An integrative assessment of phosphodiesterase 5 inhibition on cardiac function in heart failure

A thesis submitted to the University of Manchester for the degree of Doctor of Philosophy in the Faculty of Medical and Human Sciences

2014

Michael Lawless

Institute of Cardiovascular Sciences

School of Medicine

Table of contents

List of figures

List of tables

List of equations

Abstract

Heart failure is the leading cause of morbidity and mortality in the world. It is an incurable disease and most treatment strategies aim to treat the symptoms or slow the progression of the condition. Cardiac contractility is governed by calcium homeostasis within cardiac myocytes and is modulated by the sympathetic nervous system. Both mechanisms are detrimentally altered in heart failure. An important group of enzymes, phosphodiesterases, are fundamental to the sympathetic (beta-adrenergic) modulation of calcium cycling in cardiac myocytes. The selective inhibition of phosphodiesterase 5 (PDE5) has recently been considered as a potential therapy for heart failure; having beneficial effects in human and animal models of the disease. The present study employs a large animal model of tachypacing induced heart failure to test the effect of PDE5 inhibition on myocyte and whole heart contractility and beta-adrenergic function, to assess the molecular mechanisms by which PDE5 inhibition is beneficial to the failing myocardium.

In initial experiments the PDE5 inhibitor sildenafil was applied acutely to voltage clamped ventricular myocytes from uninstrumented sheep. PDE5 inhibition reduced baseline L-type calcium current and systolic calcium transient amplitude, suggesting it is negatively inotropic. Furthermore, the positive inotropic effects of beta-adrenergic stimulation were somewhat reversed by acute PDE5 inhibition. Interestingly, such negative inotropic effects of acute PDE5 inhibition were not observed in failing ventricular myocytes, which have dysfunctional calcium homeostasis and beta-adrenergic reserve. When delivered chronically over 3 weeks to tachypaced animals, PDE5 inhibition restored and augmented the systolic calcium transient and beta-adrenergic responsiveness at both the whole heart and myocyte level. These effects were associated with changes to the expression and phosphorylation status of the proteins that control calcium homeostasis in left ventricular tissue. In vivo, PDE5 inhibition prolonged longevity and reduced the onset of clinical signs of heart failure in sheep, as well as arresting cardiac dilatation and wall thinning. Chronic PDE5 inhibition however had no effect on cardiac contractility or heart failure induced changes in cardiac electrophysiology.

This study presents a novel mechanism by which PDE5 inhibition may be beneficial in a large animal model of heart failure by restoring calcium homeostasis and beta-adrenergic responsiveness. This study may have important implications for the management of heart failure in clinical practice.

Declaration

I declare that no portion of the work referred to in the thesis has been submitted in support of an application for another degree or qualification of this or any other University or institute of learning.

Michael Lawless

Institute of Cardiovascular Science

School of Medicine

Faculty of Medical and Human Sciences

Copyright statement

1. The author of this thesis (including any appendices and/or schedules to this thesis) owns certain copyright or related rights in it (the "Copyright") and s/he has given The University of Manchester certain rights to use such Copyright, including for administrative purposes.

2. Copies of this thesis, either in full or in extracts and whether in hard or electronic copy, may be made **only** in accordance with the Copyright, Designs and Patents Act 1988 (as amended) and regulations issued under it or, where appropriate, in accordance with licensing agreements which the University has from time to time. This page must form part of any such copies made.

3. The ownership of certain Copyright, patents, designs, trade marks and other intellectual property (the "Intellectual Property") and any reproductions of copyright works in the thesis, for example graphs and tables ("Reproductions"), which may be described in this thesis, may not be owned by the author and may be owned by third parties. Such Intellectual Property and Reproductions cannot and must not be made available for use without the prior written permission of the owner(s) of the relevant Intellectual Property and/or Reproductions.

4. Further information on the conditions under which disclosure, publication and commercialisation of this thesis, the Copyright and any Intellectual Property and/or Reproductions described in it may take place is available in the University IP Policy (see http://documents.manchester.ac.uk/DocuInfo.aspx?DocID=487), in any relevant Thesis restriction declarations deposited in the University Library, The University Library's regulations (see http://www.manchester.ac.uk/library/aboutus/regulations) and in The University's policy on Presentation of Theses

Acknowledgements

Firstly, I wish to thank the British Heart Foundation, as none of this would have been possible without their generous funding. They are a fantastic cause and making great waves in the battle against cardiovascular disease. I shall forever put pennies in your collection tins!

I am proud to have worked with and for the great supervisory team that is Andy and David, I owe a great deal to them for their continued help and support. Your patience and confidence in me, along with the stimulating and welcoming environment your laboratory provides has made it a very enjoyable 3 years. Thank you!

I give thanks to the wonderful support provided by my advisor Holly as well as Kat and Luigi for the debates about calcium and t-tubules.

I have made some great friends in those I worked with everyday in the lab and couldn't have asked for a better group to spend some of my most challenging days with. Those of you (past and present) on Team Sheep: Dave, Mark, Graeme, Liz, Dan, Emma, Charlie, Jess, Sarah and Charlotte are quite literally my blood brothers and sisters (post-heart harvest of course). From showing me the intricacies of whole cell patching to being there when I desperately needed a sheep holder, thank you. To Margaux, thank you for your in vivo skills, Americanisms and perfectly seasoned cakes. Little Jess (question?), I cannot thank you enough for your help and support, organisation and design skills, I promise I will one day tidy up my bay! Thank you to everyone else in the lab including Louise, Raj, Fleur and Yatong, 4pm will never be the same for me.

Also, to those in the CTF, too many to mention, thanks for putting up with my cheekiness.

To Rodolphe Fischmeister and Hind Mehel I wish to thank you for my brief stint in Paris and helping me get my head around PDEs.

Finally, I wish to thank and dedicate this work to my friends and family for keeping me sane through it all.

Thank you all!

Preface

I was born and raised on the Wirral, Merseyside. My interest in the heart began at age 14 following a rather messy dissection of a bull's heart in a memorable biology class. I subsequently moved away to study at the University of Birmingham for a Bachelor of Medical Science degree specialised in cardiovascular science. My time in the Midlands opened my eyes to the world of research and I actively sought to continue my studies. In 2010 I successfully attained a position on the 4-year British Heart Foundation PhD programme at the University of Manchester. After an initial year rotating around 3 different labs I knew I wanted to further my knowledge of cardiac physiology (and have a go at dissecting a sheep's heart). The past 3 years have been a steep learning curve, which I have relished and have certainly shaped me as a person. Following from my PhD I am about to undertake a Medicine degree at the University of Warwick making the move into the world of clinical medicine (and dissecting human hearts). The experiences, knowledge base and friends I have made along the way will undoubtedly provide an excellent foundation to continue high quality research in the future as a clinical academic.

Abbreviations

α	=	alpha
$\alpha_{1/2/3}$	=	alpha-1/2/3 (e.g. subtype)
β	=	beta
$\beta_{1/2/3}$	=	beta-1/2/3 (e.g. subtype)
β-AR	=	beta-adrenergic
γ	=	gamma
μM	=	micromolar
μmoles	=	micromoles
μm	=	micrometer
4-AP	=	4-aminopyridine
AC	=	Adenylyl cyclase
ADP	=	Adenosine di-phosphate
Ag	=	Silver
AgCl	=	Silver chloride
AKAP	=	A-kinase anchoring protein
ANOVA	=	Analysis of variance
ATP	=	Adenosine tri-phosphate
ATPase	=	Adenosine tri-phosphatase
BDM	=	2,3-butanedione monoxime
BP	=	Blood pressure
BPM	=	Beats per minute
BSA	=	Bovine serum albumin
Ca^{2+}	=	Calcium

$[Ca^{2+}]_i$	=	Intracellular calcium concentration
cAMP	=	Cyclic adenosine mono-phosphate
cGMP	=	Cyclic guanosine mono-phosphate
Cl^-	=	Chloride
DIDS	=	4,4-diisothiocyanostilbene-2,2-disulfonic acid
DBP	=	Diastolic blood pressure
DCM	=	Dilated cardiomyopathy
ECC	=	Excitation-contraction coupling
ECG	=	Electrocardiogram
EDID	=	End-diastolic internal diameter
ESID	=	End-systolic internal diameter
FKBP	=	Forskolin-binding protein
FW	=	Free wall
GDP	=	Guanosine di-phosphate
GTP	=	Guanosine tri-phosphate
G-protein	=	Guanine nucleotide binding protein
G_i	=	Inhibitory G-protein
GPCR	=	G-protein coupled receptor
G_s	=	Stimulatory G-protein
HF	=	Heart failure
HRP	=	Horseradish peroxidase
$I_{Ca\text{-}L}$	=	L-type calcium current
Iso	=	Isoprenaline
IVS	=	Intraventricular septum

K^+	=	Potassium
kDa	=	Kilodalton
L	=	Litres
LV	=	Left ventricle
MBP	=	Mean blood pressure
mg	=	Milligram
mM	=	Millimolar
Na^+	=	Sodium
NCX	=	Sodium calcium exchanger
nm	=	Nanometer
nM	=	Nanomolar
pA	=	Picoamps
PDE	=	Phosphodiesterase
pF	=	Picofarad
PKA	=	Protein kinase A
PKG	=	Protein kinase G
PLN	=	Phospholamban
PMCA	=	Plasma membrane calcium ATPase
PMT	=	Photomultiplier tube
PMSF	=	Phenylmethylsulfonyl fluoride
PP	=	Pulse pressure
PLN	=	Phospholamban
QT	=	QT interval
QTc	=	Corrected QT interval

RIPA	=	Radioimmunoprecipitation assay
R-R	=	R-R interval
RRSD	=	Standard deviation of R-R intervals
RV	=	Right ventricle
RWT	=	Relative wall thickness
RyR	=	Ryanodine receptor
SBP	=	Systolic blood pressure
SDS	=	Sodium dodecyl sulphate
Sec/s	=	Seconds
SEM	=	Standard error of the mean
Ser	=	Serine
SERCA	=	Sarco-endoplasmic reticulum calcium ATPase
Sil	=	Sildenafil
SR	=	Sarcoplasmic reticulum
TEMED	=	Tetramethylethylenediamine
Thr	=	Threonine
TnC	=	Troponin binding protein
TnI	=	Troponin inhibitory protein
TnT	=	Tropomyosin binding component
t-tubule	=	Transverse tubule
V	=	Volts

Word count: 50,343

Chapter 1

1 General Introduction

Cardiovascular disease is the leading cause of death worldwide with heart failure (HF) being the greatest cause of morbidity and mortality in the western world[1]. HF is defined as the inability for the heart to adequately perfuse body tissues and is caused by any number of risk factors, in particular lifestyle choice (tobacco use, unhealthy diet, physical inactivity)[2]. In the UK, HF affects more than 750,000 people, young and old alike, costing the NHS approximately £9 billion per annum. There currently exists no cure for HF and treatment strategies mainly target the symptoms of the disease by restoring cardiac contractility and reducing systemic vascular resistance[3, 4].

Cardiac contractility is governed by the cardiac action potential via an intracellular mechanism termed excitation-contraction coupling, which utilises Ca^{2+} ions to activate the contractile apparatus within cardiac myocytes[5]. Proper regulation of intracellular Ca^{2+} is thus fundamental to the working of the myocardium. Ca^{2+} handling is modulated by the sympathetic nervous system through tightly regulated intracellular signalling pathways mediated by cyclic nucleotide second messengers. An important group of enzymes known as phosphodiesterases (PDE) selectively hydrolyse cyclic nucleotides and thus restrict signal diffusion, resulting in highly localised and specific signal transduction.

Sympathetic signalling and Ca^{2+} handling are detrimentally altered in HF, which has been observed in both human and animal models of the disease, contributing to the disease phenotype. Many groups have explored the role of PDE inhibitors in HF, and how they may restore cardiac contractility, yet much of this work has been conducted in small animal models of disease. Thus, this thesis aims to explore the beneficial effects of PDE inhibition to the failing myocardium in a large animal model of HF, which more closely resembles the human condition.

1.1 Excitation-Contraction Coupling

1.1.1 Overview

Excitation contraction coupling (ECC) is the term given to the mechanism of myocyte contractility and is initiated by the action potential (Figure 1.1). An action potential [1] is propagated across muscular tissue through gap junctions and activates voltage gated Na^+ channels on the plasma membrane of the cardiac myocyte (sarcolemma). Myoyctes are adapted to have a large sarcolemmal surface area through invaginations deep into the centre of the cell known as t-tubules. As Na^+ channels open, Na^+ ions flood into the cell as driven by an electrochemical gradient, thus depolarising the mycoyte. L-type Ca^{2+} channels [2] densely populating the sarcolemma of the t-tubules activate in response to sarcolemmal depolarisation and Ca^{2+} freely diffuses into the cytosol (sarcoplasm). This relatively small increase in intracellular Ca^{2+} concentration ($[Ca^{2+}]_i$) results in activation of adjacent ryanodine sensitive Ca^{2+} release channels (RyR), located along the surface of the sarcoplasmic reticulum (SR) and closely associated with L-type Ca^{2+} channels. The SR acts as an intracellular reservoir for Ca^{2+}, which is both bound and freely available within this sac-like structure. Activation of RyRs [3] results in a massive efflux of Ca^{2+} from the SR into the sarcoplasm, termed the Ca^{2+} transient, which increases sarcoplasmic Ca^{2+} concentration 10 fold. This process is termed Ca^{2+}-induced Ca^{2+} release. Ca^{2+} freely diffuses throughout the sarcoplasm and activates the myofilaments [4] resulting in myocyte contraction. In the cardiac cycle this process is the main determining factor of systole.

Diastole is the relaxation phase of the myocardial contraction process. [5] Ca^{2+} is rapidly removed from the sarcoplasm by three main mechanisms. (1) Ca^{2+} is sequestered back into the SR via the sarco-endo-plasmic reticulum Ca^{2+} ATPase (SERCA) pump, which is modulated by the accessory protein phospholamban (PLN). (2) Ca^{2+} is removed from the cell via the sarcolemmal Na^+/Ca^{2+} exchanger (NCX). (3) A small proportion of Ca^{2+} is extruded from the cell via the plasma membrane Ca^{2+} ATPase (PMCA) pump and some Ca^{2+} is sequestered into mitochondria.

Each of the processes governing ECC will be described in more detail in the following chapter.

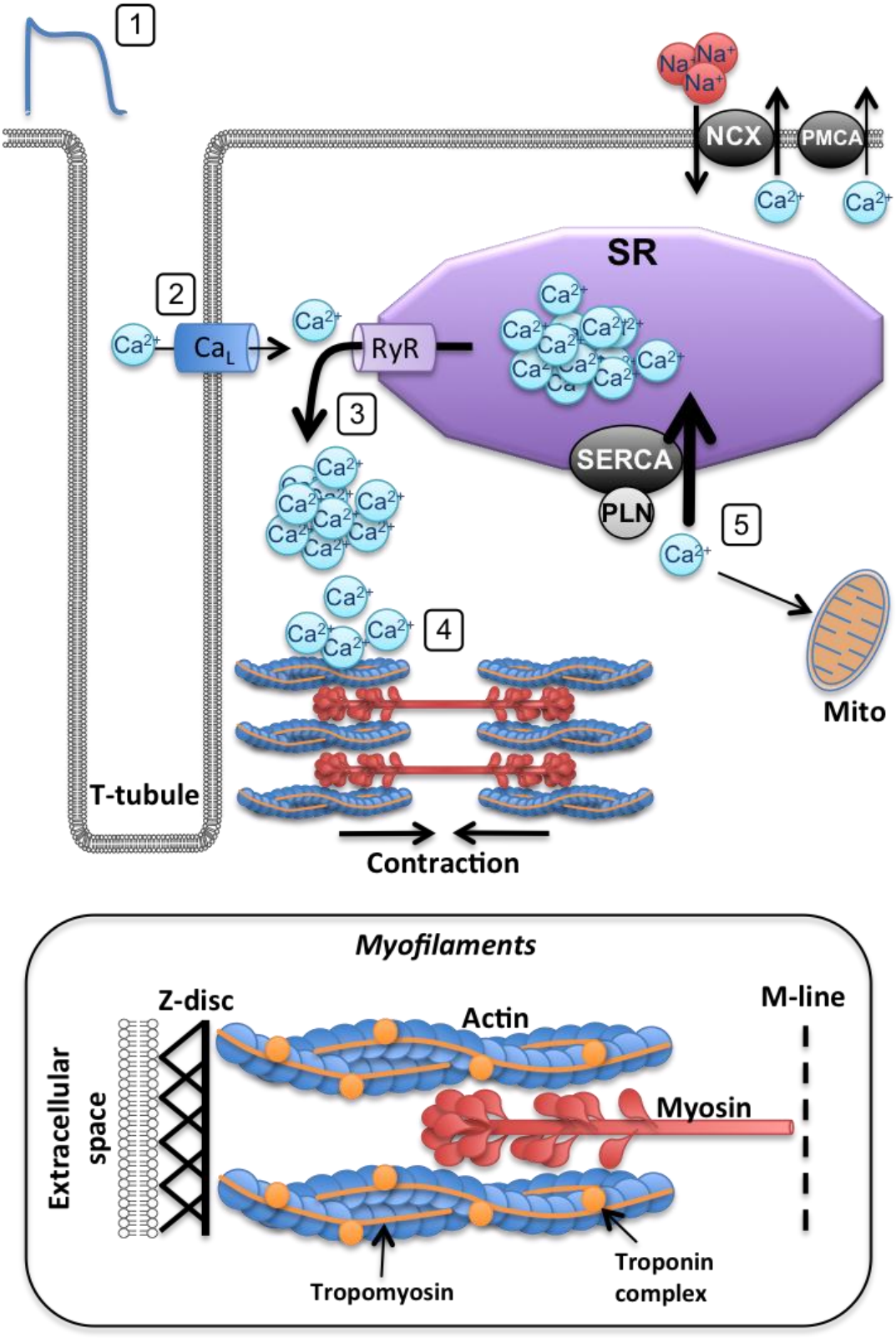

Figure 1.1 Excitation-contraction coupling.

L-type Ca^{2+} channel (Ca_L); ryanodine receptor (RyR); Na^+ Ca^{2+} exchanger (NCX); plasma membrane Ca^{2+} ATPase (PMCA); sarcoplasmic reticulum (SR); sarco-endoplasmic reticulum Ca^{2+} ATPase (SERCA); phospholamban (PLN); transverse tubule (T-tubule); mitochondria (mito).

1.1.2 Calcium influx

Calcium channels exist as a large family and are expressed in many different cell types. The current review will focus on the dihydropyridine sensitive L-type family of Ca^{2+} channels, which are highly expressed on the sarcolemma of cardiac myocytes, particularly located within t-tubules[6, 7] ([2], Figure 1.1). These channels were coined L-type due to several main characteristics: Large conductance, open for Long time and activated at Larger membrane potentials[8]. Activation occurs due to membrane depolarisation to -40mV and occurs for 2-7ms[5]. Opening of L-type Ca^{2+} channels results in a net influx of Ca^{2+} driven by a steep electrochemical gradient, resulting in a voltage dependent inward $I_{Ca\text{-}L}$. The integration of this $I_{Ca\text{-}L}$ can be used to determine the proportion of Ca entering the cell. L-type Ca^{2+} channels are located in close proximity to intracellular SR Ca^{2+} release channels and form functional coupled units with RyR called dyads[9]. This coupling facilitates Ca^{2+}-induced Ca^{2+} release by acting as the main trigger for SR release[10]. The proportion of which varies between species, being about 10% entering to 90% released from stores in rodents, to about 30% entering in larger animals[5]. Animals such as the sheep have a greater reliance on $I_{Ca\text{-}L}$ to act as a trigger for intracellular Ca^{2+} release. Moreover, Ca^{2+} influx also contributes to Ca^{2+} loading of the SR, the degree of which is also species-dependent[10, 11]. As the trigger for Ca^{2+} release occurs within the first few milliseconds then the peak of $I_{Ca\text{-}L}$ can be determined the trigger for Ca^{2+} release, with the remaining time course of $I_{Ca\text{-}L}$ being responsible for SR Ca^{2+} loading[12].

The remainder of the time course of $I_{Ca\text{-}L}$ corresponds to its inactivation. This is dependent on time, membrane potential and Ca^{2+} [5]. Initial fast inactivation of $I_{Ca\text{-}L}$ is calcium-dependent, which is enhanced by the slower voltage-dependent proportion of inactivation[13]. The latter is a negative feedback mechanism to restrict the proportion of Ca^{2+} entering the cell per beat[14]. $I_{Ca\text{-}L}$ inactivation occurs due to small local intracellular concentrations of Ca^{2+} as a result of Ca^{2+} influx, but is exacerbated by Ca^{2+} release from the SR, which was shown to reduce Ca^{2+} influx by up to 50%[15]. Inactivation typically occurs within 20ms to allow time for the next depolarisation to take place rapidly[16]. The inactivation profile of $I_{Ca\text{-}L}$ is modified by agents, which influence inotropy such as sympathetic stimulation.

1.1.3 Sarcoplasmic reticulum

The sarcoplasmic reticulum (SR) is an intracellular membrane bound compartment, which acts as a reservoir for the storage of intracellular Ca^{2+} within cardiac myocytes. The majority of the surface of the SR densely expresses Ca^{2+}-ATPase (SERCA), which actively pump Ca^{2+} into the SR. Ca^{2+} is released from the SR via RyR, which are mainly located at the terminal ends of the SR in close proximity to t-tubules and L-type Ca^{2+} channels.

SERCA2A is the main SERCA isoform expressed in cardiac and slow twitch skeletal muscle[17, 18]. SERCAs function is determined by the regulatory protein phospholamban (PLN)[19], the protein kinase-dependent phosphorylation of which increases the Ca^{2+} affinity of SERCA 2-3 fold[5].

In cardiac myocytes Ca^{2+} is stored within the SR and buffered by calsequestrin[20], which contributes to determining the total amount of Ca^{2+} to be stored within the SR: SR Ca^{2+} content. This can be experimentally measured by applying caffeine, which locks open RyR and empties the SR of Ca^{2+} [10]. The amount of Ca^{2+} stored within the SR is the main determinant of the size of the Ca^{2+} transient evoked, such that small decreases in SR content have a great impact on the amplitude of the transient[21, 22]. This highlights the importance of SR content in maintaining the size of the Ca^{2+} transient, thus contractility, which may be compromised in some disease states such as heart failure.

1.1.3.1 Ca^{2+}-induced Ca^{2+} release

The main cardiac subtype of the large family of Ca^{2+} release channels is RyR2[5], which exists functionally in vivo as a giant (2.3MDa) tetramer, acting as a junctional foot process between the SR and sarcolemma[5]. Tetrameric structural stability is determined by FK-binding proteins (FKBP), of which FKBP12.6 associates with RyR2 in the heart[23]. Disruption of this complex, for example, following protein kinase A (PKA)-dependent phosphorylation results in increased RyR open probability thus increased SR Ca^{2+} release[24, 25].

SR Ca^{2+} release occasionally occurs spontaneously and is dependent on the gating-status of the RyR; such release is termed a Ca^{2+} spark[26]. It is believed that synchronised activation and subsequent propagation of Ca^{2+} sparks by $I_{Ca\text{-}L}$ results in the generation of a Ca^{2+} transient (as reviewed[27]). This mechanism of Ca^{2+}-induced Ca^{2+} release was considered the 'local control' theory, providing an explanation for the close proximity of L-type Ca^{2+} channels and RyRs[28].

1.1.4 Transverse tubules

Transverse (t-) tubules are sarcolemmal invaginations, which project deep into the centre of the myocyte (Figure 1.1). These structures have a regular sarcomeric distribution and occur within 2μm of the z-line[29, 30]. They are the main location for L-type Ca^{2+} channels, bringing them in conjunction with the terminal ends of the SR, thus in close proximity to RyRs. They are fundamental for Ca^{2+}-induced Ca^{2+} release as mechanical loss of t-tubular density results in attenuated Ca^{2+} transients[31, 32].

T-tubules facilitate action potential induced depolarisation uniformly across the sarcolemma and thus increase the speed and synchronisation of Ca^{2+}-induced Ca^{2+} release in the myocardium. Furthermore, they are densely populated with beta-adrenoreceptors[33], which confer autonomic nervous stimulation into alterations of myocardial contractility (section 1.2). The intricate structural network of t-tubules is known to be disrupted in heart failure[34, 35], which may contribute to dysfunctional Ca^{2+} handling, contractility and sympathetic desensitisation associated with this disease.

1.1.5 Myofilaments

The sarcomere constitutes the contractile apparatus of the myocyte, consisting of thin actin and thick myosin filaments (detailed in Figure 1.1. These myofilaments occupy approximately 50% of the ventricular cell volume[5]. The sarcomere is arranged in a banding pattern with the thick filaments occurring regularly across the middle of the sarcomere and the thin filaments starting at the edges, z-bands, and projecting toward the middle, m-line (Figure 1.1). The z-band is the point at which accessory proteins attach the thin filaments to the sarcolemma[36]. Other proteins such as titin may act as a scaffold for myosin[37], which may play a role in disease induced myocardial stiffness[38].

Myocardial contractility is determined by the generation of mechanical force from chemical energy and is dependent on ATP and Ca^{2+}. Myofilament contraction occurs when the protruding 'heads' of the myosin filaments, which are attached to the 'groove' of the actin filament, actively change conformation resulting in a sliding of the actin filament past the myosin filament. When sarcomere shortening occurs uniformly across the entire cell this results in myocyte shortening and myocardial contraction. The process is regulated by tropomyosin and troponin. Tropomyosin is a long flexible molecule, which lies in the grooves of the actin filament and restricts the binding of the myosin head (Figure 1.1). The troponin complex comprises troponin-T (TnT: tropomyosin binding subunit), troponin-C (TnC: Ca^{2+} binding subunit) and troponin-I (TnI: inhibitory subunit). In the absence of

Ca^{2+} TnI specifically binds to actin and prevents myosin heads from binding. When $[Ca^{2+}]_i$ is increased it binds to TnC, which reduces the affinity of TnI for actin resulting in its removal from the actin filament. The TnC-TnI complex stimulates the removal of TnT and tropomyosin from the actin filament allowing myosin to bind to actin. Unlike skeletal muscle, cardiac muscle cannot recruit cells or fibres to increase the force of contraction; instead the force is relative to the amplitude of $[Ca^{2+}]_i$ change, thus the size of the systolic Ca^{2+} transient is fundamental to cardiac contractility.

1.1.6 Sarcolemmal Ca^{2+} removal

During diastole the majority of cytosolic Ca^{2+} is sequestered back into the SR and the remainder is extruded from the cell via two main routes: Na+ Ca^{2+} exchanger (NCX) and plasma membrane Ca^{2+}ATPase (PMCA) (Figure 1.1).

The cardiac PMCA pump contributes only 5% of Ca^{2+} extrusion on a beat-to-beat basis, and if left as the only available Ca^{2+} extrusion pathway, myocyte relaxation could take up to 60 seconds[5].

Cardiac NCX exchanges 3 Na^+ into the cell for each Ca^{2+} out[39, 40]. The relative imbalance of exchanged ions results in a charge of minus 1, causing NCX to be electrogenic as it generates an inward current: I_{NCX}[5] . Due to this effect, physiologically and experimentally altered NCX function, with either spontaneous SR Ca^{2+} release or caffeine, can generate I_{NCX}, which may result in arrhythmic contractions such as delayed after-depolarisations[5]. Generated I_{NCX} is proportional to the degree of Ca^{2+} extrusion, thus following application of caffeine to empty the SR and render SERCA redundant, quantification of Ca^{2+} extrusion from the cell is a good estimate of SR Ca^{2+} content (see 2.2.5.3).

1.2 Sympathetic neurohormonal signalling

The sympathetic nervous system modulates ECC through the agonism of adrenoreceptors on the surface of the cardiac mycoyte. Sympathetic *β*-adrenoreceptor stimulation results in increases in developed contractions (inotropy), increased rate of relaxation (lusitropy) and increased frequency of contraction (chronotropy)[41]. Together, *β*-adrenergic (*β*-AR) stimulation leads to a more spatially organised and time-synchronised depolarisation-induced Ca^{2+} release[42].

1.2.1 Adrenergic receptors

The external surface of the sarcolemma is highly specialised for modulation by both parasympathetic and sympathetic innervation[43]. Cardiac contractility is modulated by agonism of α-adrenoreceptors (α_{1a}, α_{1b} and α_{1d}) and *β*-adrenoreceptors (β_1, β_2 and β_3). Sympathetic stimulation results in the activation of all three subtypes of *β*-adrenoreceptor, which has the potential to evoke a varied response on contractility as β_1 and β_2 stimulation causes inotropy: increased force of contractility, whereas β_3 promotes negative inotropy[44, 45].

β-adrenoreceptors are G-protein coupled receptors (GPCR). G-proteins are membrane spanning multi-subunit proteins that provide a mechanism through which membrane bound receptors activate downstream signalling pathways (Figure 1.3, Figure 1.2). Those that associate with *β*-adrenoreceptors are heterotrimeric complexes consisting of an alpha ($G\alpha$) and dimeric beta-gamma ($G\beta\gamma$) subunits (Figure 1.2). They can signal through both stimulatory (G_s) and inhibitory (G_i) pathways, thus can switch on or off downstream signals (Figure 1.2A). Their mechanism of action is shown in Figure 1.2B. In the inactivated state, the GPCR has a conformation in which the $G\alpha$ and $G\beta\gamma$ subunits are closely associated, with $G\alpha$ bound to a molecule of (GDP). The subsequent binding of a ligand to the surface receptor of the GPCR and/or the exchange of GDP for GTP on $G\alpha$ results in a G-protein conformational change, which separates $G\alpha$ from $G\beta\gamma$[46]. This makes all subunits available for interaction with downstream signalling effectors. Hydrolysis of the GTP molecule results in the reformation of $G\alpha$–$\beta\gamma$ interaction thus rendering the G-protein inactive.

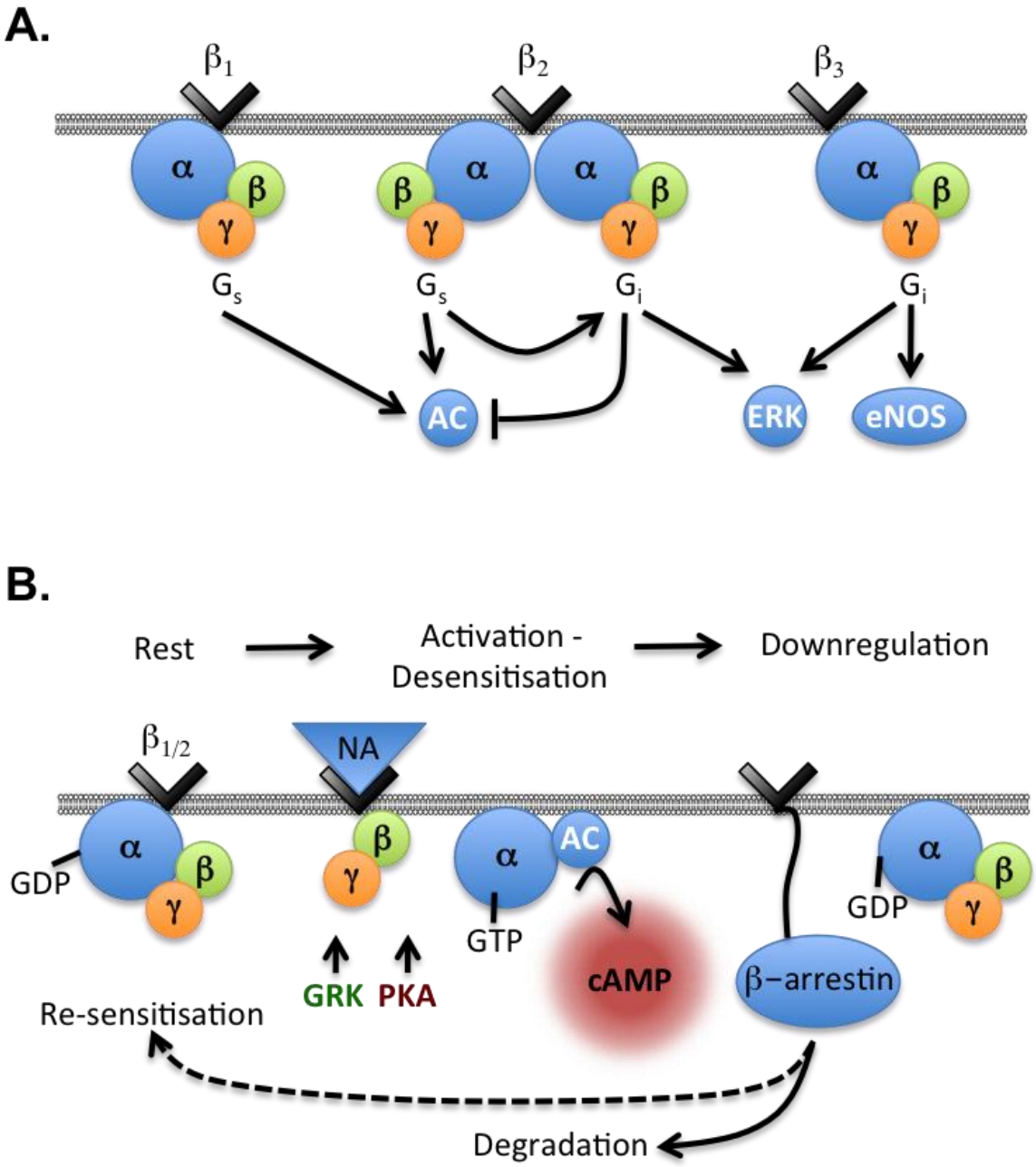

Figure 1.2. G-protein coupled receptor signalling.

(A) β-adrenoreceptors couple to either stimulatory (Gs) or inhibitory (Gi) proteins. Arrows represent activation, solid end represents inhibition. (B) Activation, desensitisation and downregulation of G-protein coupled receptor signalling. β-adrenoreceptor 1/2/3 ($\beta_{1/2/3}$); noradrenaline (NA); endothelial nitric oxide synthase (eNOS); adenylyl cyclase (AC); protein kinase A (PKA); extracellular signal-regulated kinase (ERK): cyclic adenosine monophosphate (cAMP); guanosine diphosphate (GDP); guanosine triphosphate (GTP); protein kinase G (PKG); G-receptor kinase (GRK).

β_1 and β_2 are coupled to G_s, which, when active, $G_s\alpha$ activates adenylyl cyclase (AC), which catalyses hydrolysis of ATP into cyclic adenosine monophosphate (cAMP). The downstream effector protein kinase A (PKA) phosphorylates a number of downstream effectors, which results in inotropy and lusitropy (described in more detail in section 1.2.2). The human heart expresses β_1 and β_2 in a ratio of approximately 3:1[44]. β_1 are distributed globally across the sarcolemma including both t-tubules and the sarcolemmal crest[47], whereas β_2 reside exclusively within caveolae in t-tubules[48]. Differences in membrane localisation reflect the differences in downstream signalling each subtype evokes. β_1 stimulation is coupled exclusively to G_s and results in a global cytosolic generation of cAMP[49], whereas β_2 may couple to either G_s or G_i and selective stimulation results in local sarcolemmal rises in cAMP[50,51] (Figure 1.2B). The resultant compartmentalisation of signals from the different receptor subtypes results in the activation of different downstream proteins, thus ECC is modulated differently depending on the receptor subtype stimulated. The more spatial and temporal generation of cAMP by β_1 stimulation[49], results in the activation of PKA[52] and targeted phosphorylation[50] of L-type channel[53], RyR[25], PLN and TnI[54]. On the other hand, β_2 stimulation results in increased $I_{Ca\text{-}L}$[50] with minimal downstream targeting of proteins on the SR or myofilaments[55, 56].

β-adrenoreceptors predominate in the modulation of cardiac inotropy and lusitropy[57]. They have been found to localise within both lipid and nonlipid rafts on the membrane[48], whereas there is an important role for caveolin in the normal functioning of β_2 adrenoreceptors[57]. Experiments from the Calaghan group have shown that the localisation of β_2 to caveolin is important for signalling through both G_s and G_i[58], which maintains differences in signal compartmentalisation between β_1 and β_2 (Figure 1.4). They showed that when caveolin was disrupted, a marked increase in cell shortening, Ca^{2+} transient and $I_{Ca\text{-}L}$ was observed in response to β_2 stimulation. Furthermore, they observed similar increases in myocyte contractility with β_2 stimulation following inhibition of G_i[58]. These observations are consistent with a more global generation of cAMP, akin to the mechanism of signal transduction through β_1 adrenoreceptors. Interestingly in HF β_2 adrenoreceptors are known to relocate to the sarcolemmal crest, which in turn reflects the more diffuse, poorly compartmentalised β-AR signalling observed in the failing myocardium[47].

In 1989 Alberto Kaumann reviewed data surrounding anomalous patterns of results using non-conventional agonists and antagonists for β_1 and β_2 adrenoreceptors and speculated a role for a third β-adrenoreceptor[59]. β_3 have subsequently been described at both the mRNA

and functional protein level in ventricular tissue across many species including human[60]. However, β_3 exist in much lower abundance than β_1 and β_2 adrenoreceptor protein[61]. β_3 couple predominantly to G_i[60] and selective stimulation results in decreased ventricular contractility in human[62] and canine tissue[63], as well as an observed reduction in Ca^{2+} transient amplitude and $I_{Ca\text{-}L}$ in rabbit ventricular mycoytes[64]. Furthermore, negatively inotropic responses were dependent on NO/cGMP signalling[60, 65, 64] (Figure 1.2). It is well established that β_3 are activated at higher concentrations of catecholamine than β_1 and β_2[66, 67] which may contribute to a protective counter-mechanism during sympathetic overstimulation in such conditions as HF. Moreover, β_3 are upregulated in human failing myocardium[68] and show inability to desensitise unlike β_1 and β_2 adrenoreceptors. For such reasons, β_3 adrenoreceptors have more recently attracted the attention of many as a possible therapeutic strategy in the management of human HF.

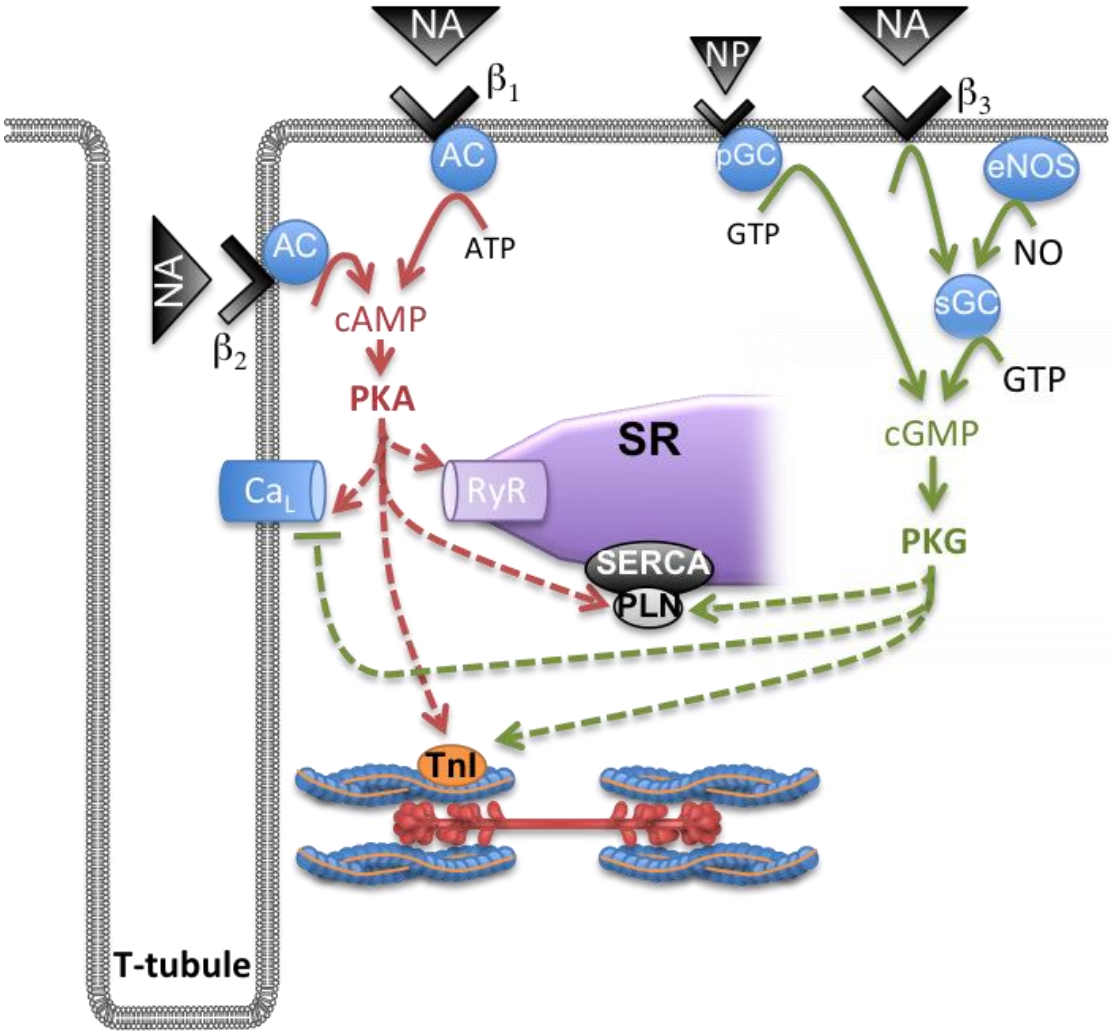

Figure 1.3 Sympathetic modulation of excitation-contraction coupling

β-adrenoreceptor 1/2/3 ($\beta_{1/2/3}$); noradrenaline (NA); natriuretic peptide (NP); endothelial nitric oxide synthase (eNOS); nitric oxide (NO); adenylyl cyclase (AC); adenosine triphosphate (ATP); cyclic adenosine monophosphate (cAMP); protein kinase A (PKA); particulate guanylyl cyclase (pGC); soluble guanylyl cyclase (sGC); guanosine triphosphate (GTP); cyclic guanosine monophosphate (cGMP); protein kinase G (PKG); L-type Ca^{2+} channel (Ca_L); ryanodine receptor (RyR); sarcoplasmic reticulum (SR); sarco-endoplasmic reticulum Ca^{2+} ATPase (SERCA); phospholamban (PLN); troponin-I (TnI); transverse tubule (T-tubule).

1.2.2 β-AR signalling pathway

Agonism of sarcolemmal β-adrenoreceptors results in the activation of G-protein subunits, which activates downstream effectors, resulting in a signal cascade with the end result being a change in mycoyte Ca^{2+} handling and contractility. The intracellular signalling pathways involved are summarised in Figure 1.3.

As discussed, β_1- and to some extent β_2-adrenoreceptors are coupled to $G_s\alpha$, which directly activates sarcolemmal bound adenylyl cyclase (AC)[69]. Of the large biological family of ACs available, AC V and VI are the most abundant and active isoforms expressed in cardiac mycoytes, which are subsequently activated by β-AR stimulation[70, 71]. AC catalyses the hydrolysis of ATP into 3'-5'-cyclic adenosine monophosphate (cAMP) and pyrophosphate. cAMP is a small, easily diffusible cyclic nucleotide, which acts as a second messenger to transmit signals within distinct sub-cellular, localised compartments[72, 73]. The most important function of cAMP, in terms of β-AR stimulation, is the activation of protein kinase A (PKA). PKA exists as a dimerised complex consisting of a regulatory subunit and a catalytic subunit. The binding of 2 cAMP to sites on the regulatory subunit results in a dissociation of the dimerised complex and allows the catalytic subunits to freely react. The resultant reaction: the transfer of terminal ATP phosphates to serine and threonine residues on protein substrates characterises the key phosphorylative role of PKA in the β-AR signalling cascade.

Stimulation of β_1 and β_2 adrenoreceptors results in PKA-dependent phosphorylation of four main intracellular targets (Figure 1.3): (1) L-type Ca^{2+} channel, increasing channel open probability and increasing $I_{Ca\text{-}L}$[74], (2) RyR, leading to enhanced open probability and greater SR Ca^{2+} release[75, 76], (3) Troponin I, reducing myofilament calcium sensitivity and encouraging enhanced lusitropy[77], (4) PLN, increasing SERCA activity and SR Ca^{2+} loading[78].

The diffusible nature of cAMP means that signal transduction must be closely regulated, thus AC, PKA and cAMP-hydrolysing phosphodiesterase (PDE) enzymes are closely associated in membrane bound complexes known as A-kinase anchoring proteins (AKAP)[79]. Following hormonal stimulation, specific pools of PKA will be locally active and thus phosphorylate a number of specific sites within that domain[80, 81, 82]. cAMP-PKA signal regulation will be discussed in more detail in section 1.4.

Functional β_3 adrenoreceptor signalling in the human myocardium was shown to decrease myocyte contractility through a G_i and NO dependent mechanism[60] (Figure 1.2, Figure

1.3). Not only can G_i directly inhibit AC[69], but there also appears to be a direct interaction between β_3, G_i and endothelial nitric oxide synthase (eNOS)[83]: a prominent source of NO in the myocardium. This highlights a negatively inotropic mechanism outside of the suppression of the AC-cAMP-PKA axis. This is the role of another second messenger 3'5'-cyclic guanosine monophosphate (cGMP).

cGMP is a similarly diffusible cyclic nucleotide as cAMP and is derived from two different intracellular sources; the freely diffusible soluble guanylyl cyclase (sGC) and the membrane bound particulate guanylyl cyclase (pGC) (Figure 1.4). Each are activated by different substrates and generate distinct, compartmentalised pools of cGMP, which signal very different downstream responses[84, 85]. Particulate GC is activated by the binding of natriuretic peptides (NP) to sarcolemmal receptors, such as brain (BNP) and atrial (ANP), which are particularly important chemokines in heart failure. NO activates soluble GC, this in turn catalyses the hydrolysis of GTP into cGMP, which activates its downstream effector protein kinase G (PKG). The resultant effects of both increased $[cGMP]_i$ and PKG activity leads to reductions in myocyte contractility because of four main reasons (Figure 1.4): (1) PKG phosphorylates the L-type Ca^{2+} channel, inhibiting $I_{Ca\text{-}L}$[86]; (2) PKG phosphorylates TnI, which has the same effect as PKA, leading to reduced myofilament Ca^{2+} sensitivity[87]; (3) PKG phosphorylates PLN; releasing its inhibition of SERCA and increasing the rate of SR Ca^{2+} uptake, thus increasing lusitropy[88]; and (4) cGMP activates the cAMP-hydrolysing enzyme phosphodiesterase 2 (PDE2), leading to a predominate cGMP signal.

It is important to note that signal transduction through cAMP and cGMP is highly regulated and compartmentalised within discrete sub-cellular locations, which is tightly controlled by an important group of enzymes, phosphodiesterases. This will be discussed in greater detail in (section 1.4.4). Firstly the effects of PKA and PKG on the most important proteins involved in Ca^{2+} handling will be discussed.

1.3 Sympathetic modulation of excitation-contraction coupling

1.3.1 Control of Ca^{2+} influx

L-type Ca^{2+} channels are the primary site for CICR, with peak $I_{Ca\text{-}L}$ providing an important trigger for SR Ca^{2+} release and a contribution to the plateau phase of the cardiac action potential. In early experiments Sperelakis and Schneider[89] and Reuter and Scholz[90] independently proposed a cAMP-PKA dependent mechanism for $I_{Ca\text{-}L}$ augmentation upon β-AR stimulation. It is now well established that $I_{Ca\text{-}L}$ modulation may occur through two main intracellular signalling pathways.

Non-selective β-AR stimulation through such agonists as isoprenaline results in marked increases in cAMP and increased peak $I_{Ca\text{-}L}$[42, 91]. These effects are associated with a direct PKA phosphorylation of Ser1989 residue on the α_{1a} subunit and on Ser478/Ser479 on the β_{2a} subunit[92], which is thought to increase the open probability of the channel[93, 94]. Leroy showed that brief pulses of isoprenaline elicited large increases in cAMP concentrations in compartments close to the plasma membrane, which was associated with increases in $I_{Ca\text{-}L}$[95]. Furthermore, AKAP-79 is known to anchor PKA close to L-type channels[96, 97, 98], which taken together, highlights the compartmentalised nature of cAMP signalling (section 1.4.3).

For a long time cGMP was known to be counteractive against prestimulated $I_{Ca\text{-}L}$[99, 100], and was directly linked to a modulation of the L-type Ca^{2+} channel [101, 102]. Moreover, selective sGC activation, resulted in $I_{Ca\text{-}L}$ inhibition in frog ventricular myocytes[103] and has more recently been linked, at least in part, to direct effects of phosphorylation by PKG[86].

1.3.2 Control of SR Ca^{2+} release

It is still widely considered that SR Ca^{2+} release under β-AR stimulation is dependent mainly on $I_{Ca\text{-}L}$ and SR loading, and not an effect of altered RyR open probability[104]. Furthermore, the close proximity of RyR to other ECC proteins has made it notoriously difficult to study. Despite this, there are several residues subject to phosphorylation on RyR. The most important residue is Ser2809, which is directly phosphorylated by PKA[24] and results in the dissociation of RyR from its regulatory/stabilising subunit FKBP12.6. This is associated with an increased in the open probability of the channel[25]. There is limited evidence to support direct RyR phosphorylation by PKG in the myocardium, although it has been shown that PKG directly targets residues on RyR in skeletal muscle[105].

1.3.3 Control of Ca^{2+} reuptake

The rate of decay of $[Ca^{2+}]_i$ during diastole is modulated by β-AR stimulation, as a faster rate of relaxation results in a faster rate of contraction. Both TnI and PLN are important targets for PKA-dependent phosphorylation, although the latter predominates. TnI phosphorylation occurs at Ser23/24[77] and results in a decrease in myofilament Ca^{2+} sensitivity due to a reduction in TnCs affinity for Ca^{2+} [5].

Ca^{2+} reuptake into the SR is determined by SERCA activity. This is positively modulated by β-AR stimulation, which results in more Ca^{2+} being pumped back into the SR before NCX has time for it to be removed, thus loading the SR with Ca^{2+} per beat and increasing the size of the systolic Ca^{2+} transient[106]. Whether SERCA itself is phosphorylated by PKA is a topic of controversy, however its regulatory protein PLN is modulated at several sites. Phosphorylation by PKA at Ser16 removes the inhibitory action of PLN from SERCA[107], thus increasing its activity, and enhancing cardiac lusitropy[108]. Targeted PLN knockout in mice results in a complete ablation of both inotropic and lusitropic observations of β-AR stimulation[109], thus PKA-dependent PLN phosphorylation is fundamental in sympathetic modulation of contractility.

Ser16 is also the site for targeted phosphorylation by PKG, which too increases the rate of Ca^{2+} sequestration[88]. The exogenous application of cGMP reduced rabbit ventricular myocyte shortening in a mechanism dependent on PKG activity[110]. PKG-dependent PLN phosphorylation has also been linked to an NO derived pool of cGMP, however such interaction was not constitutively active in the normal myocardium[111].

1.4 Regulation and compartmentalisation of β-AR signalling

The multifaceted response observed in Ca^{2+} handling following *β*-adrenoreceptor stimulation, which is just one aspect of *β*-AR signalling, provides an example for why the *β*-AR signalling pathway must be tightly controlled. Exacerbation or attenuation of the *β*-AR signal in cardiac myocytes leads ultimately to pathophysiologies such as heart failure.

1.4.1 G-protein receptor kinases and β-arrestin mediated signal regulation

The *β*-adrenoreceptor is a target of PKA. Negative feedback by PKA-dependent phosphorylation of β_2 adrenoreceptors results in G-protein switching for G_s to G_i[112], simultaneously uncoupling the *β*-adrenoreceptor from AC and activating G_i-dependent cardioprotective signalling pathways such as the anti-apoptotic/survival ERK/MAPK signalling pathways[113] (Figure 1.2A). PKA-mediated phosphorylation of *β*-adrenoreceptors is also accompanied by G-protein receptor kinase (GRK) phosphorylation[114] (Figure 1.2B). Together, this increases the binding affinity of a group of regulatory proteins: *β*-arrestins, which subsequently bind to the *β*-adrenoreceptor to promote clathrin-dependent endocytosis[115]. *β*-arrestins may function as signalling molecules as they are associated with cardioprotective signalling pathways[116] and may directly influence Ca^{2+} handling through altering the activity of SERCA2A[117].

1.4.2 Regulators of G-protein signalling

Termination of the G-protein signal is determined by the reformation of the $G\alpha$–$\beta\gamma$ complex, achieved through hydrolysis of GTP on the $G\alpha$ subunit (Figure 1.2B). Regulators of G-protein signalling (RGS) proteins act to stimulate the GTPase activity of the $G\alpha$ subunit and promote the reformation of the inactive G-protein heterotimer[118]. Of the 20+ members in this family RGS2-5 are most commonly expressed in the mammalian heart[118]. The above mechanism of RGS action is mostly restricted to $G\alpha_i$[119]. Regulation of $G\alpha_s$ occurs through direct interaction of RGS with downstream effectors[120, 121, 122]. In the case of *β*-AR signalling in the heart, RGS may directly inhibit AC and was shown to inhibit cAMP generation in the presence of the AC agonist forskolin independent of $G\alpha_s$ signalling[122]. RGS also interacts with downstream effectors of the $G\alpha_i$ signalling pathway, thus influencing cardioprotective signals[120, 121]. Furthermore, PKG can directly activate RGS proteins[121], contributing to both negative inotropy and stimulation of cardioprotective signalling pathways[123].

1.4.3 A-kinase anchoring proteins

In the early 1980s, Hayes and Brunton proposed the notion of a relationship between β-AR regulation of cardiac myocyte events and discrete compartments of cAMP[124]. They further postulated that such signals involved an interaction between sarcolemmal receptors, AC and target proteins with cytoskeletal components and structural scaffolding. This ultimately manifested in the description of A-kinase anchoring protein complexes, of which at least 50 are currently known[125], and 14 of which are expressed in cardiac mycoytes. AKAPs, by definition, associate structures such as β-ARs, L-type Ca^{2+} channels, RyRs, PLN to important signalling molecules such as AC, PKA and PDEs, in macromolecular complexes (as reviewed[126]). They are important for maintaining discrete spatial and temporal cAMP-mediated responses by bringing together source, effector and target, and reducing the chance for signal diffusion. One such example is the association of β_2-adrenoreceptors with an AKAP, which tethers PKA and L-type Ca^{2+} channels[127]. Selective stimulation of β_2 adrenoreceptors results in a PKA dependent increase in $I_{Ca\text{-}L}$, with little effect on the dynamics of other ECC proteins[50]. Furthermore, disruption of AKAP-PKA binding sites has been shown to exacerbate the phosphorylative effects of PKA both at rest and under β-AR stimulation[128]. The maintenance of these functional macromolecular complexes is therefore clearly fundamental to appropriate β-AR signalling. Surprisingly, similar complexes for cGMP-dependent signals are yet to be described in the myocardium.

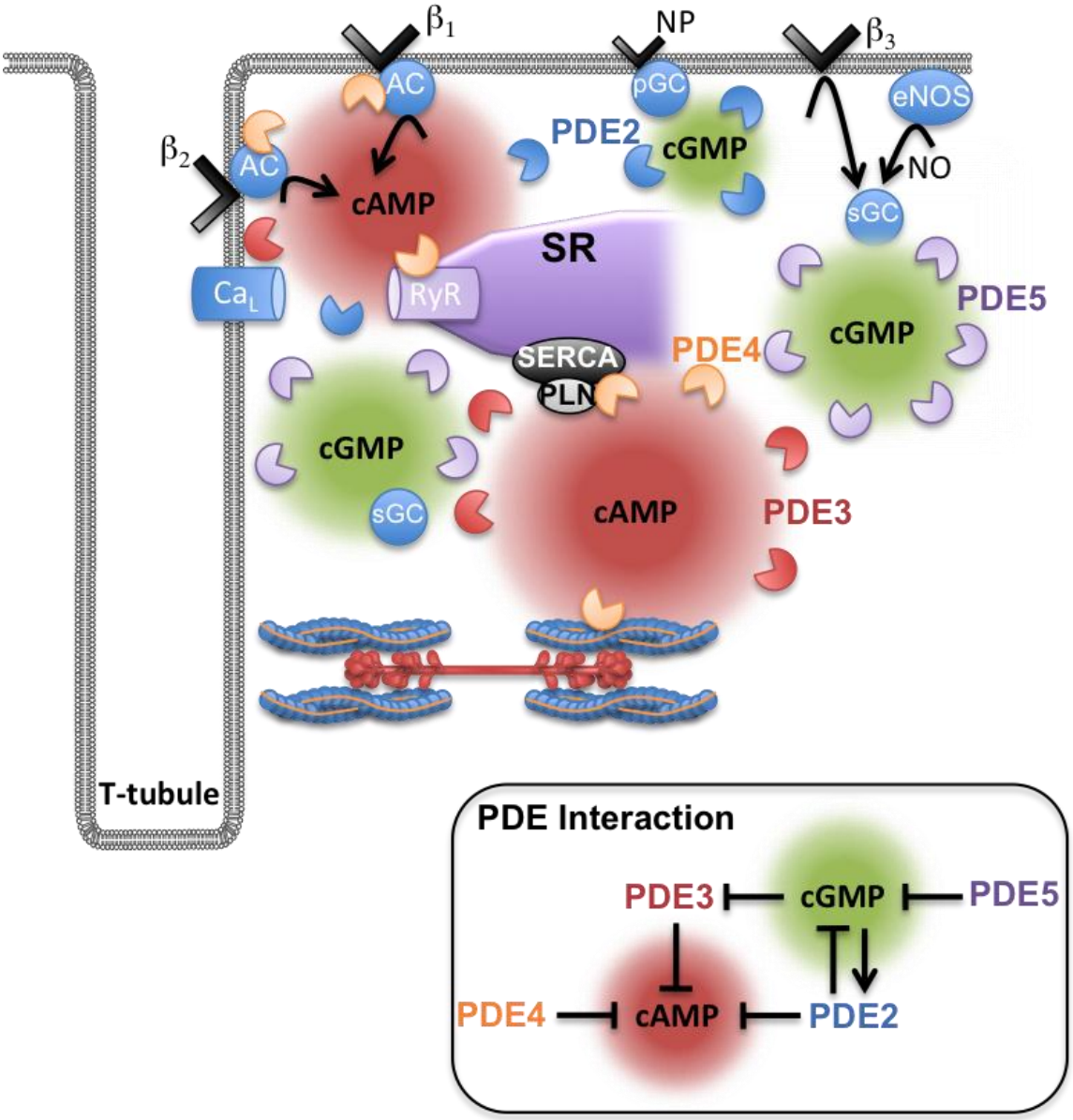

Figure 1.4 Cyclic nucleotide compartmentalisation and phosphodiesterase interaction

Cyclic nucleotides cAMP and cGMP are generated from adenylyl cyclase (AC) and guanylyl cyclase (s/pGC) activated by numerous sources inside cardiac myocyte. Cyclic nucleotides are maintained in discrete subcellular compartments via selective hydrolysis by PDEs. The complex interaction of PDE isoforms is shown in the box. Arrows represent activation and solid end represents inhibition. β-adreonreceptors ($\beta_{1/2/3}$), cyclic adenosine/guanosine monophosphate (cAMP/cGMP), transverse tubule (t-tubule), sarcoplasmic reticulum (SR), ryanodine receptor (RyR), sarcoendoplasmic reticulum Ca^{2+} ATPase (SERCA), phospholamban (PLN), phosphodiesterase (PDE).

1.4.4 Phosphodiesterase regulation of cyclic nucleotides

Phosphodiesterases (PDEs) are fundamental to the functioning of AKAPs and cytosolic bioavailability of cyclic nucleotides. Without selective hydrolysis, free diffusion of stochastically generated cAMP and cGMP would allow rapidly increasing concentrations to uniformly fill the entire cell within a fraction of a second[129]. PDEs restrict the diffusibility and concentrations of cAMP and cGMP, thus maintaining compartmentalisation and, most importantly, specificity of the β-AR signal. The complexity of signal restriction and PDE cross-talk is summarised in Figure 1.4.

PDEs belong to a vast family of enzymes in which there exists 22 different genes encoding over 60 isoforms, classifying into eleven subfamilies PDE1-PDE11[130]. The primary function for controlling cyclic nucleotide bioavailability is their direct breakdown by PDEs, however some PDEs contain N-terminal cyclic nucleotide binding sites, GAF domains[131], which may act secondarily to sequester cyclic nucleotides. PDE enzymes can be sorted in relation to their cyclic nucleotide hydrolysing specificities: PDE 4, 7 and 8 selectively hydrolyse cAMP, and PDE 5, 6 and 9 selectively hydrolyse cGMP, whereas PDE 1, 2, 3, 10 and 11 have dual specificity for both cAMP and cGMP (as reviewed[132]). In most tissues the majority of cAMP hydrolysis is achieved by PDE3 and PDE4. PDE5 is the most abundant cGMP-hydrolysing subtype, and PDE1 and 2 are the most widely expressed dual-specificity isozymes. The more obscure PDEs (6 – 11) are incompletely investigated, have not been described in cardiac tissue and are beyond the scope of the current review.

1.4.4.1 cAMP-specific PDEs

In the early 1980s Brunton and colleagues performed a series of experiments to understand how the, then considered ubiquitous, second messenger cAMP was generated in the heart. Upon stimulation with a β-adrenoreceptor agonist, cAMP was generated globally within all subcellular fractions. However, when stimulated with prostaglandin E1, cAMP was generated only within the soluble fraction, demonstrating cytosolic- and not membrane-dependent synthesis[133]. This work highlighted the complex nature of compartmentalisation of cyclic nucleotide signalling. Verde et al demonstrated the non selective PDE inhibitor IBMX increased basal $I_{Ca\text{-}L}$ similar to that observed under β-AR stimulation, an effect which was almost entirely replicated following the dual inhibition of PDE3 and PDE4[134]. Subsequently PDE3 and 4 have been shown to specifically hydrolyse cAMP and contribute approximately 90% of PDE activity in animal hearts[135].

In cardiac myocytes PDE3 exists as two isoforms: PDE3A and PDE3B[72], the former considered predominant in animal hearts[136]. Low levels of cGMP inhibit PDE3, thus cAMP hydrolysis by this isoform is also dependent on cGMP concentration (Figure 1.4). PDE3 has been isolated at both the mRNA and protein level in dog, rat and human myocardium[137], yet its importance and expression levels differ according to the species under investigation[137, 138]. Immunocytochemistry in rat cardiac myocytes has revealed that PDE3 is diffusely organised sub-cellularly demonstrating a sarcolemmal localisation[139].

The PDE4 subfamily consists of four isoforms, PDE4A-D, of which PDE4B and PDE4D contribute the majority of PDE4 activity in cardiac myocytes[139]. Both subtypes are localised to the myofilaments, PDE4B located along the m-lines and PDE4D located at the z-discs[139]. Differences in localisation between different PDE4 isoforms and their differences from PDE3 localisation reflect different sub-cellular compartments. Non-selective β-AR stimulation with agonists such as noradrenaline or isoprenaline evokes rises in cAMP, which are exacerbated following non-selective PDE inhibition with IBMX[139]. Equivalent rises in cAMP and increased PKA activities were found following selective inhibition of PDE4 with rolipram but not PDE3 with cilostamide[52, 139]. Furthermore, β-agonist evoked contractility was augmented following application of rolipram but not cilostamide[140]. In genetic knockdown studies PDE4 was shown to modulate inotropic responses to both β_1 and β_2 stimulation, whereas PDE3 only modulated β_1 evoked cAMP signalling[140, 141]. β_2 stimulation in the presence of a PDE4 inhibitor results in PLN phosphorylation, which does not happen under normal physiological conditions, suggests that PDE4 selectively controls signalling through β_2 receptors[140].

PDE4 subtypes are involved in the modulation of signalling to many ECC proteins and influence Ca^{2+} handling in cardiac myocytes (Figure 1.4). PDE4B was found to modulate compartments containing L-type Ca^{2+} channels and restricts channel phosphorylation by PKA[142]. PDE4D is responsible for the modulation of signalling to β-adrenoreceptors[143], RyR[144], SERCA2A and PLN[145, 146].

Within the PDE4D group there exist further isoforms, of which PDE4D3 and PDE4D5 are the most abundant in the heart. It has been shown that these isoforms interact with a number of membrane associated proteins including β-arrestin and AKAPs[147, 148]. PKA phosphorylation of Ser-13 and Ser-54 residues on PDE4D3 enhances its affinity for mAKAP and its catalytic efficiency of cAMP[149]. Such co-localisation has been observed at both the nuclear membrane[148] and RyR2[144]. Disruption of the latter is known to facilitate PKA-mediated RyR hyperphosphorylation resulting in arrhythmias and sudden cardiac

death[150]. The recruitment of β-arrestin in response to β_2 stimulation results in a complex formation including PDE4D3[147], which further restricts cAMP-mediated signal propagation adjunct to mechanisms to desensitise the β-adrenoreceptors[151].

1.4.4.2 Dual substrate and cGMP-specific PDEs

PDE1 is activated by calmodulin in the presence of Ca^{2+} and is widely expressed in the human myocardium[152]. The lack of specific PDE1 inhibitors has hampered the current understanding of PDE1 physiology.

PDE2 has been isolated in both the atria and ventricles of a large number of species ranging from frog to human[153, 154]. It contains a GAF domain, which when cGMP-bound, increases its cAMP-hydrolysing capacity 2-6 fold[155]. Although PDE2 only hydrolyses approximately 3% of cAMP in unstimulated cells, its function in cardiac tissues appears fundamental as it was responsible for the attenuation of β-AR stimulated cAMP-dependent responses in rabbit AV node cells[156] and rat ventricular myocytes[98]. The latter study demonstrated that such β-AR modulation was dependent on a functional NO-sGC-cGMP axis[98]. PDE2 localises to sarcomeric z-discs[98], which are commonly associated with t-tubules. Specific inhibition of PDE2 has no effect on basal $I_{Ca\text{-}L}$[134] yet enhanced cAMP-stimulated $I_{Ca\text{-}L}$[134, 157, 158], and Ca^{2+} transient amplitude[98]. PDE2 has been described as an important regulator of cyclic nucleotide cross-talk[72] because not only does it selectively hydrolyse β_1 and β_2 derived cAMP, but also its catalytic activity is enhanced by β_3 stimulated NO-derived cGMP[98] (Figure 1.4). To add to this complexity PDE2 selectively hydrolyses the natriuretic peptide-pGC-derived pool of cGMP without any effect on the NO-sGC derived pool of cGMP[84].

PDE5 is the only cGMP-specific hydrolysing enzyme in the myocardium (Figure 1.4). Its activity accounts for 30% of total myocardial cGMP degradation in mice[123] and dogs[159]. As for PDE2, PDE5 is sensitive to cGMP through the presence of a GAF domain. PDE5 contains two GAF domains, which, when bound, may increase isoenzyme catalytic activity by 10 fold[160]. Due to its ability to bind cGMP at several sites, it has been postulated that PDE5 may store and act to buffer cGMP at low cytosolic concentrations[161].

Immunolocalisation studies in isolated myocytes have shown that PDE5 co-localises with α-actinin at the sarcomeric z-discs[162]. Differing expression and activity profiles of PDE5 in different species has provoked speculation about the true role of PDE5 in the human myocardium, however the generation of a PDE5 gene silencing model settled the majority of this controversy by demonstrating its importance in cardiac myocytes[163].

Conflicting evidence exists as to the effects of PDE5 inhibition on basal ventricular myocyte Ca^{2+} handling and contractility, with differences mainly being associated to the species under investigation. Senzaki and colleagues administered the selective PDE5 inhibitor sildenafil to anaesthetised dogs and reported reduced cardiac contractility[159], which was not observed in similar experiments in mice[162, 164], or rats[85]. Acutely administered oral sildenafil to humans partially increased contractility and ejection fraction[165]. In single murine myocytes, PDE5 inhibition had no effect on baseline $I_{Ca\text{-}L}$[166], Ca^{2+} transient amplitude[85] or sarcomere shortening[85, 162]. However, in all models investigated PDE5 inhibition attenuated β-AR stimulated $I_{Ca\text{-}L}$ and Ca^{2+} transients as well as contractility in both single myocytes and whole hearts[85, 159, 162, 164, 165, 166].

In ventricular cardiac mycoytes PDE5 specifically hydrolyses the NO-sGC-derived pool of cGMP[84] (Figure 1.4), which is responsible for the PKG-dependent negative modulation of the β-AR responses described above[85, 162, 164-166]. Interestingly, the NP-pGC-derived pool of cGMP has no effect on responses to β-AR stimulation[85] and is unaffected by PDE5 inhibition[84]. Direct inhibition or genetic knockdown of eNOS leads to attenuated NO-derived pools of cGMP similar to that generated when sGC is inhibited directly[162]. Furthermore, z-disc localisation of PDE5 as described above is dependent on intact eNOS-NO-cGMP signalling[123, 162, 164].

Altogether, the evidence presented here demonstrates how different PDE isoforms control discrete, compartmentalised pools of cyclic nucleotides, which modulate ventricular myocyte Ca^{2+} handling and contractility. Alterations to this delicate and intricate system, as may occur in disease, can be devastating to cardiac function.

1.5 Heart failure

1.5.1 Pathophysiology

In 1888, Roy and Adami discussed an overstrain of the heart resulting from a requirement for the organ to perform beyond its means[167]. Today's definition of heart failure (HF) is fundamentally the same: the inability for the heart to provide adequate perfusion of peripheral tissues.

Systolic dysfunction, diastolic dysfunction or both may define heart failure. The former is characterised by impaired ventricular contractility leading to left ventricle enlargement, dilatation and hypertrophy, in order to preserve ejection fraction and cardiac output. Diastolic dysfuntion is associated with increased ventricular filling pressures due to reduced distensibility and wall compliance, ultimately leading to hypertrophy. Such pathophysiologies eventually result in an inability to maintain cardiac output, resulting in congestion and elevated blood pressures, thus fluid accumulation in the lungs, pericardium, abdomen and feet. Such haemodynamic and oedematous disorders are defining features of end stage heart failure.

1.5.2 Clinical cardiomyopathy

There are many forms of cardiomyopathy classified under heart failure; the main three are dilated (DCM), hypertrophic (HCM) and restrictive (RCM) cardiomyopathies. RCM is associated primarily with ventricular fibrosis leading to diastolic dysfunction; it is the least common form of cardiomyopathy. HCM is an autosomal dominant genetic disorder resulting in a hypertrophied, non-dilated left ventricle. DCM is the most common form of cardiomyopathy resulting in enlargement of one or both ventricles, both systolic and diastolic dysfunction and the characteristic symptoms of HF; it is the main focus of the current review.

Dilated cardiomyopathy is more common in men than women, non-specific to age or race. The prevalence of DCM in the general population is high although exact quantification is yet to be defined[168]. DCM is diagnosed in the clinic using echocardiography or MRI: ventricular dilatation and systolic dysfunction with or without mitral regurgitation. Other diagnostic indicators include cardiomegaly and signs of pulmonary oedema as revealed by chest radiograms, as well as a broad spectrum of electrocardiogram abnormalities including sinus tachycardia, atrio-ventricular arrhythmias, ST-T and Q wave changes[168]. Neurohumoral changes are another important characteristic of DCM, presenting as

dysfunctional sympathetic and renin-angiotensin system homeostasis[169]. These changes manifest in elevated systemic catecholamine[170] and natriuretic peptide[171] concentrations.

Heart failure is incurable and current therapies only aim to prevent disease progression and alleviate the symptoms of HF[172]. Some therapies globally target the cardiovascular system, such as anti-hypertensives and diuretics, which reduce cardiac loading. More invasive therapies such as cardiac resynchronisation therapy[173] and LV assist devices[174] aim to reverse remodel the failing ventricle. Other pharmacological therapies specifically target myocytes at the molecular level in order to reduce arrhythmias, e.g. amiodarone[175] and reduce the inotropic effects of elevated circulating catecholamines, e.g. β-blockers[170]. A strategy such as the latter seems counterintuitive in patients with poor inotropic reserve, however exacerbated β-AR stimulation results in uncontrolled myocardial contractility and a feed-forward spiral manifesting in further hypertrophy and dilatation. Many believe that the targeting of intracellular signalling pathways that control Ca^{2+} handling in cardiac myocytes is the future of heart failure therapy.

1.5.3 Dysfunctional calcium handling in heart failure

Calcium homeostasis governs excitation contraction coupling and is impaired in HF. Whether or not altered Ca^{2+} handling is the cause or consequence of the failing ventricle is the centre of much debate.

A force frequency relationship in ventricular tissue exists whereby increased frequency of stimulation results in increased force of contraction, which is in turn accompanied by an increase in SR Ca^{2+} content[5]. Such a relationship is lost in the failing myocardium of humans[176], guinea pigs[177] and rabbits, yet not in rodents[178]. This reduced contractile reserve in HF is associated with attenuated systolic Ca^{2+} transients[179, 180, 181]. As discussed the trigger for systolic Ca^{2+} release is peak $I_{Ca\text{-}L}$, and many studies have shown that $I_{Ca\text{-}L}$ is unchanged in HF[180-182], however those studying more severe cardiomyopathies have observed small changes in $I_{Ca\text{-}L}$[179, 183]. L-type Ca^{2+} channels are mainly located within t-tubules, which are disrupted in failing myocytes in both human and animal models[34, 184-187], which may suggest a reason for the reduction in $I_{Ca\text{-}L}$ observed in some models of HF.

Intracellular end-diastolic Ca^{2+} is increased in HF[188, 189], suggesting alterations to cytosolic Ca^{2+} removal mechanisms. The expression and activity of SERCA is reduced in human HF[190-192] as well as animal models[193], which is associated with a reduction in both PLN expression[191] and phosphorylation[194]. In the tachypaced sheep model of HF, Briston et al found no change in SERCA2A expression, however reported decreased SERCA activity

and increased protein phosphatase 1 expression associated with reduced PLN phosphorylation[179]. Further, failing ventricular myocytes in vitro regained contractile function and t-tubule density when overexpressing the SERCA2A gene[195, 196]. The failure of SERCA to sequester diastolic Ca^{2+} is concomitant with increased NCX activity[181], which will result in a decreased SR Ca^{2+} content and thus decrease the size of the systolic Ca^{2+} transient.

Intra-SR Ca^{2+} buffers such as calsequestrin are unchanged in HF[5], which suggests that any changes in SR loading will directly result in changes in SR content. The only route for Ca^{2+} release from the SR is through RyR Ca^{2+} release channels. Normal physiological function of RyR is determined by the accessory protein FKBP12.6, which is known to uncouple from RyR in HF[25] making RyR more susceptive to calcium induced calcium release from the SR. As t-tubules are lost in the failing ventricle this results in orphaned RyRs from dyads[197], which may further contribute to disorganised and dyssynchronous SR Ca^{2+} release. Together, increased Ca^{2+} leak from the SR will result in greater intracellular diastolic Ca^{2+}, reduced SR content, and a reduced Ca^{2+} transient, which will manifest in less contractile force.

1.5.4 Dysfunctional β-AR signalling in heart failure

Not only is Ca^{2+} handling itself altered in the failing ventricle, but the interplay of the signalling proteins which control Ca^{2+} cycling in response to β-AR stimulation are altered. The syndrome of HF manifests because of a pathophysiological spiral initiated by increased sympathetic drive, initially intended to improve cardiac function, but ultimately resulting in its demise (Figure 1.5). Exacerbated catecholaminergic drive is made worse by the downregulation of sympathoinhibitory reflexes such as the arterial baroreceptor reflex. Noradrenaline and adrenaline are synthesised and released from sympathetic nerves and chromaffin cells of the adrenal medulla in response to stimuli. In normal physiology these catecholamines are acutely released resulting in activation of β-adrenoreceptors and increased myocardial contractility, however in HF catecholamine production is uninhibited leading to chronic β-AR stimulation and failure[170] (Figure 1.5). Both sympathetic nerve terminals and chromaffin cells express plasmalemmal α- and β-adrenoreceptors, which when stimulated inhibit the release of noradrenaline and adrenaline as part of a negative feedback loop. GRKs are expressed in cardiac myocytes, sympathetic nerve terminals and chromaffin cells and inhibit adrenoreceptor signalling through β-arrestin mediated receptor internalisation[198, 199]. In HF GRKs are upregulated resulting in sympathetic nerve and

chromaffin cell α- and β-adrenoreceptor desensitisation, thus disinhibited noradrenaline and adrenaline release[200].

In the heart, several compensatory changes occur in order to protect it from excessive β-AR stimulation. Increased myocardial GRK expression and β-adrenoreceptor internalisation both aim to limit further β-AR signalling. In the normal myocardium the most abundant adrenoreceptor subtype is β_1[44]. In HF β_1 adrenoreceptors are downregulated[201] and may exhibit subtype switching to act more like β_2 [61]. Furthermore, β_2 relocate away from t-tubules and into the sarcolemmal crest[47], which most likely coincides with the loss in t-tubule density observed in failing myocytes[34, 184-187]. Such receptor density changes may promote β_2 dependent G_i signalling[147]. Not only does Gi signalling directly inhibit adenylyl cyclase, thus limiting further activation of downstream β-AR signalling pathways[202], but also activates PI3K-Akt cell survival pathways, which promote cardioprotection despite a loss of contractile reserve[203]. In combination with this, negatively inotropic β_3 adrenoreceptors are upregulated in human HF[68], which are not affected by GRK regulation to the same extent as β_1 and β_2 due to a lack of phosphorylation sites[97]. This highlights another compensatory mechanism whereby β_3 adrenoreceptors may promote negative inotropy in the presence of excessive β-AR stimulation. Napp et al have shown that β_3 and eNOS become uncoupled in HF[204], which may be compensatory to prevent negative inotropic β_3 signalling through NO.

Our laboratory recently reported dysfunctional ECC due to impaired β-AR signalling in a tachypaced sheep model of HF. Decreased PKA activity and concomitant reductions in PLN phosphorylation were observed in failing ventricular tissue, with reduced β-AR reserve in isolated myocytes[179]. Conversely, PKA hyperphosphorylation may accelerate the uncoupling of FKBP12.6 from RyR and increase Ca^{2+} leak from the SR[25]. Furthermore, β-adrenoreceptor antagonism resulted in restored RyR structure and function in human HF[205, 206]. Other studies have reported conflicting evidence for PKA activity in the failing ventricle. Such differences may represent the severity of HF: raised PKA activity and hyperphosphroylation of downstream targets most likely occurs in response to enhanced sympathetic drive, yet as HF progresses toward end-stage β-adrenoreceptor desensitisation and β-AR signalling impairment results in reduced PKA activity. In combination with these changes, AC generation of cAMP reduces along with altered PDE expression and activity. Decreased expression of cAMP-specific PDE3 and PDE4 in the failing ventricle has been observed in hamster[207], dogs[208], mouse[209], rat[136] and human[209]. Altered PDE expression will result in a loss of compartmentalisation and specificity of cAMP signalling,

which in conjunction with changed β-adrenoreceptor subtype density and localisation, will result in diffuse cytosolic cAMP generation[47] and uncontrolled activation of downstream targets. Reduced expression of PDE4D in particular has been linked to the hyperphosphorylation of RyR in the failing human heart[144]. Interestingly, increased expression and altered cellular localisation of cGMP-specific PDEs PDE1[210], PDE2[154], PDE5[123, 211] has been observed in both human and animal models of HF. Such changes are most likely a compensatory mechanism to counteract the negative inotropic influence of cGMP, whilst cAMP signalling is compromised. Together, this highlights the importance of compartmentalised and specific cyclic nucleotide signalling on myocyte Ca^{2+} handling, thus suggests manipulation of these altered pathways in the failing myocyte may provide therapeutic benefits for HF patients.

Altered signalling pathways in HF may be both caused by and the cause of pathology. Current therapies for HF include strategies that target β-AR signalling such as β-blockers. The lack of specificity of these agents highlights an importance for the targeting of selective downstream regulators of the β-AR signalling pathway in order to restore Ca^{2+} handling in the failing myocyte. Many studies have focused on the inhibition of phosphodiesterase enzymes as possible therapeutic targets in HF, however most have used small animal models of HF. It seems timely then that this PhD presents work exploring PDE inhibition as a potential therapy in a large animal model of HF, which more closely resembles human pathology.

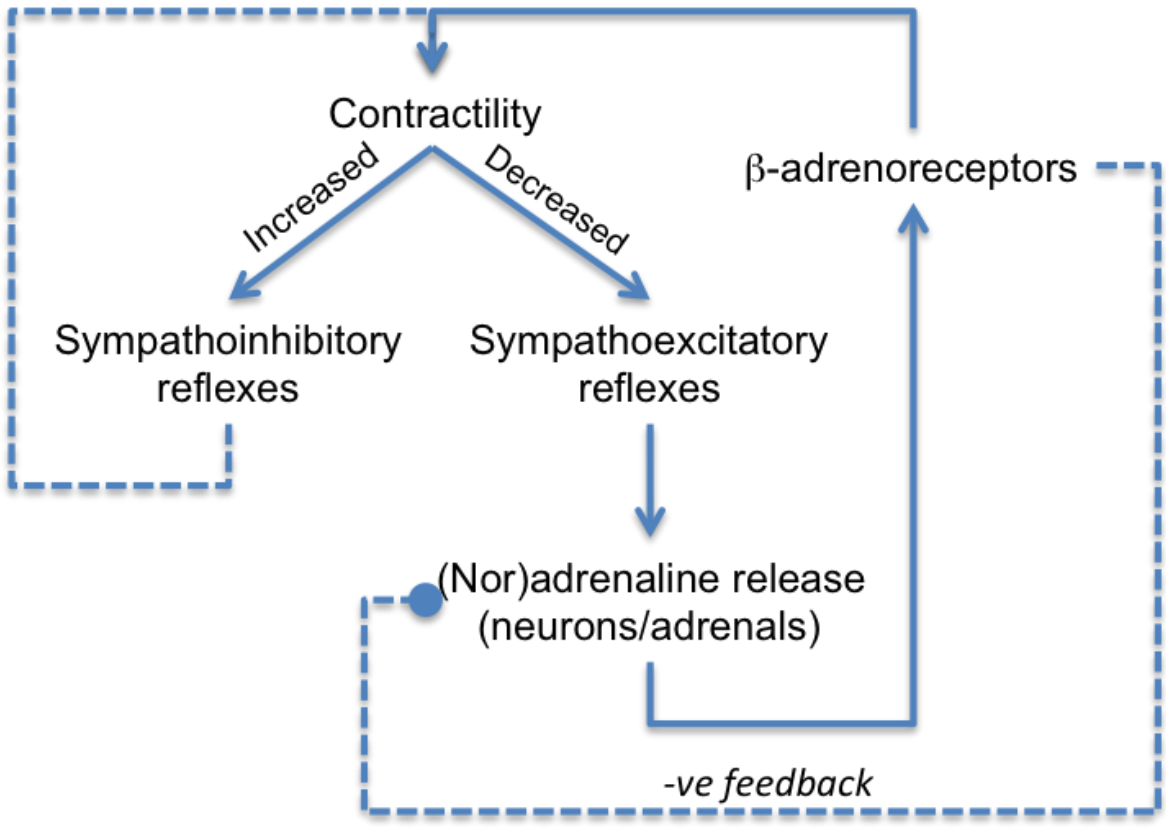

Figure 1.5 Changes in sympathetic regulation of cardiac contractility in heart failure

Dotted lines represent pathways desensitised in heart failure. Arrows represent activation, solid end represents inhibition.

1.6 Aims and objectives

The main aim of this PhD is to understand how PDE5 inhibition may be beneficial in HF.

Firstly, the role of PDE5 in the normal myocardium will be assessed using single cell electrophysiology. This is an area of the literature that until now has only included the rodent and small animal myocardium. The effect of PDE5 inhibition on ECC and its role in modulating cellular Ca^{2+} responses to β-AR stimulation will be explored. Intracellular Ca^{2+} will be measured by loading isolated ventricular myocytes with the fluorescent Ca^{2+} indicator Fura-2 and altered ionic currents will be measured using the voltage clamp whole cell patch technique.

A heart failure model will be generated in sheep using rapid ventricular pacing. The effect of PDE5 inhibition on ECC and β-AR responses will be assessed similarly as above in HF myocytes.

Following from these experiments exploring the acute effects of PDE5 inhibition in the normal and failing myocardium, a PDE5 inhibitor will be given chronically to HF sheep. In vivo techniques (echocardiography, electrocardiography, blood pressure measurements) will enable assessment of whole heart geometry, cardiovascular and electrophysiological properties of HF animals in order to determine whether PDE5 inhibition is beneficial to the failing myocardium.

Single cell electrophysiology and molecular biochemistry will be used to explore the mechanisms by which PDE5 inhibition modulates ECC and β-AR responsiveness in the failing myocardium.

Chapter 2

2 General Methods

2.1 Preparation and isolation of single cardiac myocytes

2.1.1 Animal use in scientific research

All animal experiments were performed in accordance with the Home Office Animal (Scientific Procedures) Act 1986. Mostly young adult female sheep (<18 months of age) were used in experimental methods, however some experiments employed the use of older female sheep (>8 years of age). Animal type used will be described where appropriate.

2.1.2 Animal euthanasia and heart removal

Animal sacrifice was facilitated by the cannulation of the cephalic vein using a 21G cannula. A saline flush and a 20ml bolus of heparin (10,000 units) were infused to prevent post-mortem blood clotting. Blood clots are both detrimental to proper perfusion and may influence the activity of the isolation enzymes due to the release of calcium from haematocyte lysis. The infusion of a lethal dose of pentobarbitone (Pentoject; 200mg/kg) resulted in a loss of consciousness and ultimately death, confirmed by the cessation of a blink reflex and palpable pulse. The convex nature of the sheep thorax requires an anterior midline incision through the skin layer and cutting through the ribs on either side of the sternum to allow the chest to be lifted away for heart isolation and removal.

2.1.3 Left ventricular enzymatic digestion

The heart was immediately bathed in cold isolation solution before being dissected along the coronary sulcus separating the ventricles from the atria. The left ventricle was perfused using a Langendorff preparation (Figure 2.1A) by cannulation of the anterior descending branch of the left coronary artery (Figure 2.1B) and sutured in place to occlude the cut ends of both the artery and vein. The left ventricle was initially perfused with calcium free isolation solution for ten minutes *(*Table 1*)* (12ml/min) in order to wash out the vascular bed and ensure a calcium free extracellular environment for the introduction of the digestive enzymes. A mixture of collagenase (Type IV; Worthington Biochemical Corporation, NJ, USA) and protease (Type XIV; Worthington Biochemical Corporation, NJ, USA) enzymes was then added to the isolation solution to digest the tissue. Perfusion with enzyme varied in length of time depending on the size of the heart/animal, usually between 5-7 minutes. Upon assessment of adequate tissue digestion the enzyme was washed out for 20 minutes using a low-calcium, taurine containing solution (Table 1), this

ensured minimal cytotoxicity associated with calcium overload[212] and oxidative stress[213], whilst slowly reintroducing calcium to the myocytes.

2.1.4 Isolation of single cardiac myocytes

Mid-myocardial tissue strips were excised from the remaining digested tissue and homogenised gently in taurine solution. The supernatant was filtered through a 200µm nylon mesh and the remaining tissue resuspended in taurine solution. This was repeated nine more times to ensure maximal enzyme washout and myocyte isolation. After being allowed to settle, myocyte cell pellets were resuspended in a 50:50 mix of taurine and normal tyrode's (Table 2) solutions.

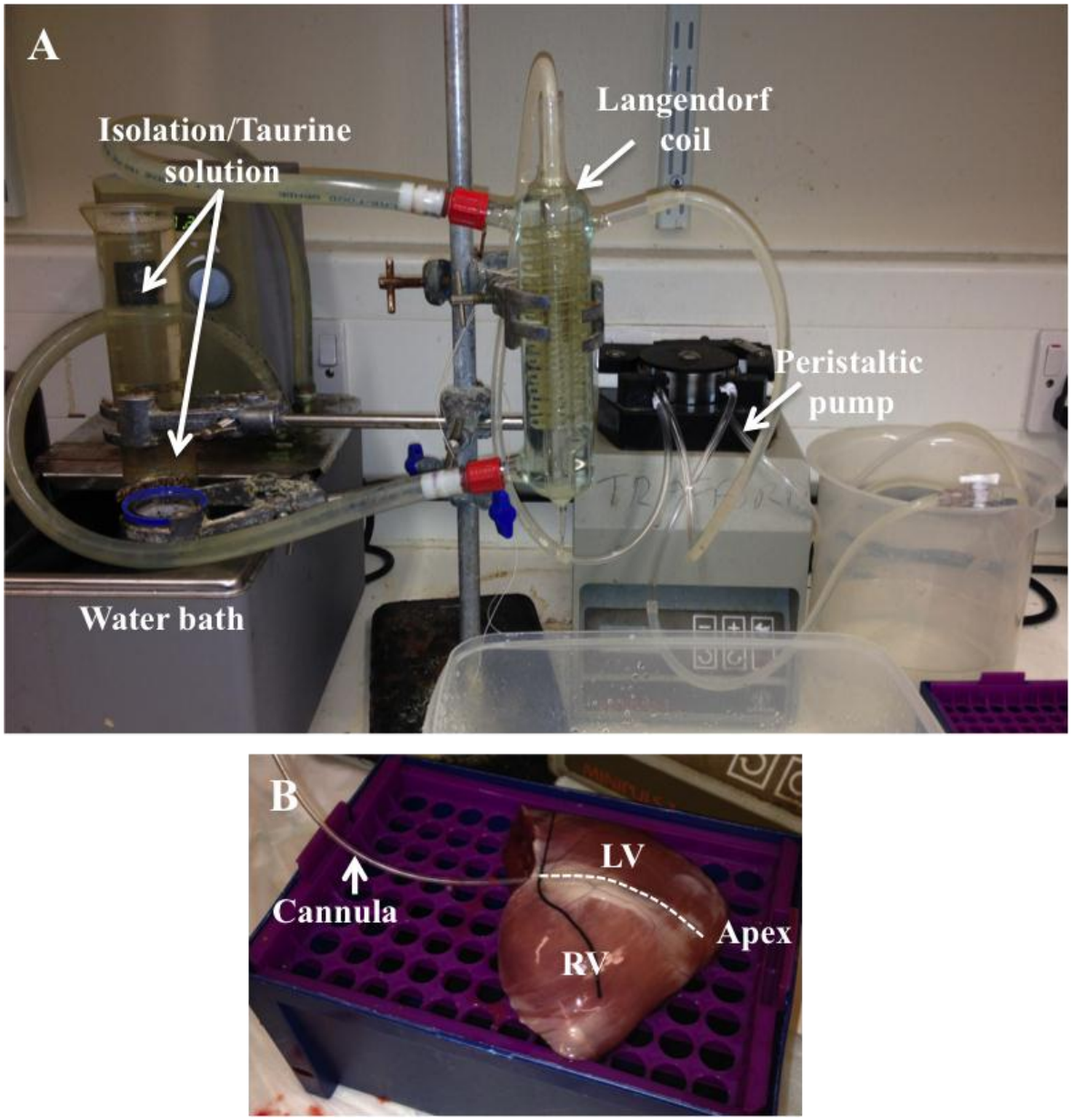

Figure 2.1 Cell isolation setup and perfusion apparatus

A) Langendorff apparatus showing the heated (37.4 ^{o}C) column through which the respective solutions pass, as driven by the peristaltic pump. (B) Solutions pass through the cannula attached to the bottom of the Langendorff coil into the left anterior descending coronary artery (dotted line) to perfuse the left ventricle (LV). The right ventricle (RV) and apex are labelled for orientation purposes.

Substance	Concentration (mM)
NaCl	134
HEPES	10
Na_2HPO_2	1.2
KCl	4
$MgSO_4$	1.2
Glucose	11
2,3-butanedione monoxime	10
Bovine Serum Albumin	0.5
$CaCl_2$	0.1
Taurine	50

Table 1. Cell isolation solutions

Standard constituents for Ca^{2+} free isolation solution above the line, the addition of the ingredients below the line produced taurine solution. Solution was titrated with NaOH to pH 7.34 at room temperature.

Substance	Concentration (mM)
NaCl	140
HEPES	10
$MgCl_2$	1
KCl	4
$CaCl_2$	1.8
Glucose	10
Probenicid	2
4-aminopyridine	5
$BaCl_2$	0.1
DIDS	0.1

Table 2. Normal Tyrode's solution and additives

Above the dark line are standard constituents of Normal Tyrode's, below the dark line are substrates used in different experimental solutions. Solutions were titrated with NaOH or HCl to pH 7.34 at room temperature.

2.2 Electrophysiological recordings and calcium imaging

2.2.1 Electrophysiological equipment setup

Isolated ventricular myocytes were allowed to settle on glass cover slips in a chamber mounted atop the objective (40x/1.3, Nikon) lens of an inverted light microscope (Nikon eclipse Ti). A heated (37^{o}C) solution changer (Temp. Controller 2 bip, NBD) provided the input of variable superfusion solutions, and chamber volume maintained constant through the use of vacuum powered suction. A reference electrode consisting of an Ag/AgCl pellet was placed in the corner of the cell bath chamber. A recording electrode was made by the insertion of a fine Ag/AgCl wire inside a pipette solution containing micro-pipette (*see 2.2.3*). The micro-pipette was lowered onto the surface of a single myocyte using an electronic micromanipulator (Scientifica, UK) to complete a continuous electrical circuit with the reference electrode, recorded through the head stage and amplifier (Axopatch 200B, Axon Instruments), converted to a digital signal and relayed to a computer for online data acquisition (Figure 2.2).

2.2.2 Calcium imaging equipment and setup

Using the video camera and monitor setup a single isolated myocyte was centred and the field of view restricted in order to minimise background signal. The cell was illuminated with a xenon light source and monochromator and emitted light passed through a dichroic mirror and recorded by a photomultiplier/amplifier (Optoscan, Cairn) and acquired in real time using the pClamp software (Molecular Devices) (Figure 2.2).

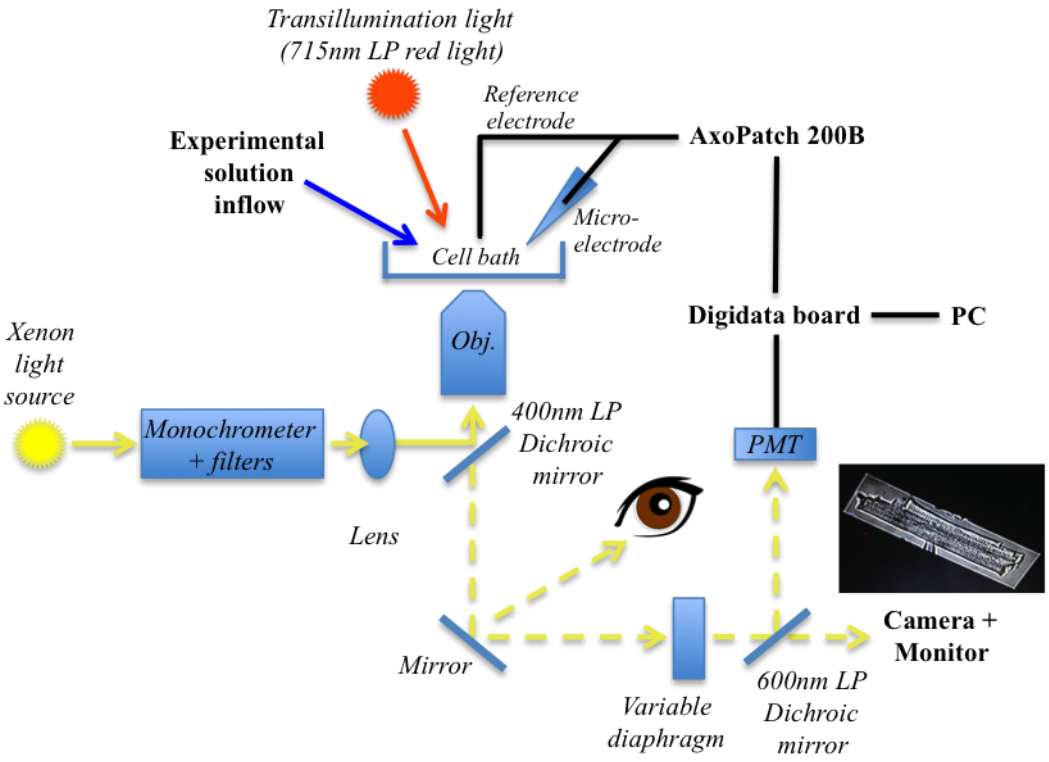

Figure 2.2 Microscope setup for electrophysiological and calcium measurements

Cells are mounted on a glass slide above an oil-immersion objective lens (Obj.) and superfused by experimental solutions warmed to 37^{o}C. Electrophysiological recordings are achieved by the creation of an electrical circuit between the reference electrode immersed within the cell bath, the microelectode and the patch clamp amplifier (AxoPatch 200B). Digital signals are output to the digidata board and to a computer (PC) for online recording/analysis. Calcium imaging requires a xenon light source, which emits through a monochrometer, which switches the wavelength of light between 340, 355 and 380nm. This is focused onto a 400nm long pass (LP) dichroic mirror and excites the cells in the bath. Excited fluorophores emit at 510nm, which passes through the dichroic mirror and reflected to the eye or passes through a variable diaphragm to restrict the level of background noise (the insert patched cell as visible on the monitor). Light excites the photomultiplier tube (PMT), which converts an optical signal into a digital one, decoded by the digidata board and sent to the PC.

2.2.3 Cytosolic calcium indicators

Changes in intracellular calcium were imaged using the fluorescent indicator Fura-2 pentapotassium (K_5) salt (100µM; Invitrogen), a cell impermeant dye loaded into the cell through the micro-pipette. Fura-2 has a single emission spectrum at a wavelength of 510nm, with dual absorption spectra: 340nm and 380nm. Calcium binding results in a changing of the emission spectrum, when excited at 340nm it increases and at 380 nm it decreases. Rapid switching of external light from a common source between wavelengths of 340 nm and 380 nm and recording the resultant alterations in emission may monitor changes in cytosolic calcium. The ratio of the two absorption signals (Fluorescence $(F)_{340}/F_{380}$), each dependent on Ca^{2+} concentration, will not be dependent on indicator concentration. This highlights the main advantage in the use of a ratiometric indicator as it is insensitive to unequal cell loading and photobleaching, which may occur over time during an experiment. In order to ensure signal integrity a third absorption spectrum wavelength of 355 nm was also measured. This wavelength falls between 340 nm and 380 nm and is termed the isosbestic wavelength as its absorbance does not change relative to changes in Ca^{2+}.

Due to a fundamental setup issue some experiments were associated with a compromised F_{380} signal, the F_{340} signal however remained consistent throughout all experiments. In order to prevent this manifesting into a problem with calcium signal analysis it was decided that the isosbestic wavelength 355nm would be used in the calculated ratio with F_{340}. It is appreciated that a ratio signal calculated from F_{340}/F_{355} will generate a smaller ratio signal than a F_{340}/F_{380} ratio however both show relative changes in Ca^{2+}.

2.2.4 Whole Cell Voltage Clamp

Voltage clamping is a useful technique for the measurement of single channel ionic currents enabled by controlling membrane voltage. A patch clamp amplifier (Axopatch 2B, Axon Instruments) was used to which a recording electrode and reference electrode were connected. An electrical circuit was made possible by using micro-pipettes, consisting of a borosilicate glass capillary tube (Harvard apparatus) pulled in a two stage process using a microelectrode puller (HEKA Electronik). The first stage involved heating the glass and gently stretching it over a distance of between 7-10mm. The second stage involved the breaking of this stretched portion of glass, producing two sharp-ended pipettes, which facilitate a circuit resistance of 2-3MΩ. The Ag/AgCl electrode was then inserted within this pipette filled with a Ca^{2+}-EGTA buffered solution that reflects the intracellular ionic environment (Table 3).

Substance	Concentration (mM)
CsCl	118
HEPES	10
$MgCl_2$	4
$CaCl_2$	0.28
Phosphocreatine	3
Na_2ATP	3.1
Na_2GTP	0.42
CsEGTA	0.02

Table 3. cGMP containing, low-EGTA Pipette Solution

Titrated with CsOH to pH 7.2 at room temperature.

The micro-electrode was carefully lowered onto the surface of the myocyte and gentle suction applied to attach a section of membrane to the tip of the pipette forming a high resistance 'giga-seal'. This electrical seal limits background noise and allows the patch of membrane to be voltage clamped. Once sealed the solution was switched from normal tyrode's solution to an experimental solution (Table 2, experiment depending). In whole cell patch clamping a brief pulse of suction is used to rupture the portion of membrane beneath the patch pipette in order to expose the whole cell contents to the microelectrode.

In discontinuous voltage clamping the recording electrode feeds forward the recorded membrane potential into the patch amplifier. An external source outputs a voltage command to the amplifier; in this instance a step-wise -60mV to +10mV voltage command was used. The voltage command, minus the membrane potential, enables the amplifier to 'hold' the cell at the defined potential (holding potential) by injecting a current equal and

opposite to cellular ionic currents. This allows accurate reproduction and recording of the currents flowing across the cell membrane. Corrections were made to compensate for series resistance and capacitance (70-80%) generated by the electrode in order to accurately reproduce ionic current measurement.

Simulation protocols were used in order to investigate the differences in EC-coupling parameters in electrically paced myocytes. Cells were stimulated at a frequency of 0.5 Hz using a ramp and step protocol. As shown in Figure 2.3 a 20 ms voltage ramp from -60 mV to -40 mV followed by a 10 ms hold was used to ensure full inactivation of voltage gated sodium channels. This was immediately followed by a voltage step to +10 mV and held for 100 ms before returning to -60 mV. Along with other ion channel blockers present in the superfusion solution, as described above, this facilitated selective investigation of voltage gated Ca^{2+} current.

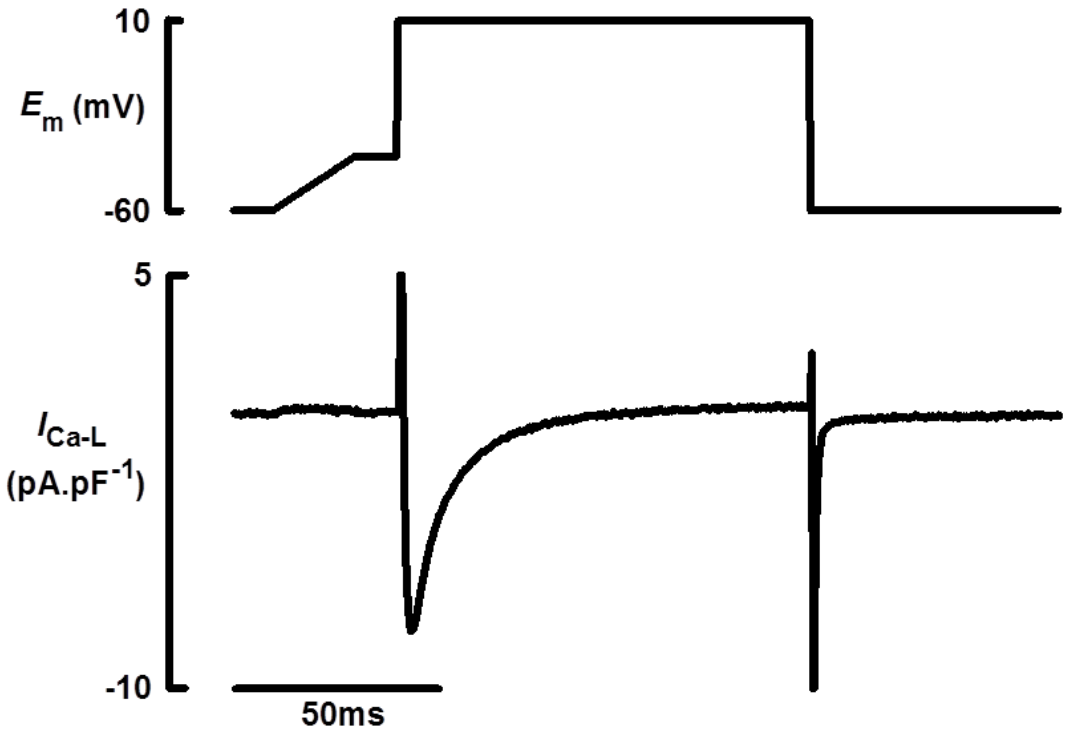

Figure 2.3 Membrane voltage protocol and associated inward $I_{Ca\text{-}L}$

The upper trace shows the voltage command: voltage from ramped from a holding potential of -60mV and held at -40mV, before being stepped to +10mV. Voltage step results in an inward $I_{Ca\text{-}L}$ as represented in the lower trace, recorded from a normal young sheep ventricular mycoyte. The voltage was held at 10mV for 100ms, in which time $I_{Ca\text{-}L}$ decays fully. $I_{Ca\text{-}L}$ is flanked by capacitance spikes.

*2.2.5 **Data analysis and interpretation***

2.2.5.1 The L-type Ca^{2+} current

Raw calcium currents (nA) were recorded (2.5kHz sampling frequency) and analysed using pClamp/Clampfit analysis software (Axon Instruments). Data sampling was obtained by averaging ten sweeps during steady state. From these average traces three useful parameters can be determined Figure 2.4: (1) peak current, which represents the trigger for intracellular Ca^{2+} release from the SR, (2) the integral of the current (the area underneath the curve of the recorded $I_{Ca\text{-}L}$) which is a measure of the total Ca^{2+} entering the cell and (3) the rate of inactivation of $I_{Ca\text{-}L}$, which describes the speed with which L-type Ca^{2+} channels close.

$I_{Ca\text{-}L}$ is expressed as a function of cell size and is therefore normalized to the recorded cellular capacitance, i.e. current (pA) divided by capacitance (pF) gives us the units for $I_{Ca\text{-}L}$: $pA.pF^{-1}$. In order to measure peak $I_{Ca\text{-}L}$, ten sweeps of steady state $I_{Ca\text{-}L}$ recording were averaged within Clampfit to give an averaged raw trace as shown in Figure 2.4A. The vertical lines represent the analysis 'cursors', which were used to select the areas of interest. Cursors 1 and 2 were positioned before and after the negative peak of $I_{Ca\text{-}L}$ trace as shown. Cursors 3 and 4 were positioned after the $I_{Ca\text{-}L}$ had inactivated back to baseline. This allowed the measurement of the maximum deflection of the $I_{Ca\text{-}L}$ to be calculated based on the actual baseline to which the $I_{Ca\text{-}L}$ decays.

The integral of the current was quantified in a similar method as described above. The analysis cursors were positioned exactly as described above, which enabled the entire area between cursor 1 and 2 to be quantified as a function of the baseline (determined by cursors 3 and 4), as shown by the hatched area in Figure 2.4Ai. The integral of $I_{Ca\text{-}L}$ was calculated as a function of $I_{Ca\text{-}L}$ (pA) over time (s), thus $nA.ms^{-1}$. This value can be used to calculate a more useful characteristic of $I_{Ca\text{-}L}$, the amount of Ca^{2+} entering the cell per beat ($\mu moles.L^{-1}$). This was calculated using the following formula:

$$\text{Calculated } Ca^{2+} (\mu moles.L^{-1}) = \mu moles \text{ of calcium} \times 1x10^{12} / \text{cell volume (pL)}$$

Equation 1

The concentration of calcium ions is calculated by dividing the calculated $I_{Ca\text{-}L}$ integral (as above) by two, as Ca^{2+} is divalent, and dividing by Faraday's constant ($9.65x10^{4}$, in order to give the magnitude of electric charge per mole of calcium. The cell volume is calculated

as the cell capacitance multiplied by 5.39 $pF.pL^{-1}$, which has previously been used in our lab as the volume correction for an ovine ventricular myocyte[214].

Finally, the rate of $I_{Ca\text{-}L}$ inactivation was calculated by fitting a double exponential to the decay phase of the averaged $I_{Ca\text{-}L}$ trace. As shown in Figure 2.4Aii the analysis cursors were repositioned to allow for the measurement the decay phase between cursors 1 and 2, and normalized to the calculated baseline between cursors 3 and 4. The double exponential fit of this curve gives two values of tau, which represents the time over which the decay occurs. The reciprocal of these values therefore provides rate constants for the time for decay of the $I_{Ca\text{-}L}$. A double exponential is used because the inactivation phase of the L-type Ca^{2+} channel is not easily fit using a single fit curve. This in turn reflects the two phases of $I_{Ca\text{-}L}$ inactivation: a fast phase and a slow phase. In terms of $I_{Ca\text{-}L}$ physiology there exists two mechanisms of $I_{Ca\text{-}L}$ inactivation: (1) a calcium-dependent mechanism, whereby Ca^{2+} negatively feeds-back to inhibit $I_{Ca\text{-}L}$ and (2) a voltage-dependent mechanism, whereby membrane voltage changes the conformation of the channel thus inhibiting $I_{Ca\text{-}L}$. In terms of the $I_{Ca\text{-}L}$ inactivation Ca^{2+} dependent inactivation generally occurs faster than voltage dependent inactivation and so for the purposes of this thesis the two tau values (rate constants) presented for $I_{Ca\text{-}L}$ inactivation will be representative of these different mechanisms. It should be noted that as the stimulated cells were twitching, the measure of $I_{Ca\text{-}L}$ inactivation might be influenced by an inward Na^{+}-Ca^{2+} current, and thus provides a limitation to the accurate measurement of $I_{Ca\text{-}L}$ inactivation.

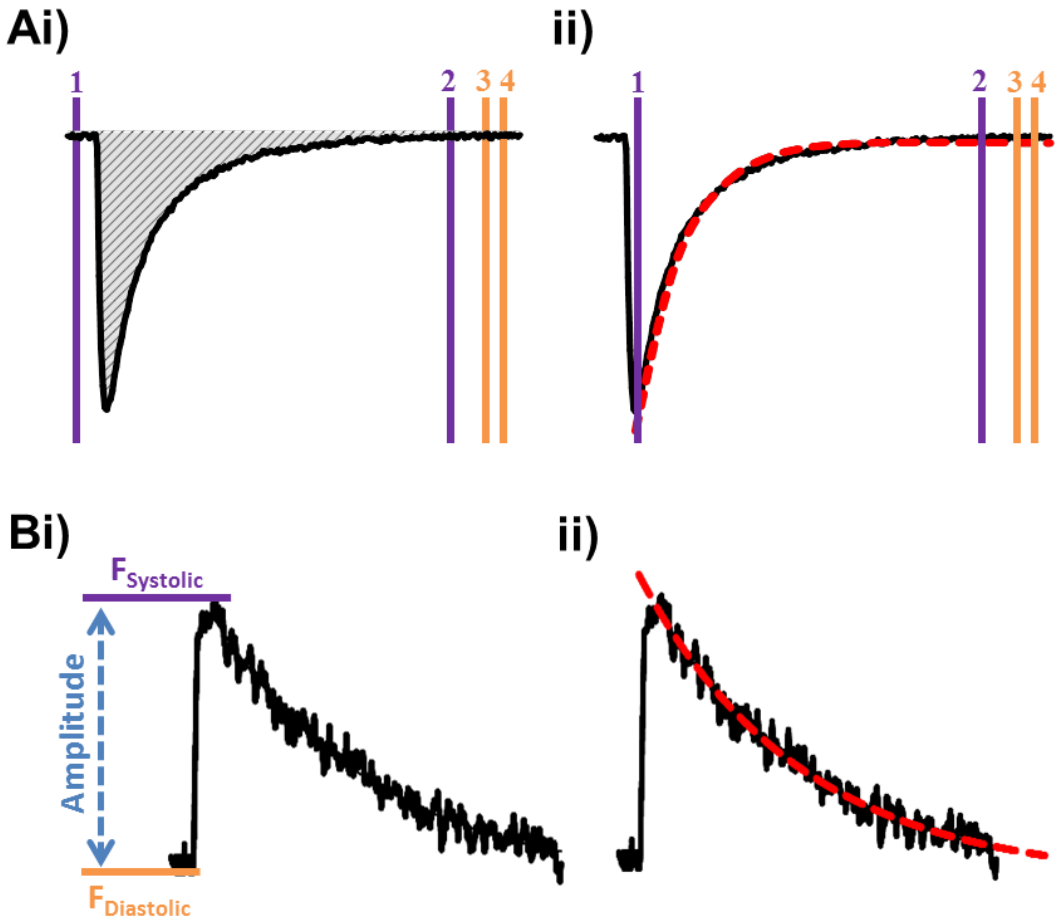

Figure 2.4 Analysis of $I_{Ca\text{-}L}$ and Ca^{2+} transient

(Ai) Analysis of Peak $I_{Ca\text{-}L}$ and Ca^{2+} influx. Analysis cursors 1 and 2 are positioned before and after $I_{Ca\text{-}L}$ deflection to determine the area of interest, cursors 3 and 4 are used to determine the baseline. Peak current is determined as the greatest point of deflection subtracting away the baseline, Ca^{2+} influx is calculated from the integral, the area underneath the $I_{Ca\text{-}L}$, shaded. (ii) Analysis of the rate of $I_{Ca\text{-}L}$ inactivation. Analysis cursor 1 is positioned just before peak $I_{Ca\text{-}L}$ and cursor 2 positioned at the point where $I_{Ca\text{-}L}$ has decayed fully, cursors 3 and 4 determine baseline. A double exponential is fitted to the decay to give time constants, of which the reciprocal is taken to calculate the rate constant of inactivation. (Bi) Analysis of Ca^{2+} transient amplitude. Fluorescence at diastole ($F_{Diastolic}$) is subtracted from the fluorescence at systole ($F_{Systole}$) to give the amplitude of the Ca^{2+} transient. (B) Analysis of the rate of Ca^{2+} transient decay. A single exponential (red line) is fitted to the decay of the transient to give a tau value, the reciprocal of which gives a value for the rate constant of decay.

2.2.5.2 Systolic Ca^{2+} transient

Changes in intracellular Ca^{2+} were recorded using the ratiometric calcium indicator Fura-2 as described above. Loading the cell with indicator via the patch pipette has the advantage that there is limited fluorescence in the surrounding bath solution/nearby cells, however in order to prevent anomalous results a baseline fluorescence level was recorded in the form of a no cell ($F_{no\ cell}$), which was subtracted away from both the F_{340} and F_{355} signals used in the final ratio:

$$R_{340/355} = \frac{F_{340} - F_{no\ cell}}{F_{355} - F_{no\ cell}}$$

Equation 2

The calcium transient is the systolic release of calcium from the SR. An average of ten steady state sweeps was exported using an 'in house' visual basic programme designed to take each ratio point recorded and corrected for background fluorescence (as described above). Analysis of the Ca^{2+} transient is performed as described in Figure 2.4B. The peak of the systolic Ca^{2+} transient is described as the transient amplitude and was calculated in Microsoft Excel using an average baseline ratio, $F_{Diastolic}$, subtracted from an average of Ca^{2+} transient peak ratio, $F_{Systolic}$.

The decay of the calcium transient represents the rate at which calcium is sequestered back into the SR and extruded from the cell during diastole. The averaged Ca^{2+} transient was drawn in Clampfit and, similar to the analysis of $I_{Ca\text{-}L}$ inactivation, two analysis cursors were used to highlight the start and end of the transient decay phase. A single exponential was fitted was fitted to this curve and the reciprocal of the tau value was then used to calculate the rate constant for Ca^{2+} transient decay (Figure 2.4Bii).

2.2.5.3 Sarcoplasmic reticulum Ca^{2+} content

SR Ca^{2+} content is determined by the application of caffeine (10mM) to an unstimulated, voltage clamped myocyte[215]. High dose caffeine massively increases the open probability of RyR, which maintains the channel in an open configuration thus negating any action of SERCA. Caffeine thus empties the SR and generates a large caffeine evoked Ca^{2+} transient. In order to maintain Ca^{2+} flux balance, cytosolic Ca^{2+} must leave the cell through NCX and to some extent PMCA. Due to the electrogenic nature of NCX, as Ca^{2+} fluxes out of the cell, Na^{+} moves in, which is recorded as an inward current (I_{NCX}). The integral of I_{NCX} is directly proportional to the amount of Ca^{2+} extruded from the cell and thus provides an accurate measurement of the amount of Ca^{2+} stored within the SR.

The integral of I_{NCX} is calculated similarly to the integral of $I_{Ca\text{-}L}$. Using analysis cursors the baseline is measured and subtracted from the integral of I_{NCX}. PMCA contributes approximately 5% of $[Ca^{2+}]_i$ extrusion in the sheep and thus in order to determine the precise amount of Ca^{2+} removed by NCX this must be corrected for. Furthermore it has been shown that the contribution of Ca^{2+} removal by PMCA varies slightly with age, thus for cells from young sheep I_{NCX} integral is multiplied by 1.41 and for old sheep I_{NCX} integral is multiplied by 1.49[216]. In order to describe the level of charge accumulation as a Ca^{2+} content the resultant value was divided by Faraday's constant, and normalized to cell volume (as with Ca^{2+} influx) to give a final calculation of SR Ca^{2+} content in μmole/L. A representative caffeine evoked Ca^{2+} transient, I_{NCX} and integral are shown in Figure 3.8.

2.2.5.4 Statistics

Data analysis was performed using SigmaPlot (Systat Software, Inc) and values given as mean ± SEM. Statistical significance was determined in paired data containing two data sets using a paired Student's t-test. If three or more paired data sets were being compared then a one-way repeated measures analysis of variance (ANOVA) and a Holm-Sidak post-hoc test was used, which enables pairwise multiple comparisons. Unpaired data was compared using a Student's t-test for two groups, or a one-/two-way ANOVA for three or more comparisons. Significance was determined as $p<0.05$.

Chapter 3

3 The effect of phosphodiesterase 5 inhibition on calcium handling in normal ovine cardiac myocytes

3.1 Introduction

The movement of Ca^{2+} into and within a ventricular myocyte determines the force of myocardial contraction. In vivo the sympathetic nervous system modulates excitation-contraction coupling, the mechanism that governs myocyte Ca^{2+} flux, through the activation of sarcolemmal β-adrenoreceptors. The stimulation of β_1 and β_2 adrenoreceptors results in an intracellular signalling cascade, governed by cAMP, resulting in the PKA-dependent phosphorylation of the L-type Ca^{2+} channel, PLN and TnI. This results in positive inotropy: a stronger myocardial contraction, and lusitropy: a faster rate of relaxation.

There is an important emphasis on the control of cAMP availability, as uncontrolled PKA-dependent phosphorylation would be detrimental to diastolic filling and may result in increased prominence of arrhythmias[217]. Cyclic AMP signalling is therefore controlled through selective hydrolysis by PDE2, PDE3 and PDE4, which maintain cAMP-PKA signalling in discrete sarcoplasmic compartments within the cardiac myocyte[153].

Negative inotropy is facilitated by cGMP, by increasing PDE2-stimulated cAMP hydrolysis[218], and by activating PKG, which decreases the L-type Ca^{2+} current ($I_{Ca\text{-}L}$)[86]. Cyclic GMP is generated through activation of β_3 adrenoreceptors[68, 219-221] coupled to eNOS[85] and is compartmentalised through selective hydrolysis by PDE5[84]. Immunolocalisation studies in isolated myocytes have shown that PDE5 colocalises with α-actinin, which corresponds to localisation at the myocardial z-bands in close proximity to t-tubules[162]. L-type Ca^{2+} channels, as well as β-adrenoreceptors and AKAPs are also found within these compartments, which highlights possible interaction between these two cyclic nucleotide-dependent signalling pathways.

Most studies investigating the role of cGMP and PDE5 in ventricular myocytes have used rodent and other small animal species, which are characteristically very different from human cardiac physiology. The present study sought to elucidate the role of PDE5 in a large animal model; sheep cardiac myocytes.

3.2 Aims

The principal aims of this chapter are as follows:

- To investigate how cGMP is controlled under steady state conditions in sheep ventricular myocytes and whether it can modulate steady state Ca^{2+} handling.
- To investigate whether cGMP exerts its effects, if any, via a PKG-dependent mechanism.
- To investigate whether cGMP modulates inotropic responses to β-AR stimulation?

3.3 Results

3.3.1 The effect of PDE5 inhibition on steady state Ca^{2+} handling

PDE5 controls specific pools of cGMP in cardiac myocytes. Several studies that have inhibited PDE5 have reported conflicting evidence for its effect on myocyte Ca^{2+} handling [99-101, 158, 222]. The present study sought to test the effect of PDE5 inhibition on Ca^{2+} handling in sheep cardiac mycoytes.

3.3.1.1 L-type Ca^{2+} current.

The first set of experiments sought to test the effect of PDE5 inhibition on $I_{Ca\text{-}L}$. Ventricular myocytes were stimulated under voltage clamp control from -40mV to +10mV for 100ms, at 0.5Hz, at 37°C. Sarcolemmal depolarisation results in an inward Ca^{2+} current as shown in Figure 3.1Ai. In normal sheep myocytes (cell capacitance = 146.7±17 pF) peak $I_{Ca\text{-}L}$ was 7.09±0.69 pA.pF^{-1}. This was associated with 2.07±0.2 μmoles.L^{-1} of Ca^{2+} entering the cell per beat. Figure 3.1B shows the acute application of the selective PDE5 inhibitor sildenafil (1μM, Sigma) for 3 minutes reduced peak $I_{Ca\text{-}L}$ by 39±13% (Figure 3.1Aii, 4.32±0.8 pA.pF^{-1}) and decreased the proportion of Ca^{2+} entering the cell, by 17±13% (Figure 3.1Aiii, 1.72±0.2 μmoles.L^{-1}).

In order to test whether PDE5 inhibition affected the rate of decay of $I_{Ca\text{-}L}$ a double exponential was fitted to the inactivation curve of $I_{Ca\text{-}L}$ as described (section 2.2.5). Figure 3.1Ci shows representative $I_{Ca\text{-}L}$ traces with the $I_{Ca\text{-}L}$ observed under PDE5 inhibition normalised to the peak of the $I_{Ca\text{-}L}$ observed in control steady state, in order to emphasise any changes in the decay phase of the currents recorded. As shown by the summary data for the rate of the voltage dependent inactivation of $I_{Ca\text{-}L}$ in Figure 3.1Cii, PDE5 inhibition slowed the rate of $I_{Ca\text{-}L}$ inactivation by 28±10%: from control rate 61±3 s^{-1} to 44±6 s^{-1}. The rate of Ca^{2+}-dependent inactivation also showed a tendency to be slowed by PDE5 inhibition, however this change did not achieve significance (-23±10%; control 226±16 s^{-1} to 173±19 s^{-1}, *p=0.09*).

The time course for the effect of PDE5 inhibition on peak $I_{Ca\text{-}L}$, shown in Figure 3.1B, revealed that there was a lag period between the exposure of the cell to sildenafil and the inhibitory effect on $I_{Ca\text{-}L}$. Figure 3.2A shows the sildenafil-induced percentage decrease in $I_{Ca\text{-}L}$ across the full 3 minutes of PDE5 inhibition. Baseline $I_{Ca\text{-}L}$ was determined as the 10 sweeps prior to the onset of sildenafil application. Mean data taken at thirty-second intervals for the full 3-minute duration of sildenafil application is shown in the histogram Figure 3.2B. The effects of PDE5 inhibition as compared with baseline $I_{Ca\text{-}L}$ are not

observed until at least 90 seconds after the application of sildenafil. Furthermore, the degree of $I_{Ca\text{-}L}$ inhibition shows that the maximal effect of PDE5 inhibition of $I_{Ca\text{-}L}$, approximately 30% decrease occurs within the 3 minutes of sildenafil application

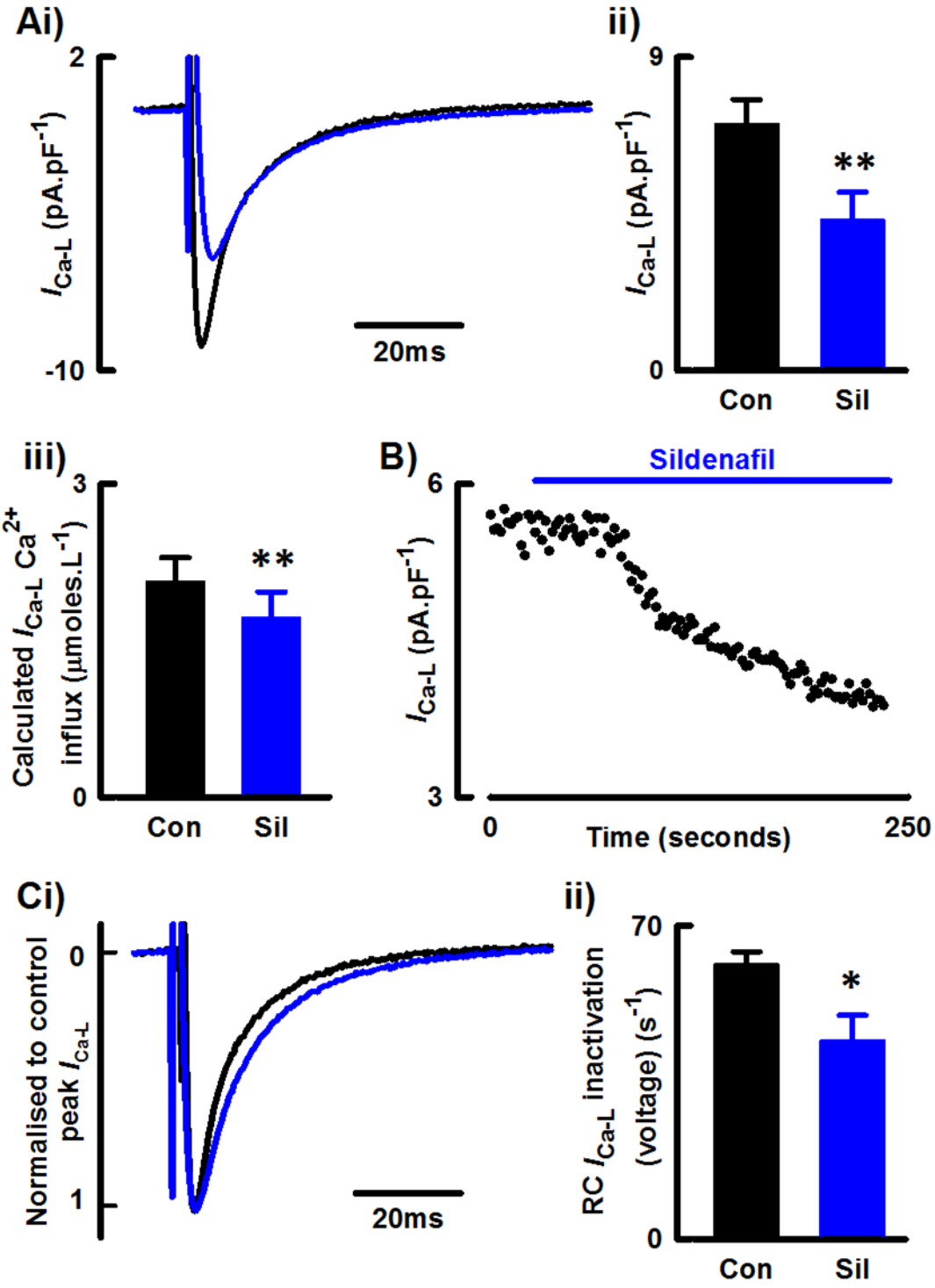

Figure 3.1 The effect of PDE5 inhibition on $I_{Ca\text{-}L}$

*(Ai) Typical $I_{Ca\text{-}L}$ recording from control sheep myocytes with summary data showing (ii) peak $I_{Ca\text{-}L}$ and (iii) calculated Ca^{2+} influx before (con, black) and after selective PDE5 inhibition with 1µM sildenafil (sil, blue). (B) Time course for the effect on $I_{Ca\text{-}L}$ of PDE5 inhibition. (Ci) $I_{Ca\text{-}L}$ normalised to control with sildenafil and (ii) summary data for change in $I_{Ca\text{-}L}$ inactivation. Mean ± SEM, differences compared using paired Student's t-test, * p<0.05, ** p<0.001. n=9 cells/ 5 animals.*

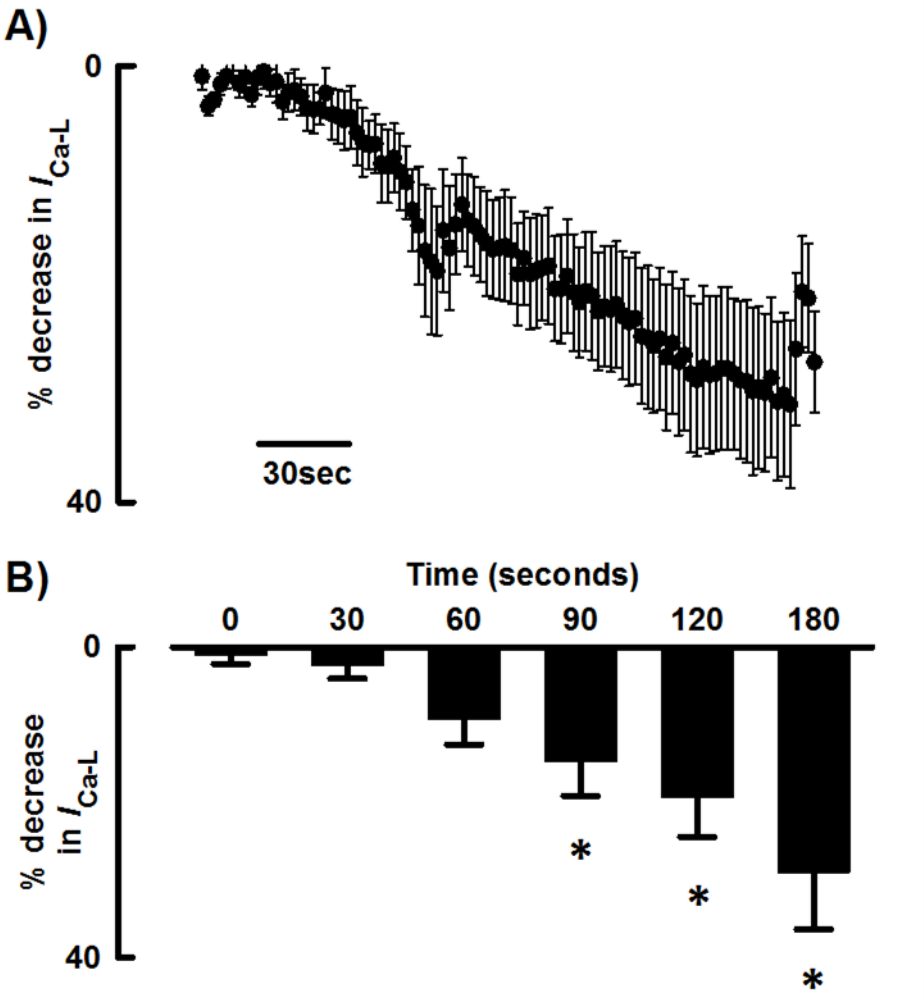

Figure 3.2 The effect of PDE5 inhibition on $I_{Ca\text{-}L}$ over time.

*(A) Mean ± SEM for the percentage decrease in $I_{Ca\text{-}L}$ in response to PDE5 inhibition with 1μM sildenafil, over time. (B) Mean ± SEM at 30 second intervals for this effect. Differences compared using one-way repeated measures ANOVA, * $p<0.05$. n=8*

3.3.1.2 Dose response for the sildenafil

Sildenafil used at high concentrations is considered to have inhibitory effects on other PDE isoforms (as reviewed[223]), especially the cGMP-hydrolysing PDE1[224]. The dose response curve in Figure 3.3 shows the dose dependent inhibition of $I_{Ca\text{-}L}$ by sildenafil at increasing concentrations up to 1 μM. The figure shows changes relative to control, therefore is given as a percentage change for each concentration. Sildenafil decreased peak $I_{Ca\text{-}L}$ at 0.03 μM by 46±5%. Similar decreases in peak $I_{Ca\text{-}L}$ were also observed at 0.3 μM and 1 μM sildenafil, 50±11% and 47±8% respectively. Together this suggests that even though sildenafil may inhibit other PDE isoforms the effect on $I_{Ca\text{-}L}$ alone is similarly negatively inotropic between 300 nM and 1 μM.

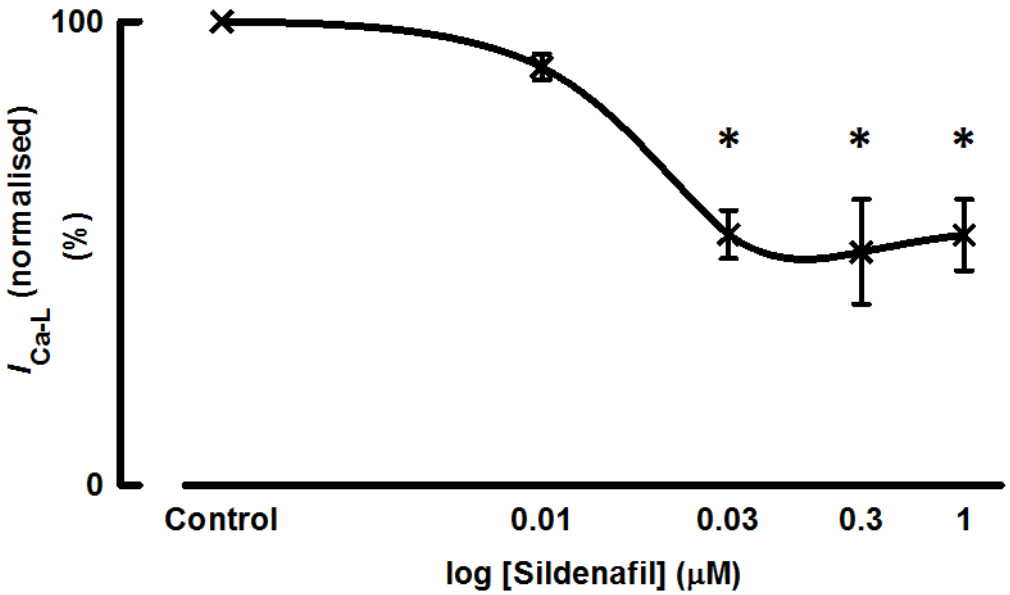

Figure 3.3 Dose dependency of the effect of PDE5 inhibition in I_{Ca-L}

*The percentage decrease in I_{Ca-L} from control in response to increasing doses of the selective PDE5 inhibitor sildenafil. Mean ± SEM, differences compared using a one-way repeated measures ANOVA, * $p<0.05$. $n = 9$*

3.3.1.3 The systolic Ca^{2+} transient.

One of the main determinants of the size of the systolic Ca^{2+} transient is the size of $I_{Ca\text{-}L}$. PDE5 inhibition reduced peak $I_{Ca\text{-}L}$, thus the next experiment tested whether sildenafil altered the systolic Ca^{2+} transient. Figure 3.4A shows PDE5 inhibition reduced the amplitude of the systolic Ca^{2+} transient by 21±8% (Summary data shown in Figure 3.4Aii: 0.018±0.01 $R_{340/355}$). Figure 3.4Bi shows the representative traces normalised to the peak of the control transient to illustrate that there was little effect of PDE5 inhibition on the decay rate of the systolic Ca^{2+} transient (Figure 3.4Bii, con: 0.094±0.15 s^{-1}, SIL: 1.075±0.18 s^{-1}).

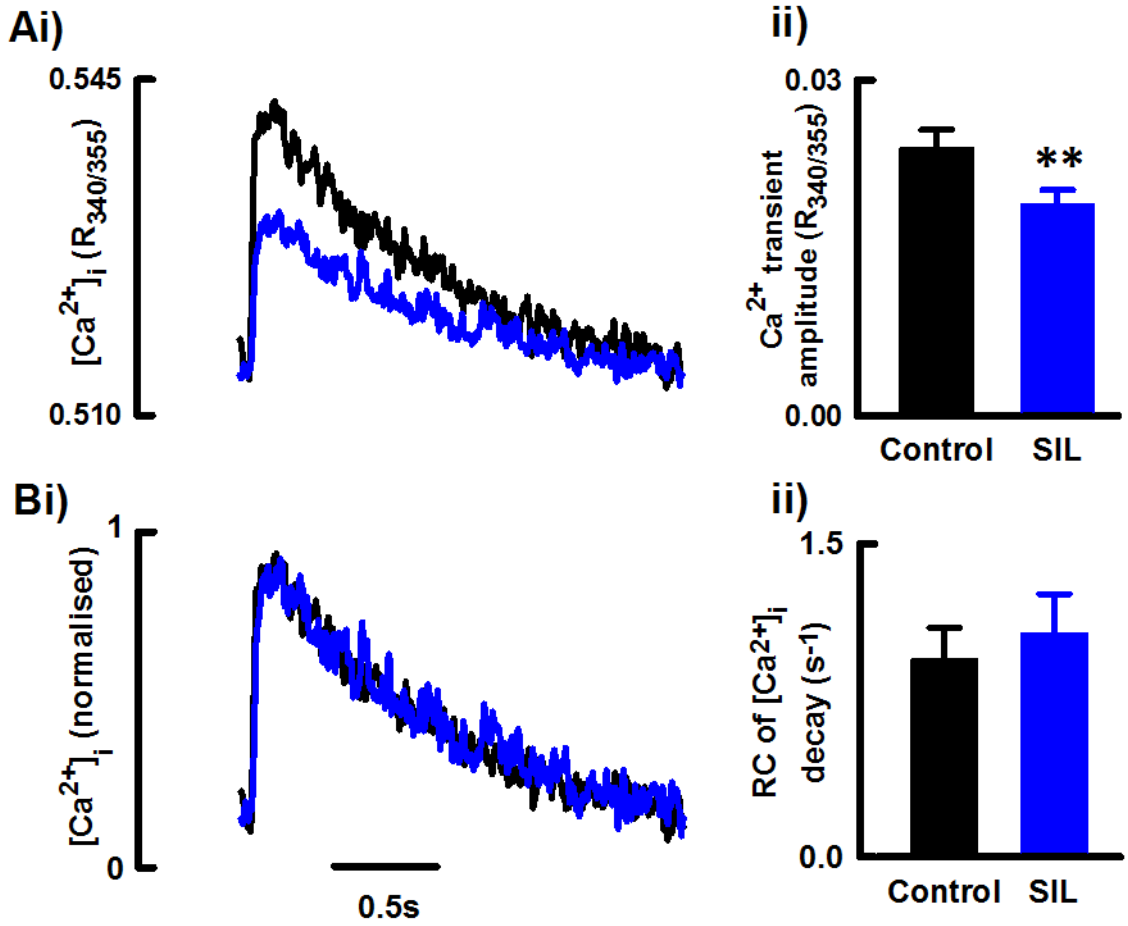

Figure 3.4 Effect of PDE5 inhibition on the systolic Ca^{2+} transient

*(Ai) Typical systolic Ca^{2+} transient from a control sheep myocyte and (ii) summary data for Ca^{2+} transient amplitude before (black) and after (blue) PDE5 inhibition with 1μM sildenafil (sil). (Bi) Ca^{2+} transients normalised to control to represent changes in $[Ca^{2+}]_i$ decay and (ii) summary data for the effect of PDE5 inhibition on the rate constant (RC) of Ca^{2+} transient decay. Mean ± SEM, differences compared using a paired Student's t-test, ** $p<0.001$. n=9 cells/ 4 animals.*

3.3.2 The effect of PKG inhibition on steady state Ca^{2+} handling

The effects observed on calcium handling in response to PDE5 inhibition could be attributed to the downstream effect of PKG. To test whether PKG is tonically active under basal conditions in ovine ventricular myocytes the PKG inhibitor KT-5823 (PKGi, 50 nM, Sigma) was acutely applied to voltage clamped cells for 3 minutes and the effects on $I_{Ca\text{-}L}$ and systolic Ca^{2+} transient were investigated.

PKG inhibition had no effect on peak $I_{Ca\text{-}L}$ (Figure 3.5Ai, control: 4.01±0.6 $pA.pF^{-1}$ versus PKGi: 4.79±0.4 $pA.pF^{-1}$). Moreover, PKG inhibition had no effect on the proportion of Ca^{2+} influxing or the rate of $I_{Ca\text{-}L}$ decay (Table 4)

	Control	**PKGi**
Calculated $I_{Ca\text{-}L}$ Ca^{2+} influx ($\mu moles.L^{-1}$)	1.51±0.1	1.53±0.1
RC for voltage-dependent inactivation of $I_{Ca\text{-}L}$ ($seconds^{-1}$)	46.2±5	49.1±3
RC for calcium dependent inactivation of $I_{Ca\text{-}L}$ ($seconds^{-1}$)	192.2±31	185.4±20

Table 4. The effects of PKG inhibition $I_{Ca\text{-}L}$

PKG inhibition (PKGi, KT-5823, 50nM); rate constant (RC) of inactivation of $I_{Ca\text{-}L}$. Mean ± SEM. Comparisons described using Student's t-test. n= 4 cells /3 animals.

PKG inhibition had no effect on $I_{Ca\text{-}L}$, however it reduced the amplitude of the Ca^{2+} transient (Figure 3.5B, control: 0.042±0.01 $R_{340/355}$ versus PKGi: 0.033±0.01 $R_{340/355}$). Furthermore, there was a possible trend for a decrease in the rate constant of decay of the Ca^{2+} transient under PKG inhibition (control 1.99±1 s^{-1} vs. PKGi 1.52±1 s^{-1}, *p=0.06*).

The changes presented here may suggest that there exists a tonic level of PKG activity in normal sheep ventricular myocytes. As PKG can phosphorylate PLN there may be a mechanism by which in the steady state PKG acts to help load the SR and maintain Ca^{2+} transient amplitude. A limitation to this hypothesis is that SR content has not been measured in the presence of the PKG inhibitor.

It should be noted that experiments using the PKG inhibitor were performed in myocytes isolated from old sheep (age > 8 years). There was no difference in cell size between the young and old cells (Table 5). However, despite no difference in calcium transient amplitude, there appeared to be a tendency for reduction in $I_{Ca\text{-}L}$ in old myocytes as compared to young myocytes.

	Young	**Old**
Cell capacitance (pF)	146.7±17	110.8±9
Peak $I_{Ca\text{-}L}$ ($pA.pF^{-1}$)	7.09±0.7	4.80±0.6
Ca^{2+} transient amplitude ($R_{340/355}$)	0.023±0.002	0.042±0.01

Table 5. Electrophysiological differences between old and young sheep

Mean ± SEM. Young n= 9 cells/5 animals, old n= 4/ 3. Comparisons described using Student's t-test.

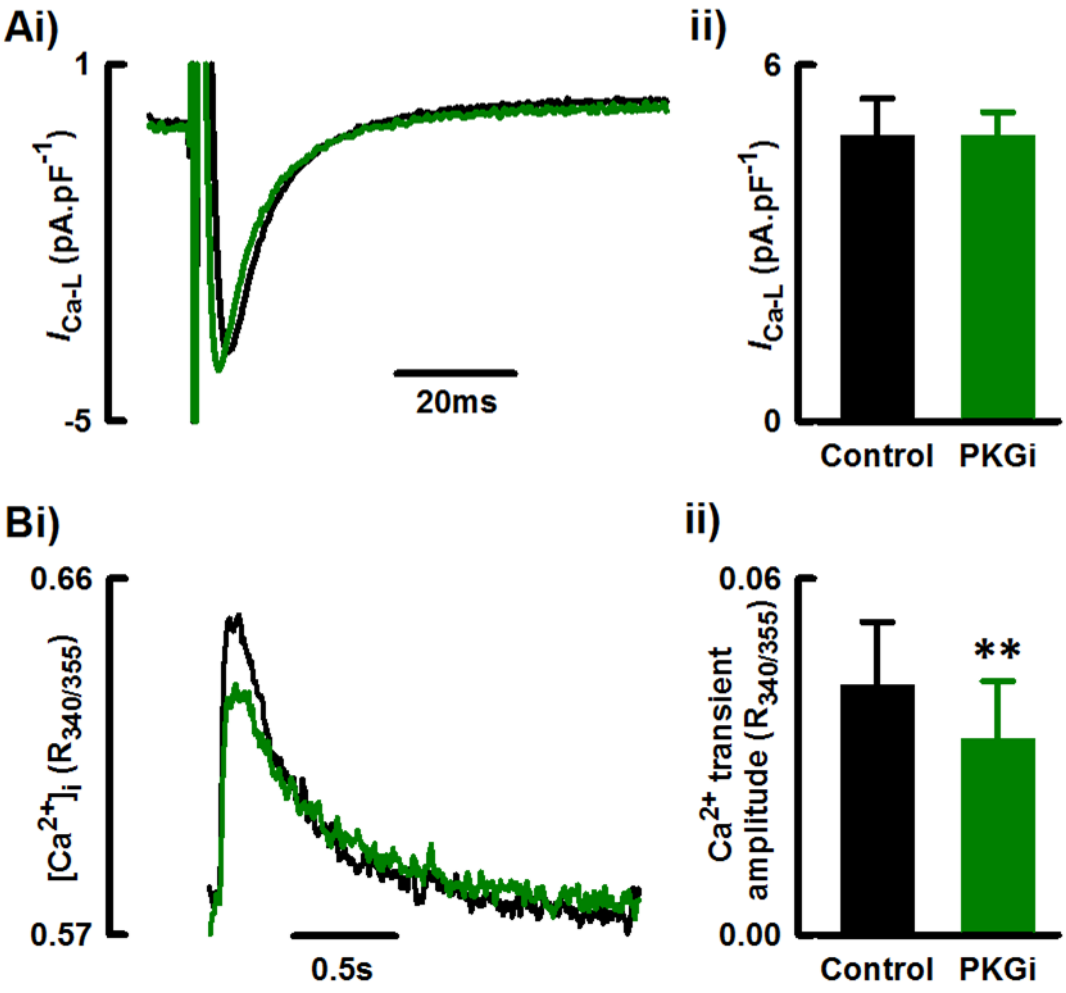

Figure 3.5 The effect of PKG inhibition on $I_{Ca\text{-}L}$ and Ca^{2+} transient

*Typical traces for (Ai) $I_{Ca\text{-}L}$ and (Bi) Ca^{2+} transient and summary data in control myocytes (black). Changes as summarised for (Aii) peak $I_{Ca\text{-}L}$ and (Bii) Ca^{2+} transient amplitude show the effect of PKG inhibition with the selective inhibitor KT-5823 50nM (PKGi, green). Mean ± SEM, differences compared using paired Student's t-test, **p<0.001. n= 4 cells/ 3 animals.*

3.3.3 The effect of β-adrenergic stimulation on steady state Ca^{2+} handling

3.3.3.1 L-type Ca^{2+} current.

This group of experiments sought to investigate the effect of β-AR stimulation on steady state $I_{Ca\text{-}L}$ in ovine cardiac mycoytes. Normal ventricular myocytes were voltage clamped and allowed to reach steady state before the application of the non-selective β-AR agonist isoprenaline (100 nM). The effect of β-AR stimulation on $I_{Ca\text{-}L}$ is shown in Figure 3.6A. β-AR stimulation resulted in a 129±41% increase in peak $I_{Ca\text{-}L}$ (Figure 3.6Aii: 5.32±0.6 $pA.pF^{-1}$ to 12.20±1.8 $pA.pF^{-1}$). Concordant increases in the proportion of Ca^{2+} influxing into the cell was also observed (Figure 3.6Aiii; 236±54% increase from 1.49±0.1 $\mu moles.L^{-1}$ to 5.01±0.7 $\mu moles.L^{-1}$).

The effect on Ca^{2+} influx is most likely due to a combination of both increased peak $I_{Ca\text{-}L}$ and a change in the inactivation profile of the $I_{Ca\text{-}L}$ under β-AR stimulation. Summary data in Figure 3.6B shows that β-AR stimulation resulted in a slower voltage-dependent $I_{Ca\text{-}L}$ inactivation (27±5% decrease from 48.2±3 s^{-1} to 35.1±2 s^{-1}), yet a faster Ca^{2+}-dependent $I_{Ca\text{-}L}$ inactivation (15±8% increase from 193.1±10 s^{-1} to 223.9±13 s^{-1}).

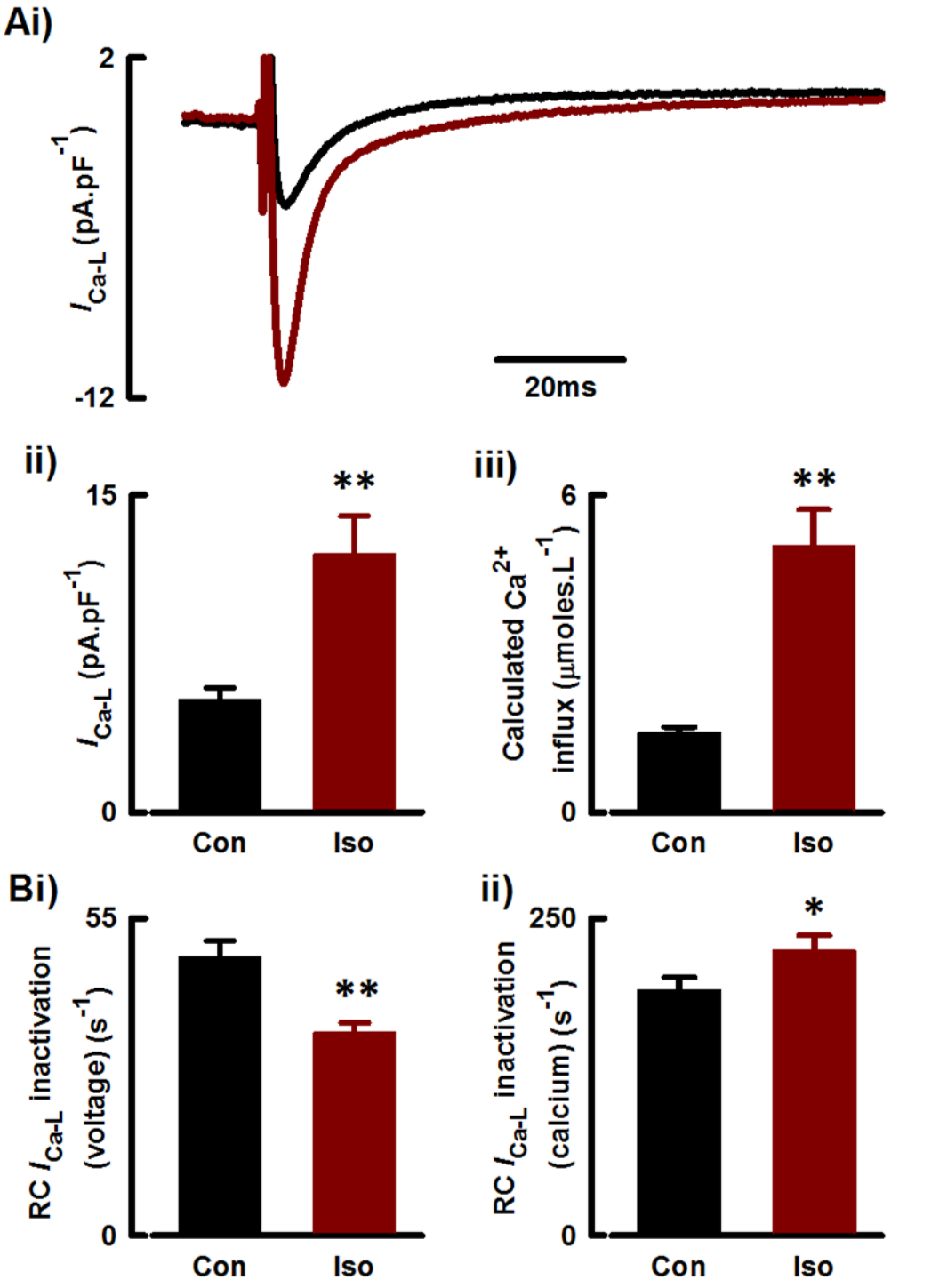

Figure 3.6 Effect of *β*-AR stimulation on $I_{Ca\text{-}L}$

*(Ai) Typical $I_{Ca\text{-}L}$ recording from control sheep myocytes with summary data showing (ii) peak $I_{Ca\text{-}L}$ and (iii) calculated Ca^{2+} influx before (con, black) and after non-selective β-AR stimulation with 100nM isoprenaline (iso, red). (B) Summary data for change in the rate constants (RC) of $I_{Ca\text{-}L}$ inactivation for (i) voltage- and (ii) calcium-dependent portion. Mean ± SEM, differences compared using paired Student's t-test, * p<0.05, ** p<0.001. n=11 cells/ 8 animals.*

3.3.3.2 The systolic Ca^{2+} transient.

β-AR stimulation increased peak $I_{Ca\text{-}L}$, the main trigger for intracellular Ca^{2+} release, thus the next experiment tested the effect of β-AR stimulation on the systolic Ca^{2+} transient.

As expected, non-selective β-AR stimulation increased Ca^{2+} transient amplitude by 263±67% (Figure 3.7A: 0.022±0.003 $R_{340/355}$ to 0.08±0.014 $R_{340/355}$). This was shown to be associated with a faster rate of decay of the Ca^{2+} transient in the presence of β-AR stimulation (Figure 3.7B; 117±38% increase from 1.7±0.2 s^{-1} to 3.8±0.4 s^{-1}).

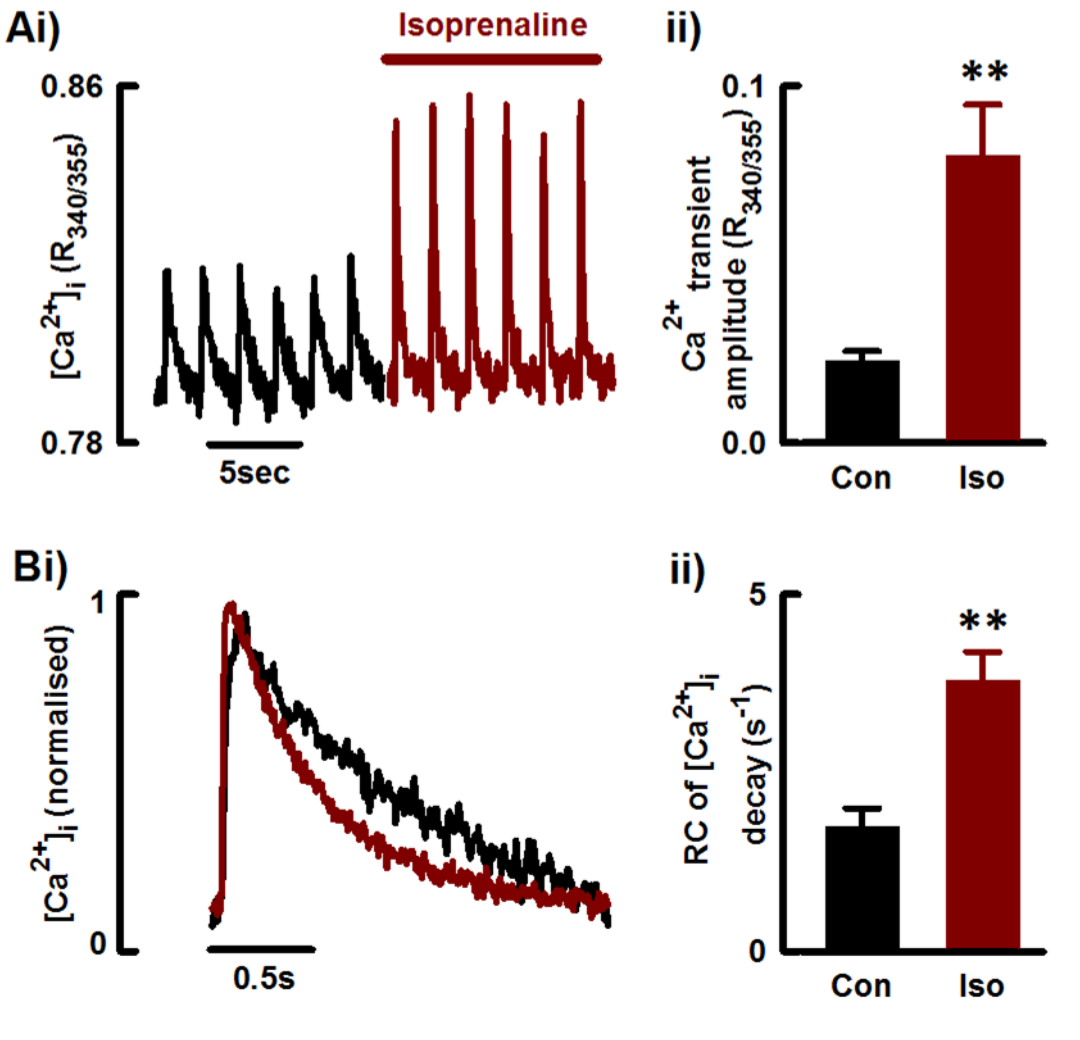

Figure 3.7 Effect of *β*-AR stimulation on systolic Ca^{2+} transient

*(Ai) Typical train of Ca^{2+} transients from a control sheep myocyte before (black) and after (red) non-selective β-AR stimulation with 100nM isoprenaline (iso). (Aii) Summary data for Ca^{2+} transient amplitude. (Bi) Ca^{2+} transients normalised to control to represent changes in $[Ca^{2+}]_i$ decay and (ii) summary data for the effect of β-AR stimulation on the rate constant (RC) of Ca^{2+} transient decay. Mean ± SEM, differences compared using a paired Student's t-test, ** p<0.001. n=10 cells/ 8 animals.*

3.3.3.3 SR Ca^{2+} content

The main factors that contribute to changes in systolic Ca^{2+} transient are the degree of trigger for SR Ca^{2+} release, peak $I_{Ca\text{-}L}$, and the amount of Ca^{2+} stored within the SR, SR Ca^{2+} content. Previous experiments have demonstrated a change in $I_{Ca\text{-}L}$ may contribute to the changes in Ca^{2+} transient following β-AR stimulation, thus the next experiment tested whether changes in SR Ca^{2+} content may also contribute.

SR content is determined by superfusing an unstimulated, voltage clamped myocyte with a saturating concentration of caffeine (10mM, see 2.2.5.3), which reversibly maintains the RyR in an open conformation, negating any action of SERCA. This generates a large release of Ca^{2+} from the SR, termed the caffeine evoked transient, which is shown by the black Ca^{2+} trace in the uppermost panel of Figure 3.8. In order to maintain Ca^{2+} flux balance, cytosolic Ca^{2+} must leave the cell through NCX and to some extent PMCA. Ca^{2+} flux out of the cell is coupled with Na^{+} influx, and due to a charge imbalance an inward current is recorded, I_{NCX}, shown by the black trace in the upper middle panel of Figure 3.8. The integral of I_{NCX} is proportional to Ca^{2+} extrusion, which provides an accurate measurement of the amount of Ca^{2+} stored within the SR, shown by the lowermost panels in Figure 3.8.

This protocol was performed following the application of 100 nM isoprenaline. β-AR stimulation increased SR Ca^{2+} content from 17.7±4 μmoles.L^{-1} to 64.7±12 μmoles.L^{-1} (Figure 3.8).

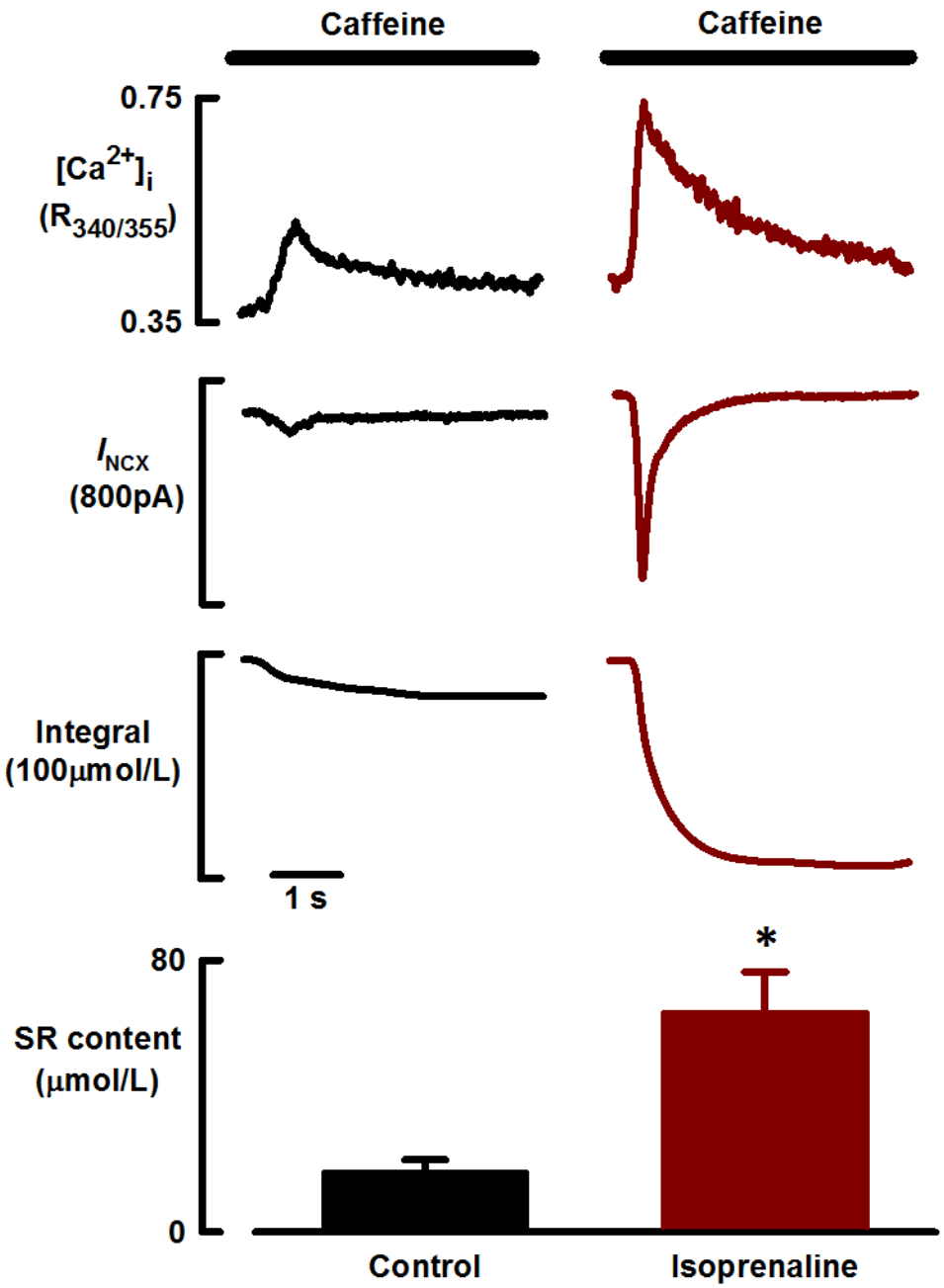

Figure 3.8 Effect of *β*-AR stimulation on SR Ca^{2+} content

SR content measured using 10mM Caffeine in control sheep myocytes (black) and following *β*-AR stimulation with 100nM isoprenaline (iso, red). Caffeine evoked Ca^{2+} transient and membrane current (I_{NCX}) and integration of current over time are shown in the upper and middle panels respectively. Quantified SR content is shown by the summary data in the bottom panel. Mean ± SEM, differences compared using a Student's t-test, * p,0.05. n= 8 cells/ 8 animals.

3.3.4 The effect of PDE5 inhibition on responses to β-AR stimulation

PDE5 inhibition was negatively inotropic: reducing $I_{Ca\text{-}L}$ and systolic Ca^{2+} transient amplitude in normal ovine ventricular myocytes. *β*-AR stimulation, however, was positively inotropic and increased $I_{Ca\text{-}L}$ and systolic Ca^{2+} transient amplitude. The next set of experiments thus sought to determine the effects of PDE5 inhibition on the *β*-AR response of ventricular myocytes. In order to test this, sildenafil was applied both before and after *β*-AR stimulation.

3.3.4.1 L-type Ca^{2+} current

As expected PDE5 inhibition decreased peak $I_{Ca\text{-}L}$ (Figure 3.9A: 7.47±1.0 pA.pF^{-1} to 4.15±1.3 pA.pF^{-1}). Upon the application of isoprenaline in the presence of sildenafil there was a trend for a further decrease in $I_{Ca\text{-}L}$ to 2.07±0.8 pA.pF^{-1}, however this change did not achieve significance (p=0.08). The application of isoprenaline increased peak $I_{Ca\text{-}L}$ from 4.74±1.0 pA.pF^{-1} to 11.44±2.4 pA.pF^{-1} (Figure 3.9B), which was reversed by PDE5 inhibition (2.41±0.9 pA.pF^{-1}). Table 6 and Table 7 shows there were limited effects of PDE5 inhibition on responses to isoprenaline for the proportion of Ca^{2+} influx or the rate of $I_{Ca\text{-}L}$ inactivation, however there was some reduction in the rate of voltage dependent $I_{Ca\text{-}L}$ inactivation.

	Control	Sil	Sil+Iso
Calculated $I_{Ca\text{-}L}$ Ca^{2+} influx ($\mu moles.L^{-1}$)	2.32±0.4	1.96±0.4	1.38±0.3
RC for voltage dependent inactivation of $I_{Ca\text{-}L}$ ($seconds^{-1}$)	58±4	49±9	23±7
RC for calcium dependent inactivation of $I_{Ca\text{-}L}$ ($seconds^{-1}$)	216±22	195±50	75±22

Table 6. The effects of PDE5 inhibition in the presence of a *β-AR* agonist on $I_{Ca\text{-}L}$

PDE5 inhibition with sildenafil (sil); β-AR stimulation with isoprenaline (iso). Mean ± SEM. Comparisons described using one-way repeated measures ANOVA. n=4 cells/ 3 animals.

	Control	Iso	Iso+Sil
Calculated $I_{Ca\text{-}L}$ Ca^{2+} influx ($\mu moles.L^{-1}$)	1.40±0.3	4.48±1.5	1.02±0.1
RC for voltage dependent inactivation of $I_{Ca\text{-}L}$ ($seconds^{-1}$)	49±6	33±2*	9±3
RC for calcium dependent inactivation of $I_{Ca\text{-}L}$ ($seconds^{-1}$)	193±10	225±28	94±44

Table 7. The effects of β-AR stimulation in the presence of PDE5 inhibition on $I_{Ca\text{-}L}$

*β-AR stimulation with isoprenaline (iso); PDE5 inhibition with sildenafil (sil). Mean ± SEM. Comparisons described using one-way repeated measures ANOVA. *p<0.05. n = 3 cells/ 2 animals.*

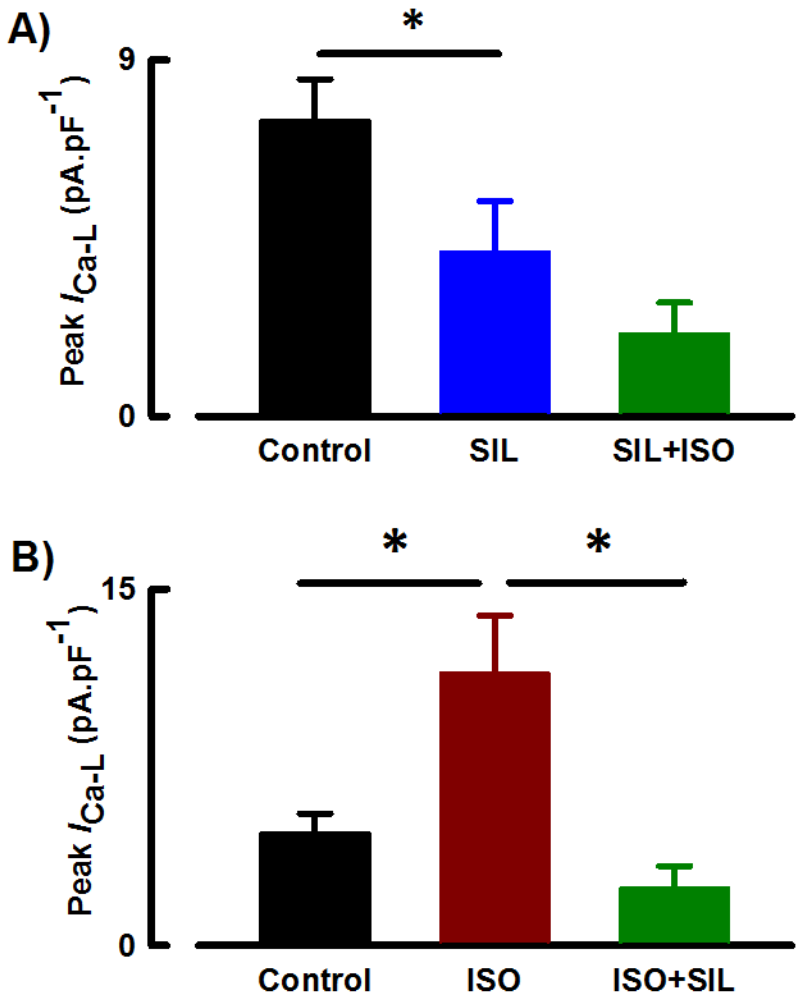

Figure 3.9 Effect of combined β-AR stimulation and PDE5 inhibition on I_{Ca-L}

*Summary data for peak I_{Ca-L} in control myocytes (black) following (A) PDE5 inhibition with 1μM sildenafil (Sil, blue) in the presence of the β-AR agonist isoprenaline (100nM, Sil+Iso, green) and (B) β-AR stimulation (Iso, red) in the presence of sildenafil. Mean ± SEM, differences compared using a one-way repeated measures ANOVA, *p<0.05. SIL+ISO n= 4 cells/ 3 animals, ISO+SIL n= 3/ 2.*

3.3.4.2 The systolic Ca^{2+} transient

Figure 3.10 shows mean data for the effects of sildenafil±isoprenaline on the amplitude of the systolic Ca^{2+} transient. The data presented here represents an n= 4/ 3 (sildenafil±isoprenaline) and n= 2/ 2 (isoprenaline±sildenafil). PDE5 inhibition showed a tendency to decrease steady state Ca^{2+} transient amplitude (Figure 3.10Ai, 0.023±0.003 $R_{340/355}$ to 0.018±0.002 $R_{340/355}$), with no effect on the rate of decay of the systolic Ca^{2+} transient (Figure 3.10Bi, 0.54±0.03 s^{-1} vs. 0.64±0.12 s^{-1}). The application of isoprenaline in the presence of sildenafil elicited a trend for an increase in Ca^{2+} transient amplitude beyond steady state (Figure 3.10Ai, 0.080±0.03 $R_{340/355}$), which was associated with a marked increase in the rate of decay of the Ca^{2+} transient (Figure 3.10Bi, 2.03±0.38 seconds).

β-AR stimulation resulted in a tendency for increased Ca^{2+} transient amplitude (Figure 3.10Aii, 0.020±0.004 $R_{340/355}$ to 0.077±0.03 $R_{340/355}$), which was unaffected by the application of the PDE5 inhibitor (0.061±0.02 $R_{340/355}$). The application of isoprenaline resulted in a trend for an increased rate of decay of the Ca^{2+} transient, which appeared to be unaffected by the application of sildenafil (Figure 3.10Bii).

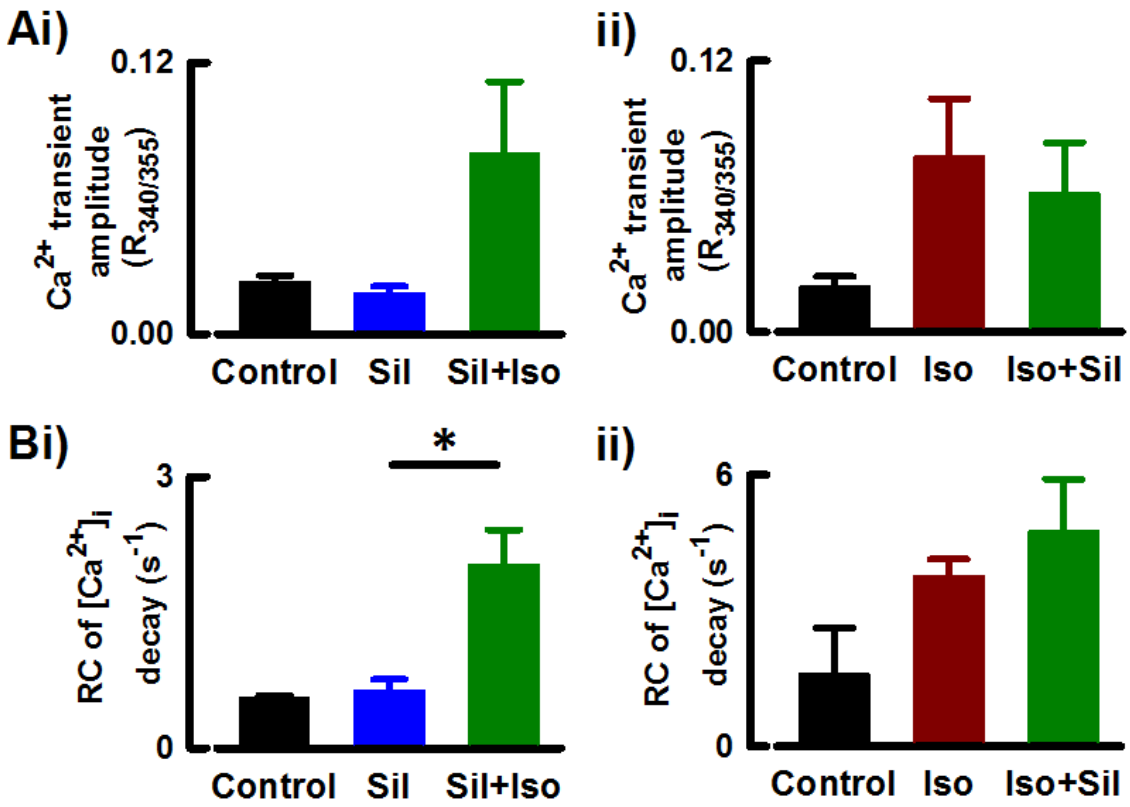

Figure 3.10 Effect of combined *β*-AR stimulation and PDE5 inhibition on the systolic Ca^{2+} transient

*(A) Summary data for Ca^{2+} transient amplitude in control myocytes (black) following (i) PDE5 inhibition with 1μM sildenafil (Sil, blue) in the presence of the β-AR agonist isoprenaline (100nM, Sil+Iso, green) and (ii) β-AR stimulation (Iso, red) in the presence of sildenafil. (B) Summary data for the rate constant for decay of the Ca^{2+} transient following the described treatments. Mean ± SEM, differences compared using a one-way repeated measures ANOVA, *p<0.05. SIL+ISO n= 4 cells/ 3 animals, ISO+SIL n= 2/ 2.*

3.3.4.3 SR Ca^{2+} content

In order to fully understand the changes in Ca^{2+} transient amplitude elicited by combined *β*-AR stimulation and PDE5 inhibition the next set of experiments sought to test the effect on SR Ca^{2+} content. Unfortunately due to time constraints and animal availability only the effect of sildenafil in the presence of isoprenaline on SR content was tested.

Caffeine was used to empty the SR of Ca^{2+}, resulting in the large caffeine evoked Ca^{2+} transient, and membrane I_{NCX}, which was increased after the application of isoprenaline (Figure 3.11, 64.7±12 μmoles.L^{-1}, n = 8 cells/ 8 animals). Further, when sildenafil was applied in the presence of isoprenaline the measured SR content was greater than steady state content, yet unchanged from that observed in the presence of isoprenaline alone (90.8±0.4 μmoles.L^{-1}, n= 2/ 2).

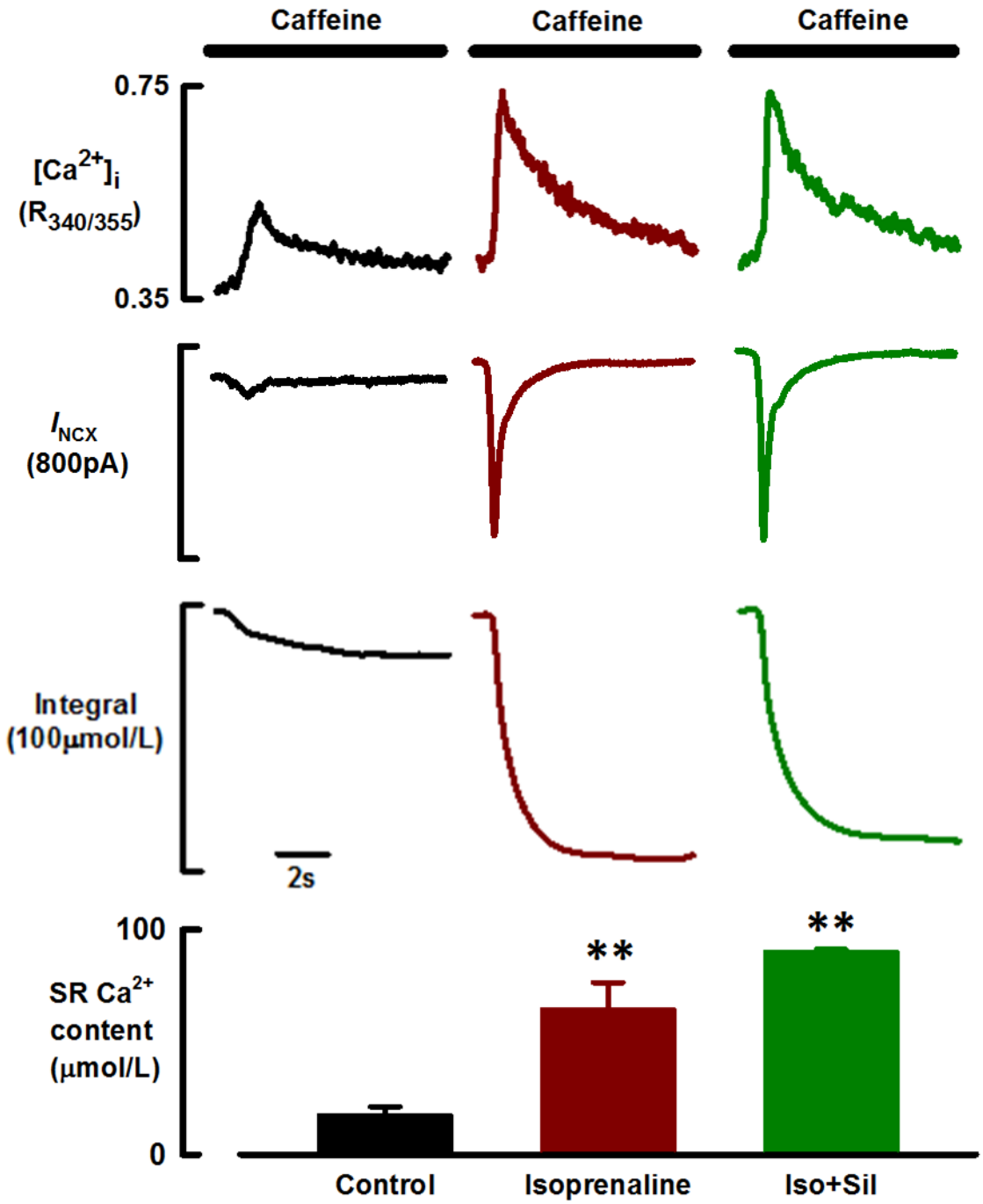

Figure 3.11 Effect of combined *β*-AR stimulation and PDE5 inhibition on SR Ca^{2+} content

*SR content measured using 10mM Caffeine in control sheep myocytes (black), following β-AR stimulation with 100nM isoprenaline (iso, red) and in the presence of the PDE5 inhibitor sildenafil (1µM, Iso+Sil, green). Caffeine evoked Ca^{2+} transient and membrane current (I_{NCX}) and integration of current over time are shown in the upper and middle panels respectively. Quantified SR content is shown by the summary data in the bottom panel. Mean ± SEM, differences compared using a one-way ANOVA, *versus control p<0.05. n= 2 cells/ 2 animals.*

3.4 Discussion

In this set of experiments we sought to test the effect of acute PDE5 inhibition, β-AR stimulation and a combination of the two on myocyte Ca^{2+} handling in control sheep. $I_{Ca\text{-}L}$, the Ca^{2+} transient and SR content are considered important determinants of myocyte contractility. The principle finding reported in this chapter is a mechanism by which PDE5 inhibition could be negatively inotropic: decreasing $I_{Ca\text{-}L}$ and the size of the Ca^{2+} transient. In contrast β-AR stimulation is positively inotropic. Furthermore, PDE5 inhibition can reverse the effects of β-AR stimulation on $I_{Ca\text{-}L}$ but not those for the Ca^{2+} transient or SR content.

3.4.1 The effect of acute PDE5 inhibition on basal calcium handling

3.4.1.1 Modulation of $I_{Ca\text{-}L}$

PDE5 inhibition in voltage clamped sheep ventricular myocytes reduced the $I_{Ca\text{-}L}$. It is known that cGMP can lead to an inhibition of $I_{Ca\text{-}L}$ through two main pathways; (1) the activation of PKG, which phosphorylates sites (Cav1.2: alpha 1c and beta2)[86] on the L-type Ca^{2+} channel leading to $I_{Ca\text{-}L}$ inhibition[100], and (2) the activation of PDE2, which will increase cAMP hydrolysis, thus reducing the effect of the inotropic effector PKA[99] (Figure 3.12).

Heterogeneous differences exist among species, such that PKG mediates $I_{Ca\text{-}L}$ inhibition in guinea pig and rat ventricular myocytes[100, 101, 225], however in frog myocytes PDE2 stimulation prevails. In humans, higher concentrations of cGMP results in $I_{Ca\text{-}L}$ inhibition, mediated by PDE2[158, 222]. In addition, PDE5 and PDE2 are known to colocalise in the same intracellular compartments, usually at the z-disk[98, 162], which brings them within compartments associated with t-tubules and L-type Ca^{2+} channels (Figure 3.12). Together, this evidence suggests that in larger animals there may be more of an effect of PDE2, on $I_{Ca\text{-}L}$, than in small animals, which are controlled more predominantly by the direct effect of PKG. The differences observed between species may be related to peak $I_{Ca\text{-}L}$, which may provide difficulties in resolving the effects of PDE5 inhibition: the mouse ventricle $I_{Ca\text{-}L}$ has been observed as $3.2\pm0.5 pA.pF^{-1}$ [166], which is much less than in the sheep ventricle (7.09 ± 0.7 $pA.pF^{-1}$). Notably, human $I_{Ca\text{-}L}$ is more physiologically similar to the sheep: 5.8 ± 0.5 $pA.pF^{-1}$ [226].

PDE5 inhibition directly affects the inactivation profile of the $I_{Ca\text{-}L}$. Current inactivation is determined by both a voltage-dependent and calcium-dependent mechanism, which were both, to some extent, affected by PDE5 inhibition. The tendency for an observed slower

calcium-dependent rate of inactivation is most likely caused by the reduced amplitude of the calcium transient by PDE5 inhibition (see 3.4.3), which is consistent with less cytosolic Ca^{2+} available to negatively feedback to the L-type Ca^{2+} channel. Furthermore, the slower voltage-dependent rate of inactivation may be due to two mechanisms, (1) the direct phosphorylation of the L-type channel by PKG could influence its sensitivity to membrane voltage, (2) a greater hydrolysis of cAMP by increased PDE2 activity could reduce the availability of active PKA and therefore reduce the basal level of phosphorylation (opening) of the L-type channel.

There was a time delay for PDE5 inhibition to have an effect on $I_{Ca\text{-}L}$. Figure 3.2 shows sildenafil took approximately 90 seconds to have a significant effect on $I_{Ca\text{-}L}$, a 40% decrease, which was sustained after 90 seconds of application. A maximal effect on $I_{Ca\text{-}L}$ inhibition with sildenafil between 90 and 180 seconds suggests that any effect of sildenafil is associated with the direct effect of the drug on the $I_{Ca\text{-}L}$.

It is well known that cAMP exists in higher basal concentrations within the sarcoplasm than does its counterpart cGMP, and is much more freely diffusible[129]. Thus for this reason it is possible that the present data suggests that the time delay for the effect of sildenafil on $I_{Ca\text{-}L}$ exists because there is a requirement for a sufficient rise in cytosolic cGMP concentration to activate sufficient PDE2 in order to exert the negative inotropic effect observed.

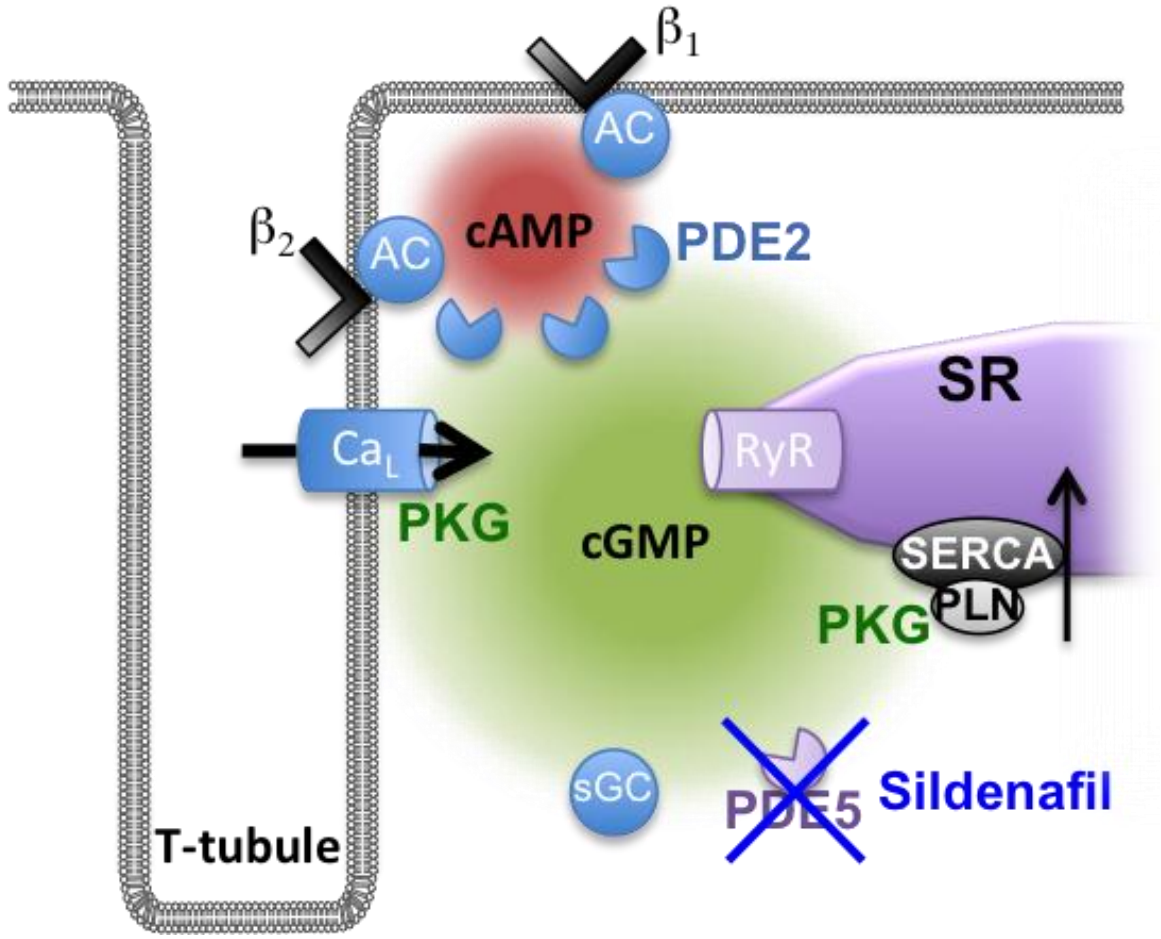

Figure 3.12 Mechanism by which PDE5 inhibition modulates $I_{Ca\text{-}L}$ and Ca^{2+} transient

*Arrow represents Ca^{2+} movement. β-*adreonreceptors (*$\beta_{1/2/3}$), adenylyl cyclase (AC), soluble guanylyl cyclase (sGC), cyclic adenosine/guanosine monophosphate (cAMP/cGMP), protein kinase G (PKG), L-type Ca^{2+} channel (Ca_L), ryanodine receptor (RyR), sarcoplasmic reticulum (SR), sarco-endoplasmic reticulum Ca^{2+} ATPase (SERCA), phospholamban (PLN), transverse tubule (t-tubule), phosphodiesterase (PDE).*

3.4.2 Appropriate use of sildenafil concentration for selective PDE5 inhibition

The use of sildenafil as a selective inhibitor of PDE5 in cardiac myocytes is well established and has been used for nearly 20 years. However, much debate has arisen about the specificity of its action and the most appropriate concentration to be used in different cell types. The selectivity of PDE5 inhibitors: sildenafil, tadalafil and vardenafil (as reviewed by Bischoff[223]), is under scrutiny as they are known to interact with both PDE1 and PDE6, which are both expressed in ventricular cardiac mycoytes. Takimoto *et al* showed whole mouse heart contractility was suppressed by 0.1-1 μM sildenafil[85], while Lee *et al* demonstrated reduced sarcomere shortening in single mouse mycoytes with 1μM sildenafil[221]. Moreover, in voltage clamped guinea pig ventricular myocytes, Chiang *et al* showed a dose dependent inhibition of $I_{Ca\text{-}L}$ with sildenafil 1 – 100 μM[227]. Previous studies have also used the PDE5 inhibitor zaprinast[166], however this is known to be much less selective than sildenafil[228]. The present study showed decreases in $I_{Ca\text{-}L}$ of approximately 40% over a 3-minute application of 1 μM sildenafil, which was shown to be similarly negatively inotropic as 0.03 μM and 0.3 μM sildenafil. This to my knowledge is the first time sildenafil has been acutely applied to isolated sheep ventricular myocytes, thus as there were little differences in the effect of sildenafil between 0.03 μM and 1 μM it could be concluded that PDE1, which is known to only be inhibited by 1 μM sildenafil[224], is either less active in sheep ventricular cardiac mycoytes or unaffected by the high dose of sildenafil.

3.4.3 Modulation of the systolic Ca^{2+} transient

$I_{Ca\text{-}L}$ acts as the main trigger for intracellular Ca^{2+} release, thus using the calcium indicator Fura-2, simultaneous recordings of intracellular Ca^{2+} fluxes allowed the investigation of PDE5 inhibition on the systolic Ca^{2+} transient. PDE5 inhibition reduced the amplitude of the systolic Ca^{2+} transient by 21% in sheep ventricular myocytes.

There are three main sites for controlling the systolic Ca^{2+} transient; (1) $I_{Ca\text{-}L}$, which acts as the trigger for intracellular Ca^{2+} release, (2) RyR open probability, the site for Ca^{2+} release from the SR, and (3) SR content, the amount of Ca^{2+} stored in the SR. The movement of calcium in and out of the cell per beat is known to be in direct influx-efflux balance. That is, that there is no net gain or loss of Ca^{2+} within the cell, under steady state conditions. The calcium that moves into the sarcoplasm, via $I_{Ca\text{-}L}$ must be removed from the cell by NCX and PMCA[229]. Furthermore, the nature of this requirement for influx-efflux balance suggests that despite any changes to RyR open probability, there will still be a maintained

Ca^{2+} flux balance in steady state conditions. Ca^{2+} transient amplitude is predominantly affected only by Ca^{2+} entry via $I_{Ca\text{-}L}$ and SR content (reviewed by Trafford *et al*[230]). As the present study has shown that PDE5 inhibition decreases Ca^{2+} transient amplitude, this effect must be associated with the effect of the cGMP-PKG axis on either $I_{Ca\text{-}L}$ or SR content (Figure 3.12). This study has shown PDE5 inhibition is sufficient to decrease $I_{Ca\text{-}L}$ within an acute three-minute application; this may therefore be translated directly into an overall reduction in Ca^{2+} release from the SR.

Trafford et al has previously shown that increases in $I_{Ca\text{-}L}$ are associated with increases in Ca^{2+} transient amplitude, which were shown to be largely independent of SR content[216]. This suggests that any PDE5 inhibitor modulated decrease in $I_{Ca\text{-}L}$ could be responsible for decreases in Ca^{2+} transient amplitude, independent of SR content. This highlights a limitation to this study, as due to experimental constraints I was unable to obtain data for the direct effect of sildenafil on SR content, which would provide the most reliable view of its mechanism of action. However, I have shown that PDE5 inhibition has no effect on the decay rate of the systolic Ca^{2+} transient. The main route of sarcoplasmic Ca^{2+} extrusion is resequestration into the SR, through SERCA, which is modulated by the accessory protein PLN. Both PKA and PKG are known to phosphorylate PLN[78, 88], which in turn removes its inhibitory effect on SERCA, thus increasing its function. The proposed mechanism could proceed as follows. Under PDE5 inhibition the sarcoplasmic level of cGMP will increase, thus increasing the activity of PKG. If PKG was directly influencing PLN to a greater extent, then one would expect the rate of Ca^{2+} uptake back into the SR to be increased, which would increase the rate of the inactivation of the Ca^{2+} transient (Figure 3.12). I believe this therefore suggests changes in the Ca^{2+} transient amplitude are independent of SR content and are due to the observed decreases in $I_{Ca\text{-}L}$ with sildenafil.

Together, the above findings suggest a mechanism by which PDE5 inhibition results in an elevation of cGMP in a compartment localized to the z-lines/t-tubules. This compartment is densely populated by L-type Ca^{2+} channels, which are closely associated with AKAPs containing protein kinases and PDEs. As discussed in detail previously (see 1.4.4.2 and 3.4.1.1), eElevation of cGMP in this compartment will directly activate PDE2, which in turn will hydrolyse local cAMP, thus reducing the activity of PKA within that same compartment. This would reduce L-type Ca^{2+} channel phosphorylation resulting in a smaller inward $I_{Ca\text{-}L}$, which in turn reduces the corresponding Ca^{2+} transient (Figure 3.12).

3.4.4 The effect of PKG inhibition on basal calcium handling

In order to test the above conclusion that the mechanism by which PDE5 inhibition is negatively inotropic is due mainly to the effect of PDE2 activation and not PKG activation, the next set of experiments investigated whether PKG is active under baseline/steady state conditions.

In early experiments into the existence of a functioning cGMP-PKG axis, Méry *et al*[101] showed that direct application of exogenous cGMP and PKG had no effect on basal Ca^{2+} handling in voltage clamped rat ventricular myocytes. Under cAMP-stimulated conditions the activation of the cGMP-PKG axis was negatively inotropic. The present study hypothesised that large animal myocytes appear to be more dependent on the interaction of cGMP and cAMP-dependent PDEs in order to exert negative inotropy. When the PKG inhibitor KT-5823 was applied to isolated sheep ventricular myocytes, there was no effect on $I_{Ca\text{-}L}$, however a modest reduction in Ca^{2+} transient amplitude and a tendency for a slower rate of transient decay was observed. Together this suggests that baseline activity of PKG in normal myocytes has little effect on the L-type Ca^{2+} channel, however may be important in the functioning of SR filling. Unfortunately, due to experimental constraints I have not been able to present data for the effect of PKG on SR content however the effect on both the amplitude and decay rate of the Ca^{2+} transient suggests that some baseline level of PLN phosphorylation is maintained by a local domain of active PKG[88]. The resultant inhibition of PKG would reduce the level of PLN phosphorylation and reduce the activity of SERCA, resulting in both a slower rate of SR refilling and overall reduction in SR content per beat. As $I_{Ca\text{-}L}$ is unaffected by PKG inhibition, the proportion of calcium entering the cell would still be appropriately matched by Ca^{2+} effluxing the cell, but the slower rate of refilling of the SR may result in an incomplete refill upon the next beat. To test this hypothesis further a beat-by-beat time controlled experiment would be most useful, in which the SR would be depleted of Ca^{2+} using a saturating concentration of caffeine plus and minus the PKG inhibitor.

It is possible that the effects observed are due to non-specific interaction of KT-5823 with other target sites, however the dose (50nM) has previously been used in similar studies to investigate the role of PKG in cGMP signalling[231].

Due to animal type availability at the time of this data set, this set of experiments was performed exclusively in myocytes isolated from old sheep. Of those cells tested the recorded cell capacitance, $I_{Ca\text{-}L}$ and Ca^{2+} transient amplitude are demonstrated in Table 5. There existed no significant differences between cell capacitance or calcium transient

amplitude when compared with the young myocytes used in other experiments, with a trend for a reduced peak $I_{Ca\text{-}L}$ in the old cells (*p=0.067*). Any differences/lack of differences observed must be treated with caution as this group only contained and 4 animals and cells. A greater sample size may reveal actual differences as the Trafford group have previously shown that aged ventricular cells have greater cell capacitance, $I_{Ca\text{-}L}$ and Ca^{2+} transient amplitude[216]. Despite the underpowered nature of this data set, the present data suggests that in those cells tested with the PKG inhibitor, there was little difference between them and myocytes taken from young sheep, thus I believe the data can be reliably extrapolated into the young myocardium.

3.4.5 The effect of β-adrenergic stimulation on calcium handling

The next group of experiments sought to investigate the effect of *β-AR* stimulation on steady state calcium handling in normal sheep ventricular myocytes.

Cardiac myocytes are highly subjected to stimulation by the sympathetic nervous system. Agonism of *β*-adrenoreceptors on the sarcolemma results in a varied response, as detailed previously (section 1.2.1). Briefly, β_1 and β_2 adrenoreceptors are coupled with G-proteins, which activate AC, thus stimulating an increase in cAMP and the activation of PKA. β_3 adrenoreceptors couple to G-proteins, which stimulate guanylyl cyclase to generate cGMP, summarised in Figure 3.13B. The expression levels of the former are much greater than the latter, thus global, non-selective activation of sarcolemmal *β*-adrenoreceptors evokes an inotropic and lusitropic response in ventricular cardiac myocytes[41], predominantly due to β_1 dominance.

The response to *β*-AR stimulation in cardiac myocytes is well established and is reliant on compartmentalized cAMP signals[232] (Figure 3.13). Plasma membrane associated [cAMP] rise rapidly and transiently in response to *β*-AR stimulation[95], this activates PKA, which associates closely with the plasma membrane and L-type Ca^{2+} channels[68, 97, 98, 218]. This results in phosphorylation of sites on the L-type Ca^{2+} channel and in turn increases its open probability[92]. The data presented in this study concurs with this: marked increases in peak $I_{Ca\text{-}L}$ and the amount of calcium entering per beat. The phosphorylation of the L-type Ca^{2+} channel by PKA is most likely the main cause for the delayed rate of voltage-dependent $I_{Ca\text{-}L}$ inactivation, whereas the larger evoked calcium transient and thus a larger proportion of local cytosolic Ca^{2+} will result in a greater Ca^{2+} evoked inactivation of the $I_{Ca\text{-}L}$[233].

$I_{Ca\text{-}L}$ acts as the main trigger for intracellular Ca^{2+} release and thus the increase in peak $I_{Ca\text{-}L}$ following *β*-AR stimulation provides one explanation for the marked increase in systolic Ca^{2+} transient amplitude. It must also be noted that there was an increase in the decay rate of the Ca^{2+} transient under *β*-AR stimulation, which is most likely due to the PKA dependent phosphorylation of PLN[234], thus increasing the activity of SERCA. Furthermore, this in turn encourages more Ca^{2+} to be sequestered back into the SR per beat, which explains the observed increased SR content[104, 106, 235] and will also evoke increases in Ca^{2+} transient amplitude.

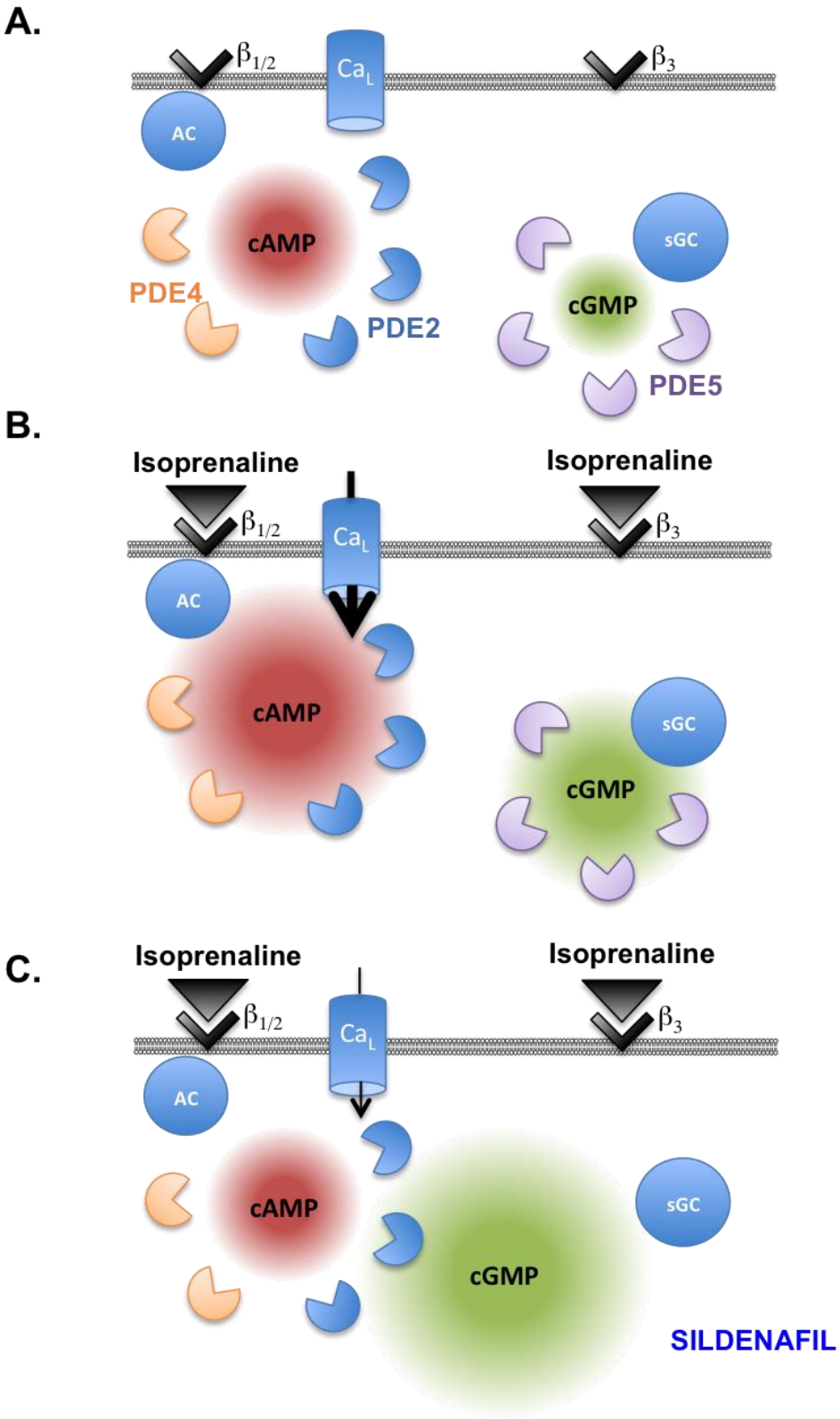

Figure 3.13 Mechanism of how PDE5 inhibition modulates β-AR Ca^{2+} handling

(A) Steady state compartmentalization of signals. (B) β-AR stimulation. (C) β-AR stimulation in the presence of the PDE5 inhibitor sildenafil. L-type Ca2+ channel (CaL); cyclic adenosine/guanosine monophosphate (cAMP/cGMP); adenylyl cyclase (AC); soluble guanylyl cyclase (sGC).

3.4.6 The effect of combined β-AR stimulation and PDE5 inhibition

In sheep ventricular myocytes, isoprenaline generated a positive inotropic response as facilitated by increased $I_{Ca\text{-}L}$, Ca^{2+} transient amplitude and SR Ca^{2+} content[179]. In addition, I have demonstrated PDE5 inhibition is negatively inotropic in these same cells. The next set of experiments sought to investigate the effect of a combined stimulation of the *β*-AR system and the inhibition of PDE5 in sheep ventricular myoyctes.

cAMP and cGMP are maintained in discrete cellular compartments in order to limit their signalling power (Figure 3.13A). Most studies investigating the interaction of these signalling cyclic nucleotides have been performed in murine species, thus the question remains to how they interact in sheep cardiac myocytes. Initial experiments sought to test the effect of cyclic nucleotide co-stimulation on $I_{Ca\text{-}L}$. As hypothesised and as described above, in cells exposed to the selective PDE5 inhibitor sildenafil, which will increase cytosolic [cGMP], $I_{Ca\text{-}L}$ was decreased. Conversely, in cells exposed to the non-selective *β*-AR agonist isoprenaline, which will increase cytosolic [cAMP], $I_{Ca\text{-}L}$ was increased. This demonstrates the polar relationship that exists between these two cyclic nucleotide second messengers. Interestingly, when applied in the presence of each other there appeared to be a unified response, a reduction in $I_{Ca\text{-}L}$. The PDE5 inhibitor was sufficient to eradicate the *β*-AR stimulated increases in $I_{Ca\text{-}L}$ and *β*-AR stimulation appeared, if not significant (which is most likely due to an underpowered data set), to exacerbate the effect of PDE5 inhibition.

A wealth of studies have previously investigated the effects of the cGMP-PKG axis on *β*-AR stimulated $I_{Ca\text{-}L.}$ Investigation into the interaction of cAMP and cGMP showed that exogenous cGMP was sufficient to blunt $I_{Ca\text{-}L}$ in frog[236] and guinea pig ventricular myocytes following prestimulation with isoprenaline or exogenous cAMP. Furthermore, Sumii and Sperelakis showed that exogenous PKG produced a similar degree of attenuation of $I_{Ca\text{-}L}$ responses to isoprenaline in rat ventricular myocytes[225]. This concurs with the findings presented in this study, and may provide some explanation to the mechanism by which PDE5 inhibition attenuates $I_{Ca\text{-}L}$ responses to *β*-AR stimulation in sheep ventricular myocytes. As I have not tested whether or not the direct effects of sildenafil on current are cGMP/PKG related, then I can only speculate as to the mechanism of action, but it may be that there is a requirement for the involvement of PDE2, which is allosterically stimulated by cGMP to increase cAMP hydrolysis. This could be confirmed with further work using a PDE2 inhibitor, and/or a PKG inhibitor/activator, in order to

evaluate which is more influential in determining the interaction between cAMP/cGMP signals and $I_{Ca\text{-}L}$ in the larger animal.

This study employed the use of a PDE5 inhibitor, which would increase cytosolic cGMP levels, however this effect has not directly been tested, thus are the effects seen here related to cGMP/PKG axis, or an allosteric effect of the inhibitor? The Ziolo group have used the PDE5 inhibitor zaprinast against responses to isoprenaline, and observed marked attenuation of $I_{Ca\text{-}L}$ in guinea pigs[237] and mice[166], which suggest that the responses observed in the present study are consistent with an actual effect of raised cytosolic cGMP levels.

To my knowledge this is the first study to test the effect of PDE5 inhibition against β-AR stimulated calcium handling in voltage clamped large animal ventricular myocytes. It is also the first to show that PDE5 inhibition not only reverses the effects on $I_{Ca\text{-}L}$ observed with isoprenaline, but also that isoprenaline may ($p=0.07$, n=4 cells /4 animals) exacerbate PDE5 inhibitor elicited decreases in $I_{Ca\text{-}L}$. Isoprenaline is a non-selective β-AR agonist, which, when applied to ventricular myocytes generates a cAMP/PKA dependent positive inotropic response (reviewed by Bers[41]). The signalling pathway here is summarized in Figure 3.13B. This response is associated with the activation of both β_1 and β_2 adrenoreceptors, which both couple to adenylyl cyclase. β_3 adrenoreceptors are also expressed in ventricular myocytes, which are associated with eNOS and sGC, thus stimulate the generation of cGMP. The application of isoprenaline to these cells will therefore appropriate a multifaceted intracellular signalling cascade resulting in the generation of not only cAMP, but also cGMP (Figure 3.13C). PDE5 is solely responsible for controlling the sGC derived pool of cGMP, and thus, when inhibited will prevent the hydrolysis of cGMP allowing this pool to spill over into other compartments. The proposed theory is that the close proximity of cGMP pools controlled by PDE5 and PDE2 (which solely controls membrane derived cGMP) facilitates the activation of PDE2 by uncontrolled isoprenaline stimulated sGC-cGMP. This in turn will encourage cAMP hydrolysis at the membrane and reduce the activity of PKA local to L-type Ca^{2+} channels; decreasing $I_{Ca\text{-}L}$ further.

As PDE5 inhibition can attenuate β-AR $I_{Ca\text{-}L}$ modulation, the next experiments sought to elucidate how PDE5 inhibition affects β-AR evoked changes in systolic Ca^{2+} transient. Kass *et al* have spent the past decade investigating the effect of PDE5 inhibition on calcium handling in murine ventricular myocytes. Their work has become the basis for the current study, in that experimental design was maintained consistent. They have shown on

multiple occasions that sildenafil has no effect on basal sarcomere shortening and Ca^{2+} transient amplitude in field stimulated myocytes[85, 162]. The present study has shown that in voltage clamped myocytes sildenafil significantly reduces basal Ca^{2+} transient amplitude. In previous studies sildenafil reduced isoprenaline induced myocyte contractility and Ca^{2+} transient amplitude in mice[85, 85, 162, 166, 221], which was not observed in sheep. The observed attenuation of β-AR stimulated Ca^{2+} transient amplitude in mice is dependent on the β_3-eNOS-sGC derived pool of cGMP[162, 221], which is consistent with literature surrounding the compartmentalisation of PDE5 signalling. Moreover, Lee et al showed that the effect of sildenafil on isoprenaline stimulated Ca^{2+} transients was unaffected by the selective PDE2 inhibitor, Bay 60-7550[221]. These studies did not measure SR Ca^{2+} content and only Wang *et al* used patch clamped myocytes, thus measured $I_{Ca\text{-}L}$, which as described was reduced also[166]. In sheep there was an increased SR Ca^{2+} content with isoprenaline, which was unaffected by PDE5 inhibition. Despite reductions in the trigger for SR Ca^{2+} release ($I_{Ca\text{-}L}$) with PDE5 inhibition following isoprenaline, it may be that the unaffected SR Ca^{2+} content is sufficient to maintain Ca^{2+} transient amplitude. This may highlight an important species difference for SR content:transient ratio between mice and sheep. The present study has shown that the Ca^{2+} transient is sensitive to PKG inhibition in the steady state, which may mean that an elevated PKG tone (following PDE5 inhibition) could increase SERCA activity, through PLN phosphorylation, and be paramount in the maintenances of SR Ca^{2+} content/Ca^{2+} transient amplitude in larger animals. One method to test this hypothesis would be to apply the PKG inhibitor KT-5823 alongside the PDE5 inhibitor in the presence of isoprenaline.

3.5 Study limitations

The present study has sought to understand the role of PDE5 and cGMP in normal Ca^{2+} handling in sheep ventricular myocytes. The results show that PDE5 inhibition with sildenafil reduces $I_{Ca\text{-}L}$ and Ca^{2+} transient amplitude, which has been concluded to be related to downstream effects of cGMP. This study has not used alternative PDE isoform inhibitors, thus the possibility of signal interaction and PDE cross-talk cannot be ruled out. An alternative approach would be to firstly use the non-specific PDE inhibitor IBMX to test the effects of individual PDE inhibitors against total PDE inhibition to give a better indication of the role of each isoform in the sheep ventricular myocyte.

Further, without selective markers for visualisation or inhibitors of cGMP and PKG in the presence of the PDE5 inhibitor then it is difficult to conclude that the observations reported for the effects on Ca^{2+} handling are due to activation of these pathways. However, I believe that the findings of the present study in conjunction with that observed by others provides a good indication that the effects observed here are reflective of an activation of the cGMP-PKG axis.

Due to experimental constraints the effects of PDE5 and PKG inhibitors were not tested against caffeine responses to provide data for SR Ca^{2+} content. The limitation here is that the lack of this evidence makes it difficult to conclude their effects on the Ca^{2+} transient. In addition, further work to elucidate the effect of these inhibitors on SR Ca^{2+} content would reveal any changes occurring in the activity of SERCA.

In addition to the work required to further the present data set as alluded to above, more experiments would be required to answer questions such as the effects of PDE5 inhibition on SR content. Such experiments are discussed in more detail in Chapter 6.4.

3.6 Conclusion

The work presented in this first chapter has shown that in normal ovine ventricular myocytes there exists a tonic level of cGMP, which interacts with Ca^{2+} handling proteins and is specifically hydrolysed by PDE5. Upon inhibition of PDE5 it may be speculated that increases in cGMP are sufficient to decrease steady state $I_{Ca\text{-}L}$ and systolic Ca^{2+} transient, which may be dependent on changes in activity of PKG, PDE2 or both. When ovine ventricular mycoytes were challenged with a β-AR agonist, $I_{Ca\text{-}L}$, Ca^{2+} transient amplitude and SR Ca^{2+} content were augmented. As previous studies in murine models have shown that PDE5 inhibition can attenuate responses to β-AR induced contractility it was surprising to see little effect on the Ca^{2+} transient, despite a reversal in β-AR stimulated $I_{Ca\text{-}L}$ by PDE5 inhibition. It is concluded that a preservation of SR Ca^{2+} content following PDE5 inhibition in the presence of β-AR stimulation facilitates maintained Ca^{2+} transient amplitude, which may highlight important physiological differences between small and large mammals.

The next chapter will seek to investigate the effect of PDE5 inhibition in heart failure.

Chapter 4

4 The effect of PDE5 inhibition on calcium handling in failing ovine cardiac myocytes

4.1 Introduction

Heart failure is one of the leading causes of morbidity and mortality in the western world[1]. It is associated with reduced cardiac contractility observed at both the level of the single myocyte[238] and whole heart[104]. Attenuated β-AR signalling is a hallmark of heart failure[239] and a number of therapeutic strategies have been designed to restore normal functioning in the failing heart. However, targeting of the symptoms of HF or slowing its progression, as is the aim of most current treatment strategies[4, 175, 240], is not necessarily a treatment. Thus further understanding of the molecular mechanisms underlying HF is fundamental for future therapeutic strategies.

4.1.1 Current therapeutic strategies for HF

In order to sustain cardiac contractility in HF patients, many have investigated targeting the β-AR signalling pathway. The most successful strategy is the use of β-blockers in human HF, which improves survival in these patients[3, 241], but is most commonly administered as an adjunct therapy alongside angiotensin-converting enzyme inhibitors. The main aim of β-blockers is to attenuate the exacerbated catecholamine levels circulating in HF patients[242]. Their mechanism of action is poorly understood and their use remains paradoxical: to administer a negatively inotropic agent to an already cardiac-compromised patient. Nonetheless β-blockers are associated with reduced HR, BP and a decreased prevalence of arrhythmias. However, the effect of such therapy on Ca^{2+} handling has remained unclear for many years. PKA hyperphosphorylation has been suggested as an important component in the failing ventricle, yet a rather controversial topic. In a series of experiments, Marx and Reiken et al found that the RyR is an important target for PKA phosphorylation and results in defective channel function in HF[25]. They further showed that in dog tachypaced HF, β-1 blockade resulted in RyR Ca^{2+} release[205, 206] and ultimately restored cardiac function in human HF[12].

It is well known that the cAMP-PKA axis is reduced in failing hearts[243]. Recently, Briston et al investigated the effect of HF on Ca^{2+} handling in the failing sheep ventricle, finding that $I_{Ca\text{-}L}$ and Ca^{2+} transient amplitude were reduced in failing ventricular myocytes, which were markedly less responsive to β-AR stimulation than normal sheep myocytes[179]. As HF results in a multifaceted attenuation of intracellular signalling it seems almost inappropriate to non-selectively inhibit the system in order to modulate excessive Ca^{2+}

signalling, as is the case with β-blocker therapy. In light of this, downstream effectors of the β-AR signalling cascade have been targeted as potential therapies for HF.

4.1.2 PDEs in HF

Restoration of β-AR signalling and Ca^{2+} handling in the failing myocardium has been achieved by targeting PDEs in order to exert greater control over cyclic nucleotide signalling. Selective PDE inhibition has been used to treat a variety of cardiovascular diseases including intermittent claudication[244], COPD[245], pulmonary hypertension[246], erectile dysfunction[247], and heart failure[248].

Heart failure is associated with the downregulation of cAMP-PDEs in the left ventricle[249, 250, 136]. In genetic knockdown models, PDE3/4 null mice did not spontaneously develop HF, which suggests their downregulation reflects a compensatory mechanism to maximise cAMP signalling to maintain ventricular contractility, rather than being the primary cause of pathology[251]. In the clinic, cAMP-PDE inhibitors have been used to combat the reduced inotropic reserve in HF patients with great success. PDE3 inhibitors milrinone, amrinone and anoximone have been used to treat congestive HF resulting in greater inotropy and chronotropy[252, 253, 254, 255]. PDE3 inhibition results in enhanced phosphorylation of L-type Ca^{2+} channels[256], RyR and PLN[257], leading to greater SR loading and release. Furthermore, milrinone decreased vascular resistance and enhanced coronary blood flow providing greater clinical benefit than either inotropic agents or vasodilator agents alone[254]. However, these beneficial effects of PDE3 inhibition occur only in the short term as chronic treatment in severe HF results in increased SR Ca^{2+} leak manifesting in fatal ventricular arrhythmias and sudden cardiac death[240, 258]. Moreover, PDE3 inhibition in juxtaglomerular cells leads to increased renin secretion, which ultimately exacerbates the HF phenotype[259]. Their detrimental effect in HF patients has since limited the use of PDE3 inhibitors in the clinic to more short term inotropic enhancing roles in patients undergoing cardiac surgery and for weaning from cardiac bypass[260, 261]. Selective inhibition of PDE4 has yielded similar effects as observed following PDE3 inhibition in HF patients[250], and their use is mainly limited to treating other disorders such as asthma and COPD[262].

4.1.3 PDE5 as a therapeutic target

In 1998 the popularity of PDE5 rose exponentially as its selective inhibitor sildenafil became the first oral medication for impotence[263]. Since then PDE5 has become the target of therapeutic strategies for pulmonary hypertension[264] and more recently HF[265]. There exists a paradoxical relationship between brief periods of myocardial ischaemia and

cardioprotection to injury such as myocardial infarction[266]. The activation of a cGMP-dependent signalling pathway is known to govern such protective effects in the heart, which led to an understanding that PDE5 inhibition is beneficial to the failing myocardium[267, 268]. This concurs with reports of increased cGMP-PDE expression in HF[269, 270]. PDE5 inhibition with sildenafil has subsequently been shown to reduce ventricular arrhythmias in dogs[271], prevent and reverse cardiac hypertrophy in mice[123, 272], increase inotropy and chronotropy in dogs[273] and restore cellular contractility in failing mouse myocytes[274]. Altogether these promising effects have led to a small-scale clinical trial in humans, which after 1 year of treatment revealed improvements in systolic and diastolic function in those patients[265].

4.1.4 Aims

The literature surrounding the beneficial effect of PDE5 inhibition on Ca^{2+} handling in HF is relatively limited and to my knowledge non have investigated the effect of PDE5 inhibition in voltage clamped myocytes in a large animal model of HF. Thus the principle aims of this chapter are as follows:

- To investigate whether 4 weeks of tachypacing alters Ca^{2+} handling in sheep ventricular myocytes to the same extent as that observed in end-stage HF.
- Are there any such alterations in responsiveness to β-AR stimulation?
- To investigate the effect, if any, of acute PDE5 inhibition on Ca^{2+} handling in failing cardiac myocytes.
- To investigate any differences in steady state Ca^{2+} handling in cardiac myocytes following chronic PDE5 inhibition.
- Can chronic treatment with a PDE5 inhibitor be beneficial in heart failure through alteration to myocyte sensitivity to β-AR stimulation?

4.2 Methods

4.2.1 Experimental animals

As described previously, all animal experiments were performed in accordance with the Home Office Animal (Scientific Procedures) Act 1986. Young adult female wild type sheep (<18 months of age) were used in experimental models unless otherwise stated.

4.2.2 Large Animal Model of Heart Failure

The Trafford laboratory employs the use of an ovine tachypacing model of dilated cardiomyopathy[179]. Heart failure was induced by the insertion of a pacemaker with pacing leads in the right ventricle to rapidly pace the heart for approximately 4 weeks (model depending).

4.2.3 Detail of surgical intervention

4.2.3.1 Anaesthesia

Anaesthesia was administered initially through a passive ventilator using a gas mask and a breathing combination of 2-chloro-2-(difluoromethoxy)-1,1,1-trifluoro-ethane (5% Isoflurane) and a mix of 4L/min oxygen and 4L/min air. Isoflurane is a halogenated ether and, as with many anaesthetics, its mechanism of action is incompletely understood, however it acts to decrease nociception and relax muscles. The eye blink reflex was used as a test for depth of anaesthesia and when lost the animal was deemed sufficiently 'under' to be transferred to a positive pressure mechanical ventilator. To facilitate this, tracheal intubation was performed using a veterinary laryngoscope. Initially, upon depression of the epiglottis and visualisation of the glottis a local anaesthetic was applied topically (xylocaine) to paralyse the pharynx, thus allowing the easy passage of a tracheal tube (type, size) into the trachea. It is difficult to 100% confirm correct tube placement however visualisation, breath sounds and the tidal movement of a ventilator bag were used as a guide. Upon successful tracheal tube placement a balloon cuff located on the tube was inflated to seal the tracheobrachial tree from leakage of ventilated gases and to prevent any pulmonary aspiration of gastric contents, mucus, blood etc. Finally, the tube was secured to the lower jaw of the animal using a fast-release, simple bow-tie.

Ventilation was achieved using a mechanical tidal ventilator, keeping ventilation rate at around 15 breaths per minute, a flow rate of 4L/min oxygen and 4L/min air, and constant anaesthesia with 3% isoflurane.

The depth of anaesthesia was constantly monitored using the eye blink reflex rule of thumb as described above, as well as the recording of a multitude of vital signs. An electronic sphygmomanometer (*Cardell Veterinary Monitor 9402, Sharn, USA*) fitted with a tail cuff for arterial plethysmography was used to assess blood pressure. A laser Doppler pulse oximeter was used to determine arterial oxygen saturation and a five lead electrocardiogram (ECG) recording was used to monitor heart rate.

4.2.3.2 Actions against pain and infection and blood loss

Animals were treated with a long lasting analgesic (meloxicam 0.5mg/kg) and a long lasting antibiotic (oxytetracycline 20μg/kg), administered subcutaneously using a 21G needle, upon induction of anaesthesia. During surgery blood loss was kept to a minimum although to prevent hypovolemia an intravenous catheter was inserted into the cephalic vein to infuse 0.9% saline (NaCl) at a rate of 10ml/kg/hr.

4.2.3.3 Pacing lead positioning and pacemaker implantation

Once stably anaesthetised the first approach was to isolate the right jugular vein. An incision approximately 4cm long was made using an 11 blade scalpel and the jugular was isolated using blunt dissection. The rostral end of the vein was ligated with a 2.0 silk suture tie and the caudal end was temporarily occluded using an untied suture; any venous branches were ligated as above. A small incision was made to gain access to the jugular lumen and a pacemaker lead (Medtronic) was advanced caudally. The position of the lead was tracked using fluoroscopy, which employs x-rays in order to provide a real-time image, as shown in Figure 4.1A. The lead was tracked along the jugular, into the superior vena cava and into the right atrium. In order to position the pacing lead at the apex of the right ventricle the guide stylet within the pacing lead, which provides stability during insertion, was switched for one with a slight curve in it. Changing the angle of the lead tip facilitated an easy advance across the tricuspid valve and into the right ventricle. Once positioned at the apex (Figure 4.1) the lead was secured in place: depending on the lead make and model this was achieved either passively with tines located at the tip of the lead (Figure 4.1B, left), which anchor the lead to the trabecular network at the apex, or actively fixed using a screw device deployed from within the tip of the lead (Figure 4.1B, right), which fixes the lead to the ventricular wall. As tested by a pacemaker programmer, lead placement was tested by ensuring an R-wave greater than 10mV, an impedance of 500-1000Ω and a pacing threshold of less than 4.

For the majority of animals, single lead pacing was achieved through the attachment of a double-header device (Figure 4.1D). This device quite simply takes two inputs, which can be connected to the two channels on the pacemaker (Figure 4.1C, Medtronic Adapta/Sensia) and converts it to a single output, i.e. the single ventricular pacing lead. In some cases two pacing leads were inserted, without the need for a double header device. In these instances two leads were affixed to the RV apex (not shown). Alternatively an intracardiac device (ICD), with a single lead was positioned exactly as described above (not shown). In all cases the leads were secured at the point of entry at the jugular using silk 2.0 sutures. Where needed a double header device was attached and the free ends of the pacing leads were secured into a pacemaker device. The pacemaker box and any excess lead were positioned within a muscular pocket above the jugular and securely closed using silk 2.0 sutures. The implant wound was closed in 3 layers, closing the muscular fascia, the subdermal tissue and finally the cutaneous layer.

The animal was recovered from anaesthesia in isolation before being returned to shared housing. No further intervention was performed for one week in order to ensure full recovery from surgery as well as to allow the pacing leads to settle in their intracardiac positions.

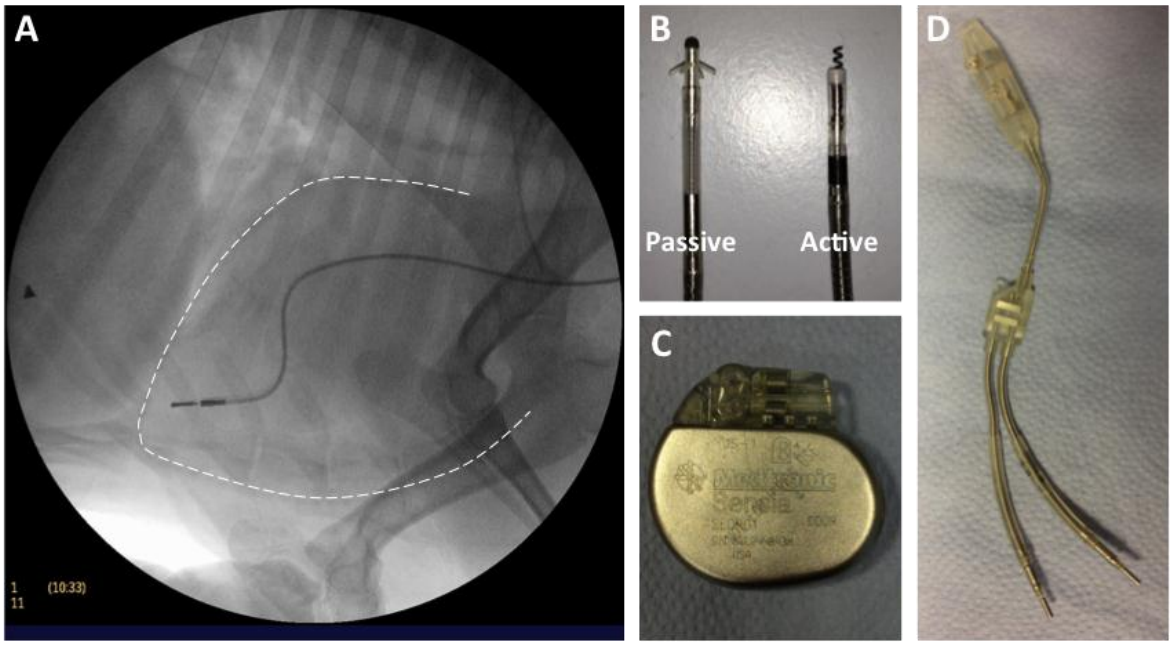

Figure 4.1 Pacing devices

(A) Fluoroscopy image demonstrating lead positioning at the right ventricular apex. Dotted line has been added for orientation purposes. (B) Two types of lead fixing are used, either Passive fix, which has a tined end to secure the lead to trabeculae, or an Active fix, which deploys a screw from the head of the pacing lead to secure it to the ventricular wall. (C) Pacemaker device, contains the battery and lead sockets (at the top of the image), programmable via telemetry. (D) A custom-built double-header device, enabling ventricular pacing from a single lead.

4.2.4 Pacing parameters

The implanted pacemaker can be communicated with non-invasively using a telemetry device connected to a pacemaker programmer (Medtronic). Animals were seated under gentle restraint and connected to a 5 lead electrocardiogram (ECG) whilst the pacemaker was interrogated.

Pacemaker programming works via a 3 letter code: Pacing, Sensing, Response if sensed, which corresponds to the cardiac chamber being paced or sensed. The code follows that V = ventricle, A=atria, D=Both/dual, O=none. Such that VVI mode describes ventricular pacing, ventricular sensing, inhibit if sensed.

Pacing was initiated at 3 times the resting heart rate (e.g. from 70bpm to 210bpm) by programming the pacemaker to (1) single lead configuration: DOO, lower rate 105bpm, (2) two lead configuration: VOO, lower rate 210bpm, or (3) an 'in house' high rate pacing override patch was programmed to facilitate tachypacing through an ICD, 214bpm.

For the 4-week HF animals (n=10) pacing was maintained for 29.9±1.1 days and for end-stage HF animals (n=5) were paced for 42.6±4.1 days. Importantly the pacemaker was switched to ODO (off) mode at least 10 minutes before the measurement of any in vivo data collection.

4.2.5 Tadalafil treatment protocol

The current study aimed to test the effect of a specific PDE5 inhibitor on HF. Animals to be treated (n=15) were implanted at the same time as those destined for 4-week pacing and after 29.1±1.4 days, were given one tadalafil tablet (20mg, Cialis, Eli Lilly) every day taken orally for the next 22±0.6 days whilst the pacing was continued (Figure 4.2).

Figure 4.2 Pacing protocol

Animals were allowed to recover for one week after pacemaker implant before the pacemaker was switched to VOO/DOO, facilitating a myocardial tachypacing of 210bpm as assessed by ECG. Pacing was continued for a further 4 weeks for those animals in the 4-week HF group, at which point they were sacrificed with a lethal injection of pentobarbitone. Animals destined for tadalafil treatment were fed one 20mg Cialis tablet every day for the next three weeks before being euthanised. Animals destined for 'end-stage' HF were sacrificed when symptoms of HF were presented: ascites, dyspnea, cachexia.

*4.2.6 **Molecular Techniques***

4.2.6.1 Protein Sample Preparation and Quantification

At the point of heart removal full thickness ventricular samples were dissected and snap frozen in liquid nitrogen and stored accordingly for use later. When necessary these frozen ventricular samples were defrosted for protein extraction and homogenised on ice in cold radioimmunoprecipitation assay (RIPA) buffer containing protease inhibitors (0.1 mg/ml phenylmethylsulfonyl fluoride; PMSF, 100mM sodium orthovanadate, 1 mg/ml aprotonin and 1 mg/ml leupeptin). Insoluble material was removed by centrifugation (1300 x *g* 2^{o}C, 10 min) and samples were stored at -80^{o}C until use.

Substance	Concentration
Phosphate Buffered Saline	Total volume
Igepal CA360	1%
Sodium deoxycholate	0.5%
SDS	0.1%

Table 8 RIPA Buffer

Protein sample concentration was determined using a colorimetric assay; Bio-Rad DC Protein Assay (Hercules, USA). The assay was carried out on a 96-well plate and absorbance values of the resulting reduced species, which have a characteristic blue colour with absorbance between 405nm and 750nm, were quantified using a spectrophotometer and Gen5 analysis software (BioTEK).

4.2.6.2 Sodium Dodecyl Sulfate – Polyacryllamide Gel Electrophoresis (SDS-PAGE)

Protein separation was achieved by Western blotting. using Novex Bis-Tris or Tris-Acetate gels (NuPAGE, Invitrogen, USA). Samples were heated to 75^{o}C for ten minutes with Novex sample buffer and reducing agent. Samples were loaded alongside the molecular weight marker and an internal control and run at 150-200V in running buffer containing 500µl NuPAGE Antioxidant, which maintains the proteins in a reduced state during gel electrophoresis.

4.2.6.3 Protein transfer to nitrocellulose membrane

Proteins were transferred to Hybond-C nitrocellulose membranes (Amersham, UK) using the *XCell SureLock Mini-Cell* electronic transfer kit (Invitrogen, USA). Blotting paper and nitrocellulose membrane were cut to size to match the gels and stacked along with foam pads to form a cassette to be inserted within the transfer chamber between the anode and cathode. The transfer chamber was filled with transfer buffer containing methanol, which prevents gel swelling, and antioxidant (as before), and run at 25V for 75 minutes.

Successful protein transfer was assessed by incubation with 10ml Ponceau-S solution (Sigma-Aldrich) for 5 minutes (Figure 4.3), and subsequently washed off using TBS-T.

4.2.6.4 Blocking and Antibody

False-positive results may be observed if the primary antibody binds non-selectively to areas on the nitrocellulose membrane outside of the protein of interest band. In order to prevent this, the membrane was blocked with a dilute protein solution. The nitrocellulose membrane was incubated in blocking solution (refer to Table 2 for different blocking proteins used) for 1 hour at room temperature on a rocking table to ensure all the membrane was exposed to blocker. Membranes were then washed 3 times with TBS-T before being incubated for 16 hours at 4^{o}C with primary antibody (*see Table 2*), which was prepared in a dilute solution of blocker.

4.2.6.5 Protein detection

Following immunoblotting, membranes were washed 3 times with TBS-T and incubated for a further 1 hour at room temperature with a horseradish peroxidise (HRP) conjugated secondary antibody, which had been raised in the same species as the primary antibody. Following a final 3 times wash with TBS-T, the nitrocellulose membrane was prepared for immunodetection using the Pierce Super Signal® West Pico Chemiluminescent system. Preparation involves incubation of the membrane with 1ml of a chemiluminescent substrate and 1ml of a luminol-enhancer solution for 5 minutes. The HRP-conjugated secondary antibody catalyses the hydrolysis of the chemiluminescent substrate, which results in a signal generation and is detected by a digital imaging system (Syngene Chemi Genius Bio Imaging System or FluorChem 8900, Alpha Innotech). Representative blots are shown in Figure 4.3.

4.2.6.6 Data Acquisition and Analysis

Quantification of band intensity was performed using the GeneSnap band quantification software and compared to the intensity of the internal control band to provide a corrected value. Values are representative of mean±SEM of three repeats and are shown as protein expression in control versus heart failure. Statistical significance was determined using a student's t-test and determined as $P<0.05$.

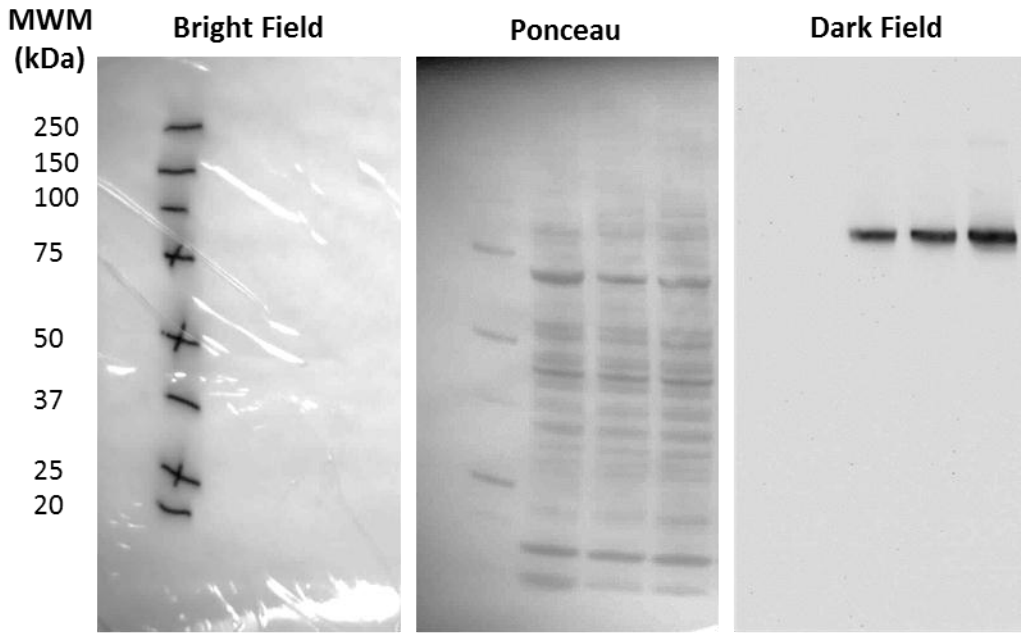

Figure 4.3 Western blot band detection

Representative blot to demonstrate the different band sizes shown by the molecular weight marker (MWM) in the bright field image and all proteins detected by ponceau staining. Dark field shows the protein of interest imaged following HRP-conjugated antibody staining.

Target Protein	W.Blot method used	Total amount of protein loaded (µg)	Blocking Solution	Primary Antibody	1° Ab. dilution	Secondary Antibody	2° Ab. dilution
PDE3A	Poly-acrylamide	20	Superblock, Thermo Scientific 1hr @ Room temperature	Santa Cruz, sc-11830. Polyclonal goat	1:1000	Santa Cruz. HRP-conjugated anti-goat raised in donkey.	1:5000
PDE4B	Bis-Tris	20	Superblock, Thermo Scientific 1hr @ Room temperature	Santa Cruz, sc-25812. Polyclonal rabbit.	1:200	Santa Cruz. HRP-conjugated anti-rabbit raised in goat.	1:40000
PDE4D	Bis-Tris	10	Superblock, Thermo Scientific 1hr @ Room temperature	Santa Cruz, sc-25814. Polyclonal rabbit	1:500	Novis. HRP-conjugated anti-rabbit raised in donkey.	1:10000
SERCA2A	Bis-Tris	5	Superblock, Thermo Scientific 1hr @ Room temperature	Santa Cruz, sc73022. Monoclonal mouse	1:5000	Santa Cruz. HRP-conjugated anti-mouse raised in goat.	1:40000
PLN_T	Bis-Tris	5	Superblock, Thermo Scientific 1hr @ Room temperature.	Badrilla A010_14. Monoclonal mouse	1:10000	Santa Cruz. HRP-conjugated anti-mouse raised in goat.	1:40000
P-PLN_{Ser16}	Bis-Tris	20	Superblock, Thermo Scientific 1hr @ Room temperature	Badrilla A010_12. Polyclonal rabbit.	1:10000	Santa Cruz. HRP-conjugated anti-rabbit raised in goat.	1:40000
P-PLN_{Thr17}	Bis-Tris	20	Superblock, Thermo Scientific 1hr @ Room temperature	Badrilla A010_13. Polyclonal rabbit.	1:5000	Santa Cruz. HRP-conjugated anti-rabbit raised in goat.	1:40000

Table 9. Summary of Western blot reagent sources and conditions

Phosphodiesterase (PDE); Sarco-endoplasmic reticulum Ca^{2+} ATPase (SERCA); phospholamban total (PLN_T); phosphorylated phospholamban Serine 16 (P-PLN_{Ser16}); phosphorylated phospholamban Threonine 17 (P-PLN_{Thr17}). PDE4B blot performed by Miss Jessica Caldwell.

4.2.7 Radioactive PDE activity assay

The activity of the cAMP and cGMP hydrolyzing PDEs were measured using a radioactive assay based on the method of Thompson and Appleman with some modifications[275]. Experiments were supervised and contributed to by Dr Hind Mehel in the laboratory of Professor Rodolphe Fischmeister in INSERM, University Paris-Sud.

The assay relies on active PDE isoforms present within a protein sample to hydrolyse tritium bound 3',5'-cAMP/cGMP (1 µM cAMP and 10^5 cpm ^{3}H-cAMP; 5 µM cGMP and 10^5 cpm ^{3}H-cGMP) into 5'-AMP/GMP, which is further hydrolysed into ^{3}H-adenosine/guanosine using snake venom. The degree of radiation detected corresponds to the activity of PDEs present. This assay identifies total cAMP- or cGMP-hydrolytic enzyme activity, which can be compared to samples in which selective PDE inhibitors have been added in order to calculate the relative hydrolytic contribution of a particular PDE isoform. Selective PDE inhibitors used are summarized in Table 10.

PDE isoform	Selective PDE inhibitor	Concentration (µM)
PDE2	BAY 60-7550	0.1
PDE3	Cilostamide	1
PDE4	Rolipram	10
PDE5	Sildenafil	1

Table 10. Summary of PDE inhibitors used to determine relative PDE isoform activity

Total PDE activity is used to compare the observed activities in the presence of different PDE inhibitors in order to determine the relative contribution of cyclic nucleotide hydrolysis by each isoform. PDE2 has a dual specificity for cAMP and cGMP, PDE3 and PDE4 are selective for cAMP and PDE5 is selective for cGMP.

The relative PDE activity was determined by subtracting activity with inhibitor from the total PDE activity. Each relative activity was presented as a percentage of total activity and repeats were expressed as mean ± SEM. Data was interpreted in Sigma plot and samples from control animals were compared with samples from heart failure animals using a Student's t-test. Significance was determined as $p<0.05$.

4.2.8 Cyclic nucleotide assay

The assessment of the availability of cAMP and cGMP in a protein sample was performed using the Cell Signalling Technology cAMP and cGMP XP Assay Kit. The protocol was carried out according to the manufacturer's instructions. In brief, the assay was performed

in 96-well plates coated with an anti-cAMP/cGMP rabbit monoclonal antibody to which tissue homogenates and a fixed amount of HRP conjugated cAMP/cGMP were added. The cAMP/cGMP within the test sample competes with the HRP conjugate samples for the antibody bound to the plate. Upon the addition of a HRP substrate a colour change develops, which was read at 405nm by a plate reader. The competitive nature of this assay means that the magnitude of the absorbance is inversely proportional to the amount of cyclic nucleotide present within the test sample.

In order to accurately determine cAMP/cGMP concentration a standard curve was produced using different known concentrations of cAMP/cGMP. Each sample of interest was repeated 3 times and normalized to a blank sample containing no protein/cyclic nucleotide sample. The data was analysed using Sigma plot and presented as relative cyclic nucleotide concentration to show differences between cyclic nucleotide bioavailability between control, heart failure and tadalafil treated tissue samples. Significance was assessed using a one-way ANOVA and represented as $p<0.05$.

4.3 Results

4.3.1 The effect of the time course for pacing on cellular electrophysiological characteristics

Our laboratory has developed and utilised an ovine tachypaced model of HF[179, 276, 277]. This involves rapidly pacing the heart beyond physiological levels, 210bpm, which restricts diastolic filling and over time results in a reduced cardiac output, leading to HF. Traditionally this laboratory determined the end point of the experiment as the presentation of clinical symptoms of HF (dyspnea, cachexia, peripheral oedema), which would present between 4 and 8 weeks of pacing. The present study used this established model and incorporated a chronic drug treatment strategy. As symptoms often present from 4 weeks the present study used this as the heart failure time point, from which drug treatment was given for a further 3 weeks.

In order to assess HF at the 4-week pacing time point preliminary experiments sought to test the difference between Ca^{2+} handling in isolated ventricular myocytes from HF animals paced until 'end-stage' and myocytes from animals paced for 4-weeks. Table 11 shows there were no differences between the two groups of paced animals for the main cellular electrophysiological characteristics: cell capacitance, $I_{Ca\text{-}L}$, Ca^{2+} transient amplitude, and SR Ca^{2+} content.

	esHF	**4 wk**	***n***
Cell capacitance (pF)	163.40±24.60	162.70±16.00	6/4
Peak $I_{Ca\text{-}L}$ (pA.pF^{-1})	2.88±0.43	2.72±0.40	3/2
Ca^{2+} transient amplitude ($R_{340/355}$)	0.014±0.002	0.018±0.003	4/4
SR Ca^{2+} content (μmoles.L^{-1})	20.51±6.68	15.22±6.59	2/4

Table 11. Cellular electrophysiological differences with paced duration

End-stage HF (esHF); 4-week paced HF (4 wk). n = number of cells/ number of animals. Mean ± SEM. Differences compared using Student's t-test.

As no differences were observed between the two time courses of pacing, the proceeding group of experiments will be representative of mean data from a mixture of animals paced for 4-weeks and paced until end-stage. The group will therefore be generically termed HF, unless otherwise stated.

4.3.2 The effect of heart failure on $I_{Ca\text{-}L}$

HF is defined as being the inability for the heart to pump enough blood to meet the demands of the body. HF is associated with both diastolic and systolic impairments. $I_{Ca\text{-}L}$ is important for myocardial contractility and has previously been reported to play a role in the systolic dysfunction of HF[278]. This experiment sought to test whether $I_{Ca\text{-}L}$ is impaired in sheep ventricular myocytes following tachypacing.

Ventricular myocytes were isolated and voltage clamped in the whole cell configuration. Table 12 shows little difference in the cell capacitance recorded between myocytes from control animals and those from animals in HF.

	Control	**HF**
Cell capacitance (pF)	153.5±13	163.0±13
RC of voltage-dependent $I_{Ca\text{-}L}$ inactivation (s^{-1})	54.1±2	49.1±5
RC of Ca^{2+}-dependent $I_{Ca\text{-}L}$ inactivation (s^{-1})	207.9±10	182.7±14*

Table 12. Electrophysiological differences in heart failure

*Mean±SEM, control n=20 cells/13 animals, HF n=11-12/6. Comparisons described using a Student's t-test, *p<0.05.*

In myocytes taken from normal animals peak $I_{Ca\text{-}L}$ was 6.12±0.5 $pA.pF^{-1}$ as shown by the representative black trace in Figure 4.4*A*. Peak $I_{Ca\text{-}L}$ is summarized in the histogram in Figure 4.4B, which was 55±5% smaller in HF myocytes than in control (2.78±0.23 $pA.pF^{-1}$). This reduction in $I_{Ca\text{-}L}$ was associated with a 48±6% reduction in Ca^{2+} influxing into the cell (Figure 4.4*C*) between control 1.75±0.13 $\mu moles.L^{-1}$ and HF 0.91±0.09 $\mu moles.L^{-1}$.

The kinetics of the $I_{Ca\text{-}L}$ are summarised in Table 12. HF myocytes appeared to show no difference in the voltage dependent portion of inactivation of the $I_{Ca\text{-}L}$, however exhibited a slower rate of calcium-dependent inactivation.

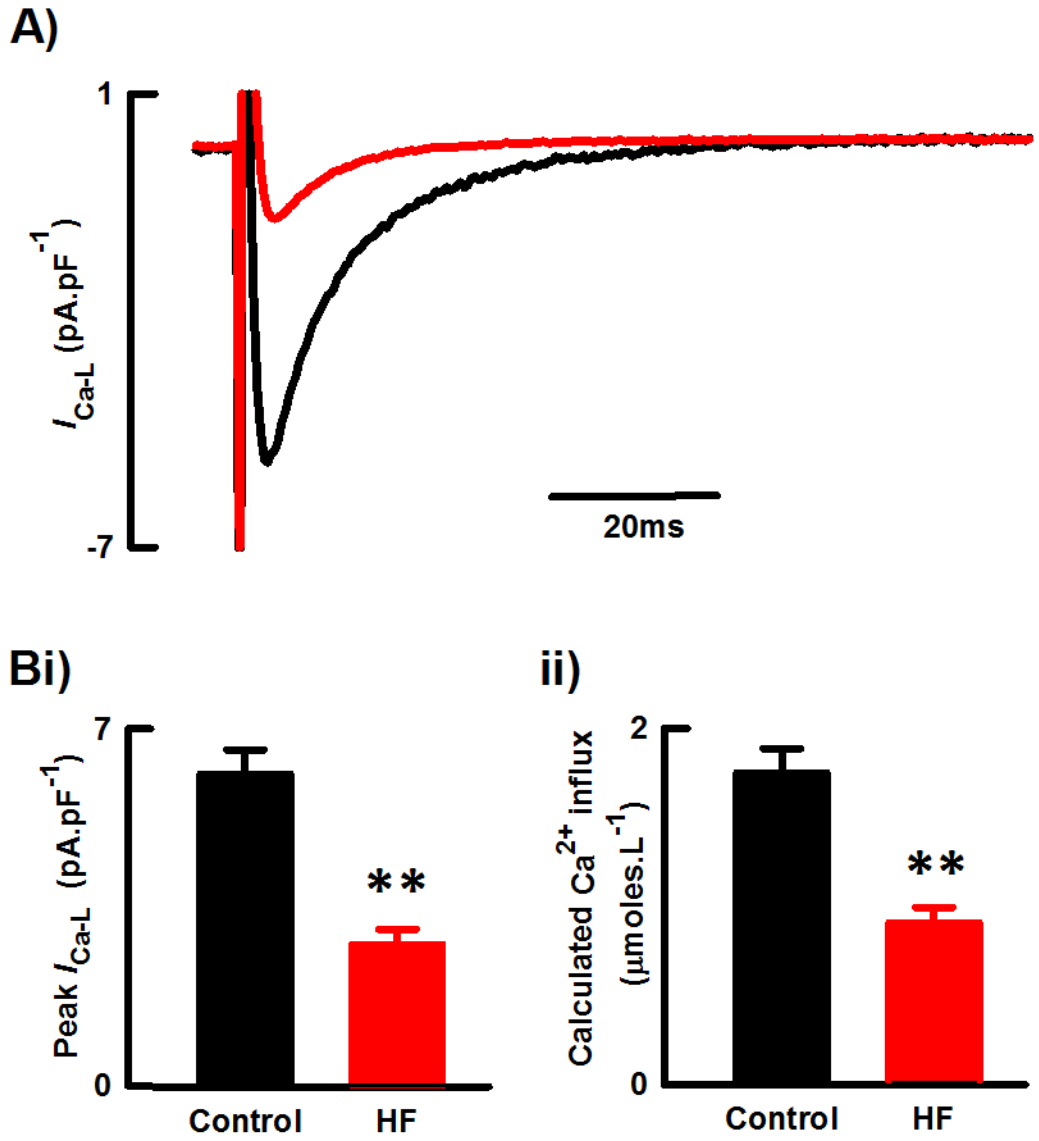

Figure 4.4 The effect of heart failure on I_{Ca-L}

*(A) Typical I_{Ca-L} recording from control (black) and failing (red) sheep left ventricular myocytes. (B) Mean data for the effect of heart failure on (i) peak I_{Ca-L} and (ii) calculated Ca^{2+} influx. Mean ± SEM, statistical significance assessed using a Student's t-test. **vs control p<0.01. Control n=20 cells/13 animals. HF n=11-12/6.*

4.3.3 The effect of heart failure on the systolic Ca^{2+} transient

Changes in the $I_{Ca\text{-}L}$ observed in HF may cause changes in the systolic Ca^{2+} transient. This was investigated by loading cells with the Ca^{2+} indicator Fura-2 as described (section 2.2.3).

Figure 4.5*A* shows a typical Ca^{2+} transient recorded from a voltage clamped normal sheep myocyte. Ca^{2+} transient amplitude was 34% lower in HF myocytes (Figure 4.5*A/B*, 0.015±0.002 $R_{340/355}$) than in control (0.023±0.007 $R_{340/355}$). Despite changes in amplitude, HF appeared to have no effect on the rate constant of decay of the Ca^{2+} transient (Figure 4.5*C*, control: 1.4±0.2 s^{-1}, versus HF: 1.3±0.2 s^{-1}).

In additional experiments SR Ca^{2+} content was measured by applying a saturating dose of caffeine to voltage clamped myocytes. SR content in normal cells was measured as 17.7±4 μmoles.L^{-1} (*n*= 8 cells/ 8 animals), which was shown to be no different in HF, 18.8±5 μmoles.L^{-1} (*n*=5/2). The attenuated Ca^{2+} transient observed in HF myocytes is thus most likely due to the reduced trigger for Ca^{2+} release.

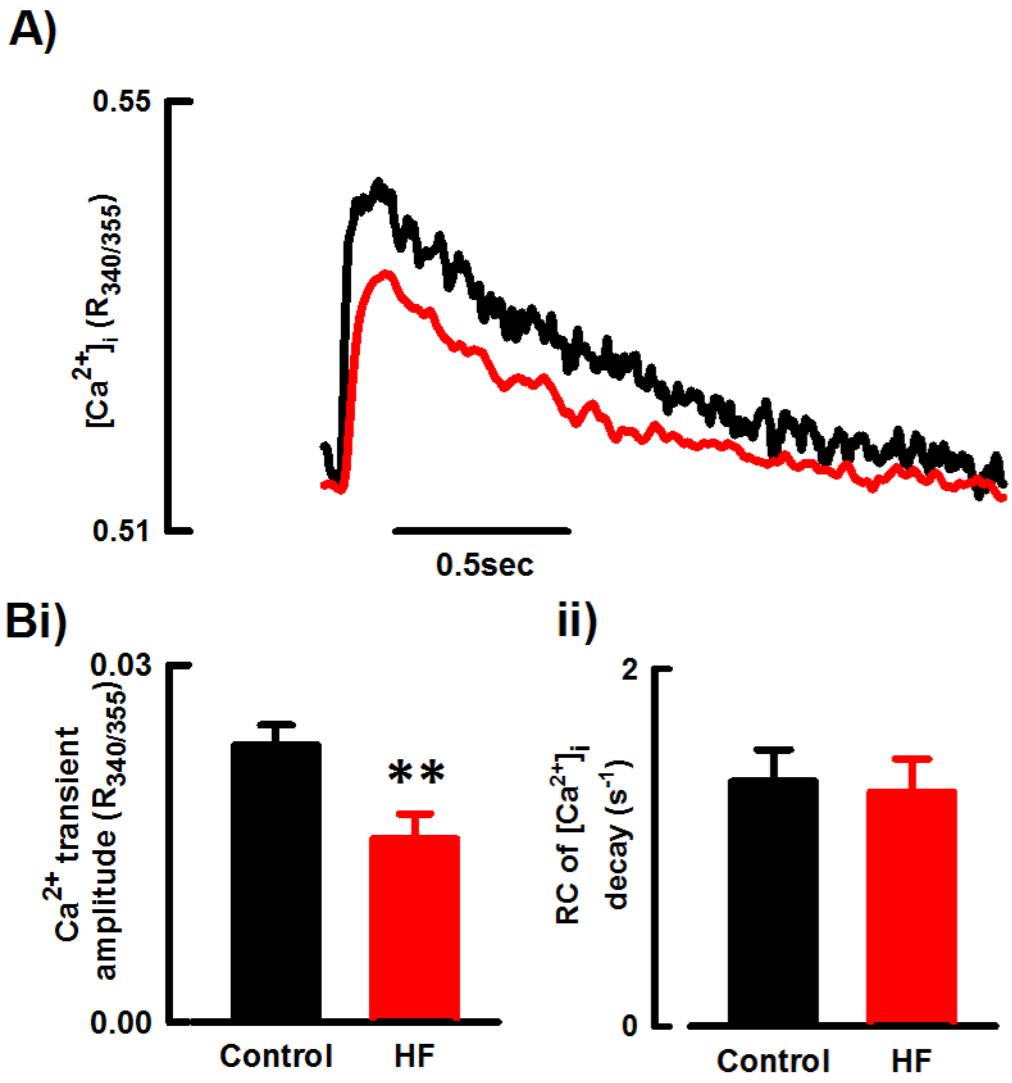

Figure 4.5 The effect of heart failure on the systolic Ca^{2+} transient

*(A) Typical systolic Ca^{2+} transient ($[Ca^{2+}]_i$) recording from control (black) and failing (red) sheep left ventricular myocytes. (B) Mean data for the effect of heart failure on (i) Ca^{2+} transient amplitude and (ii) the rate constant (RC) of decay of the Ca^{2+} transient. Mean ± SEM, statistical significance assessed using a Student's t-test. **vs control $p<0.01$. Control n=17-19 cells/12 animals. HF n=7-9/4.*

4.3.4 The effect of acute PDE5 inhibition on Ca^{2+} handling in heart failure

The work presented in Chapter 3 showed that acute PDE5 inhibition attenuated steady state $I_{Ca\text{-}L}$ and Ca^{2+} transient amplitude and therefore promotes negative inotropy in normal sheep ventricular myocytes. The next series of experiments sought to investigate whether acute PDE5 inhibition had an effect on Ca^{2+} handling in the failing myocardium.

4.3.4.1 The effect on $I_{Ca\text{-}L}$

PDE5 inhibition with sildenafil decreased $I_{Ca\text{-}L}$, which was most likely due to a cGMP-PKG dependent mechanism. Figure 4.6*A* shows representative traces for the effect of selective PDE5 inhibition (sildenafil, 1 μM) on $I_{Ca\text{-}L}$ in myocytes from HF animals. The histogram in Figure 4.6*B* shows the application of sildenafil resulted in a tendency to decrease peak $I_{Ca\text{-}L}$ by 35±16% (p=0.16), which was associated with a tendency for a decreased overall amount of Ca^{2+} entering per beat (Figure 4.6*C*, 0.95±0.1 μmoles.L^{-1} to 0.67±0.1 μmoles.L^{-1}, p=0.09). The low sample number in this group (*n*= 5 cells/ 2 animals) suggests these changes may not be significant due to being underpowered.

Analysis of $I_{Ca\text{-}L}$ kinetics revealed that PDE5 inhibition had a tendency to decrease the rate of both the voltage (p=0.06) and calcium (p=0.18) dependent portion of $I_{Ca\text{-}L}$ inactivation (Table 13).

	Control	**Sildenafil**
RC for voltage-dependent $I_{Ca\text{-}L}$ inactivation (s^{-1})	60.0±8	37.2±9
RC for calcium-dependent $I_{Ca\text{-}L}$ inactivation (s^{-1})	195.9±25	124.7±31

Table 13. The effect of PDE5 inhibition on the rate of $I_{Ca\text{-}L}$ inactivation in HF

Mean±SEM, all pairwise, n= 5 cells/ 2 animals. Differences compared using paired Student's t-test.

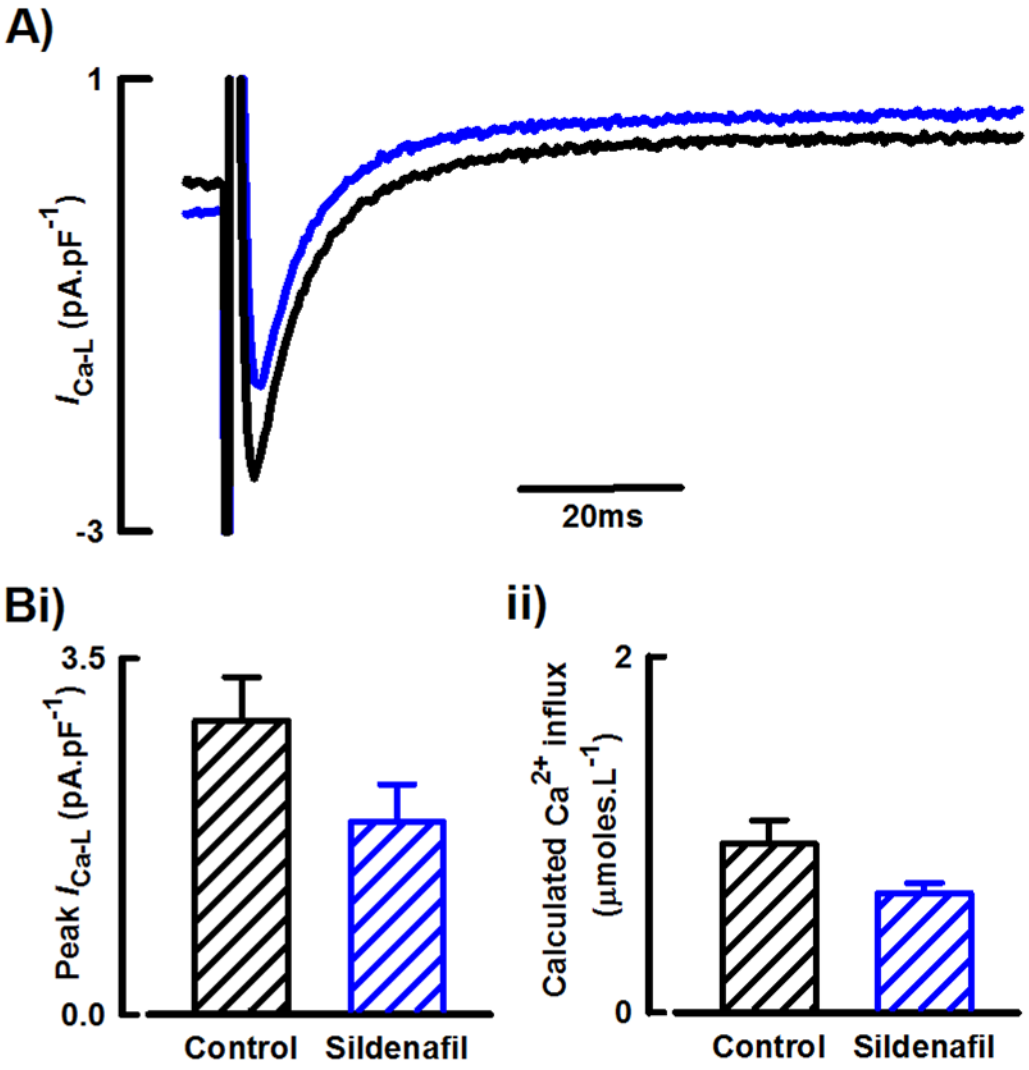

Figure 4.6 The effect of acute PDE5 inhibition on $I_{Ca\text{-}L}$ in failing myocytes

(A) Typical $I_{Ca\text{-}L}$ recording from a failing sheep left ventricular myocyte at steady state (control, black) and following PDE5 inhibition (sildenafil, 1μM, blue). (B) Mean data for the effect of PDE5 inhibition on (i) peak $I_{Ca\text{-}L}$ and (ii) calculated Ca^{2+} influx. Mean ± SEM. Differences compared using a paired Student's t-test. Control n=5 cells/2 animals. Sildenafil n=5/2.

4.3.4.2 The effect on the systolic Ca^{2+} transient

In simultaneous experiments we tested whether the effects of PDE5 inhibition on $I_{Ca\text{-}L}$ in failing myocytes manifested in changes to the systolic Ca^{2+} transient. The representative trace and mean data presented in Figure 4.7*A* show that PDE5 inhibition had no effect on the amplitude of the systolic Ca^{2+} transient (control: 0.012±0.002 $R_{340/355}$ versus sildenafil: 0.011±0.001 $R_{340/355}$, p=0.48). There appeared to be a small increase in the rate of transient decay following PDE5 inhibition (Figure 4.7*B*, control: 1.040±0.20 s^{-1} versus sildenafil: 1.28±0.21 s^{-1}, p=0.27), but the underpowered nature of this data set makes it difficult to accurately comment on any changes.

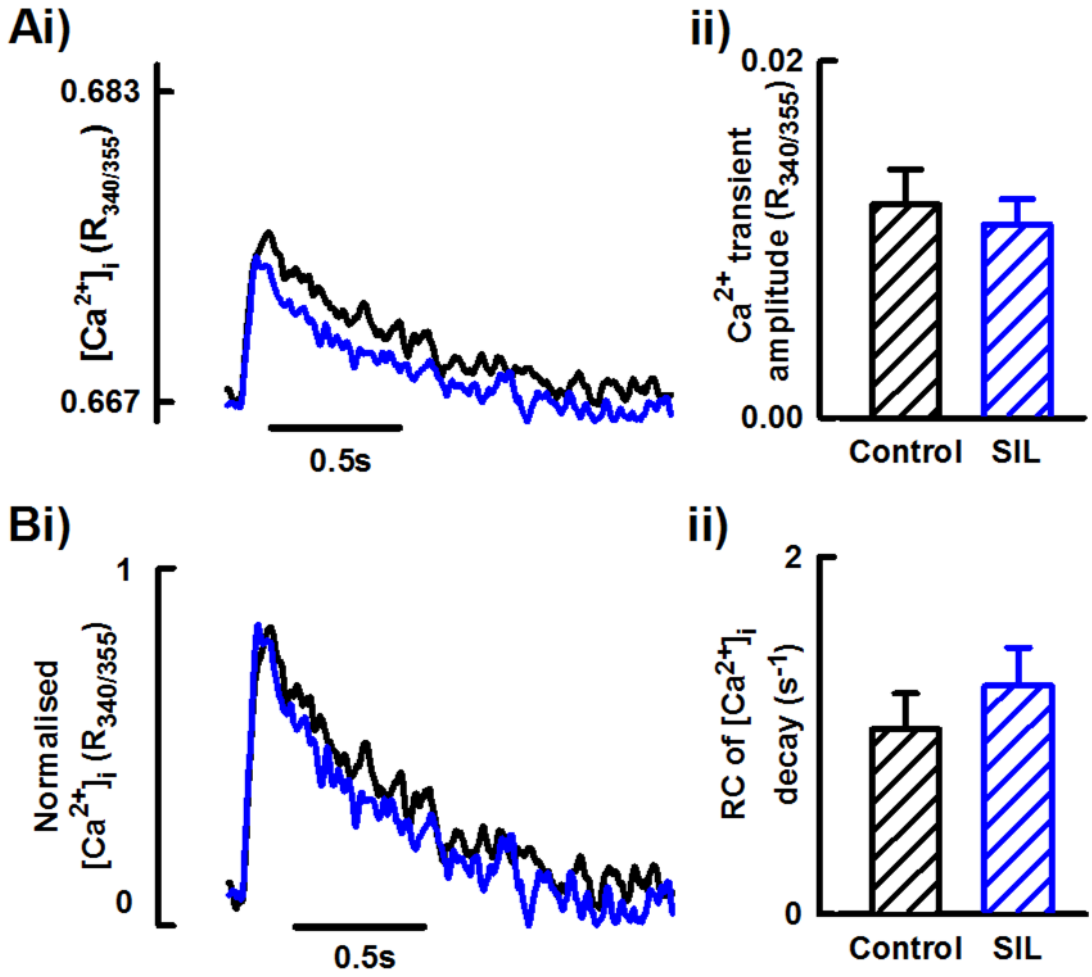

Figure 4.7 The effect of acute PDE5 inhibition on the systolic Ca^{2+} transient in failing myocytes

(A) Typical Ca^{2+} transient ($[Ca^{2+}]_i$) recording from a failing sheep left ventricular myocyte at steady state (control, black) and following PDE5 inhibition (sildenafil, 1μM, blue). (B) Mean data for the effect of PDE5 inhibition on (i) Ca^{2+} transient amplitude and (ii) the rate constant (RC) of Ca^{2+} transient decay. Mean ± SEM. Differences compared using a paired Student's t-test. Control n=5 cells/2 animals. Sildenafil n=5/2.

4.3.5 The effect of chronic PDE5 inhibition on steady state Ca^{2+} handling in heart failure

Targeting of the β-AR signalling pathway in the treatment of heart failure has been commonplace for many years[279]. Such treatment strategies include the use of β-blockers and PDE inhibitors. The popularity of PDE5 as a potential target for HF therapy has more recently increased[265]. As such this study is the first to chronically inhibit PDE5 in a large animal model of HF in order to investigate the effects on Ca^{2+} handling.

4.3.5.1 The effect on $I_{Ca\text{-}L}$

Animals destined for chronic PDE5 inhibitor treatment were paced for 4 weeks alongside other HF animals. At this point animals were paced for a further 3 weeks and treated with one tadalafil tablet daily (20 mg, Cialis, Eli Lilly). For nomenclature purposes HF animals treated with the PDE5 inhibitor will be referred to as Tadalafil animals.

Myocytes isolated from Tadalafil animals were subject to whole cell voltage clamp to assess the effect of treatment on $I_{Ca\text{-}L}$. For comparison purposes the data presented in Figure 4.8 shows $I_{Ca\text{-}L}$ in Tadalafil animals presented alongside data for normal and HF animals, which was described earlier in this chapter (see *4.3.2*).

Myocytes isolated from Tadalafil animals were no different in size than control or HF myocytes (Table 14). As described (see 4.3.2) HF myocytes had an attenuated $I_{Ca\text{-}L}$, which was characterized both by reduced peak and reduced Ca^{2+} influx. Figure 4.8 shows that tadalafil treatment did not lead to a restoration of peak $I_{Ca\text{-}L}$ (2.81 ± 0.23 $pA.pF^{-1}$) or influxing Ca^{2+} (0.99 ± 0.08 $\mu moles.L^{-1}$). Furthermore, kinetics of $I_{Ca\text{-}L}$ were unchanged in animals chronically treated with the PDE5 inhibitor: calcium-dependent $I_{Ca\text{-}L}$ inactivation was similar to that observed in HF myocytes (Table 14) and voltage-dependent $I_{Ca\text{-}L}$ inactivation had a tendency to be slower than that observed in HF (Table 14, $p=0.06$).

	Control	HF	Tadalafil
Cell capacitance (pF)	154±13	163±13	176±12
RC of voltage-dependent $I_{Ca\text{-}L}$ inactivation (s^{-1})	54.1±2	49.1±5	42.1±4
RC of Ca^{2+}-dependent $I_{Ca\text{-}L}$ inactivation (s^{-1})	207.9±10	182.7±14	189.2±17

Table 14. The effect of chronic PDE5 inhibition on cellular electrophysiology in HF.

Mean data for Tadalafil animals presented alongside reproduced data for control and HF used here for comparison purposes. Mean±SEM, control n=20 cells/13 animals, HF n=12/6, Tadalafil n=19/6. Statistical significance assessed using a one-way ANOVA.

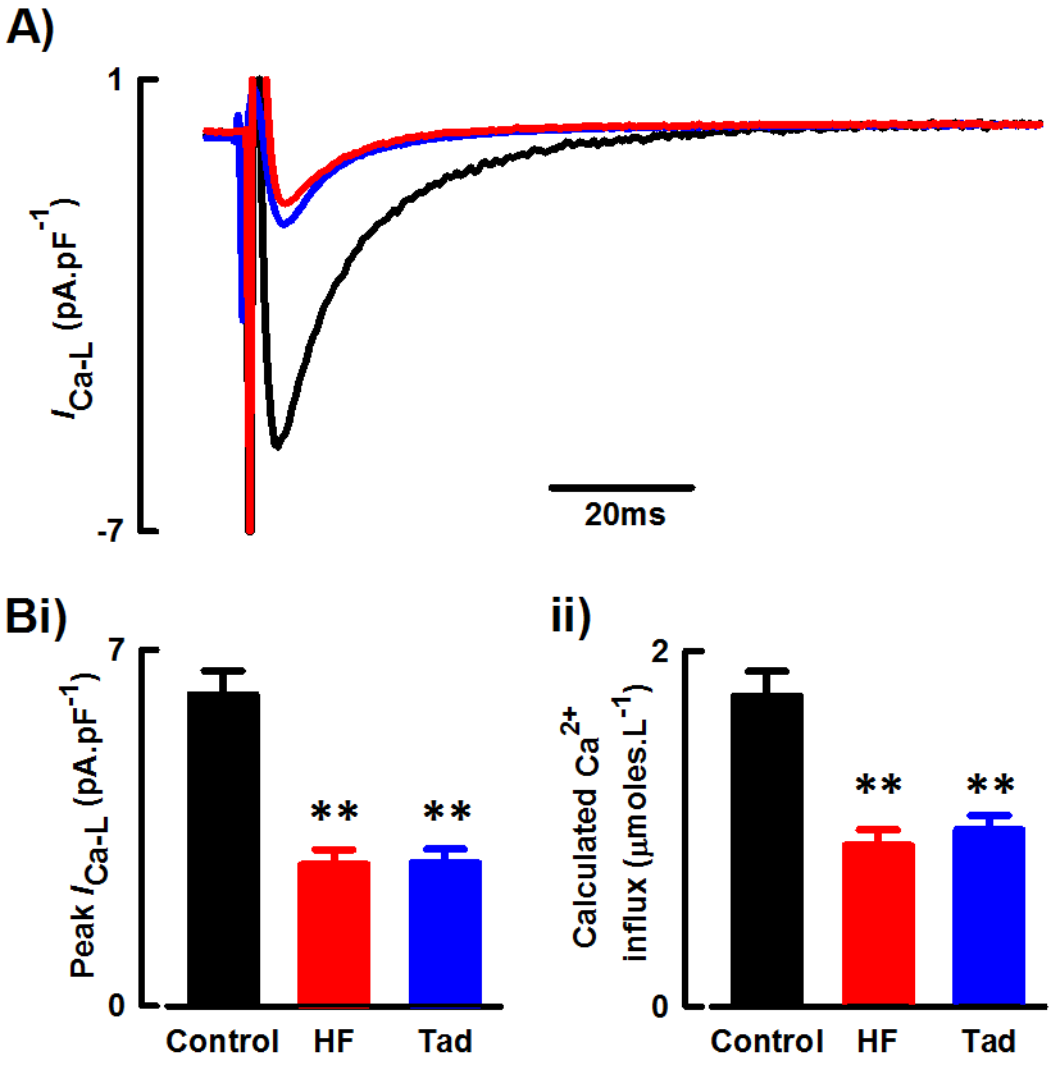

Figure 4.8 The effect of chronic PDE5 inhibition on I_{Ca-L}

*(A) Typical I_{Ca-L} recording from control (black), failing (red) and chronic PDE5 inhibitor treated (Tadalafil, blue) sheep left ventricular myocytes. (B) Mean data for the effect of chronic PDE5 inhibition on (i) peak I_{Ca-L}. (ii) calculated Ca^{2+} influx. Mean data for tadalafil animals presented alongside data shown previously in this chapter (control and HF) used here for comparative purposes. Mean ± SEM, statistical significance assessed using a one-way ANOVA. **vs control p<0.01. Control n=20 cells/13 animals. HF n=11-12/6. Tadalafil n=20/6.*

4.3.5.2 The effect on the systolic Ca^{2+} transient

As above, the data presented in Figure 4.9 represents the effects observed in Tadalafil animals alongside previously described (see 4.3.3) data for Ca^{2+} transient dynamics in normal and HF sheep.

As $I_{Ca\text{-}L}$ is an important determinate of Ca^{2+} transient amplitude, decreases in peak $I_{Ca\text{-}L}$ observed in HF go some way to describing decreases in Ca^{2+} transient amplitude. Tadalafil treatment had no effect on the attenuated $I_{Ca\text{-}L}$, however as shown by the representative trace and mean data in Figure 4.9 there was a substantial increase in Ca^{2+} transient amplitude following 3 weeks of PDE5 inhibitor treatment (0.062±0.004 $R_{340/355}$). Increases in transient amplitude exceeded even transient size observed in control sheep ventricular myocytes by 170%. Furthermore, increases in the size of the Ca^{2+} transient in Tadalafil animals were associated with a faster rate of decay of the Ca^{2+} transient (4.49±0.56 s^{-1}).

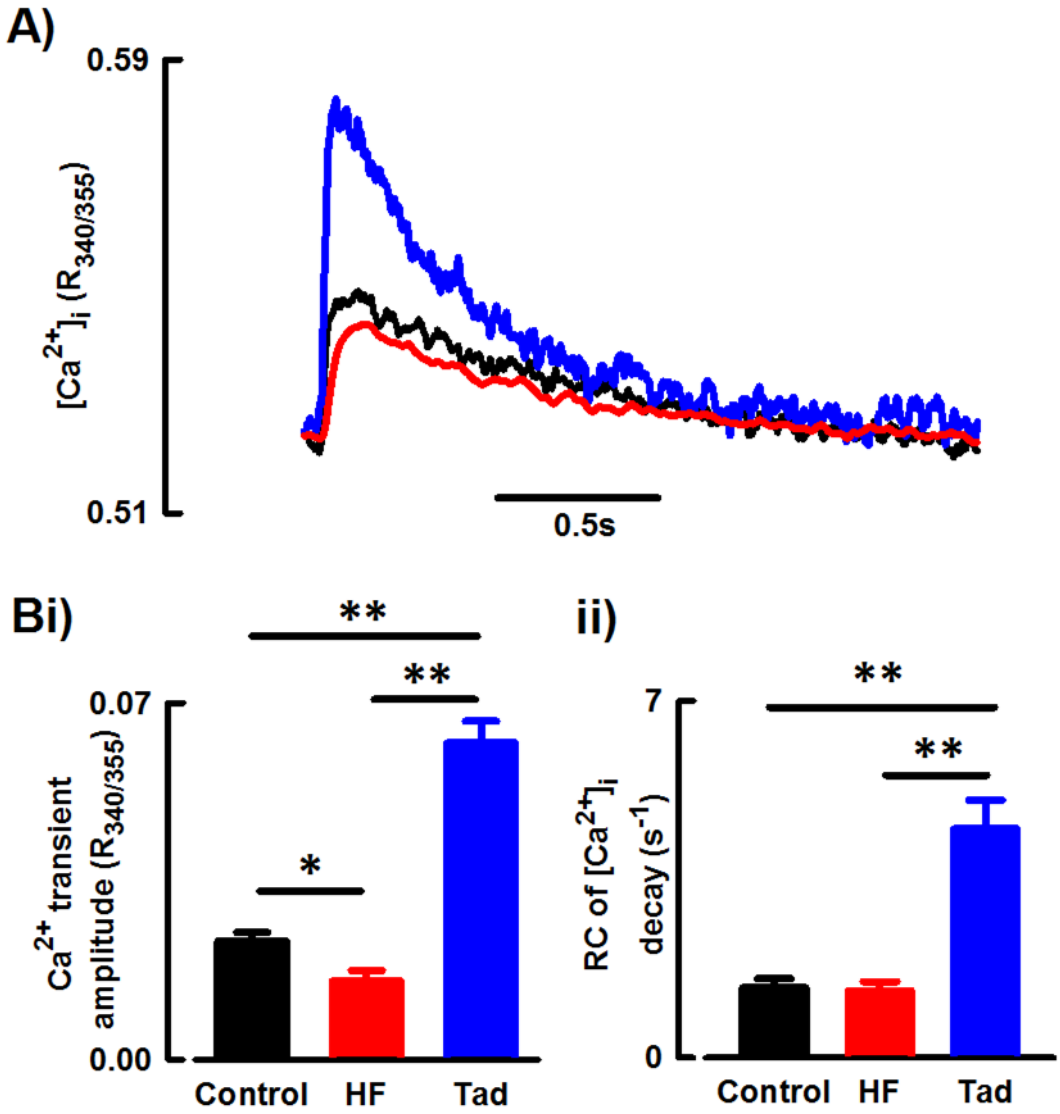

Figure 4.9 The effect of chronic PDE5 inhibition on the systolic Ca^{2+} transient

*(A) Typical systolic Ca^{2+} transient ($[Ca^{2+}]_i$) recording from control (black), failing (red) and chronic PDE5 inhibitor treated (Tadalafil, blue) sheep left ventricular myocytes. (B) Mean data for the effect of chronic PDE5 inhibition on (i) Ca^{2+} transient amplitude and (ii) the rate constant (RC) of decay of the Ca^{2+} transient. Mean data for tadalafil animals presented alongside data shown previously in this chapter (control and HF) used here for comparative purposes. Mean ± SEM, statistical significance assessed using a one-way ANOVA. *p<0.05, ** p<0.01. Control n=19 cells/9 animals. HF n=9/4. Tadalafil n=9/3.*

4.3.6 The effect of chronic PDE5 inhibition on β-AR stimulation in heart failure

The findings presented so far in this chapter suggest that chronic PDE5 inhibition (3 weeks) modulates steady state Ca^{2+} handling in the failing myocardium. The next series of experiments, albeit preliminary, sought to investigate changes to β-AR signalling in the failing heart and whether any such changes were modulated by chronic PDE5 inhibition.

4.3.6.1 The effects of β-AR stimulation on Ca^{2+} handling in heart failure

The present study reports that steady state $I_{Ca\text{-}L}$ was attenuated following 4 weeks of tachypacing (see 4.3.2). This concurs with previous reports of reduced $I_{Ca\text{-}L}$ in end-stage heart failure in tachypaced sheep[179]. Moreover, Briston et al also demonstrated diminished β-AR responsiveness, which is a key characteristic of human HF.

The effect of non-selective β-AR stimulation with isoprenaline (100 nM) on ventricular myocytes from normal and HF animals and the specific effects on $I_{Ca\text{-}L}$ are shown in Figure 4.10*A*. β-AR stimulation in HF animals resulted in a tendency for an increased peak $I_{Ca\text{-}L}$ (Figure 4.10*Aii, p=0.10*) concomitant with an increase in Ca^{2+} influx (Figure 4.10*Aiii*). These changes were associated with a tendency for a slower voltage-dependent $I_{Ca\text{-}L}$ inactivation and a slower rate of calcium-dependent inactivation.

In normal ventricular cells β-AR stimulation resulted in a 130±42% increase in peak $I_{Ca\text{-}L}$, whereas there was only a 61±17% increase in $I_{Ca\text{-}L}$ observed in HF animals. This reveals a diminished sensitivity to β-AR stimulation in failing myocytes.

The size of the systolic Ca^{2+} transient is proportional to myocyte contractility, thus in normal cells β-AR stimulation evokes a greater Ca^{2+} transient to promote greater myocardial contraction: positive inotropy. In HF a reduced responsiveness to β-AR stimulation, in particular a reduced Ca^{2+} transient is responsible for poor cardiac function. The present study has reported in normal sheep ventricular myocytes β-AR stimulation resulted in a 248±68% increase in Ca^{2+} transient amplitude (see 3.3.4.2). In HF myocytes there was a tendency for an increase in Ca^{2+} transient amplitude following β-AR stimulation (Figure 4.11*Aii*), however this data set is underpowered and further work would be required to more reliably comment on the changes observed.

4.3.6.2 The effect of β-AR stimulation on Ca^{2+} handling in heart failure animals chronically treated with a PDE5 inhibitor

Chronic PDE5 inhibition is beneficial to both human and animal models of HF. The present study has shown a paradoxical variety of effects of PDE5 inhibition on Ca^{2+} handling: acute PDE5 inhibition appeared to be negatively inotropic to isolated ventricular myocytes, chronic PDE5 inhibition had little effect on steady state $I_{Ca\text{-}L}$, yet increased the size of the steady state Ca^{2+} transient in the failing ventricle (see 3.3.1). In light of this it is hypothesised that the beneficial effects of PDE5 inhibition may be related to a restoration of impaired *β*-AR signalling in the failing ventricle.

Ventricular myocytes from tadalafil treated HF animals responded to *β*-AR stimulation similarly to control myocytes: an 184±50% increase in peak $I_{Ca\text{-}L}$ and a 300±85% increase in Ca^{2+} influx (Figure 4.10*B*). Furthermore, *β*-AR stimulation in PDE5 inhibitor treated myocytes showed a trend for slower voltage-dependent and faster calcium-dependent inactivation of $I_{Ca\text{-}L}$. Together; this suggests that PDE5 inhibition restores the responsiveness of $I_{Ca\text{-}L}$ to *β*-AR stimulation in HF.

Tadalafil treatment elicited a large increase in baseline inotropy, manifesting in substantially greater steady state Ca^{2+} transients. As $I_{Ca\text{-}L}$ was significantly modulated by *β*-AR stimulation the next experiment sought to test whether similar sensitivity is demonstrated with regards to the systolic Ca^{2+} transient. Figure 4.11*Bii* shows *β*-AR stimulation resulted in a strong tendency for increased Ca^{2+} transient amplitude and a faster rate of transient decay (Figure 4.11*iii, p=0.051 and p=0.056 respectively*). However, the *β*-AR evoked fractional change in Ca^{2+} transient amplitude in Tadalafil (65±24%) was relatively small in comparison to those observed in control cells (248±68%). This is most likely due to SR capacity and the effect of tadalafil treatment on the size of the steady state Ca^{2+} transient. It is difficult to draw too heavily on these latter findings due to the limited sample size currently available.

PDE5 inhibition appears to be beneficial to the failing sheep myocardium by restoring Ca^{2+} handling and *β*-AR sensitivity. The next series of experiments presented in this chapter aim to understand the mechanisms via which these beneficial effects manifest. The change in expression of EC-coupling proteins, concentrations of cyclic nucleotides and activities of the most important PDE subtypes will be investigated.

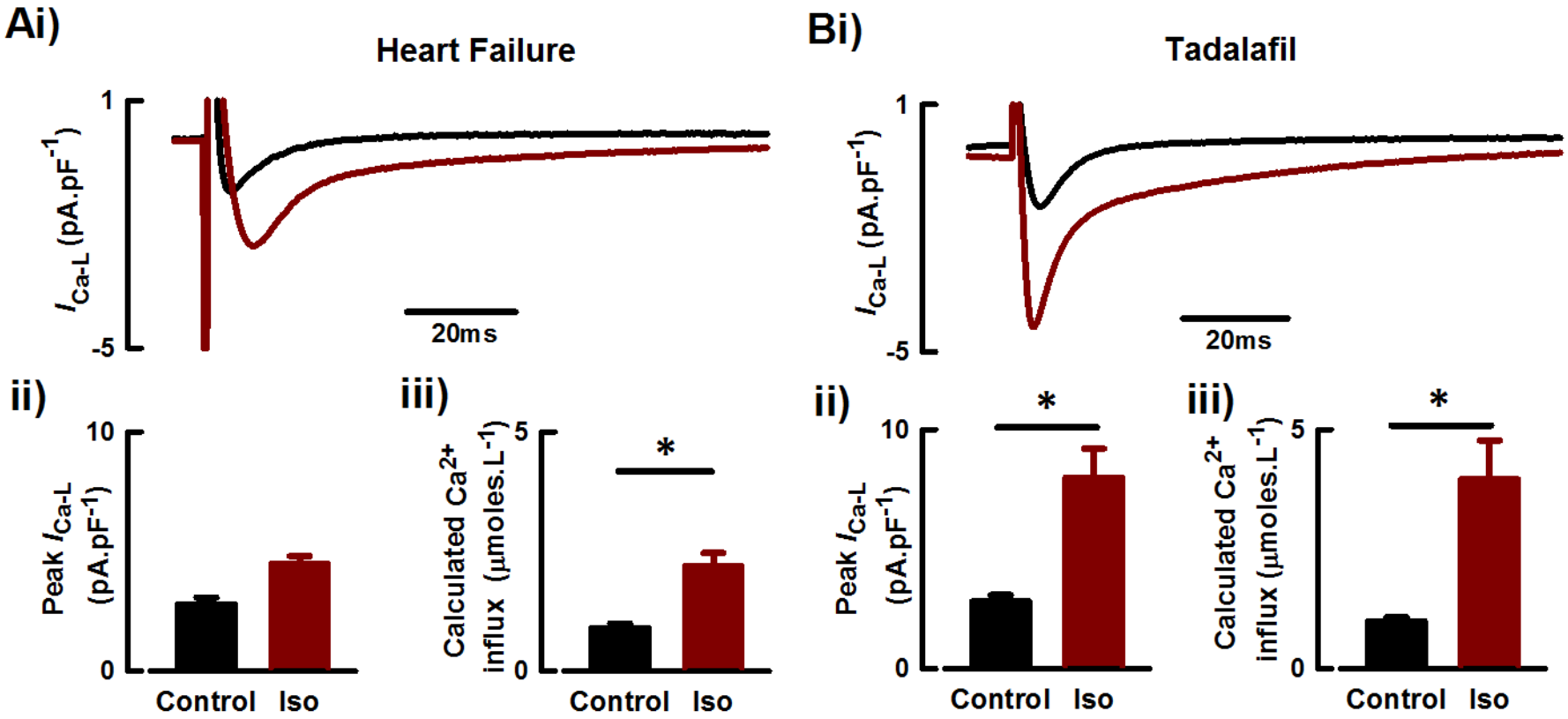

Figure 4.10 The effect of β-AR stimulation on $I_{Ca\text{-}L}$ in HF.

*The effect of the non-selective β-AR agonist isoprenaline (100nM, red) on $I_{Ca\text{-}L}$ (black, at steady state) in myocytes from (A) heart failure and (B) tadalafil treated HF animals. (i) Typical $I_{Ca\text{-}L}$ recording. (ii) Summary data for peak $I_{Ca\text{-}L}$. (iii) Summary data for calculated Ca^{2+} influx. Mean ± SEM, statistical significance assessed using a paired t-test. *vs control $p<0.05$. Heart Failure n=2 cells/2 animals. Tadalafil n=5/2.*

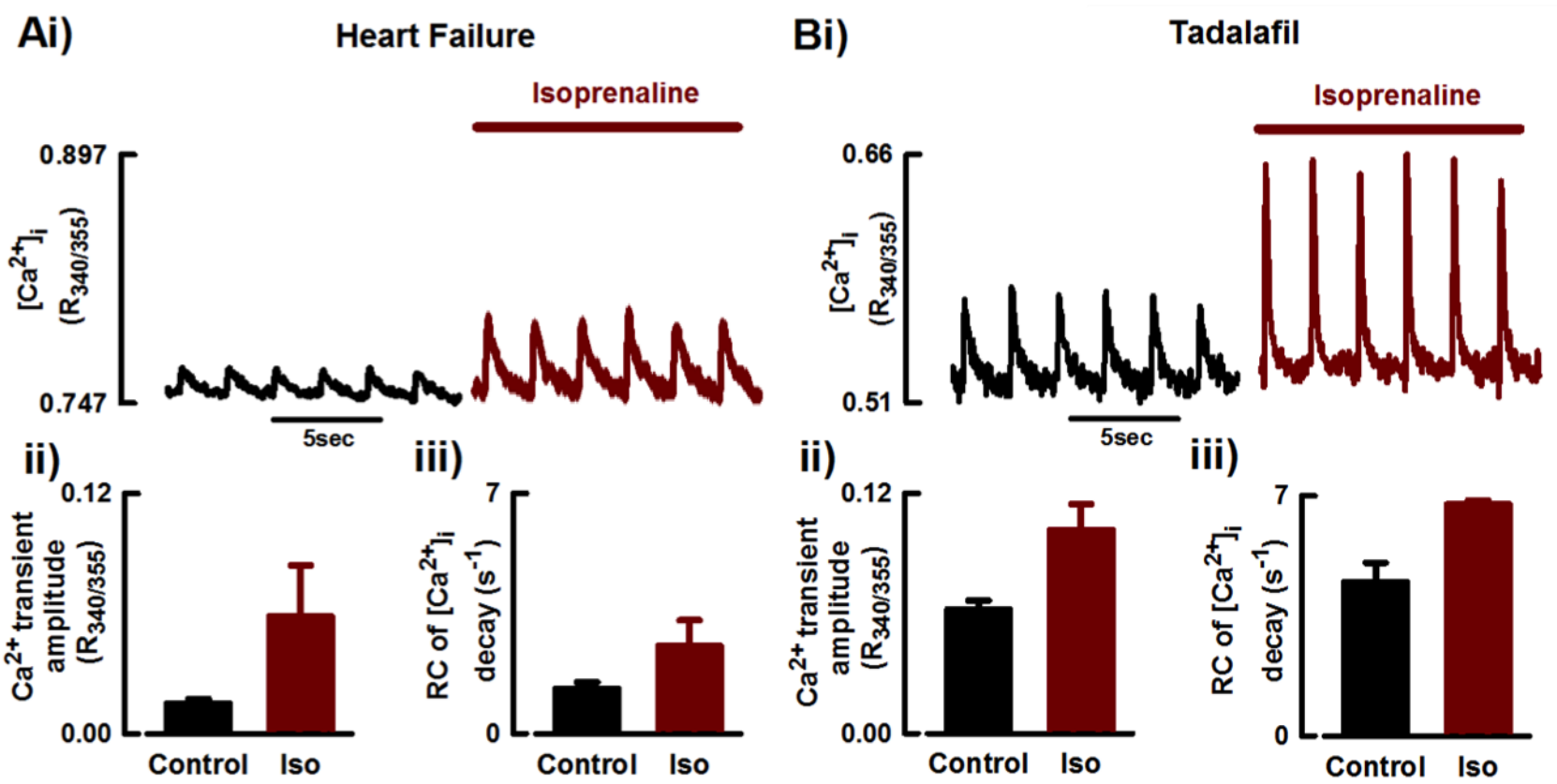

Figure 4.11 The effect of β-AR stimulation on Ca^{2+} transient in HF.

The effect of the non-selective β-AR agonist isoprenaline (100nM, red) on Ca^{2+} transient (black, at steady state) in myocytes from (A) heart failure and (B) tadalafil treated HF animals. (i) Typical $[Ca^{2+}]_i$ recording. (ii) Summary data for Ca^{2+} transient amplitude. (iii) Summary data for the rate constant of Ca^{2+} transient decay. Mean ± SEM, statistical significance assessed using a paired t-test. Heart failure n=4 cells/2 animals. Tadalafil n=3/1.

*4.3.7 **Biochemical assessment of the proteins and signalling molecules involved in modulating calcium handling***

4.3.7.1 Differences in E-C coupling protein expression

The present study has demonstrated that Ca^{2+} handling is modulated in the failing heart with and without chronic PDE5 inhibition. One of the most striking findings was the substantial increase in the size of the steady state Ca^{2+} transient following 3 weeks of tadalafil treatment. Due to experimental constraints I was unable to record SR Ca^{2+} content using caffeine in Tadalafil animals, however as SR Ca^{2+} is regulated by the activity of SERCA, which in turn is modulated by the accessory protein PLN, the expression of these two proteins was examined.

Using Western blotting the SR Ca^{2+} ATPase, SERCA2A, was found to be decreased in the failing ventricle, Figure 4.12*Ai*, which was also observed in ventricular tissue from Tadalafil animals. Furthermore, the regulatory protein PLN was shown to be unchanged in heart failure with or without PDE5 inhibitor treatment (Figure 4.12*Aii*). As PLN inhibits SERCA activity, the reduced expression of SERCA:PLN, as shown by the summary data in Figure 4.12Aiii, shows that there is likely a greater proportion of PLN-dependent inhibition of SERCA in the failing ventricle. The altered ratio as observed here would suggest a greater inhibition of SR Ca^{2+} uptake.

The phosphorylation of PLN results in a conformational change in the tertiary structure of the protein and thus removes its inhibition of SERCA[78]. Such phosphorylation is achieved by both PKA and PKG at identical residues, Ser16 and Thr17, on the protein[88, 107]. Thus the phosphorylation status of PLN is an important indicator of protein kinase activity in ventricular myocytes. The phosphospecific Western blots presented in Figure 4.12B show that phosphorylation of Ser16 and to some extent (although not significant) Thr17 was attenuated in heart failure. In Tadalafil animals there was a greater phosphorylation of Ser16, although maintained lower than normal animals, which was accompanied by a possible similar increase in Thr17 phosphorylation. Together, this may suggest that protein kinase activity is greater in response to chronic PDE5 inhibition and may indicate a mechanism by which greater Ca^{2+} loading of the SR in tadalafil animals may contribute to the greater Ca^{2+} transient observed. Moreover, this hypothesis may corroborate the increased rate of Ca^{2+} transient decay observed in Tadalafil cells.

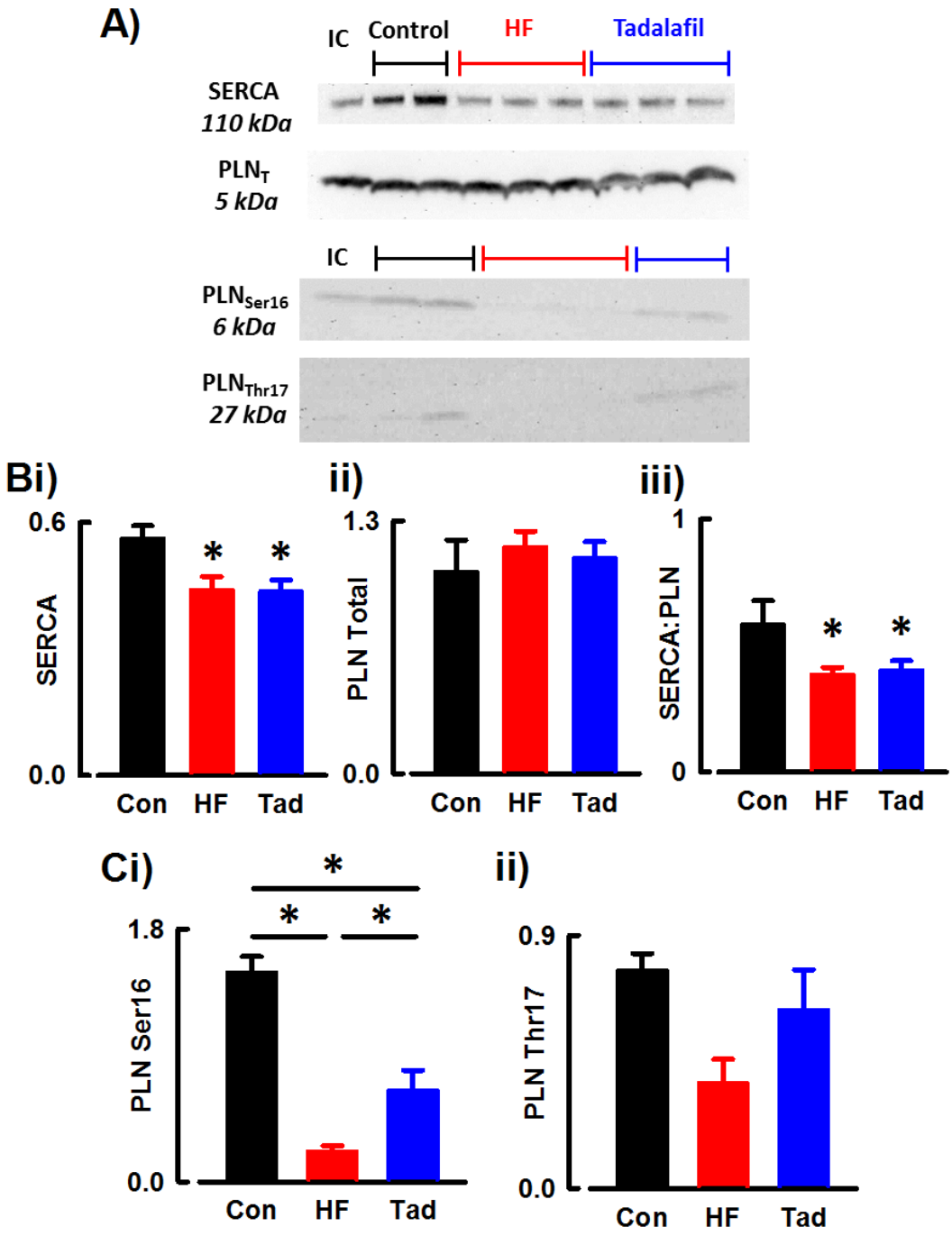

Figure 4.12 The effect of HF on ECC protein expression.

*Differences in expression in left ventricular tissue from control animals (black), HF (red) and Tadalafil (blue). (A) Representative Western blots. (B) summary data for (i) sarcoendoplasmic reticululm Ca^{2+} ATPase (SERCA2A), (ii) total phospholamban (PLN_T) and (iii) the difference in the ratio between the two. (C) Summary data for phosphospecific Western blotting (i) Ser^{16} and (ii) Thr^{17} phosphorylated phospholamban. Mean ± SEM as compared to internal control (IC) and representative of 3 repeats (for SERCA and PLN only). Statistical significance assessed using a one-way ANOVA. *p<0.05 Control n=4. Heart failure n=7. Tadalafil n=5.*

4.3.7.2 Differences in cyclic nucleotide availability in heart failure

Cellular data presented earlier in this chapter shows that *β*-AR modulation of Ca^{2+} handling may be altered in heart failure, which suggests that *β*-AR signalling may become disrupted in the failing ventricle. As *β*-AR signalling is highly reliant on the availabilities of cyclic nucleotides the next experiment sought to test whether relative cAMP and cGMP concentrations are altered in the failing ventricle before and after chronic PDE5 inhibition (Figure 4.13). The summary data for (Ai) relative cAMP and (Bi) relative cGMP concentrations in ventricular tissue reveal that there were minimal overall effects on cyclic nucleotide bioavailability. The analysis performed for this data series meant the values presented are relative to total cyclic nucleotide availability, thus absolute values are shown, as reflected by the lack of error presented. There was a tendency for an increased cyclic nucleotide level (both cAMP and cGMP) in the failing ventricle, however such differences were not observed in Tadalafil tissue. The standard curves shown in Figure 4.13*B* show that the ELISA, as performed to manufacturer's instructions, produced a normal concentration curve, suggesting that the data analysis used to determine the relative cyclic nucleotide concentrations in Figure 4.13*A* is accurate.

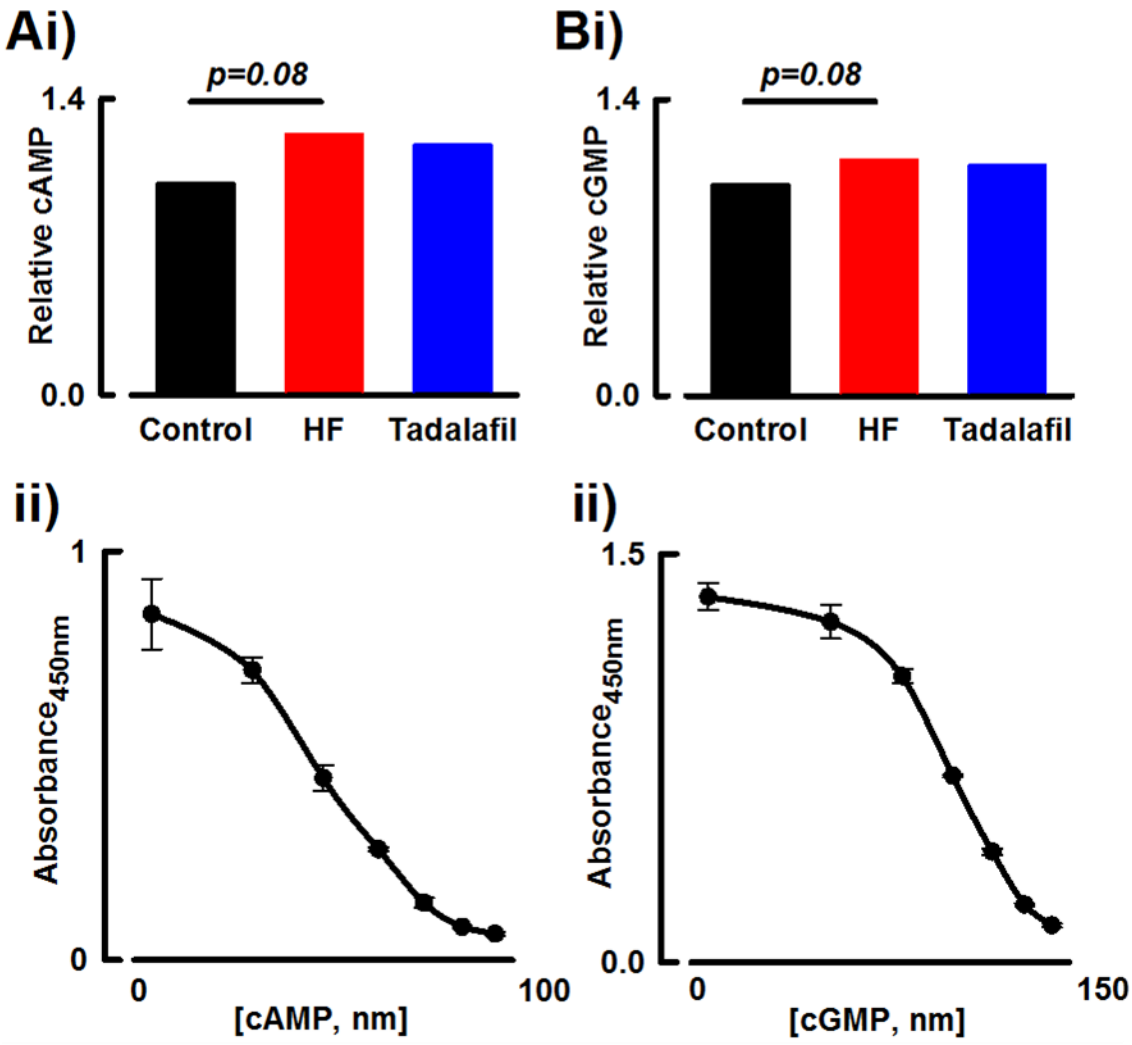

Figure 4.13 The effect of HF and chronic PDE5 inhibitor treatment of HF on cyclic nucleotide cytosolic bioavailability

The relative abundance of (A) cAMP and (B) cGMP in ventricular tissue from control (black), heart failure (HF, red) and tadalafil treated HF (Tadalafil, blue) sheep. (i) Summary data as normalised to control and (ii) standard curve used to calculate relative concentrations. Means shown only, statistical significance assessed using a one-way ANOVA. Control n=8. Heart failure n=8. Tadalafil n=7.

4.3.7.3 Alterations in PDE expression and activity in heart failure

The observed effects on steady state and β-AR stimulated Ca^{2+} handling are most likely due to a multifaceted alteration in intracellular signalling, protein expression and phosphorylation status. Small changes in cyclic nucleotide availability may be due to changes in the expression or activity of phosphodiesterase enzymes, thus this next set of experiments tested whether this changes in HF.

The majority of cAMP hydrolysis is achieved by PDE3 in the mammalian myocardium[280]. Figure 4.14*A* and Figure 4.15*Ai* show that PDE3 is expressed in the normal sheep ventricle and provides 68.36±3.1% of cAMP hydrolysis. Furthermore, in the failing ventricle PDE3 expression was reduced (Figure 4.14*A*), which was accompanied by a trend for a reduction in activity (Figure 4.15*Ai*).

PDE4 is the only cAMP specific PDE isoform in the mammalian myocardium, of which the two most ubiquitously expressed are PDE4B and PDE4D, both of which are expressed in the sheep ventricle (Figure 4.14*B*). Both isoforms of PDE4 and their collective activities were shown to be decreased in the failing ventricle (Figure 4.14*B and* Figure 4.15*Aii)* which may explain to some extent the possible increases in cAMP abundance in heart failure (Figure 4.13*Ai*).

Antibodies for cGMP-hydrolysing PDEs do not cross-react adequately with ovine myocardium, thus expression analysis for PDE2 and PDE5 has not been undertaken in the present study. Analysis of both cGMP-hydrolysing isoforms revealed that both PDE2 and PDE5 are active in the sheep myocardium (Figure 4.15*B/C*) and have preserved activity in the failing ventricle, with possible tendencies for their activity to be increased. It must be noted that cGMP-PDE activity analysis revealed an approximately 50% discrepancy between total cGMP-PDE activity and the combination of PDE2 and PDE5, which suggests possible tonic cGMP-hydrolysis by other PDE isoforms.

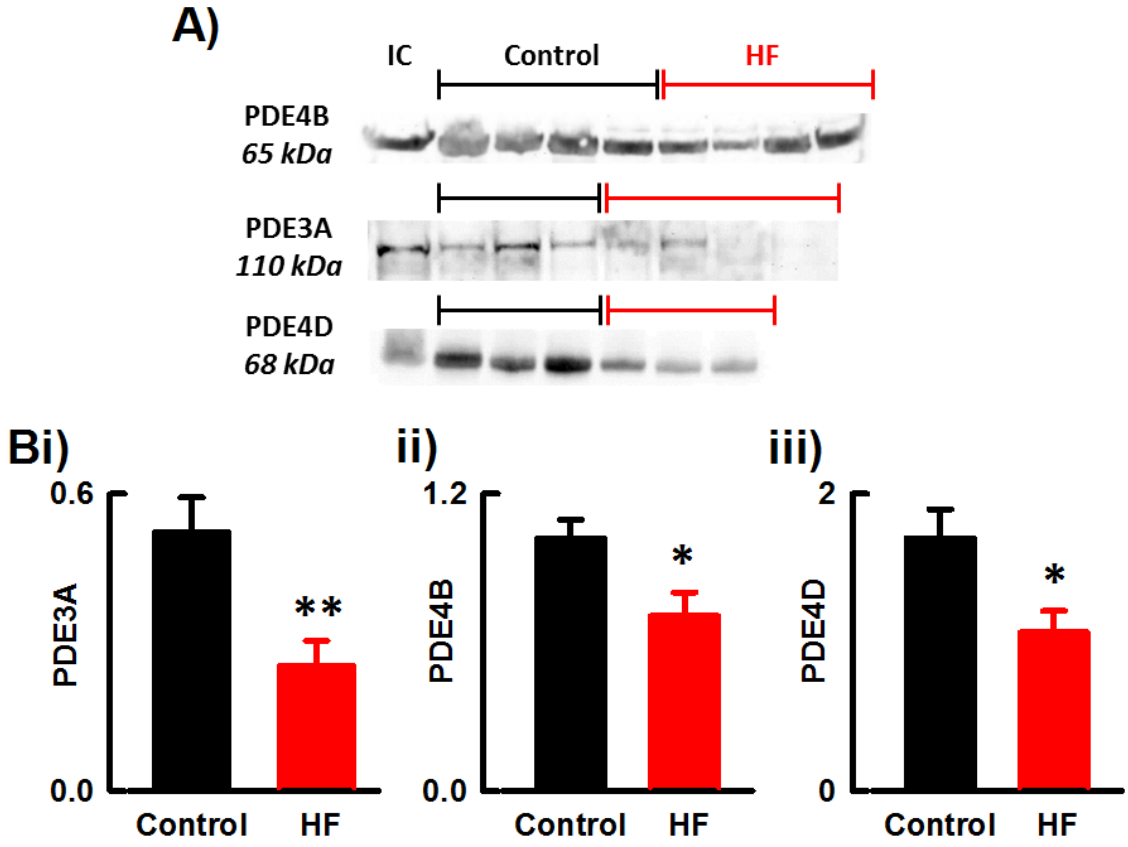

Figure 4.14 The effect of HF on PDE protein expression.

*Differences in expression of cAMP-hydrolysing PDE isoforms in left ventricular tissue from control (black) and heart failure (red) animals. (A) Representative Western blots. (B) Summary data for (i) PDE3A, (ii) PDE4B and (iii) PDE4D. PDE4B blot performed by Miss Jessica Caldwell presented here with permission. Mean ± SEM as compared to internal control (IC) and representative of 3 repeats. Statistical significance assessed using a Student's t-test. * p<0.05 Control n=6-7. Heart failure n=6.*

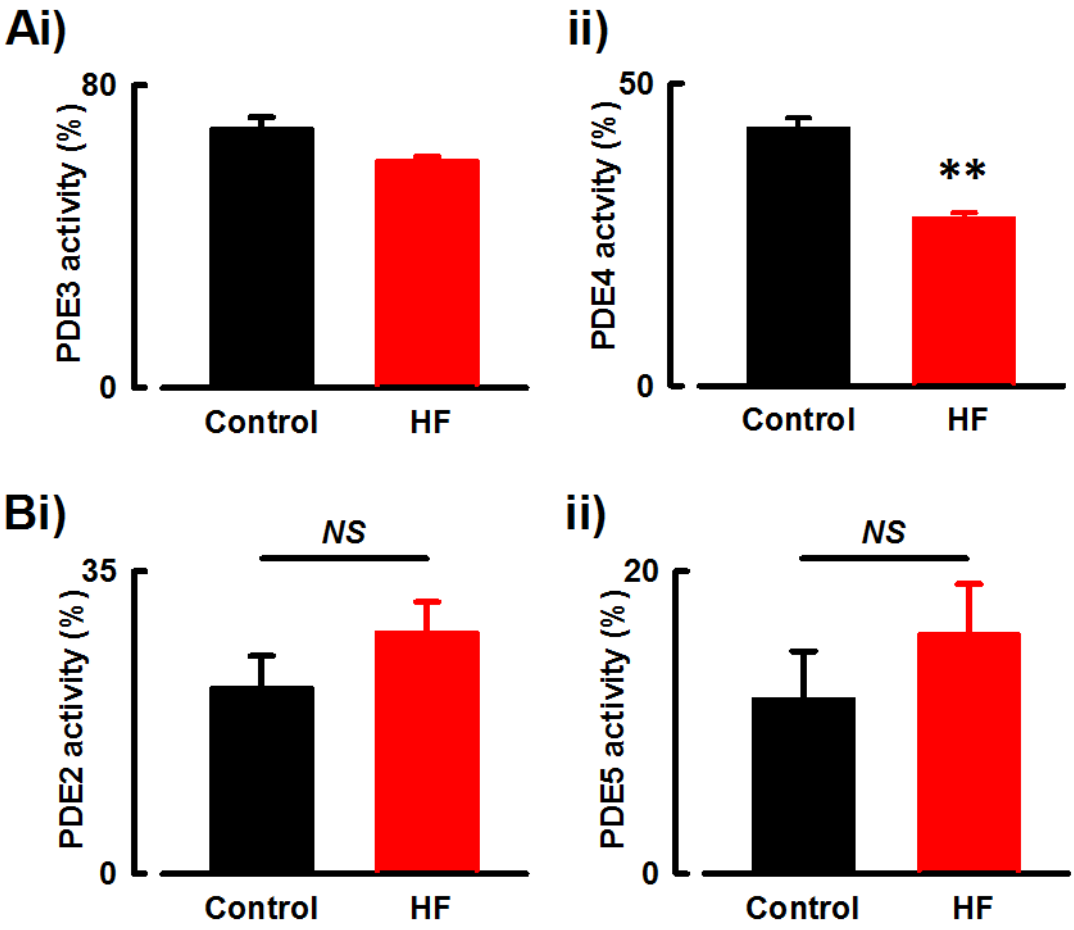

Figure 4.15 The effect of HF on PDE activity.

*Differences in the percentage activities of PDE isoforms in left ventricular tissue from control (black) and heart failure (HF, red) animals. Summary data for the activity of the (A) cAMP-hydrolysing PDEs (i) PDE3 and (ii) PDE4, (Bi) the dual specificity isoform PDE2 and (ii) the selective cGMP-hydrolysing isoform PDE5. Activity assays performed alongside Dr Hind Mehel, University Paris-Sud, presented here with permission. Mean ± SEM, statistical significance assessed using a Student's t-test. ** $p<0.01$. Control n=5-9. Heart failure n=4-8.*

4.4 Discussion

This series of experiments sought to investigate the effect of PDE5 inhibition in voltage clamped myocytes in a large animal model of HF. The current findings show that the negative inotropic effects of acute PDE5 inhibition on Ca^{2+} handling in normal cardiac myocytes are attenuated in failing myocytes, and β-AR responsiveness is diminished following 4-weeks of tachypacing. Conversely, chronic PDE5 inhibition resulted in an increased baseline Ca^{2+} transient amplitude and resensitisation of failing cardiac myocytes to β-AR stimulation. Together, these findings suggest that chronic PDE5 inhibition, at the cardiac myocyte level, may be beneficial to Ca^{2+} handling in heart failure.

4.4.1 The effect of heart failure on EC-coupling

Whether or not heart failure is associated with changes in $I_{Ca\text{-}L}$ is a controversial topic. Mukherjee and Spinale discussed that a large proportion of the animal models of HF used show a variety of differences in peak $I_{Ca\text{-}L}$, which was linked to varying severity of the cardiomyopathy investigated[183]. This review demonstrated that of the larger animals investigated $I_{Ca\text{-}L}$ was mostly decreased: severe right and left ventricular failure in cats, guinea pigs, also tachypaced pigs and in human heart failure. More recently our laboratory has shown that $I_{Ca\text{-}L}$ was reduced in tachypaced sheep ventricular myocytes[179]. The present study investigated the effect of HF on $I_{Ca\text{-}L}$ after just 4 weeks of tachypacing in order to facilitate a novel drug treatment strategy. Similar attenuation of $I_{Ca\text{-}L}$ was observed at 4 weeks of pacing, when animals were relatively symptom-free, as that recorded in ventricular myocytes from symptom presenting 'end-stage' animals, as used previously by Briston et al[179].

Peak $I_{Ca\text{-}L}$ has been described as the trigger for intracellular Ca^{2+} release from the SR, and can therefore modify the size of the systolic Ca^{2+} transient[281]. In animal models of heart failure reduced Ca^{2+} transients have been ubiquitously described[182, 282], however not all models show changes in $I_{Ca\text{-}L}$[5]. Briston et al observed reduced Ca^{2+} transient amplitude in tachypaced sheep ventricular myocytes associated with unchanged SR Ca^{2+} content[179], which concurs with the findings of the present study. A decreased Ca^{2+} transient may be caused by a multitude of factors, however one could speculate that in the absence of changes in SR Ca^{2+} content in the present study then the attenuated $I_{Ca\text{-}L}$ observed provides a mechanism for these changes in systolic Ca^{2+}. Furthermore, due to poor antibody cross-reactivity with sheep proteins immunoblotting was not possible to investigate any changes

in L-type Ca^{2+} channel protein expression in heart failure. Such experiments could be very useful in understanding the electrophysiological changes observed.

The rate of Ca^{2+} resequestration into the SR is determined by the activity of SERCA, which in turn is regulated by the inhibitory peptide PLN. This study shows that SERCA2A expression was reduced in HF ventricular tissue as previously shown[192], with no change in the expression of PLN. The shift in SERCA:PLN ratio would suggest that there would be a greater inhibition on SERCA and thus an overall reduced activity would be expected. The present study has not measured SERCA activity, but the main route for diastolic cytosolic Ca^{2+} removal is via SERCA, resequestering it back into the SR. Findings by Briston et al suggest that increased NCX activity would be the main reason for a compensation of the reduced SERCA activity[179], thus maintaining the rate of Ca^{2+} transient decay in HF, however such experiments have not been performed in the present study.

4.4.2 The effect of heart failure on β-AR signalling

Dysregulation of β-AR signalling is considered an important mechanism responsible for impaired contractility in HF. Not only are there changes to β-adrenoreceptor density and subtype switching[68], but also increased expression of G-protein receptor kinases[283] and protein phosphatases[179], which further impair their downstream signals. This study has shown that $I_{Ca\text{-}L}$ appeared to be less sensitive to β-AR modulation than Ca^{2+} transient responsiveness, which was relatively unchanged in comparison to control. Our lab has previously shown that both $I_{Ca\text{-}L}$ and Ca^{2+} transient were attenuated in end-stage HF[179], thus the current findings concur with others that the cellular phenotype of HF worsens with disease progression.

The present study found that there was marginally elevated cAMP concentrations in failing tissue, which may be explained by decreased expression and activity of cAMP-specific PDE isoforms: PDE3 and PDE4, as previously observed[136, 249]. It is established that β-adrenoreceptor subtype switching results in a greater sarcolemmal distribution of β_2, which, unlike in the normal myocardium, act more like β_1 adrenoreceptors by generating global cytosolic cAMP concentrations[47]. A combination of this and exaggerated stimulation by increased circulating catecholamines in HF would most likely result in the generation of greater diffuse cAMP. Paradoxically we found that PLN was dephosphorylated in failing as compared with normal ventricular tissue. The residues Ser16 and Thr17 on PLN are targets of PKA phosphorylation, which is directly activated

by cAMP. It has been noted that PKA activity may be rendered inadequate by greater protein phosphatase activity[284], which directly dephosphorylates target residues, as has been shown to occur in the failing sheep ventricle[179]. Moreover, the finding of a possible trend for increased PDE2 activity may highlight an attempt of cellular compensation to regain control of spiralling cAMP concentrations, which concurs with observations from human HF[154].

4.4.3 The modulatory effects of PDE5 inhibition in HF

Over the last 10 years there has been increasing interest in the targeting of the cGMP-PKG axis in various animal models of cardiomyopathy. Chapter 3 showed PDE5 inhibition was negatively inotropic in normal sheep ventricular myocytes, yet many recent studies have shown that PDE5 inhibition with sildenafil improves Ca^{2+} handling[274], reverses cardiac hypertrophy[123, 272], and improves systolic and diastolic function in human heart failure[265]. As the sheep model of heart failure shows similar characteristics to human heart failure at the myocyte level the present study sought to test the effect of PDE5 inhibition on Ca^{2+} handling in HF.

The effect of acute PDE5 inhibition with sildenafil on Ca^{2+} handling has never been tested in patch clamped myocytes from failing hearts. Thus, it was surprising to find that PDE5 inhibition had very little effect on steady state Ca^{2+} handling, particularly the Ca^{2+} transient amplitude in HF. In an *in vivo* study, acute selective PDE5 inhibition caused decreases in cardiac contractility in normal dog hearts, which was not observed following 4 weeks of left ventricular tachypacing[159]. When taken together with possible increases in cGMP availability and PDE5 activity observed in the failing sheep heart, this may suggest that as part of the compensatory changes the heart undergoes in HF, the cGMP-PKG axis may be intrinsically targeted to promote contractility through the cAMP-PKA pathway, which in turn is ultimately detrimental, as occurs with compensatory increases in circulating catecholamines.

Chapter 3 showed that β-AR stimulation in the presence of a PDE5 inhibitor exacerbated the negative modulation of $I_{Ca\text{-}L}$ with little effect on the Ca^{2+} transient. Due to experimental constraints this was not tested in HF cells. However, in vivo data in tachypaced dog hearts showed that β-AR stimulation with dobutamine enhanced PDE5 inhibitor-dependent decline in contractility in normal animals, which was not observed following 4 weeks of pacing[159]. This group concluded that a loss of function of PDE5 in HF is associated with a

loss of protein expression and disrupted localisation from the z-bands[159]. Moreover, t-tubules, which are known to concomitantly localize along the z-bands[285], are partially lost from ventricular myocytes in HF from many species including dog[184] and human[34], as well as in sheep[187]. Such a loss of t-tubules in HF may therefore demonstrate a similar dissociation of PDE5 localisation in our model of HF, and may provide a possible mechanism by which PDE5 inhibition may modulate of β-AR responses in HF.

If PDE5 inhibition manifests negatively inotropic in the sheep model of HF then can it really be beneficial in this model? The following series of experiments sought to elucidate the effects of chronic PDE5 inhibition on the sheep failing myocardium, as others have shown it to be beneficial.

4.4.4 Generating the model of chronically treated HF

As discussed earlier in this chapter, targeting PDE5 came into favour a decade ago, when several reports demonstrated a beneficial effect of PDE5 inhibition in reversing hypertrophy[123] and providing cardioprotection[267] against myocardial injury. The present study aimed to investigate whether chronic PDE5 inhibition was beneficial in the established tachypaced sheep model of heart failure.

PDE5 inhibition is used currently in the treatment of erectile dysfunction and more recently pulmonary hypertension. Many studies have used the common, selective inhibitor sildenafil, being tested in a variety of animal models and used at varying concentrations. The current study opted for the less common PDE5 inhibitor tadalafil, branded as Cialis by Eli Lilly. Tadalafil is known to be more selective than sildenafil for PDE5, without having any effect on PDE6, unlike other PDE5 inhibitors[286]. Furthermore, tadalafil is a long-acting PDE5 inhibitor and has been observed to be effective up to 36 hours in men[287]. A concurrent dose (to the present study, 20mg) was shown to increase intraocular pressure in age and weight matched sheep for up to 2 days after the dose was given, whereas the effects in those animals treated with sildenafil wore off after 1 hour[288]. Together these advantages provide the reasons for why PDE5 inhibition to chronically modulate cardiovascular effects was achieved using tadalafil over sildenafil in the present study.

The tachypaced sheep model of heart failure as used in our laboratory was first described by Briston et al[179]. As shown in the present study, 4-weeks of right ventricular tachypacing was sufficient to induce heart failure in the sheep, with dysfunction observed at both the whole animal (Chapter 4), tissue and myocyte level. As we have previously found HF

symptoms in the sheep are observed between 5 and 8 weeks of rapid pacing[179], thus the current study used this as a benchmark for the time frame for tadalafil treatment. Previous studies have used PDE5 inhibitors chronically for between 2 and 5 weeks[123, 272, 274], thus the current study decided on a 3 week tadalafil treatment period, which put the time frame for total pacing at 7 weeks.

4.4.5 The effect of chronic PDE5 inhibition on calcium handling in heart failure

Rapid right ventricular pacing induced HF reduced $I_{Ca\text{-}L}$ and Ca^{2+} transient amplitude in sheep ventricular myocytes. Chronic PDE5 inhibition with tadalafil resulted in an increase in steady state Ca^{2+} transient amplitude with no effect on $I_{Ca\text{-}L}$. Our laboratory has previously demonstrated that Ca^{2+} transient amplitude is determined mainly by SR Ca^{2+} content, having a cubic relationship[281], although Ca^{2+} release is determined predominantly by peak $I_{Ca\text{-}L}$. An important study limitation is the lack of assessment of SR Ca^{2+} content in tadalafil treated cardiac myocytes, which is fundamental in allowing us to properly understand why the Ca^{2+} transients in these HF myocytes were considerably large. Biomolecular investigation into the proteins that control the SR Ca^{2+} content, SERCA and PLN, showed that their expression was decreased and unchanged respectively in tadalafil treated tissue, which was unchanged from 4-week paced HF. However, there was an increase in the phosphorylation status of PLN, which removes the inhibitory effect from SERCA and may suggest an increased SR loading is facilitated by a mechanism dependent on cGMP, as proposed in Figure 4.16. Furthermore, the increased rate of decay of the Ca^{2+} transient in tadalafil treated myocytes is consistent with such a hypothesis.

Nagayama et al saw similar recovery of the Ca^{2+} transient in a hypertrophic cardiomyopathy mouse model achieved by pressure overload (transverse-aortic constriction, TAC)[274]. Following 4 weeks of TAC, mice were treated orally with sildenafil for a further 5 weeks with the TAC remaining. Ca^{2+} transients were significantly larger than those from 9 week TAC mycoytes, and appeared greater than control levels, which the authors concluded was related to a similar SR loading mechanism proposed by the present study, as they too found increased Ser-PLN phosphorylation following chronic PDE5 inhibition. Together these findings are consistent with an increased activity of PKG, however increased protein phosphatase activity, as found in our sheep model of HF, cannot be ruled out[179].

β-AR signalling was positively modulated in Tadalafil animals. The present study originally hypothesised that PDE5 inhibition would be beneficial in the failing myocardium partly due to resensitisation of cardiac myocytes to sympathetic activation, akin to β-blockers[289], which aim to attenuate exacerbated β-AR signalling in response to increased circulating catecholamines. This study has shown that 3 weeks of tadalafil treatment restored both $I_{Ca\text{-}L}$ and systolic Ca^{2+} transient responsiveness to non-selective β-agonism with isoprenaline to levels similar to that seen in control sheep ventricular myocytes. As the sample size used in this experimental cohort was relatively small the data has been approached with caution, however one can appreciate a restoration of responsiveness to β-AR stimulated Ca^{2+} handling in Tadalafil animals.

The Kass group have demonstrated sustained Ca^{2+} transient responses to isoprenaline in sildenafil treated mice, although they reported minimal effects of TAC on Ca^{2+} transient size, which may be an important defining difference between our model of HF and TAC induced cardiomyopathy[274]. In vivo recordings in a tachypaced model of HF in dogs showed a reduction of β-AR responsiveness (dobutamine) following 4 weeks of pacing, which was unaffected by acute PDE5 inhibition[159] administered intravenously. Together, these findings suggest that it is the chronic effects of PDE5 inhibition that facilitate the restoration of β-AR responsiveness in HF and not the direct effect of the PDE5 controlled signalling cascade itself, i.e. it appears there must be substrates aside from the cGMP/PKG pathway which become constitutively active over time with chronic PDE5 inhibition/cGMP elevation. I propose that this represents a role for other signalling molecules, which are modulated by cGMP and PKG such as PDE2 and PDE3 (Figure 4.16*B*).

Further to this, unpublished data from our lab shows that t-tubules are lost in HF and restored in Tadalafil animals similar to those restored in a model of HF recovery, achieved by pacing cessation. We propose that the regeneration of t-tubules recuperates signal compartmentalization through the redistribution of PDE isoforms to their primary locations, such as PDE2 and PDE5 to the z-bands. Such investigation is beyond the scope of the current study, however immunohisto- and cyto-chemistry may present an interesting future direction to understand this further. T-tubule recovery may result in changes to cellular capacitance (possibly revealed by the tendency for changes observed in Table 14), which may affect the estimation of cell volume. As this has not been accurately measured then this is a notable limitation to the present study.

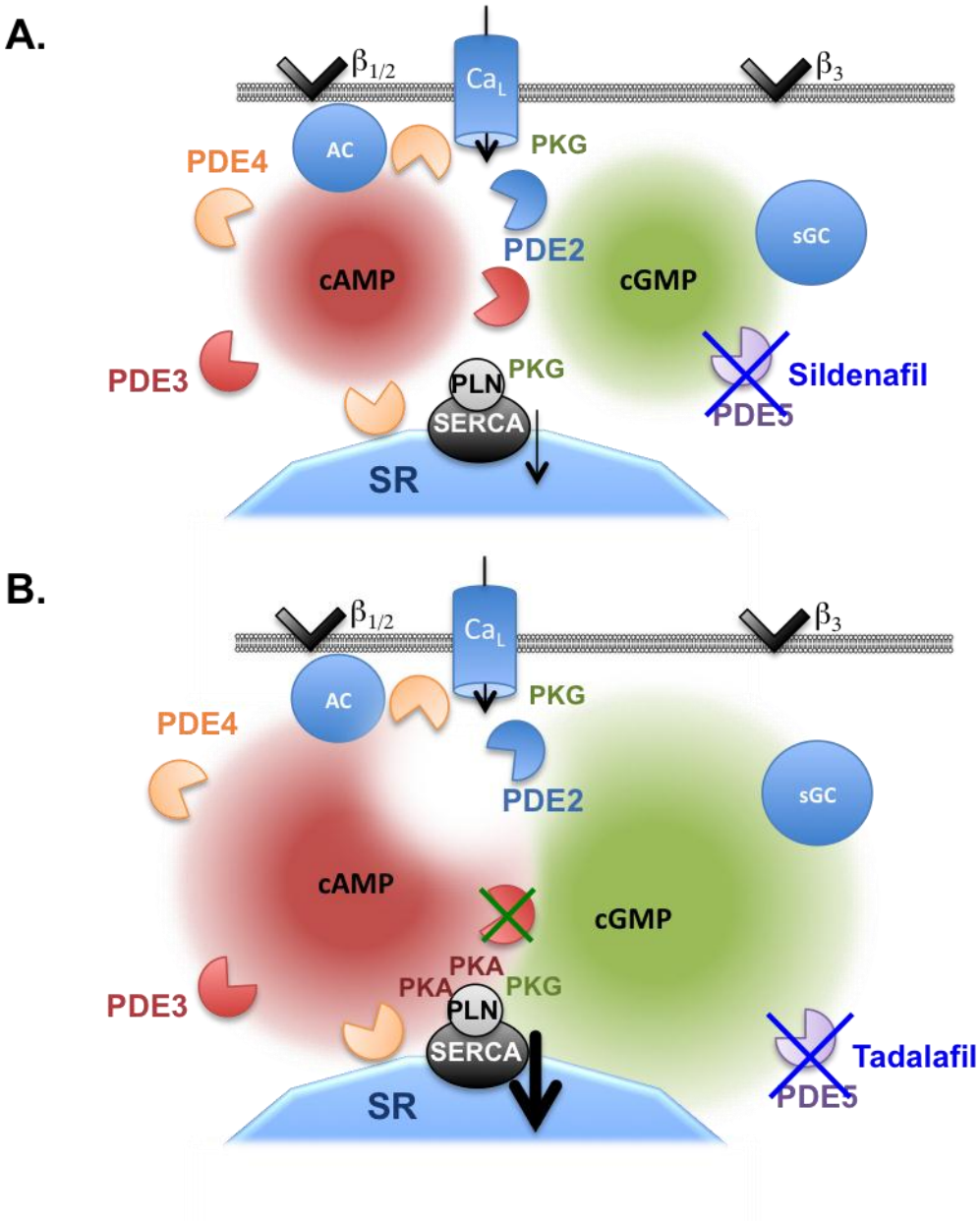

Figure 4.16 The effect of acute and chronic PDE5 inhibition on Ca^{2+} handling.

A potential mechanism for the differential effects of (A) acute and (B) chronic PDE5 inhibition in HF. Crosses represent inhibition. Phosphodiesterase (PDE); β-adrenoreceptor 1/2/3 ($\beta_{1/2/3}$); cyclic adenosine/guanosine monophosphate (cAMP/cGMP); L-type Ca^{2+} channel (Ca_L); protein kinase A/G (PKA/PKG); phospholamban (PLN); sarco-endoplasmic reticulum Ca^{2+} ATPase (SERCA); sarcoplasmic reticulum (SR).

4.4.6 *Ca^{2+} handling is modulated differently in HF by acute and chronic PDE5 inhibition: a mechanism*

The following provides a potential mechanistic framework to explain the differences observed in Ca^{2+} handling in HF with acute and chronic PDE5 inhibition.

This present study has shown a trend towards decreases in $I_{Ca\text{-}L}$ in HF myocytes in response to acute sildenafil application (underpowered), with no concurrent changes in Ca^{2+} transient. Figure 4.16*A* demonstrates that PDE5 inhibition results in increased cGMP accumulation, which will lead to PKG activation and the direct inhibition of the L-type Ca^{2+} channel. PKG will also phosphorylate PLN, thus encouraging SR loading, which may explain small increases in Ca^{2+} transient decay rate. Increased SR loading will maintain Ca^{2+} transient size despite a decreased trigger for Ca^{2+} release.

Figure 4.16*B* shows what happens in chronic PDE5 inhibition in HF, PDE5 inhibition results in tonically generated cGMP, which will (1) bind and inhibit PDE3, resulting in increased global cAMP. PDE3 is located throughout the cytosol and thus will allow cAMP to freely diffuse in the microsomal fraction, activate PKA and thus tonically increase phosphorylation of PLN. (2) cGMP will directly increase the activity of PKG, which will in turn phosphorylate and inhibit the L-type channel, and PLN. (3) cGMP will bind and activate PDE2[154], located mainly at the membrane and increase its hydrolysing activity of cAMP in the particulate fraction, thus decreasing local PKA activity and reducing L-type channel open probability. Together, these effects will result in a decreased $I_{Ca\text{-}L}$ and increased SR loading, which results in a greater steady state Ca^{2+} transient amplitude.

β-AR stimulation is restored in tadalafil treated myocytes. *β_1 and β_2* are known to act more like each other in HF[68], which is beyond the scope of the current study to test whether β-adrenoreceptor subtypes change location in response to tadalafil treatment. Based on them acting as they do in HF, then both β_1 and β_2 will generate global cAMP concentrations in response to stimulation with isoprenaline. This in turn will activate PKA and increase both $I_{Ca\text{-}L}$ and SR loading through PLN phosphorylation. Simultaneously, β_3 activation by isoprenaline will increase cGMP concentrations resulting in (1) increased PKG dependent phosphorylation of PLN and increased SR loading, and (2) increasing an already tonically inhibited PDE3, which will further increase cAMP.

4.5 Conclusion

The present study has shown and proposed a mechanism by which chronic PDE5 inhibition is beneficial to steady state Ca^{2+} handling in heart failure. The systolic Ca^{2+} transient is a function of myocardial contractility, which may suggest that changes in intracellular Ca^{2+} handling may result in overall propagation of restored cardiac function in heart failure following PDE5 inhibition. The findings presented here have strong clinical implications and provide important cellular and molecular explanations for positive systolic and diastolic effects observed in HF patients currently treated with PDE5 inhibitors.

The next chapter will outline the effects of chronic PDE5 inhibition on clinical assessment of heart failure in the large animal.

Chapter 5

5 The effect of chronic PDE5 inhibition in heart failure: in vivo measurements.

5.1 Introduction

The previous chapter demonstrated that chronic PDE5 inhibition provides some restoration of both Ca^{2+} handling and β-AR responsiveness to ventricular myocytes in a large animal model of HF. The focus was to elucidate the cellular and molecular mechanisms responsible for beneficial effects of PDE5 inhibition. This next chapter will present data for the effect of chronic PDE5 inhibition on the whole animal, thus will employ a range of in vivo techniques to assess the holistic pathophysiology of HF in the sheep.

The aims of this chapter are as follows:

- To assess the clinical progression of HF in tachypaced sheep.
- To assess the longevity of animals in HF chronically treated with the PDE5 inhibitor compared with those untreated.
- To use echo- and electrocardiography to assess the changes in cardiac geometry and electrophysiology during HF progression and any improvements elicited by chronic PDE5 inhibition.
- To extrapolate from cellular improvements in β-AR responsiveness by chronic PDE5 inhibition by assessing β-AR reserve in vivo.

5.2 Methods

5.2.1 Lung weight to body weight ratio

All animals were weighed before the period of pacing and then again after 4-weeks of pacing (or end-stage). For those animals chronically treated for a further 3 weeks then a final weight was recorded prior to euthanasia.

After the removal of the heart the trachea was dissected as high as possible from within the thorax and the lungs were removed intact. Superfluous connective and pericardial tissue was removed were appropriate. The wet weight was recorded in grams.

Final body weight was compared with the weight of the lungs to give a calculation of the lung:body weight ratio (LW:BW), which is often used as a useful function of disease. LW:BW was compared between control, heart failure and tadalafil treated animals using a one-way ANOVA in Sigma plot.

5.2.2 Blood pressure

Blood pressure was recorded using tail cuff plethysmography in all animals prior to the period of pacing and then again after 4-weeks of pacing (or end-stage). For those animals that were then chronically treated for a further 3 weeks then a final BP recording was completed prior to sacrifice. In both latter cases, BP measurements were taken after the pacemaker had been turned off for at least 10 minutes. All recordings were performed in conscious, standing, minimally restrained animals using an appropriately sized tail cuff. For all animals a series of measurements were taken and the last 5 results averaged to ensure minimal variation relating to stress. Systolic blood pressure (SBP) and diastolic blood pressure (DBP) were recorded directly and pulse pressure (PP=SBP-DBP) and mean blood pressure (MBP=DBP+1/3PP), were calculated offline. Heart rate (HR) was also recorded simultaneously through the tail cuff.

As data was paired for all animals SBP, DBP, MBP and HR from control, heart failure and tadalafil animals (where appropriate) were compared using a one-way repeated measures ANOVA and the Holm-Sidak post-hoc test. Significance was interpreted as $p<0.05$.

5.2.3 Echocardiography

Echocardiography was performed using a 5-1 MHz phased array probe and recorded on a Sonosite MicroMaxx (BCF Technology, Scotland) in all animals prior to the period of

pacing and then again after 4-weeks of pacing (or end-stage). For those animals that were then chronically treated for a further 3 weeks then final recordings were made prior to sacrifice. In both latter cases, echocardiography was performed after the pacemaker had been turned off for at least 10 minutes and in all cases animals were conscious and seated, under gentle restraint.

A right-sided transthoracic window was utilised to acquire both short-axis and long-axis parasternal views.

5.2.3.1 Short axis measurements

Short axis echocardiographs were recorded by finding a cross section through the left ventricle just below the mitral valve. This view is used to measure end-systolic area (ESA) and end-diastolic area (EDA), which can be used to calculate the fractional are change per cardiac cycle.

$$\text{Fractional area change} = \frac{\text{EDA} - \text{ESA}}{\text{EDA}}$$

Equation 3

Short axis measurements were made by converting 6 second .avi files to .bmp image sequences using Virtual Dub and using image analysis software (ImageJ, USA) to select which images show systole or diastole. Once selected, the polygonal selection tool was used to manually draw around the area of the ventricle lumen at both systole and diastole (Figure 5.1). A minimum of 3 cardiac cycles were measured and the mean taken.

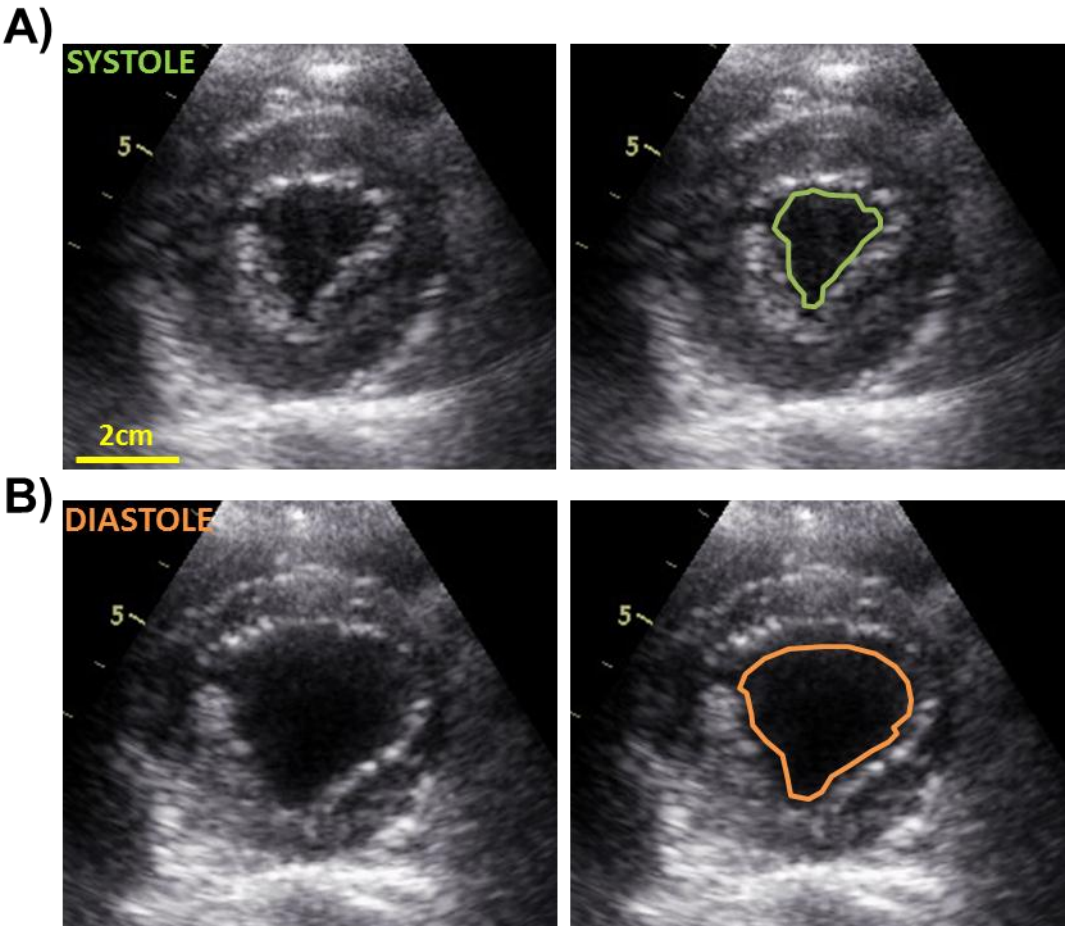

Figure 5.1 Representative short-axis echocardiogram

Images captured using transthoracic parasternal echocardiographic window in a control animal during (A) Systole and (B) Diastole. The right hand panels show the traced area at end-systolic (ESA) and end-diastolic (EDA), the difference between the two is the fractional area change.

5.2.3.2 Long axis (M-mode) measurements

Long axis echocardiography is used to measure ventricular lumen dimensions: end-systolic internal diameter (ESID) and end-diastolic internal diameter (EDID), as well as wall thickness at both systole (SWT) and diastole (DWT). M-mode echocardiography is useful as it shows a cross section through the ventricular lumen over time, as shown in Figure 5.2. In humans ejection fraction would be calculated from the ratio of ventricular volume between diastole and systole, however a 4-chamber view is required, which is unobtainable in the sheep due to their cardiac anatomy. Alternatively, in order to calculate ventricular contractile function the present study measured fractional shortening using the following equation:

$$\text{Fractional shortening} = \frac{\text{EDID} - \text{ESID}}{\text{EDID}}$$

Equation 4

Furthermore, as changes in wall thickness occur between systole and diastole, relative wall thickness was calculated as follows:

$$\text{Relative wall thickness} = \frac{2 \times \text{DWT}}{\text{EDID}}$$

Equation 5

5.2.3.3 Data interpretation

All variables were assessed pairwise for each animal across the course of their paced duration. Sigma plot was used to graphically present each variable between control, heart failure and tadalafil treated. One-way repeated measures ANOVA with a $p\text{-value}<0.05$ was assessed as statistically significant.

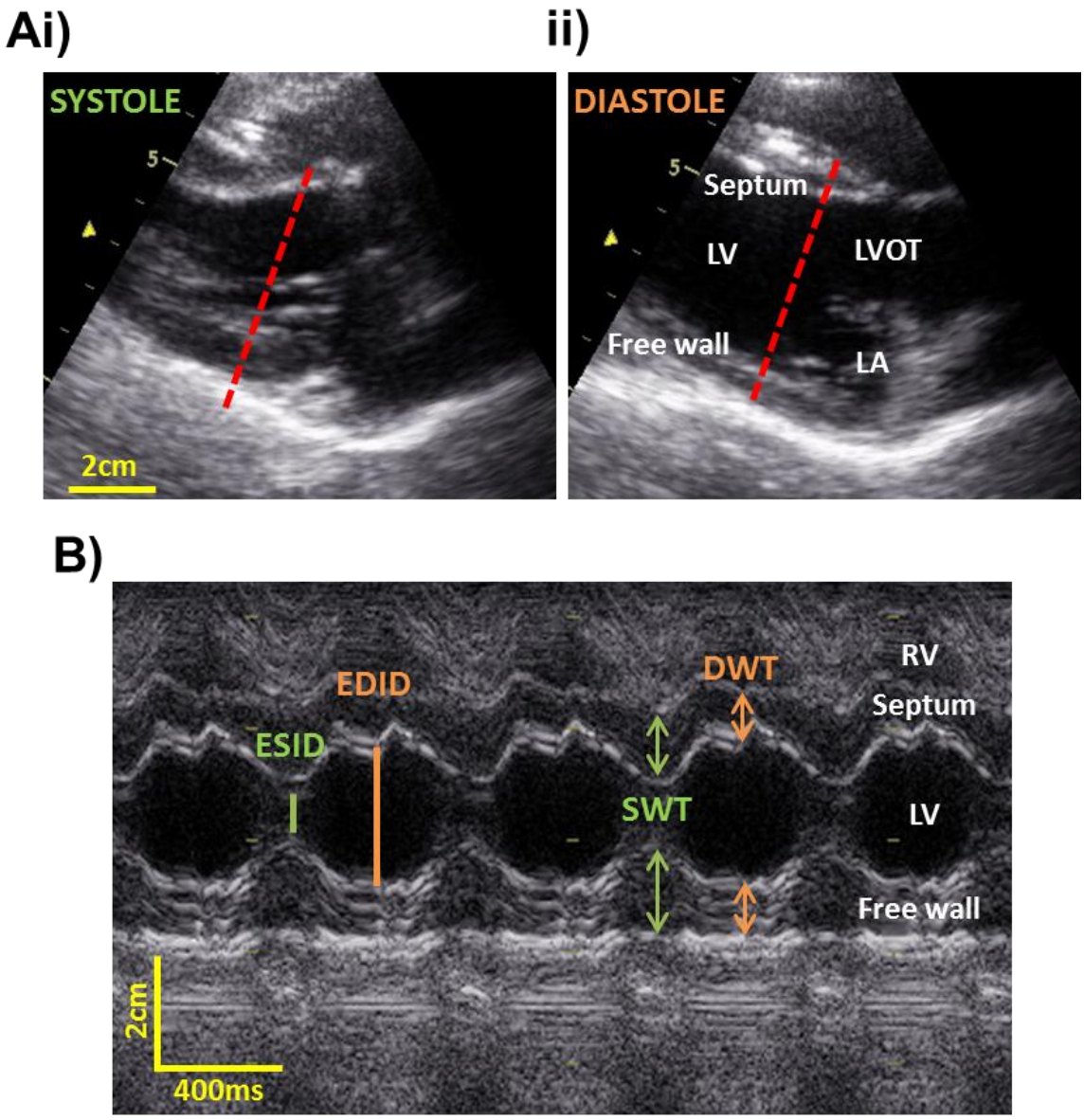

Figure 5.2 Representative long-axis and M-mode echocardiogram

Images captured using transthoracic parasternal echocardiographic window in a control animal during (Ai) Systole and (ii) Diastole. Red line represents the probe position for m-mode cross section in (B). M-mode view shows contractility over time and methods for measurements of end-systolic and end-diastolic internal diameters (ESID/EDID) and wall thicknesses (SWT/DWT). Left ventricle (LV), right ventricle (RV), left atrium (LA), left ventricular outflow tract (LVOT).

5.2.4 Animal Survival

The three different models used in this study correspond to the number of days each animal was paced: 4-week HF, end-stage HF and tadalafil treated HF. In order to demonstrate the effect of tadalafil treatment on symptomless survival a Kaplan-Meyer survival plot was used. The number of animals alive per day was recorded for the full length of each animal's paced duration. Paced duration itself was compared using a one-way ANOVA between end-stage HF and tadalafil treated HF. Significance was determined as $p<0.05$.

5.2.5 Electrocardiography

Animals were allowed to settle in a seated position under light restraint as five electrodes were attached to clipped limbs and chest. The electrocardiogram (ECG) was recorded using a PC with IOX software (EMKA Technologies, France). Electrical conductivity through the limb leads was maximised using a light spray of water. A 10-minute ECG was recorded once the animal was settled a relaxed. Paced animals had the pacemaker switched off for at least 10 minutes before any ECG was recorded.

ECG analysis was done offline. Firstly raw ECG traces (.mkt files) were opened in ECG-Auto (EMKA Technologies, France) and 5 minutes of clean ECG was chosen. The chosen .mkt files were then converted into tab delimited .txt files and re-opened in Labchart for analysis. Labchart software enabled the user to create a library of reference waveforms for several parameters to be accurately analysed. Waveforms chosen were: the start and end of the P wave, the start of the Q wave, peak of the R wave, the peak and end of the T wave. At least 1 minute of the selected ECG trace was analysed to measure R-R interval, heart rate (HR) and QT interval.

In order to assess the influence of the autonomic nervous system on HR a measure of heart rate variability (HRV) was calculated. This involves measuring the standard deviation of the R-R interval (RRSD). As HR increases or decreases the conduction through the heart also changes, thus QT interval changes. In order to give an accurate measure of QT interval a correction for HR is required, QT correction (QTc). In this study the correction used was the Bazett's formula:

$$QTc = \frac{QT\ interval}{\sqrt{(60/HR)}}$$

Equation 6

All variables were assessed pairwise for each animal across the course of their paced duration. SigmaPlot was used to graphically present each variable between control, heart failure and tadalafil treated. One-way repeated measures ANOVA with a p-value<0.05 was assessed as statistically significant.

5.2.5.1 Dobutamine stress test

A dobutamine stress test was used to assess the *β*-AR reserve in vivo. In order to do this the forearm of the animal was cannulated (as described) and a saline flush administered, followed by the attachment of a 50ml syringe filled with 500μg.ml^{-1} dobutamine. This syringe was connected to an infusion pump and ECG was recorded. After recording 10 minutes of baseline ECG the dobutamine infusion was started and the flow rate of dobutamine was increased every 3 minutes. Increasing the flow rate resulted in an increased effective dose of dobutamine being delivered to the animal: 0.5, 1, 2.5, 5, 10, 20 μg.kg^{-1}.min^{-1}. *β*-AR responsiveness was assessed via monitoring of the animal's heart rate (HR). A doubling of baseline HR was considered a sufficient *β*-AR evoked response. The stress test was completed pre-paced, post-4 weeks pacing and post-tadalafil treatment. At baseline, all animals had at least a doubling of HR following 10μg.kg^{-1}.min^{-1}, thus none were stressed with higher doses of dobutamine. At the beginning and end of the test an echocardiogram was recorded to monitor the change in *β*-AR induced contractility.

The R-R interval at each dose of dobutamine was analysed from the raw ECG traces as described above. Mean data ± standard error of the mean was collated in Microsoft Excel and R-R interval at each dose was normalised to the R-R interval at baseline (before dobutamine) in order to give an assessment of the change in R-R interval (HR) with the *β*-AR agonist. Significance was assessed using SigmaPlot using a two-way repeated measures ANOVA, p<0.05 was deemed significant. Contractility was measured using echocardiography analysis as explained in section 5.2.3.

5.3 Results

Heart failure is one of the world's leading causes of morbidity and mortality, which has been approached by a number of therapeutic strategies. The present study has shown that chronic PDE5 inhibition may improve left ventricular myocyte Ca^{2+} cycling and sensitivity to β-AR agonists. In light of these positive effects, we tested whether chronic PDE5 inhibition is beneficial to the general health of an entire animal by assessing heart failure progression with and without PDE5 inhibitor treatment using a range of in vivo measurements.

5.3.1 The effect of HF and chronic PDE5 inhibition on animal weight

As cachexia, weight loss, is a symptom of human heart failure, the current study tested whether sheep undergo similar weight loss following tachypacing. In a paired cohort of animals baseline body weight (BW) measurements was 29.6±1.3 kg, reduced to 27.7±1 kg following 4 –weeks of rapid ventricular pacing (p>0.01, n=21). In a tadalafil treated cohort of animals baseline BW was 28.7±1 kg, which was relatively unchanged by 4-weeks of pacing 27.2±1 kg, with a possible trend for an increase toward control levels following 3-weeks of tadalafil treatment 28.1±1 kg. The error is relatively high in this cohort, which is reflected by the low sample number (n=9), and proved underpowered for appropriate statistical testing. A limitation here is that body weight was unfortunately not recorded for the end-stage HF animals.

Lung weight (LW) was measured post-mortem from animals in each group, control, 4-weeks, and Tadalafil, to allow a calculation of LW:BW, which is considered the primary morphometric measure of heart failure. Lung weight can be representative of the degree of pulmonary oedema, which is known to occur in end-stage HF. The data in Table 15 shows there was little difference between the three groups of animals, however it should be appreciated that in the sheep this is a crude assessment of pathology.

	LW:BW	***n***
Control	0.019±0.001	15
4-wk	0.019±0.002	10
Tadalafil	0.018±0.001	14

Table 15. Lung weight to body weight measurement as a function of heart failure

Mean ± SEM. Comparison determined using one-way ANOVA.

5.3.2 The effect of heart failure and chronic PDE5 inhibition on blood pressure

Human heart failure can be described as a syndrome consisting of oedamatous, haemodynamic and neurohormonal disorders manifesting simultaneously. As heart failure is associated with changes in cardiac output, heart rate and blood pressure, the next series of measurements aimed to assess the cardiovascular status of the tachypaced sheep.

Blood pressure recording was achieved using tail cuff plethysmography and readings were taken at least 10 minutes after the pacemaker had been turned off. Raw data is summarised in Table 16. Following 4-weeks of tachypacing, animals presented with a reduced systolic blood pressure, with relatively unchanged diastolic pressures (Figure 5.3*A/B*. This in turn manifested into a reduction in pulse pressure (systolic BP –diastolic BP, Figure 5.3*D*) and mean arterial blood pressure (diastolic BP / 0.33 x pulse pressure) (Figure 5.3*C*). In end-stage HF animals there was a tendency for a reduced diastolic BP (*p=0.09*) and MABP (*p=0.08*), however this may reflect the underpowered nature of this group (Table 16).

PDE5 inhibitors such as tadalafil are commonly used in the treatment of vascular disorders such as erectile dysfunction and pulmonary hypertension. The subsequent increases of cGMP in vascular endothelial cells results in endothelial-dependent relaxation of vascular smooth muscle and vasodilatation. Despite these known effects 3 weeks of tadalafil treatment seemingly had very little effect on blood pressure in comparison to that observed after 4-weeks of pacing (Figure 5.3).

	Control	**4 wk**	**Tadalafil**	**esHF**
Systolic (mmHg)	116±3	99±1*	98±5*	102±5
Diastolic (mmHg)	68±5	62±2	55±5	57±5
MABP	89±5	78±2*	74±4*	72±5
PP	48±4	37±1*	42±4	45±3

Table 16. Summary data for blood pressure in HF and following PDE5 inhibitor treatment

*Measurements taken before commencement of pacing (control), at 4-weeks of pacing (4 wk) and after 3-weeks of further pacing concomitant with tadalafil treatment. Differences tested using a one-way repeated measures ANOVA (n=5). Measurements at the point of euthanasia for the end-stage HF (esHF) animals are shown for comparison purposes, differences between this group and other time points were tested using a one-way ANOVA (n=5). Mean ± SEM, *p<0.05 versus control. (MABP=mean blood pressure, PP=pulse pressure).*

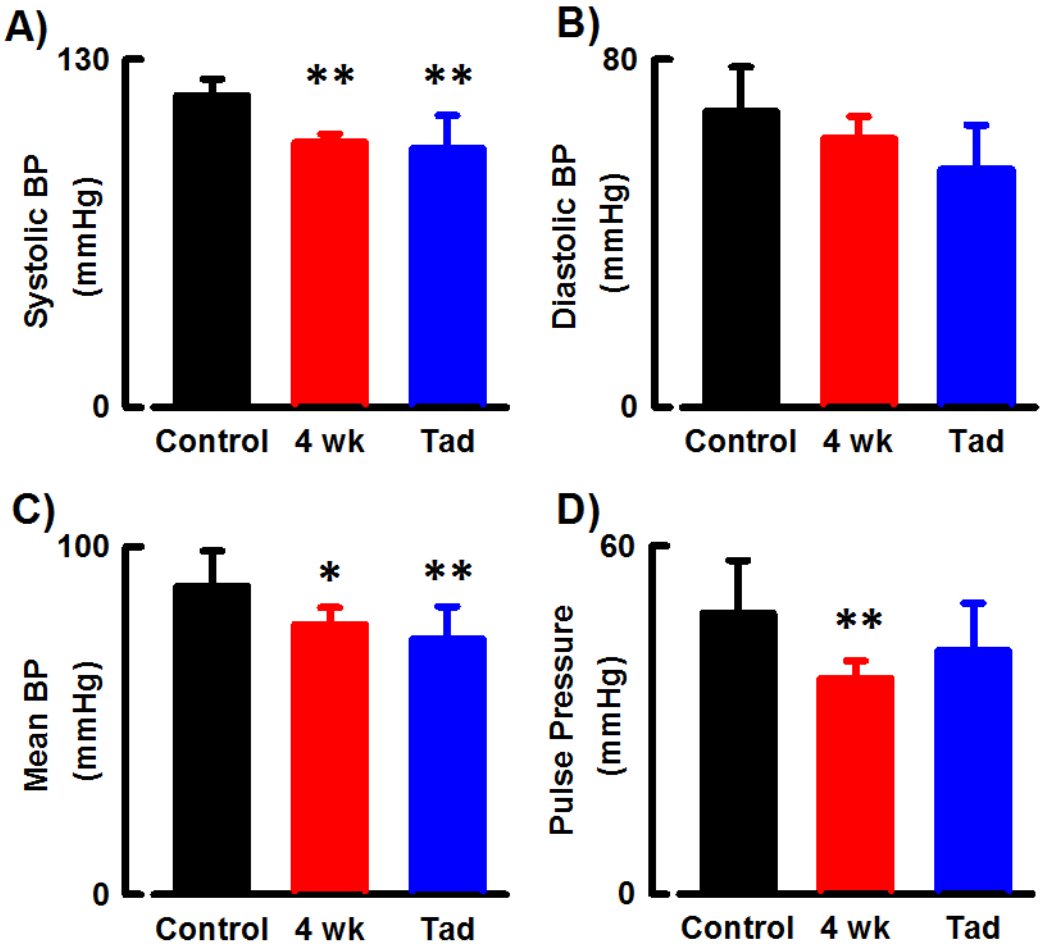

Figure 5.3 Mean data for blood pressure and heart rate measurements

*All measurements are pairwise, taken pre-pacing (Control, black), at 4-weeks of pacing (4-wk, red) and after 3-weeks of further pacing concomitant with tadalafil treatment (Tadalafil, blue). Measurements shown are for (A) systolic blood pressure, (B) diastolic blood pressure, (C) mean blood pressure and (D) pulse pressure. Mean ± SEM. Differences compared using a one-way repeated measures ANOVA and holm-sidak post-hoc test. Versus control *p<0.05, **p<0.01.*

5.3.3 The effect of HF and chronic PDE5 inhibition on animal survival

In accordance to Home Office legislation, the development of symptoms (cachexia, dyspnea, and fluid accumulation) requires the animal to be sacrificed, thus we use the term 'end-stage' HF as the point at which symptoms prevail to the point where it is considered necessary to euthanise the animal.

Figure 5.4 shows a Kaplan-Meier plot demonstrates the relative survival of animals paced until the end of the study. HF animals treated with a PDE5 inhibitor live longer than untreated animals.

In terms of paced duration Tadalafil treated animals were tachypaced for 30±1.1 days, approximately 4 weeks, and treated for a further 20.7±0.3 days, approximately 3 weeks, with the selective, long-acting PDE5 inhibitor tadalafil. Animals destined for end-stage HF were paced on average for 42.6±4 days at which point they had developed symptoms of HF and were sacrificed. In total, tadalafil animals were paced for 50.7±1.4 days, which equates to a total pacing time of 15.9±8.4% greater than end-stage HF animals (p=0.03, n=15).

Taken together, tadalafil treatment improves survival and cellular Ca^{2+} handling in animals with HF without effects on vascular resistance, which suggests that the beneficial effects of PDE5 inhibition are not due to changes in cardiac loading. The next set of experiments sought to elucidate changes to cardiac function in HF and following tadalafil treatment.

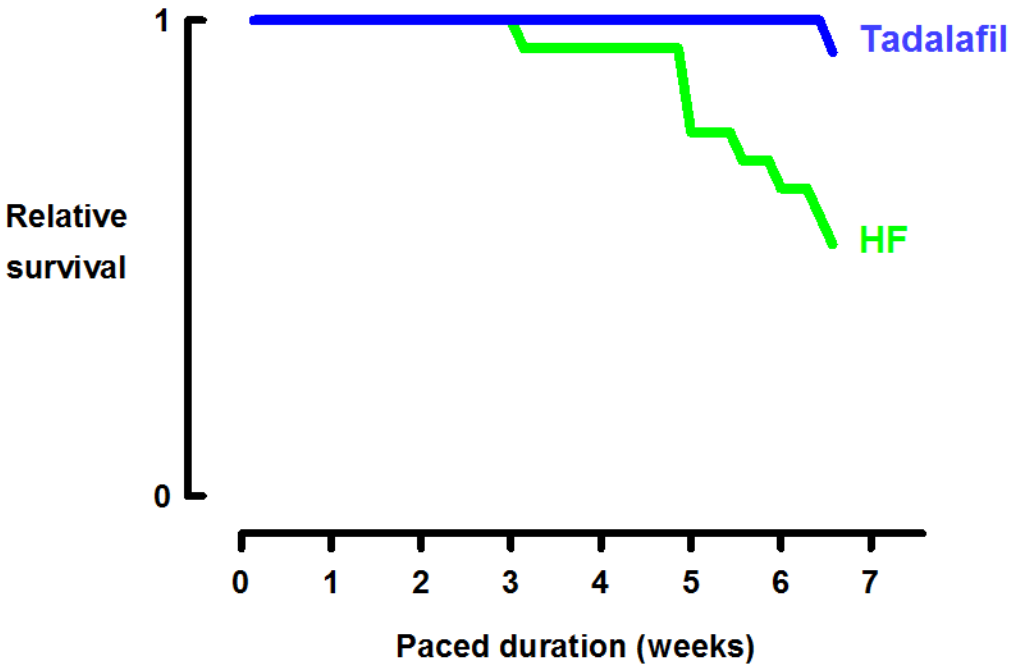

Figure 5.4 Relative symptom free survival in PDE5 inhibitor treated HF animals

Animals were paced for 4 weeks at which point some were treated chronically with the PDE5 inhibitor tadalafil and paced for a further 3 weeks (blue line), other animals deemed for 'end-stage' HF were paced continually until they presented clinical symptoms of HF (green line), at which point they were sacrificed (n=15).

5.3.4 The effect of heart failure and chronic PDE5 inhibition on left ventricular dimension and systolic function

5.3.4.1 Fractional area change

Short axis echocardiography using b-mode (brightness/2-dimensional mode) allows a cross-sectional view through the heart to be analysed. Measuring the cross-sectional area of the ventricular lumen, inferior to the mitral valves, provides us with chamber dimensions that can be measured at both systole and diastole (Figure 5.5*A*). From these the fractional area change can be calculated, which is a function of cardiac contractility. Control corresponds to observations before commencement of tachypacing: pre-pacing. Summary data in Figure 5.5*B/C* shows that 4-weeks of tachypacing reduces contractility (pre-pacing: 0.73±0.02 cm, versus 4-week: 0.46±0.03 cm), similar to the dysfunction observed in end-stage heart failure (0.40±0.08 cm). Furthermore, chronic treatment with tadalafil had little effect on contractility compared with that observed at both 4-week and end stage HF (0.51±0.05 cm, Figure 5.5*B/D*). Also, note the accumulation of pericardial fluid in representative paced images (pericardial effusion (PE) marked on Figure 5.5A), as this demonstrates fluid decompensation associated with dilated cardiomyopathy.

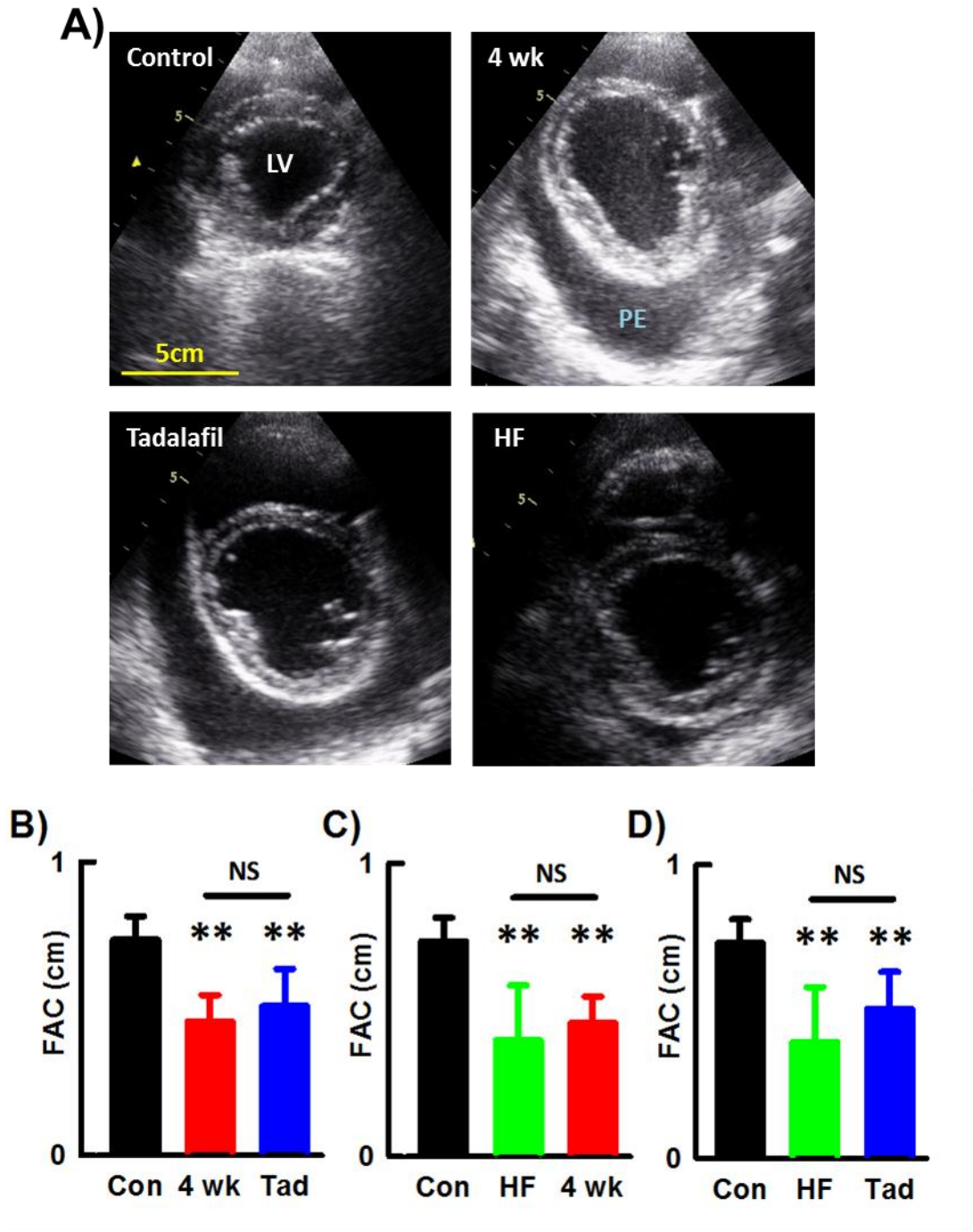

Figure 5.5 The effect of PDE5 inhibition in heart failure on fractional area change

*Echocardiography performed before pacing (control), at 4 weeks of pacing (4-wk), after a further 3-weeks of pacing plus tadalafil treatment (Tadalafil), and in animals paced to end-stage HF (HF). PE = pericardial effusion. (A) Representative short axis echocardiograms. Summary data for fractional area change (B) pairwise and (C/D) unpaired to show comparisons with HF. Data presented as fractional area change (end-systolic minus end-diastolic area, 1 being total area change, discussed in Chapter 5.2). Mean±SEM. Differences compared using a one-way repeated measures ANOVA and holm-sidak post-hoc test for pairwise data and a one-way ANOVA for unpaired data. Versus control *p<0.05, **p<0.01. NS=not significant.*

5.3.4.2 Fractional shortening

Long-axis echocardiography using m-mode (motion) allows specific ventricular lumen dimensions to be measured, such as internal diameters and wall thicknesses at both systole and diastole. The movement of the free- and septal- ventricular walls can be measured during systole and diastole to calculate the fractional shortening. The anatomy of the sheep thorax makes it impossible to obtain a 4-chamber apical view, which would be the usual method of calculating ejection fraction (an accurate measure of ventricular contractile function), thus fractional shortening, together with fractional area change, provides the only available indications in this model. Figure 5.6*B/C* show both 4-weeks of pacing and end-stage HF are associated with decreased ventricular contractility (pre-pacing: 0.55±0.03 cm, versus 4-week: 0.31±0.02 cm, and HF: 0.22±0.02 cm). Furthermore, as disease progresses with prolonged pacing from 4-weeks to the presentation of symptoms of end-stage HF, ventricular function worsens (Figure 5.6*D*, -29.9±8.8%, $p<0.001$). There was little difference observed between ventricular function in Tadalafil and end-stage HF (0.21±0.03 cm, Figure 5.6*E*), which showed a trend to be worse than the function observed at 4-weeks of pacing (p=0.06, Figure 5.6*B*).

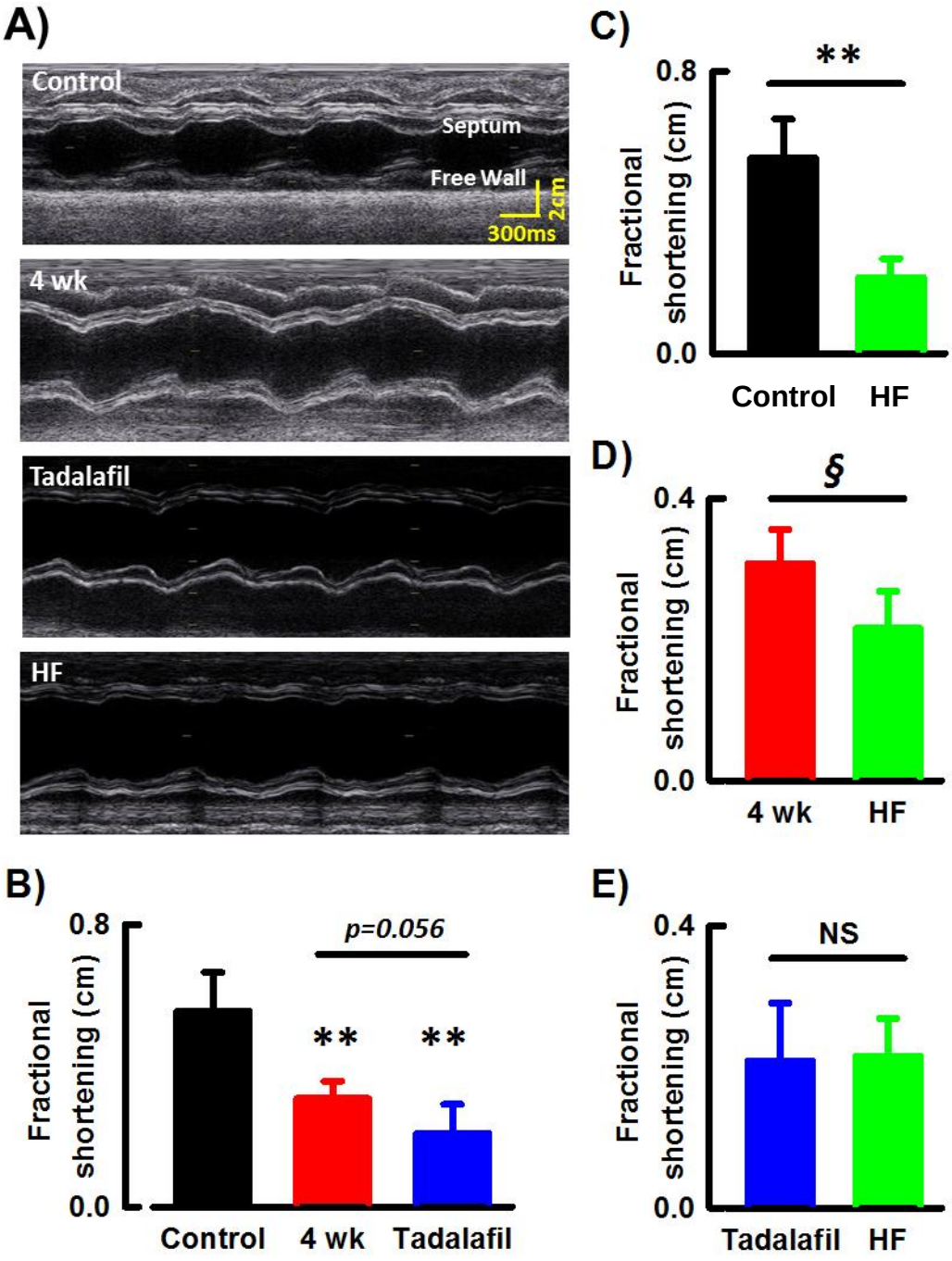

Figure 5.6 The effect of PDE5 inhibition in heart failure on fractional shortening

*Echocardiography performed before pacing (control), at 4 weeks of pacing (4-wk), after a further 3-weeks of pacing plus tadalafil treatment (Tadalafil), and in animals paced to end-stage HF (HF). PE = pericardial effusion. (A) Representative long axis echocardiograms. Summary data for fractional shortening (B) pairwise and (C/D) unpaired to show comparisons with HF. Data presented as a fraction end-diastolic internal diameter (1 being total shortening, discussed in Chapter 5.2) Mean±SEM. Differences in paired data compared using a one-way repeated measures ANOVA and holm-sidak post-hoc test, or a paired Student's t-test. Unpaired data compared using a Student's t-test. Versus control **p<0.01. Versus 4-wk §p<0.01. NS=not significant.*

End-diastolic and end-systolic internal diameter (EDID and ESID respectively) measurements provide an indication of the level of ventricular dilatation associated with heart failure. Summary data presented in Figure 5.7 and Figure 5.8 show that both EDID (pre-pacing: 3.34±0.4 cm) and ESID (pre-pacing: 1.55±0.3 cm) were increased after 4-weeks of pacing (3.68±0.2 cm and 2.65±0.3cm respectively), which was not as bad as the dilatation observed in end-stage HF hearts (EDID: 4.79±0.3 cm, ESID: 3.76±0.3 cm). Following 3 weeks of PDE5 inhibitor treatment there was neither any significant difference between chamber dimensions at 4-weeks nor at end-stage (EDID: 3.94±0.3 cm, ESID: 3.13±0.3 cm), which suggests tadalafil treatment arrested any further chamber dilatation.

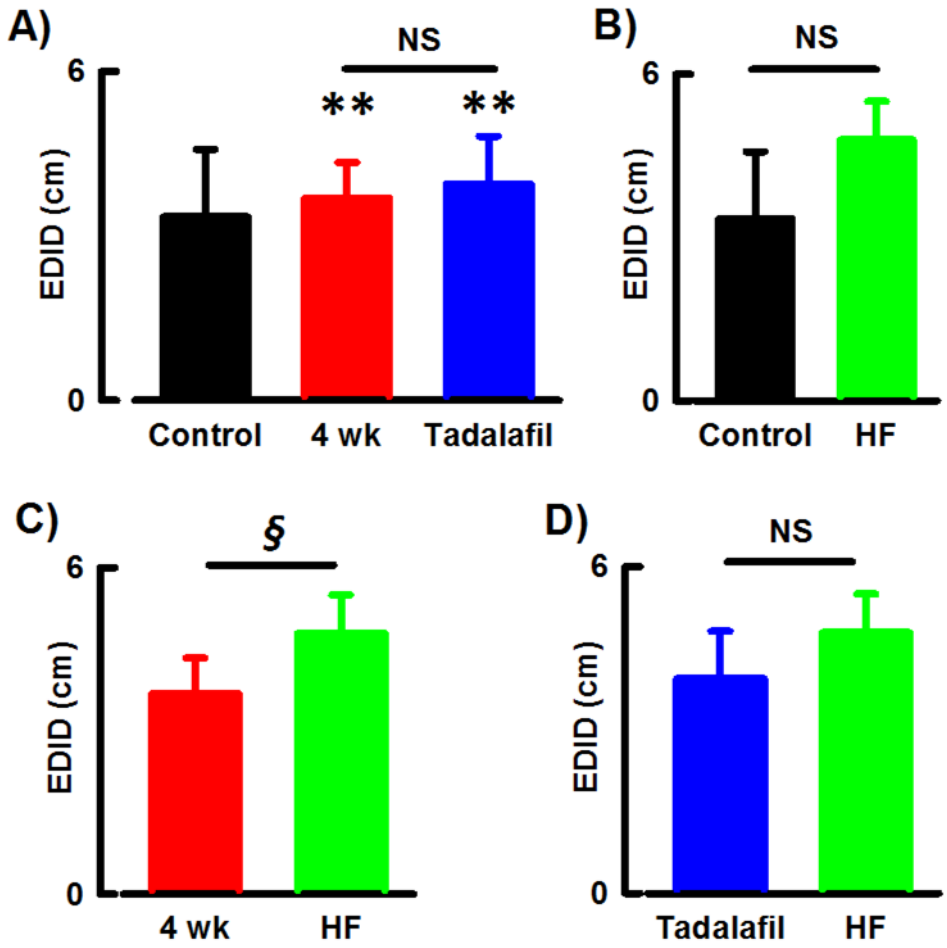

Figure 5.7 The effect of PDE5 inhibitor treatment in heart failure on end-diastolic internal diameter (EDID)

*(A) Paired summary data for EDID as measured from m-mode echocardiography for control (black), 4-week paced (4 wk, red), 3-week further pacing plus tadalafil treatment (Tadalafil, blue). (B) Paired summary data for EDID between control and end-stage HF (green). (C) Unpaired summary data for EDID between 4 wk and HF. (D) Unpaired summary data for EDID between HF and Tadalafil. Mean±SEM. Differences in paired data compared using a one-way repeated measures ANOVA and holm-sidak post-hoc test, or a paired Student's t-test. Unpaired data compared using a Student's t-test. Versus control **p<0.01. Versus 4-wk §p<0.01. NS=not significant.*

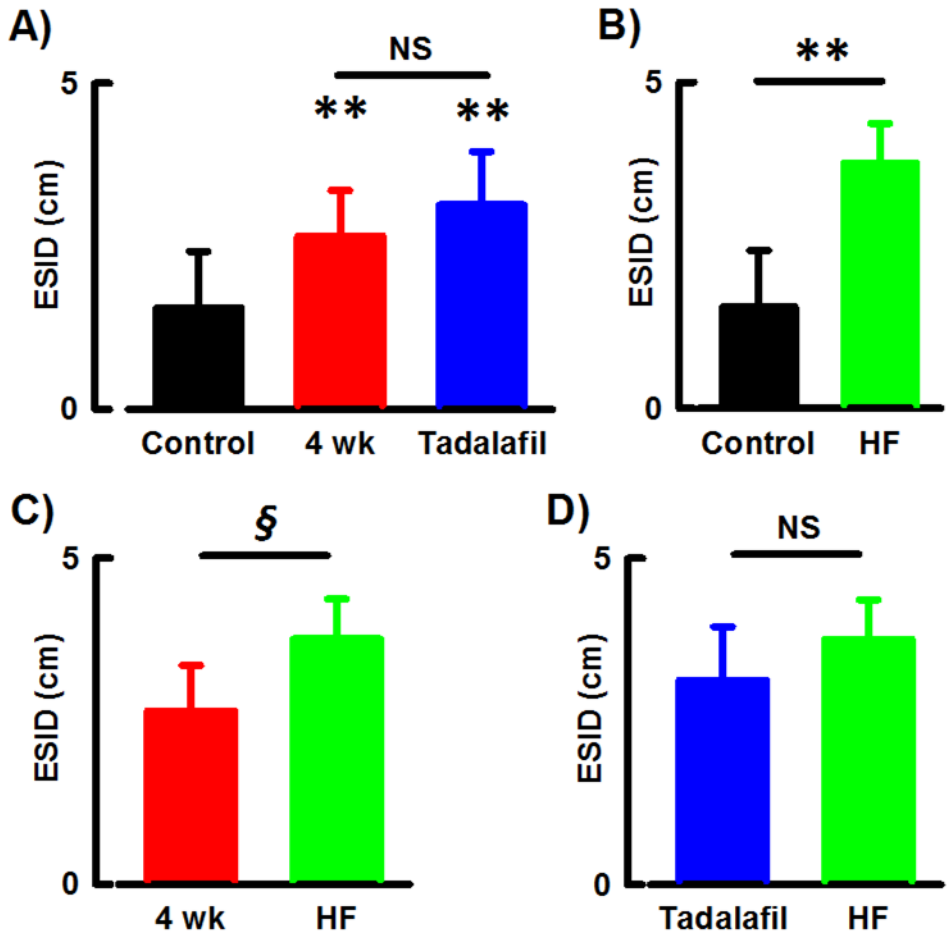

Figure 5.8 The effect of PDE5 inhibitor treatment in heart failure on end-systolic internal diameter (ESID)

*(A) Paired summary data for ESID as measured from m-mode echocardiography for control (black), 4-week paced (4 wk, red), 3-week further pacing plus tadalafil treatment (Tadalafil, blue). (B) Paired summary data for ESID between control and HF (green). (C) Unpaired summary data for ESID between 4 wk and HF. (D) Unpaired summary data for ESID between HF and Tadalafil. Mean±SEM. Differences in paired data compared using a one-way repeated measures ANOVA and holm-sidak post-hoc test, or a paired Student's t-test. Unpaired data compared using a Student's t-test. Versus control **p<0.01. Versus 4 wk §p<0.05. NS=not significant.*

Different animal models of heart failure use different substrates to induce cardiomyopathy. Pressure overload models induced by transverse aortic constriction generate hypertrophic cardiomyopathy, whereas tachypaced models, such as the present study, generate dilated cardiomyopathy. We have shown that chamber dilatation occurs in the present model of HF, thus we next tested whether hypertrophy is observed by measuring ventricular wall thickness. Figure 5.9 shows that 4-weeks of tachypacing resulted in a reduction in free wall thickness (pre-pacing: 0.60±0.06 cm, versus 4-weeks: 0.32±0.02 cm, p=0.002) similar to that observed in end-stage HF (0.35±0.03 cm, p=0.08), a 45.8±5.9% and 40.9±7.4% reduction respectively.

The intraventricular septum thickness was also measured (pre-pacing: 0.69±0.07cm), which too was reduced following 4-weeks of pacing (45.4±6.4%, 0.37±0.02 cm, p<0.001), which was seemingly worse than the reduced thickness observed in end stage HF (29.8±9.9%, 0.48±0.05 cm, p=0.06). Together, these changes correspond to the ventricular dilatation observed in both diastole and systole as described above.

Tadalafil treatment had no effect on either free wall (0.36±0.05 cm) or septal wall (0.39±0.05 cm) thickness as compared with either 4-weeks of pacing or end stage HF.

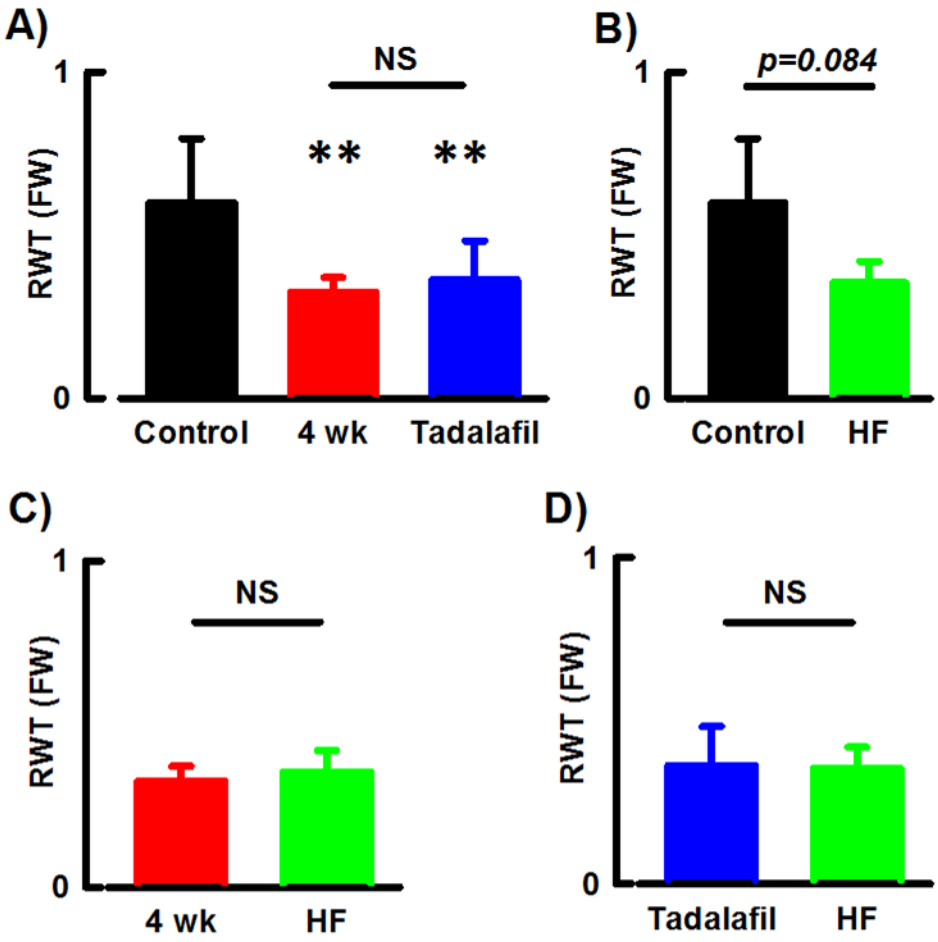

Figure 5.9 The effect of PDE5 inhibitor treatment in heart failure on relative wall thickness (RWT) of the left ventricular free wall (FW)

*(A) Paired summary data for RWT FW as measured from ventricular free wall thickness in diastole (see text) using m-mode echocardiography for control (black), 4-week paced (4 wk, red), 3-week further pacing plus tadalafil treatment (Tadalafil, blue). (B) Paired summary data for RWT FW between control and HF (green). (C) Unpaired summary data for RWT FW between 4 wk and HF. (D) Unpaired summary data for RWT FW between HF and Tadalafil. Mean ± SEM. Differences in paired data compared using a one-way repeated measures ANOVA and holm-sidak post-hoc test, or a paired Student's t-test. Unpaired data compared using a Student's t-test. Versus control **p<0.01. NS=not significant.*

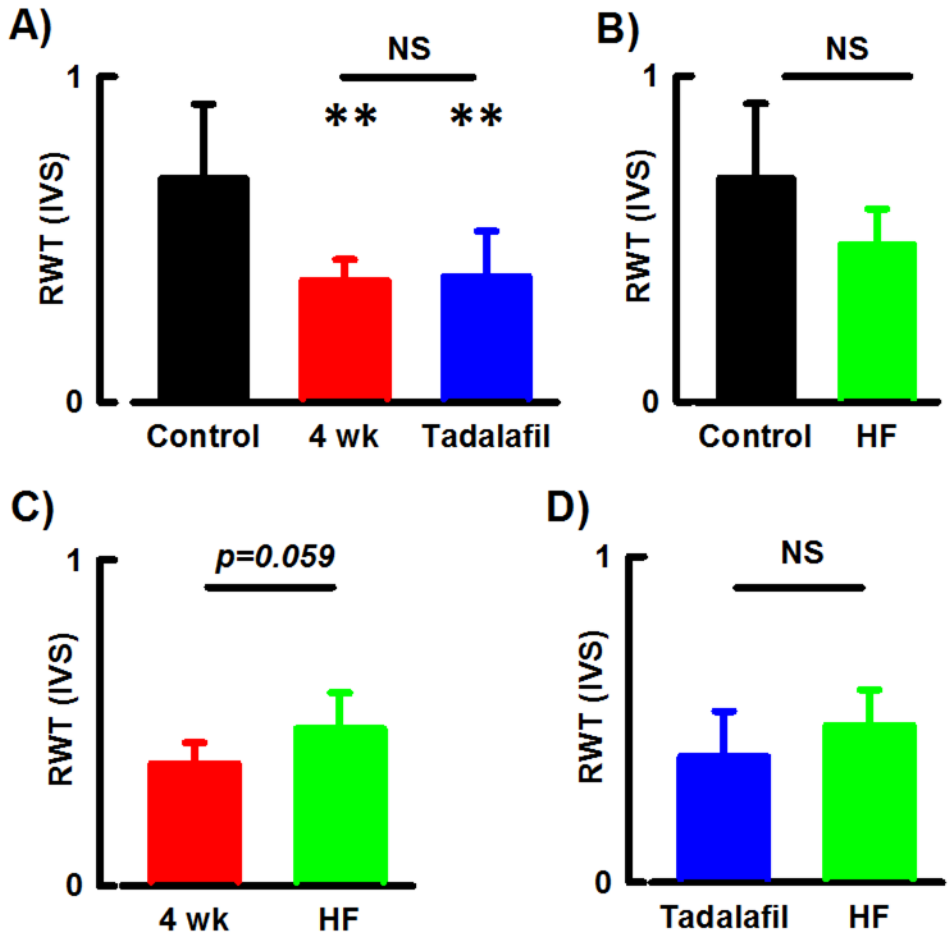

Figure 5.10 The effect of PDE5 inhibitor treatment in heart failure on relative wall thickness (RWT) of the intraventricular septum (IVS)

*(A) Paired summary data for RWT IVS as measured from intraventricular septum wall thickness in diastole (see text) using m-mode echocardiography for control (black), 4-week paced (4 wk, red), 3-week further pacing plus tadalafil treatment (Tadalafil, blue). (B) Paired summary data for RWT IVS between control and HF (green). (C) Unpaired summary data for RWT IVS between 4 wk and HF. (D) Unpaired summary data for RWT IVS between HF and Tadalafil. Mean ± SEM. Differences in paired data compared using a one-way repeated measures ANOVA and holm-sidak post-hoc test, or a paired Student's t-test. Unpaired data compared using a Student's t-test. Versus control **p<0.01. NS=not significant.*

5.3.5 The effect of heart failure and chronic PDE5 inhibition on in vivo electrophysiological remodelling in HF

Contractility is determined by electrical activity, which transmits throughout the heart and can be recorded non-invasively using electrocardiography (ECG), example traces are shown in Figure 5.11. Electrical impulses are generated by the sinoatrial node, which transmits electrical impulses across the atria resulting in atrial systole, the P wave on the ECG. Electrical impulses are channelled down into the ventricles along the His-Purkinje system located in the ventricular septum, which result in ventricular systole and correspond to the QRS complex on the ECG. Ventricular diastole and the dissipation of the electrical signal correspond to the T wave on the ECG. A number of parameters were measured from the ECG recorded in animals before pacing, at 4-weeks of pacing and following tadalafil treatment and are summarised in Table 17. The R-R interval as shown in Figure 5.12*Ai* corresponds to the time between each R wave and provides an indication of heart rate. R-R interval before pacing (561.5±42 ms) had a tendency to be decreased following 4-weeks of pacing (486.3±20 ms, p=0.07) and maintained decreased following tadalafil treatment (473.8±25 ms p=0.07). The change in R-R interval would suggest an increase in heart rate (HR) in the tachypaced animals, we observed possible increases in HR (pre-pacing: 112±9 bpm, versus 4-weeks: 125±6 bpm, Tadalafil: 130±7 bpm, Figure 5.12*Aii*), however these changes did not achieve significance, most likely reflective of the low sample size presented in this study.

The standard deviation of the R-R interval (SD R-R) is used as an indication of the amount of variability of heart rate over time, which is indicative of the autonomic control of heart rate. R-R variability was decreased from pre-pacing (36.8±8.5 ms, Figure 5.12Aiii) following 4-weeks of tachypacing (17.7±2.8 ms, p=0.009) and maintained similarly decreased after tadalafil treatment (18.0±3.1 ms, p=0.01). This may suggest that there is a degree of autonomic dysfunction present in our model of HF unchanged by tadalafil treatment.

For the other parameters investigated there was no difference in P-wave duration (p=0.75), P-R interval (p=0.21) or QRS duration (p=0.68) as summarised in Table 17, however there appeared to be a tendency for an increase in Q-T interval following 4-weeks of tachypacing (control: 0.34±0.01s, versus 4-week: 0.36±0.01s, p=0.08, Figure 5.12*B*), which showed a tendency to be restored to control following tadalafil treatment (0.35±0.01s).

	Control	4 wk	Tadalafil
P-wave duration (ms)	30±2	30±2	30±5
P-R interval (ms)	80±4	100±8	90±10
QRS duration (ms)	50±4	40±3	40±3

Table 17. Summary data for changes in ECG parameters

Mean ± SEM, n=8, differences compared using one-way repeated measure ANOVA.

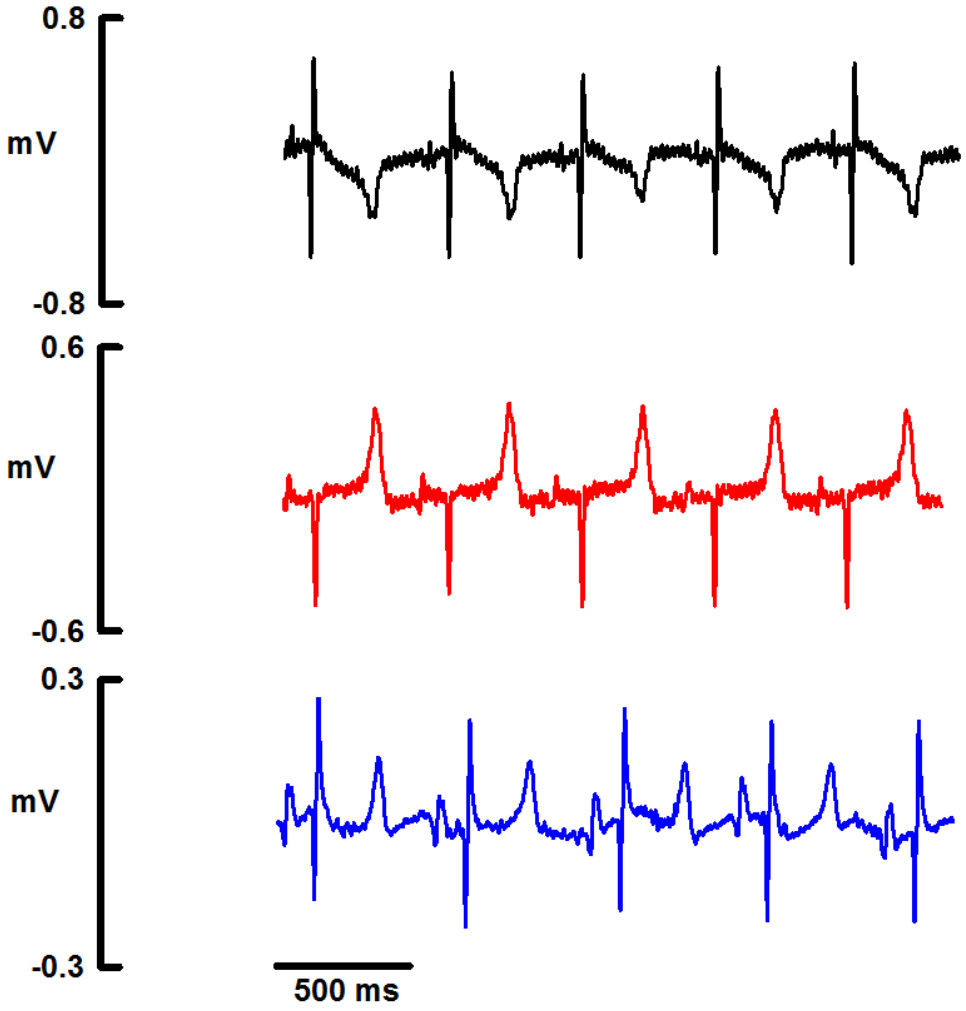

Figure 5.11 Representative ECG traces.

Example traces for ECGs from one animal (top to bottom), at baseline (black), following 4 weeks of pacing (red), following a further 3 weeks of pacing and tadalafil treatment (blue).

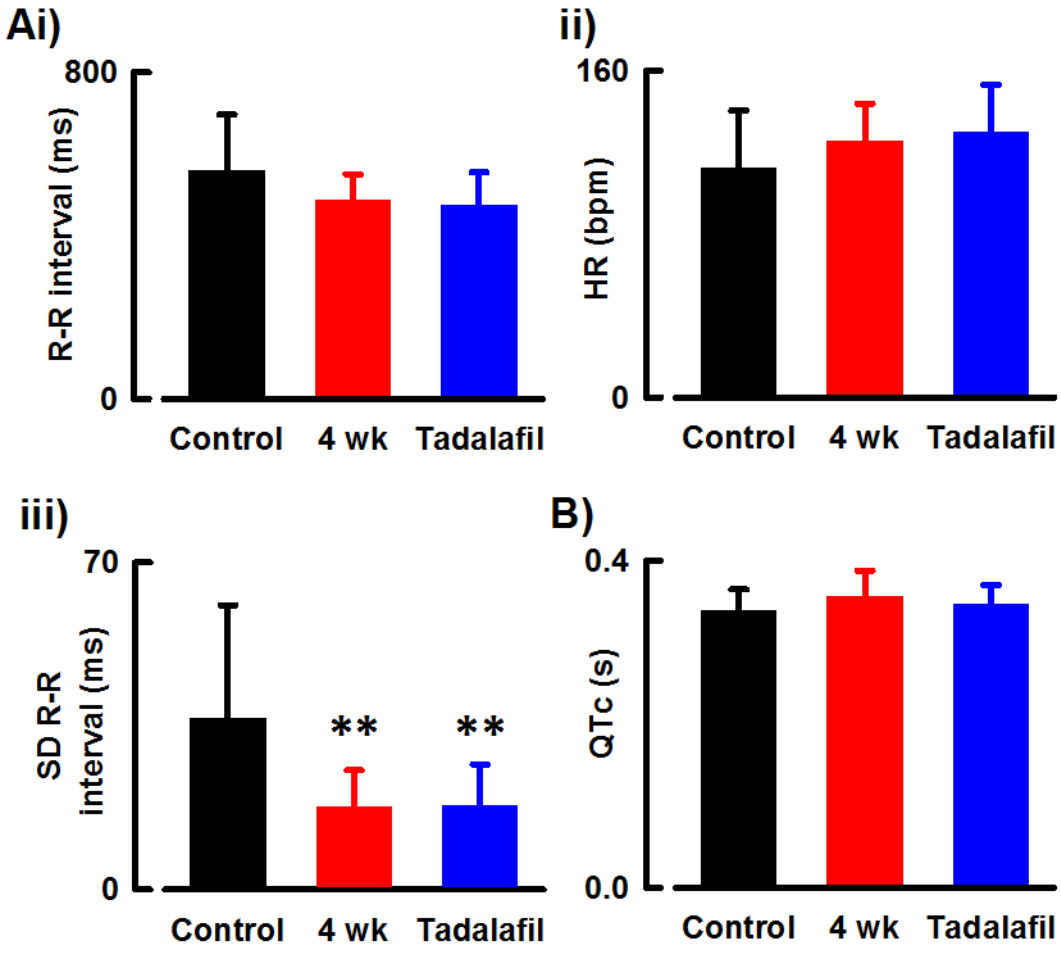

Figure 5.12 The effect of PDE5 inhibitor treatment in heart failure on electrical activity in the heart

*Differences in ECG parameters pre-pacing (black), post 4-weeks pacing (4 wk, red) and following further 3 weeks of pacing and tadalafil treatment (blue). (Ai) interval between R-waves (R-R interval) (ii) heart rate (HR) and (iii) R-wave variability (standard deviation (SD) R-R interval). (B) Changes in corrected Q-T duration (QTc). Differences in paired data compared using a one-way repeated measures ANOVA and holm-sidak post-hoc test Versus control **p<0.01.n=8*

5.3.6 The effect of β-AR stimulation on HR in heart failure

As shown in previous chapters of this thesis, 4-weeks of tachypacing resulted in altered *β*-AR signalling, which was modulated by chronic PDE5 inhibition. This next set of experiments sought to investigate whether *β*-AR responsiveness is altered at the whole heart/animal level.

Increasing doses of the selective β_1 agonist dobutamine were used to stress the *β*-AR capacity of the conscious sheep. Figure 5.13*A* shows the decreases in R-R interval (inverse analogue of HR) as the dose of dobutamine was increased from 0.5 to 20 μg/kg/min.

Following 10 minutes of baseline ECG recording incremental increased doses of dobutamine were infused to produce a decrease in R-R interval until at least a 50% decrease was observed. Pre-pacing, dobutamine at increasing doses 5 and 10 μg/kg/min resulted in a dose dependent decrease in R-R interval, 34±6% and 44±11% respectively, which is consistent with β_1 dependent elevation of HR (Figure 5.13*Ci*). Following 4-weeks of pacing sensitivity to the agonist was lost, resulting in a lack of significantly decreased R-R from baseline at either 5 or 10μg/kg/min (5±6% and 14±3% decrease respectively). A dose of 20μg/kg/min was required to generate a 23±3% decrease in R-R interval. Figure 5.13*Cii* shows that in different animals paced to end stage there was almost no change in R-R interval observed following 5 and 10μg/kg of dobutamine.

Chronic treatment with tadalafil revealed an increase in sensitivity to the *β*-AR agonist at all three doses of dobutamine (5, 10 and 20μg/kg/min) showing dose-dependent decreases in R-R interval (15±4%, 26±5%, 33±5% decrease respectively, $p<0.05$ versus control no drug). These results correspond to the cellular data, suggesting that chronic PDE5 inhibition restores *β*-AR sensitivity in HF.

After administering a dose of dobutamine great enough to produce a >50% change in R-R interval (or HR) from baseline, a short axis echocardiogram was recorded to measure the dobutamine evoked fractional area change, summary data shown in Figure 5.13*B*. In animals paced for 4-weeks and to end stage HF, cardiac contractility was reduced, however following treatment with the PDE5 inhibitor fractional area change was still lower than that observed at baseline, yet revealed greater contractile capacity as compared with the failing hearts.

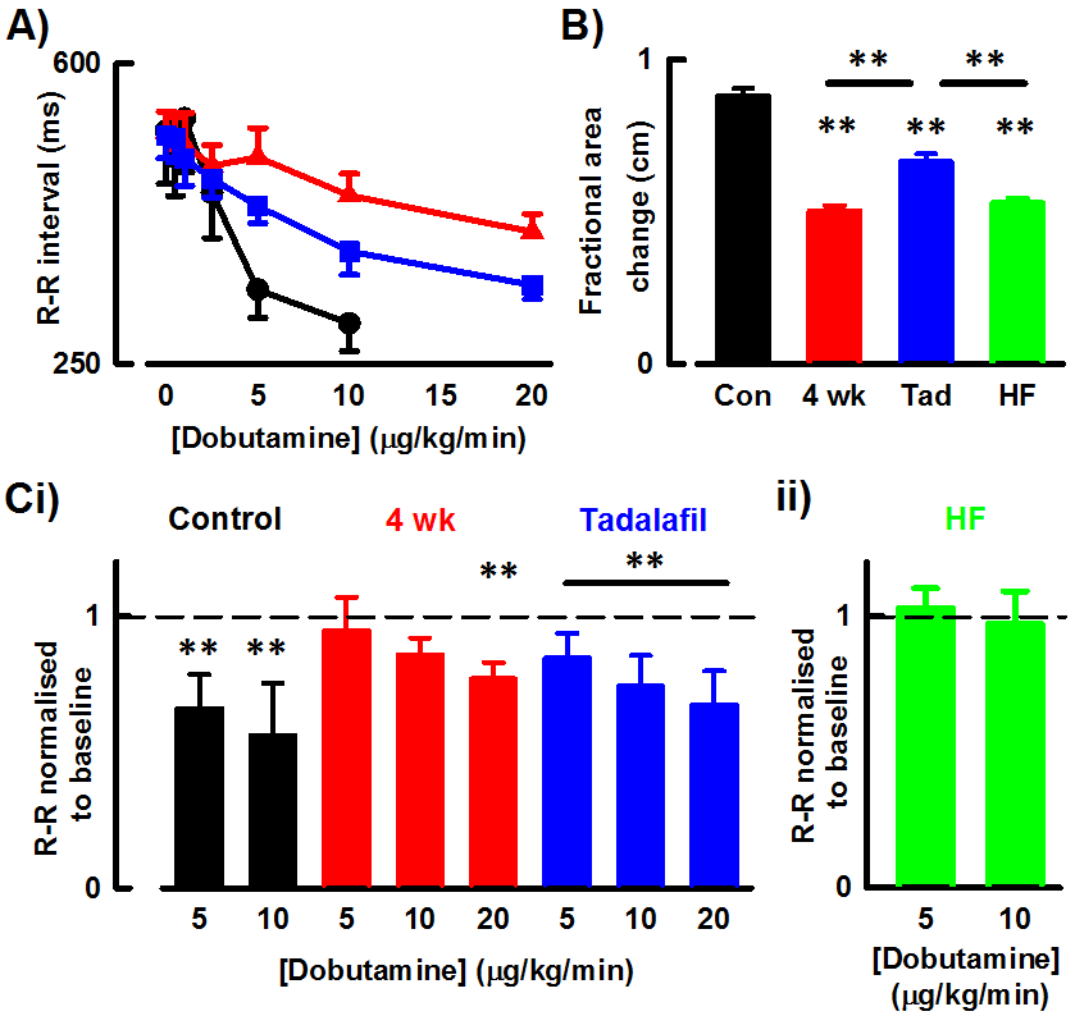

Figure 5.13 The effect of β-AR stimulation in HF

*Differences in the effects of β_1 stimulation in animals: pre-pacing (black), post 4-weeks paced (red) and following a further 3 weeks of pacing plus tadalafil treatment (blue) and end-stage HF (green). (A) Effect of increasing concentrations of infused β_1 agonist dobutamine on R-R interval values are mean ± SEM. (B) The effect of a maximum dose of dobutamine required to significantly decrease R-R interval on cardiac fractional area change as assessed by transthoracic echocardiography. (C) Summary data for the effect of increasing doses of infused dobutamine (5-20µg/kg/min) on R-R interval as normalised to baseline R-R interval. HF data in Cii provided by Dr M. Horn and shown here for comparison purposes. For A and B: differences compared using a one-way repeated measures ANOVA and holm-sidak post-hoc test Versus control **p<0.01, solid lines represent alternative differences. For Ci differences were compared using a two-way repeated measures ANOVA and holm-sidak post-hoc test. Cii data is unpaired from Ci. Versus 1 **p<0.01, solid line represents all points different from 1.*

5.4 Discussion

Chronic treatment with the PDE5 inhibitor Tadalafil prolongs the life of an animal in HF. Phenotypically those animals treated with the drug have unaltered cardiovascular characteristics to untreated animals with little differences in cardiac contractility. However, chronic PDE5 inhibition restores responsiveness to β-AR stimulation in vivo. The data presented here provides evidence for the beneficial effects of PDE5 inhibition in a large animal model of HF.

5.4.1 Large animal model of dilated cardiomyopathy (DCM)

The present study has employed the use of a large animal model of dilated cardiomyopathy induced by rapid ventricular pacing. DCM is characterized by prominent increases in myocardial mass and volume secondary to (bi-)ventricular dilatation. This results in the myocardium developing a more globe-like appearance. Raised wall stress, depressed systolic function, abnormal diastolic filling and wall thinning are all common in a DCM phenotype[290].

In human patients symptoms of DCM include dyspnea and a reduced capacity for exercise, followed by cachexia and peripheral oedema in the latter stages of disease progression. Our group has developed and utilised a sheep model of heart failure induced by tachypacing for 5-8 weeks[179, 276, 277], which reflects an end-stage model of HF. The present study has determined HF as the phenotype presented at four weeks of tachypacing and showed in Chapter 4 that cellular physiology impairment is similar to that observed at end stage[179]. In addition, animals paced for four weeks showed cachexia with ascites and cardiac effusion. HF animals were dyspnoeic with observed fluid accumulation in the lungs at the time of killing, yet there was no difference in LW to BW ratio between normal and paced animals. This may be a result of the necessity to rapidly extract the heart from the chest cavity post-mortem, which in turn results in the lungs stagnating in residual blood before they too could be extracted. As a function of HF, LW to BW ratio would be more reliable if dry lung weight was measured, alternatively BW to tibia length ratio could be calculated.

Left ventricular dysfunction as induced by tachypacing was first described by Whipple et al[291] and has since become a common methodology to reliably produce a DCM and chronic HF phenotype in larger animals including dogs[292], pigs[293] and sheep[294]. Tachypacing induced cardiomyopathy results in the generation of a model closely resembling human DCM as animals undergo similar cellular, structural and neurohumoral alterations[290]. After

four weeks of tachypacing systolic, mean and pulse pressures were reduced in the sheep, which corresponds to previous findings in different large animal species[276, 292, 293, 295]. Clinical studies suggest that heart failure in humans is generally associated with an elevated blood pressure, however concurrent vascular diseases and pharmacological interventions (ACE inhibitors, Ca^{2+} channel blockers, β-AR blockers) may be responsible for such findings. This study showed a tendency for reduced R-R interval in HF, corresponding to a trend for an increase in HR. Tachypaced dogs have presented with increased[295] and unchanged[296] HR and one study found no change in sheep HR following six weeks of tachypacing at a similar rate to the current study. The nature of tachypacing prevents compensatory HR changes occurring, thus upon pacing cessation one may expect concomitant increases in HR. Typically at least 10 minutes was allowed for animals to recover once pacing was ceased, which has proved adequate for HR to stabilise. Moreover, handling is stressful to the animals and so this also allows catecholamine surges to stabilize. This suggests that any changes in HR observed here are due to intrinsic compensations to rescue cardiac output from the failing ventricle.

Systolic and diastolic dysfunction are important characteristics of DCM and are diagnosed in the clinic using echocardiography to assess myocardial internal diameters and wall thickness. DCM ultimately results in a failure for the heart to provide adequate perfusion of tissues, thus is concordant with a decreased ejection fraction. Cardiac anatomy in the sheep prevents capture of four-chamber apical views using echocardiography, thus precluding measurement of ejection fraction and chamber volumes. The present study has, as before[179, 276], used 2-dimensional views to calculate fractional area change and m-mode views to calculate fractional shortening in order to provide an indirect measure of ejection fraction. Both fractional area change and shortening were reduced in the sheep left ventricle following four weeks of pacing, of which the latter was further reduced as HF progressed. Moreover, this was accompanied by systolic and diastolic dilatation that too worsened toward end-stage HF. Byrne et al demonstrated similar progression of HF in sheep, finding increasing left ventricular area and decreased fractional shortening from three to 10 weeks of rapid pacing[294]. In accordance with the limitation to using echocardiography in the sheep as discussed above it is difficult to obtain appropriate trans-thoracic views to measure mitral flow, which would be a useful factor in determining valve regurgitation associated with the myocardial dilatation observed.

DCM in humans as well as animal models is accompanied by ventricular wall thinning[276, 294, 295], which is secondary to eccentric hypertrophy. The present study found no difference in cellular capacitance (see 4.3); unlike previously reported in the tachypaced sheep model[179], which also showed increases in myocyte length. However, similar decreases in left ventricular free and septal wall thicknesses were observed in the present study as previously reported[179, 276, 294]. Surprisingly, the intraventricular septum appeared to be thinner at 4-weeks of pacing than at end stage, however this may highlight the limitation of using one technique as the sole determinate of wall dimensions, as an oblique parasternal image in m-mode can result in overestimation of dimensions. Increasing the power of this group would allow a more robust assessment of any such changes.

The heart is greatly influenced by the autonomic nervous system. Increased circulating catecholamines measured in HF patients results in a greater sympathetic tone, which ultimately leads to β-AR dysfunction, is associated with a concomitant decrease in parasympathetic tone leading to further left ventricular dysfunction[297]. The resultant loss of autonomic tone may manifests in the loss of heart rate variability as observed in the current study. Precise blockade of both sympathetic and parasympathetic nervous systems would be required to examine the exact changes in autonomic contribution occurring in the sheep model of HF.

The QT interval is a standard measure of ventricular repolarization and thus corresponds to the action potential duration, which can be measured from both whole hearts in vivo and single myocytes in vitro. As HR increases, the refractory period and thus the time for repolarisation of the ventricles must also increase[298]. Therefore it is well documented that action potential duration (APD) and thus QT will change with alterations in HR. For this reason QT has been corrected for using a Bazett's correction, which is most commonly used for humans in a clinical setting[299]. As this formula is derived using normal human HR (60 bpm) as a correction factor there may be some limitation to its use for correcting sheep QT interval (resting HR >80 bpm). Human heart failure is associated with both structural and electrical changes to the myocardium and as such is associated with a prolongation of the APD[300, 301]. Moreover, in a canine model of HF a prolonged APD was observed in vivo following 3 weeks of rapid pacing[302], which may indicate the possible prolonged QT interval observed in the current study. As action potentials were not measured in this study such changes to QT interval can only be speculated and further work would be required to measure the APD in the present model of HF.

5.4.2 The effect of PDE5 inhibition on the DCM phenotype

PDE5 inhibitor therapy was originally developed for the treatment of angina, with subsequent therapeutic targeting of erectile dysfunction and pulmonary hypertension. PDE5 inhibition thus traditionally is considered a therapy for vascular disorders. The present study has shown that BP and HR was unaffected by chronic tadalafil treatment. When administered acutely the PDE5 inhibitor sildenafil transiently decreased BP in both normal and HF patients with no effect on HR[303]. In studies of HF patients chronically treated with sildenafil there were no effects on BP or HR observed[304]. Some have shown that chronic PDE5 inhibition may have varying effects on both pulmonary and systemic vascular resistance[165, 248, 305-307]. Changes in cardiac output could facilitate changes in vascular resistance without effects on blood pressure, which may explain this conflicting evidence. Further investigation into the effect of chronic PDE5 inhibition on pulmonary wedge pressures and systemic vascular resistance in the sheep model of HF are required to confirm any such differences. It should be noted that a limitation to the present study is the lack of BP data for animals at end-stage HF, however it is possible that chronic PDE5 inhibition is preventing any worsening of BP.

The present study has shown that Ca^{2+} handling in the failing ventricle is positively modulated by chronic PDE5 inhibition, which appears to be independent of changes in BP. The amplitude of the systolic Ca^{2+} transient is an important determinate of myocardial contractility, which is attenuated by at least 4-weeks of tachypacing in the sheep. Measurements of left ventricular area change and shortening determine relative myocardial contractility and provide an estimate of ejection fraction. As discussed above, the tachypaced sheep model of HF is associated with decreased ventricular function. Despite any changes in Ca^{2+} handling facilitated by chronic PDE5 inhibition, there was no change in ventricular contractility. Furthermore, cardiac contractility in Tadalafil animals was tantamount to that observed in end-stage HF animals. Chronic PDE5 inhibition is known to recover contractility in TAC mice[123, 274], in rats with a compromised mitral valve[308] and following PDE5-siRNA targeting in post-MI mice hearts. Furthermore, chronic PDE5 inhibitor treatment improved contractility in humans with left and right heart failure[265, 309, 310].

The majority of these studies also report that PDE5 inhibition reduced both systolic and diastolic ventricular dimension, of which there was no reversal following three weeks of PDE5 inhibition in the tachypaced sheep heart. Our laboratory has previously reported that

the sheep model of HF is associated with wall thinning and eccentric hypertrophy[179, 276], the former of which was shown to some extent unaffected by chronic PDE5 inhibitor therapy in the current study. PDE5 inhibition is known to reverse pre-existing hypertrophy through inhibition of the pro-hypertrophic calcineurin/NFAT and ERK1/2 signalling pathways[123]. Such signalling pathways are beyond the present investigation but further work would be required to firstly test whether they are activated in a tachypaced model of HF and whether PKG signalling interacts in this scenario.

Little difference was observed in most electrophysiological parameters of the whole heart of animals treated chronically with the PDE5 inhibitor than that observed following 4-weeks of pacing. However, the small increases in the QT interval following 4 weeks of rapid pacing were no longer observed following chronic PDE5 inhibitor treatment. As discussed above, such changes in QT interval may be associated with changes in APD. Such discussion here is limited by the lack of evidence from the current study to support this. Although as APD is determined by several ionic conductances it is likely that changes in these may contribute to the changes in QT interval observed. Eisner et al reviewed that changes in potassium and calcium currents along with NCX and calcium activated chloride currents all contribute to action potential duration[311], of which the current study has shown no difference in steady state $I_{Ca\text{-}L}$, which suggests that further work may elucidate changes in those other contributing currents.

Most studies maintained PDE5 inhibition for between 3 weeks and 1 year using sildenafil to inhibit PDE5 at concentrations of 100 mg/kg/day for rodents and 100-150 mg/day in humans. To my knowledge no previous studies investigated the effect of tadalafil as a PDE5 inhibitor on haemodynamics in HF. Tadalafil is >1000x selective for PDE5 than sildenafil and therefore makes it more appropriate for a 'once-a-day' therapy[312, 313]. Moreover 20mg tadalafil was shown to increase intraocular pressure in sheep, which shows such a dose is effective for eliciting haemodynamic responses. The plasma concentration of tadalafil was not measured in the present study, however Figure 5.4 provides compelling evidence for the effectiveness of this therapy on the survival of sheep in HF.

5.4.3 PDE5 inhibition resensitises the failing heart to β-AR stimulation

Heart failure is associated with a decreased sensitivity of the myocardium to *β*-AR stimulation, which is observed at both the whole animal and myocyte level. Such

desensitisation has been observed in tachypacing induced HF, including the sheep[179, 314], which may be due to increased circulating catecholamines[294], as consistent with human HF.

Unlike that observed previously by our laboratory, the current study revealed that 4-weeks of pacing was not sufficient to completely attenuate the β-AR responsiveness of isolated mycoytes (see 4.3.6.1); demonstrating a reduced response of β-AR stimulation on changes to $I_{Ca\text{-}L}$, yet no difference in the size of the evoked Ca^{2+} transient. In order to test the β-AR capacity of HF animals in vivo increasing doses of the β-AR agonist dobutamine were infused Figure 5.13. As the systolic Ca^{2+} transient is an analogue of myocardial contractility it was surprising that cardiac contractility in response to β-AR stimulation, as assessed by echocardiography, was attenuated following 4-weeks of pacing to a similar level to those animals paced until end-stage HF. Furthermore, 4-week paced animals required up to 20 μg/kg/min of dobutamine before significant changes in HR were observed, which may also suggest sinus node dysfunction in these animals. The underpowered nature of the in vitro data may suggest a possible reason for the discrepancy observed here, however as dobutamine is more selective for β_1 adrenoreceptors and isoprenaline (see Chapter 3) is a non-selective β-adrenoreceptor agonist, changes to β-adrenoreceptor density cannot be ruled out. Further work would be required to assess differences in sarcolemmal distribution and expression of β-adrenoreceptors in the tachypaced sheep model of HF.

Animals chronically treated with the PDE5 inhibitor tadalafil are more responsive to β-AR stimulation at both the myocyte and whole heart level. Heart rate was dose-dependently increased above baseline following 5 to 20 μg/kg/min of dobutamine, and β-AR stimulated contractility was equally greater than that measured at 4-weeks of pacing and end-stage HF. The dobutamine stress test was performed in animals immediately before the time of killing and so the previous tadalafil treatment was provided the day before. This was ensured to prevent any acute interactions of PDE5 inhibition with the study as increases in systolic and diastolic function evoked by dobutamine in HF patients was markedly blunted when pre-treated with sildenafil[165]. In humans with congested HF 12 weeks of sildenafil treatment facilitated a tendency for an increase in capacity for a 6 minute walk stress test, which was not observed in a placebo treated cohort[315]. Furthermore, in a rodent model of mitral regurgitation resulting in chronic left ventricular dysfunction, four months of sildenafil treatment restored exercise capacity[308]. Together with the findings of the present

study this suggests that chronic PDE5 inhibition positively modulates β-AR signalling in the failing ventricle.

5.5 Study limitations

Here the limitations to the use of the HF and chronically treated model will be explored with reference to the experiments presented in both this and the previous chapter.

The rapid ventricular pacing model of HF is well established in our laboratory[179, 276, 277]. Generally the length of time of pacing is correlated with the severity of HF, however as severity is a complicated spectrum it is almost impossible to tell, especially in the sheep, the degree of HF presented. For the animals at end stage, HF is determined as the point of fluid accumulation and breathlessness, which was generally not as obvious at the 4-week point of pacing. Thus as tadalafil treatment was initiated at the 4-week point it is impossible to tell at which stage of severity of HF the animals were at. This uncertainty may account for the premature loss of one animal during the study.

In vivo measurements were always performed at least 10 minutes after the pacemaker was turned off in order to allow the heart to stabilise, however this does not take into account the stress of handling the animal and the likely increased level of circulating catecholamines, which may influence blood pressure and heart rate. Furthermore, in the present study ECG analysis was performed on 1-5 minute periods of ECG recordings, which would usually be assessed over a 24-hour period in humans. Body temperature and hormonal influences and genetic variability have not been corrected for in the analysis, which may confer inconsistencies in the measurements obtained.

Tadalafil is considered a more selective PDE5 inhibitor than sildenafil and appears to be beneficial to the failing myocardium. When applied acutely to myocytes sildenafil was negatively inotropic, however the present study has not tested the acute effects of tadalafil. Further, tadalafil treatment was only administered to a HF group of animals; a control group was not treated alongside. In HF, tadalafil treatment had no effect on blood pressure or HR; however from the present study we cannot be certain of the alternative cardiovascular effects PDE5 inhibition may have in the normal population. Although, treating HF similarly to the present study is more applicable to human physiology as HF treatment would not normally be provided prophylactically.

In order to assess the availability of cAMP and cGMP in tissue from the different experimental animal models used the present study used a colorimetric cyclic nucleotide ELISA, however one would question the reliability of such an experimental procedure as we know that cyclic nucleotides bind substrates to activate them, thus effectively lowering their cytosolic concentrations. Furthermore, cyclase inhibitors were not used, which may result in further production of cyclic nucleotides beyond physiologically relevant levels. I believe that a more reliable method of assessing cyclic nucleotide availability would be to test the activity of PKA and PKG in protein samples.

Time constraints prevented PDE expression and activity assays to be performed in tissue from Tadalafil animals, which restricts the ability to compare and conclude any changes to that observed in HF. These experiments are required to confirm the validity of the mechanisms proposed.

5.6 Conclusion

Chronic PDE5 inhibition prevents the progression of heart failure and resensitises the myocardium to β-AR stimulation. These beneficial effects in HF are most likely due to the positive effects observed at the myocyte level described in Chapter 2 and are unlikely due to mechanical unloading of the heart as blood pressures were unaffected. Steady state contractility was not altered and the dilatation and wall thinning phenotypical of HF were not reversed, however the current study is limited by only a 3-week period of treatment. When PDE5 is chronically inhibited in the rodent heart challenged with transverse aortic constriction then hypertrophy and function was restored, however the different pathophysiology of a tachypaced heart, which resembles more similarly human DCM, such anti-hypertrophic benefits were not seen. Further work is required to assess the pathways involved in the cardioprotection provided by chronic PDE5 inhibition as it remains that the effects described here may be attributed to the large spectrum of species variation in the myocardium between small and large mammals.

Chapter 6

6 General Discussion

The aim of this thesis was to understand the role of cGMP and PDE5 in the ovine ventricular myocardium and whether they can be manipulated in order to be beneficial in HF. This study has shown that acute PDE5 inhibition was negatively inotropic, yet paradoxically to the failing ventricle chronic PDE5 inhibition had positive effects on steady state Ca^{2+} handling, improved β-AR reserve and prolonged longevity.

6.1 Acute PDE5 inhibition is negatively inotropic

In the normal ventricular myocyte PDE5 is located at the z-disk and exclusively commands control of the NO-stimulated sGC-derived pool of cGMP. Acute PDE5 inhibition results in cGMP accumulation, which results in three possible outcomes, (1) PKG-dependent phosphorylation of the L-type Ca^{2+} channel, PLN and TnI, promoting reduced inotropy and increased lusitropy, (2) activation of PDE2 resulting in increased cAMP hydrolysis, and (3) inhibition of PDE3 resulting in decreased cAMP degradation. The latter two effects are determined by the concentration of cGMP. Two out of the three outcomes result in a reduction in cardiac contractility. Many previous studies have described relative degrees of negative modulation of contractility, species depending, following acute PDE5 inhibition, to which we can now include the sheep. Sildenafil reduced $I_{Ca\text{-}L}$ and Ca^{2+} transient in control sheep ventricular myocytes.

A reduction in $I_{Ca\text{-}L}$, Ca^{2+} transient and SR Ca^{2+} content was observed in the failing ventricular myocyte as compared with a control cell. The observation of reduced cAMP-PDE expression and activity, as well as trends for increased cGMP-PDE activity reveals a mechanism by which cyclic nucleotide signalling is altered in the failing ventricle. In addition, β-AR responsiveness was reduced in HF, which suggests a role for either β-adrenoreceptor dysfunction, altered downstream signalling or a combination of the two. However, despite apparent dissociation of intracellular signalling pathways PDE5 inhibition still showed tendencies to negatively modulate myocyte contractility: reduced $I_{Ca\text{-}L}$. The lack of effect on the Ca^{2+} transient is most likely due to disruption of compartmentalised cGMP resulting in stochastic PKG activation.

6.2 Chronic PDE5 inhibition improves Ca^{2+} transients and β-AR responsiveness

The main aim of this study was to understand how PDE5 inhibition is beneficial to the failing myocardium. Chronic PDE5 inhibition prolonged the life of HF animals, reducing

the onset of clinical signs. PDE5 inhibition in HF substantially increased baseline Ca^{2+} transient and maintained whole heart contractility. Chronic PDE5 inhibition also restored the β-AR responsiveness of the failing myocardium at both the myocyte and whole heart level. Structurally, there was no reverse remodelling observed following PDE5 inhibition, however at the myocyte level there was a partial recovery of the t-tubular network. Mechanistically, chronic PDE5 inhibition results in greater phosphorylation of downstream targets of PKA and PKG, thus it appears that this therapy leads to a restoration of cyclic nucleotide signalling in failing myocytes.

6.3 Why is chronic PDE5 inhibition beneficial to the failing myocardium?

The present study shows that PDE5 inhibition is beneficial to the failing myocardium. I have discussed the intracellular signalling pathways that may interact to enable recovery of Ca^{2+} handling and β-AR responsiveness following PDE5 inhibition in HF, such as PDE2 activation and PDE3 inhibition. However more work is still required to fully understand how chronic PDE5 inhibition is beneficial. Inhibition of PDE5 ultimately leads to increased cGMP and thus increased PKG activation. I have discussed the effects of downstream PKG activity in previous discussions and so the following discussion will explore some other ways in which PDE5 inhibition may be beneficial in HF, they are summarised in Figure 6.1.

Regulators of G-protein signalling (RGS) initiate the termination of the G-protein by stimulating the GTPase activity of the Gα subunit, thus promoting the reformation of the inactive G-protein heterotimer[118]. Gαq signalling is important for stimulating the intracellular signalling pathways involved in cardiac hypertrophy and remodelling following pressure overload[316] and is selectively targeted by RGS2[317]. Selective RGS2 knockout in mice results in a faster progression of cardiac remodelling in response to pressure overload[121]. The present study has shown that animals survive longer following treatment with a PDE5 inhibitor. PDE5 inhibition results in increased cGMP concentrations and PKG activity. Such increased PKG activity has previously been shown to be responsible for cardioprotection in pressure overloaded mice[123]. Furthermore, PKG can directly activate RGS proteins[121, 318]. In RGS2 knockout mice PDE5 inhibition did not have similarly cardioprotective effects, yet still increased PKG activity to the same extent as control[121]. Experiments to assess the activity and expression of RGS in the sheep myocardium in HF and chronic tadalafil treatment may reveal more about the mechanism of prolonged longevity in this model.

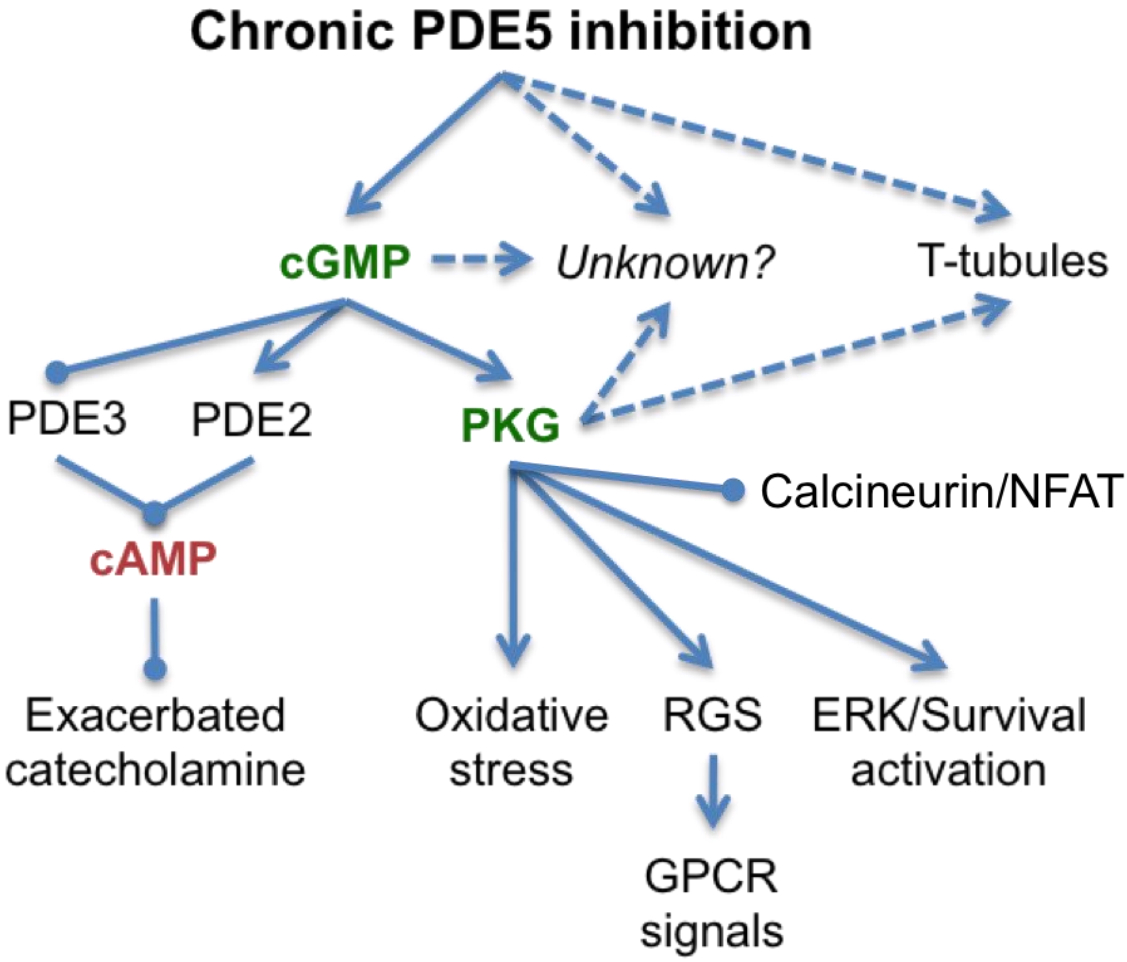

Figure 6.1 How is PDE5 inhibition beneficial in HF?

Phosphodiesterase (PDE); transverse-tubules (t-tubules); cyclic adenosine/guanosine monophosphate (cAMP/cGMP); protein kinase G (PKG); regulators of G-protein signalling (RGS); extracellular signal-regulated kinase (ERK); G-protein couples receptor (GPCR). Arrows represent activation, solid end lines represent inhibition.

Oxidative stress is considered an important aspect of the pathophysiology of the failing ventricle (as reviewed[319]). Increased free radicals cause mitochondrial damage and ultimately lead to cardiac remodelling and apoptosis. Pressure overloaded mice undergo left ventricular chamber remodelling which is associated with the expression of myocardial oxidative stress markers[272]. Interestingly, this study reported increased PDE5 expression, which was attenuated following treatment with antioxidants. Furthermore, the cardioprotective effect of chronic PDE5 inhibition was linked to the attenuation of increased myocardial oxidative stress[272]. This may have implications for the results reported in the present study.

Cellular proliferation, differentiation and survival are dependent on signalling through ERK proteins, a member of the mitogen activated protein kinase family[320]. Cardioprotection against ischaemia-reperfusion injury and myocardial infarction have been linked to ERK signalling[321, 322]. Other pathways involved in cardiac remodelling include Akt-PI3K and their downstream effector GSK3β. Such signalling pathways are activated following pressure overload in mice[123]. All of these pathways are phosphorylated by PKG, induced by chronic PDE5 inhibition and contribute to the remodelling and cardioprotection proffered by PDE5 inhibition[123, 323]. The models used in these studies are very different to the tachypacing induced failure presented in this study, however it would be very interesting to test whether these pathways are involved here.

Cardiac hypertrophy and remodelling are important pathophysiological aspects of heart failure. The calcium dependent phosphatase calcineurin is involved in the activation of downstream signalling pathways associated with remodelling including ERK[324]. The main hypertrophic role of calcineurin is through dephosphorylation of nuclear factor of activated T-cell (NFAT) transcription factors, encouraging their translocation to the cell nucleus, resulting in cardiac transcription[325]. Inhibition of this pathway reduces cardiac hypertrophy and heart failure progression in animal models of the disease[325]. Calcineurin signalling is inhibited by PKG, the activation of which resulted in an NO-dependent reduction in cardiac myocyte hypertrophy[326]. Furthermore, chronic treatment of the PDE5 inhibitor sildenafil in a TAC model of heart failure resulted in reduced calcineurin expression and calcineurin/NFAT signalling as compared with untreated animals[123]. Together, this suggests that chronic PDE5 inhibition can attenuate remodelling pathways in heart failure, which may suggest a role for the arrested chamber dilatation observed in the present study.

It would be very interesting to explore such remodelling signalling pathways in greater detail

T-tubules are an important component in the compartmentalization of signals as they are densely populated with β-adrenoreceptors, L-type Ca^{2+} channels and AKAPs. The organization of these specialized membrane invaginations is disrupted in HF leading to a large reduction in cell capacitance. Mechanical detubulation can result in a 60% reduction in $I_{Ca\text{-}L}$[327], which most likely contributes to the attenuated $I_{Ca\text{-}L}$ observed in the failing ventricle. At 4-weeks of pacing t-tubules are severely disrupted in the tachypaced sheep heart, which is partially recovered following 3-weeks of PDE5 inhibition (personal communication, Jessica Caldwell). Similarly in rats with right ventricular failure following pulmonary pressure overload, chronic treatment with the PDE5 inhibitor sildenafil reversed t-tubule remodelling[328]. Further, in an infarct model of left ventricular HF Chen et al reported β-blocker therapy similarly restored t-tubule density[329]. The present study reported very little vascular effect of PDE5 inhibition in the sheep, suggesting that t-tubule remodelling is not secondary to a reduction in left ventricular unloading. Together this may present a mechanism by which t-tubule reverse remodelling as activated by intracellular signalling pathways contributes to the restored Ca^{2+} handling associated with chronic PDE5 inhibition in the failing myocardium.

Indeed, there may be other mechanisms by which cGMP, PKG and even direct PDE5 inhibition alone may be beneficial to the failing myocardium.

6.4 Further work

Following on from the work presented here the most important question that needs to be answered is whether PDE5 inhibition alters SR Ca^{2+} content and if so, how? By applying caffeine to isolated cardiac myocytes in the presence of the PDE5 inhibitor and in myocytes taken from animals chronically treated with a PDE5 a much clearer picture of how cGMP modulates Ca^{2+} handling in the normal and diseased myocardium.

A greater insight into the altered signalling pathways involved in the chronically treated animals would be beneficial. By determining the expression and activity level of GRK, β-arrestin and RGS it could be determined whether chronic PDE5 inhibition modulates the control of β-adrenoreceptors themselves. This may highlight an important mechanism by which PDE5 inhibition restores β-AR responsiveness in the failing sheep heart.

In personal communication with another PhD student we know that there is a partial restoration to the t-tubular network in HF animals chronically treated with the PDE5 inhibitor. β-adrenoreceptors and L-type Ca^{2+} channels are mainly localized in t-tubules. As these structures are disrupted in HF, which is associated with decreased β-AR responsiveness and reduced $I_{Ca\text{-}L}$, there would be scope for immunostaining of these proteins to understand how they are relocated in HF. Further, PDE2 and PDE5 localise in similar regions, thus immunostaining could reveal whether chronic PDE5 inhibition restores intracellular compartments, which may reveal mechanisms by which β-AR responsiveness and Ca^{2+} handling are restored in HF.

Using super resolution microscopy it would be possible to visualize cyclic nucleotide compartmentalisation, which would further reveal whether there is a reorganisation of signalling in failing myocytes chronically treated with the PDE5 inhibitor. Alternatively many studies have employed the use of a FRET-based sensor for cyclic nucleotide signalling, which can be used to study local PDE activity.

As the present study has shown that chronic PDE5 inhibition prolongs the life expectancy of HF animals it would be very interesting to test how long a tachypaced animal could survive whilst being chronically treated with the PDE5 inhibitor. This may reveal reverse remodelling of the heart as observed in the longer chronic treatment studies of Kass et al.

Finally, further experiments need to have a greater number of cells added to the mean data e.g. PDE5 inhibition and β-AR responsiveness in HF.

6.5 General conclusion

Chronic PDE5 inhibition improves ventricular function in the failing human ventricle, by which mechanism is not fully understood. HF is associated with altered Ca^{2+} handling and β-AR reserve, which was shown in this study to be improved following chronic PDE5 inhibition. The exact mechanisms by which PDE5 inhibition provides these beneficial effects are yet to be elucidated, however this study shows to some degree that a restoration in the signalling pathways that govern myocardial contractility are improved. Furthermore, the evidence in this study may be more directly comparable to human disease than those previous studies, which have used mostly small animal and rodent models of HF. It is unlikely that 'a magic bullet' therapy for HF will ever be discovered, however the present study provides evidence, which may implicate the introduction of chronic PDE5 inhibition as a contender for future therapeutic strategies for this disease.

References

7 References

1. Lloyd-Jones DM, Larson MG, Leip EP, Beiser A, D'Agostino RB, Kannel WB, Murabito JM, Vasan RS, Benjamin EJ, Levy D. Lifetime risk for developing congestive heart failure - the framingham heart study. *Circulation*. 2002;106:3068-3072
2. WH O. Http://www.Who.Int/mediacentre/factsheets/fs317/en/. 2013
3. Packer M, Bristow MR, Cohn JN, Colucci WS, Fowler MB, Gilbert EM, Shusterman NH. The effect of carvedilol on morbidity and mortality in patients with chronic heart failure. *New England Journal of Medicine*. 1996;334:1349-1355
4. Digitalis Investigation G. The effect of digoxin on mortality and morbidity in patients with heart failure. *New England Journal of Medicine*. 1997;336:525-533
5. Bers DM. *Excitation-contraction coupling and cardiac contractile force*. Dodrecht: Kluwer Aacdemic Publishers; 2001.
6. Benitah JP, Gomez AM, Virsolvy A, Richard S. New perspectives on the key role of calcium in the progression of heart disease. *Journal of Muscle Research and Cell Motility*. 2003;24:275-283
7. Wehrens XHT, Lehnart SE, Marks AR. Intracellular calcium release and cardiac disease. *Annual Review of Physiology*. 2005;67:69-98
8. Nowycky MC, Fox AP, Tsien RW. 3 types of neuronal calcium-channel with different calcium agonist sensitivity. *Nature*. 1985;316:440-443
9. Scriven DRL, Dan P, Moore EDW. Distribution of proteins implicated in excitation-contraction coupling in rat ventricular myocytes. *Biophysical Journal*. 2000;79:2682-2691
10. Fabiato A. Simulated calcium current can both cause calcium loading in and trigger calcium release from the sarcoplasmic-reticulum of a skinned canine cardiac purkinje-cell *Journal of General Physiology*. 1985;85:291-320
11. Brette F, Salle L, Orchard CH. Differential modulation of l-type ca2+ current by sr ca2+ release at the t-tubules and surface membrane of rat ventricular myocytes. *Circulation Research*. 2004;95:E1-U9
12. Eisner DA, Trafford AW. What is the purpose of the large sarcolemmal calcium flux on each heartbeat? *American Journal of Physiology-Heart and Circulatory Physiology*. 2009;297:H493-H494
13. Kass RS, Sanguinetti MC. Inactivation of calcium-channel current in the calf cardiac purkinje-fiber - evidence for voltage-mediated and calcium-mediated mechanisms. *Journal of General Physiology*. 1984;84:705-726
14. Grantham CJ, Cannell MB. Ca2+ influx during the cardiac action potential in guinea pig ventricular myocytes. *Circulation Research*. 1996;79:194-200
15. Puglisi JL, Yuan WL, Bassani JWM, Bers DM. Ca2+ influx through ca2+ channels in rabbit ventricular myocytes during action potential clamp - influence of temperature. *Circulation Research*. 1999;85:E7-E16
16. Sipido KR, Callewaert G, Carmeliet E. Inhibition and rapid recovery of ca2+ current during ca2+ release from sarcoplasmic-reticulum in guinea-pig ventricular myocytes. *Circulation Research*. 1995;76:102-109
17. Brandl CJ, Green NM, Korczak B, Maclennan DH. 2 ca-2+ atpase genes - homologies and mechanistic implications of deduced amino-acid-sequences. *Cell*. 1986;44:597-607
18. Brandl CJ, Deleon S, Martin DR, Maclennan DH. Adult forms of the ca-2+ atpase of sarcoplasmic-reticulum - expression in developing skeletal-muscle. *Journal of Biological Chemistry*. 1987;262:3768-3774
19. Tada M, Katz AM. Phosphorylation of the sarcoplasmic-reticulum and sarcolemma. *Annual Review of Physiology*. 1982;44:401-423
20. Campbell KP, Maclennan DH, Jorgensen AO, Mintzer MC. Purification and characterization of calsequestrin from canine cardiac sarcoplasmic-reticulum and identification of the 53,000 dalton glycoprotein. *Journal of Biological Chemistry*. 1983;258:1197-1204

21. Bassani JWM, Yuan WL, Bers DM. Fractional sr ca release is regulated by trigger ca and sr ca content in cardiac myocytes. *American Journal of Physiology-Cell Physiology*. 1995;268:C1313-C1319
22. Trafford AW, Diaz ME, Sibbring GC, Eisner DA. Modulation of cicr has no maintained effect on systolic ca2+: Simultaneous measurements of sarcoplasmic reticulum and sarcolemmal ca2+ fluxes in rat ventricular myocytes. *Journal of Physiology-London*. 2000;522:259-270
23. Timerman AP, Onoue H, Xin HB, Barg S, Copello J, Wiederrecht G, Fleischer S. Selective binding of fkbp12.6 by the cardiac ryanodine receptor. *Journal of Biological Chemistry*. 1996;271:20385-20391
24. Valdivia HH, Kaplan JH, Ellisdavies GCR, Lederer WJ. Rapid adaptation of cardiac ryanodine receptors - modulation by mg2+ and phosphorylation. *Science*. 1995;267:1997-2000
25. Marx SO, Reiken S, Hisamatsu Y, Jayaraman T, Burkhoff D, Rosemblit N, Marks AR. Pka phosphorylation dissociates fkbp12.6 from the calcium release channel (ryanodine receptor): Defective regulation in failing hearts. *Cell*. 2000;101:365-376
26. Cheng H, Lederer WJ, Cannell MB. Calcium sparks - elementary events underlying excitation-contraction coupling in heart-muscle. *Science*. 1993;262:740-744
27. Wier WG, Balke CW. Ca2+ release mechanisms, ca2+ sparks, and local control of excitation-contraction coupling in normal heart muscle. *Circulation Research*. 1999;85:770-776
28. Stern MD. Theory of excitation-contraction coupling in cardiac-muscle. *Biophysical Journal*. 1992;63:497-517
29. Brette F, Orchard C. T-tubule function in mammalian cardiac myocytes. *Circulation Research*. 2003;92:1182-1192
30. Brette F, Orchard C. Resurgence of cardiac t-tubule research. *Physiology*. 2007;22:167-173
31. Kawai M, Hussain M, Orchard CH. Excitation-contraction coupling in rat ventricular myocytes after formamide-induced detubulation. *American Journal of Physiology-Heart and Circulatory Physiology*. 1999;277:H603-H609
32. Brette F, Komukai K, Orchard CH. Validation of formamide as a detubulation agent in isolated rat cardiac cells. *American Journal of Physiology-Heart and Circulatory Physiology*. 2002;283:H1720-H1728
33. Zhou YY, Yang D, Zhu WZ, Zhang SJ, Wang DJ, Rohrer DK, Devic E, Kobilka BK, Lakatta EG, Cheng HP, Xiao RP. Spontaneous activation of beta 2-but not beta(1)-adrenoceptors expressed in cardiac myocytes from beta(1)beta(2) double knockout mice. *Molecular Pharmacology*. 2000;58:887-894
34. Lyon AR, MacLeod KT, Zhang Y, Garcia E, Kanda GK, Lab MJ, Korchev YE, Harding SE, Gorelik J. Loss of t-tubules and other changes to surface topography in ventricular myocytes from failing human and rat heart. *Proceedings of the National Academy of Sciences of the United States of America*. 2009;106:6854-6859
35. Crossman DJ, Ruygrok PR, Soeller C, Cannell MB. Changes in the organization of excitation-contraction coupling structures in failing human heart. *Plos One*. 2011;6
36. Price MG, Sanger JW. Intermediate filaments in striated muscle. A review of structural studies in embryonic and adult skeletal and cardiac muscle. *Cell and muscle motility*. 1983;3:1-40
37. Gautel M, Goulding D. A molecular map of titin/connectin elasticity reveals two different mechanisms acting in series. *Febs Letters*. 1996;385:11-14
38. Brady AJ. Mechanical-properties of isolated cardiac myocytes. *Physiological Reviews*. 1991;71:413-428
39. Pitts BJR. Stoichiometry of sodium-calcium exchange in cardiac sarcolemmal vesicles - coupling to the sodium-pump. *Journal of Biological Chemistry*. 1979;254:6232-6235
40. Philipson KD, Nicoll DA. Sodium-calcium exchange: A molecular perspective. *Annual Review of Physiology*. 2000;62:111-133
41. Bers DM. Cardiac excitation-contraction coupling. *Nature*. 2002;415:198-205

42. Song LS, Wang SQ, Xiao RP, Spurgeon H, Lakatta EG, Cheng HP. Beta-adrenergic stimulation synchronizes intracellular ca2+ release during excitation-contraction coupling in cardiac myocytes. *Circulation Research*. 2001;88:794-801
43. Shcherbakova OG, Hurt CM, Xiang Y, Dell'Acqua ML, Zhang Q, Tsien RW, Kobilka BK. Organization of beta-adrenoceptor signaling compartments by sympathetic innervation of cardiac myocytes. *Journal of Cell Biology*. 2007;176:521-533
44. Brodde OE. Beta-adrenoreceptors in cardiac disease. *Pharmacology & Therapeutics*. 1993;60:405-430
45. Heubach JF, Rau T, Eschenhagen T, Ravens U, Kaumann AJ. Physiological antagonism between ventricular beta1-adrenoceptors and alpha1-adrenoceptors but no evidence for beta2- and beta3-adrenoceptor function in murine heart. *British Journal of Pharmacology*. 2002;136:217-229
46. Hamm HE. The many faces of g protein signaling. *Journal of Biological Chemistry*. 1998;273:669-672
47. Nikolaev VO, Moshkov A, Lyon AR, Miragoli M, Novak P, Paur H, Lohse MJ, Korchev YE, Harding SE, Gorelik J. Beta(2)-adrenergic receptor redistribution in heart failure changes camp compartmentation. *Science*. 2010;327:1653-1657
48. Rybin VO, Xu XH, Lisanti MP, Steinberg SF. Differential targeting of beta-adrenergic receptor subtypes and adenylyl cyclase to cardiomyocyte caveolae - a mechanism to functionally regulate the camp signaling pathway. *Journal of Biological Chemistry*. 2000;275:41447-41457
49. Nikolaev VO, Buenemann M, Schmitteckert E, Lohse MJ, Engelhardt S. Cyclic amp imaging in adult cardiac myocytes reveals far-reaching beta(1)-adrenergic but locally confined beta(2)-adrenergic receptor-mediated signaling. *Circulation Research*. 2006;99:1084-1091
50. Kuschel M, Zhou YY, Cheng HP, Zhang SJ, Chen Y, Lakatta EG, Xiao RP. G(1) protein-mediated functional compartmentalization of cardiac beta(2)-adrenergic signaling. *Journal of Biological Chemistry*. 1999;274:22048-22052
51. Chen-Izu Y, Xiao R-P, Izu LT, Cheng H, Kuschel M, Spurgeon H, Lakatta EG. Gi-dependent localization of beta2-adrenergic receptor signaling to l-type ca2+ channels. *Biophysical Journal*. 2000;79:2547-2556
52. Soto D, De Arcangelis V, Zhang J, Xiang Y. Dynamic protein kinase a activities induced by beta-adrenoceptors dictate signaling propagation for substrate phosphorylation and myocyte contraction. *Circulation Research*. 2009;104:770-U121
53. Hulme JT, Westenbroek RE, Scheuer T, Catterall WA. Phosphorylation of serine 1928 in the distal c-terminal domain of cardiac ca(v)1.2 channels during beta 1-adrenergic regulation. *Proceedings of the National Academy of Sciences of the United States of America*. 2006;103:16574-16579
54. Sulakhe PV, Vo XT. Regulation of phospholamban and troponin-i phosphorylation in the intact rat cardiomyocytes by adrenergic and cholinergic roles of cyclic-nucleotides, calcium, protein-kinases and phosphatases and depolarization. *Molecular and Cellular Biochemistry*. 1995;149:103-126
55. Calaghan SC, Colyer J, White E. Cyclic amp but not phosphorylation of phospholamban contributes to the slow inotropic response to stretch in ferret papillary muscle. *Pflugers Archiv-European Journal of Physiology*. 1999;437:780-782
56. Xiao RP, Avdonin P, Zhou YY, Chen HP, Akhter SA, Eschenhagen T, Lefkowitz RJ, Koch WJ, Lakatta EG. Coupling of beta(2)-adrenoceptor to g(i) proteins and its physiological relevance in murine cardiac myocytes. *Circulation Research*. 1999;84:43-52
57. Xiang Y, Kobilka BK. Myocyte adrenoceptor signaling pathways. *Science*. 2003;300:1530-1532
58. Calaghan S, White E. Caveolae modulate excitation-contraction coupling and beta(2)-adrenergic signalling in adult rat ventricular myocytes. *Cardiovascular Research*. 2006;69:816-824

59. Kaumann AJ. Is there a 3rd heart beta-adrenoceptor. *Trends in Pharmacological Sciences*. 1989;10:316-320
60. Gauthier C, Tavernier G, Charpentier F, Langin D, LeMarec H. Functional beta(3)-adrenoceptor in the human heart. *Journal of Clinical Investigation*. 1996;98:556-562
61. Moniotte S, Vaerman J, Kockx MM, Larrouy D, Langin D, Noirhomme P, Balligand J. Real-time rt-pcr for the detection of beta-adrenocepto messenger rnas in small human endomyocardial biopsies. *Journal of Molecular and Cellular Cardiology*. 2001;33:2121-2133
62. Rozec B, Gauthier C. Beta(3)-adrenoceptors in the cardiovascular system: Putative roles in human pathologies. *Pharmacology & Therapeutics*. 2006;111:652-673
63. Dessy C, Balligand J-L. Beta3-adrenergic receptors in cardiac and vascular tissues: Emerging concepts and therapeutic perspectives. *Cardiovascular Pharmacology: Heart and Circulation*. 2010;59:135-163
64. Audigane L, Kerfant B-G, El Harchi A, Lorenzen-Schmidt I, Toumaniantz G, Cantereau A, Potreau D, Charpentier F, Noireaud J, Gauthier C. Rabbit, a relevant model for the study of cardiac beta(3)-adrenoceptors. *Experimental Physiology*. 2009;94:400-411
65. Angelone T, Filice E, Quintieri AM, Imbrogno S, Recchia A, Pulera E, Mannarino C, Pellegrino D, Cerra MC. Beta(3)-adrenoceptors modulate left ventricular relaxation in the rat heart via the no-cgmp-pkg pathway. *Acta Physiologica*. 2008;193:229-239
66. Ursino MG, Vasina V, Raschi E, Crema F, De Ponti F. The beta(3)-adrenoceptor as a therapeutic target: Current perspectives. *Pharmacological Research*. 2009;59:221-234
67. Emorine LJ, Marullo S, Briendsutren MM, Patey G, Tate K, Delavierklutchko C, Strosberg AD. Molecular characterization of the human beta-3-adrenergic receptor. *Science*. 1989;245:1118-1121
68. Moniotte S, Kobzik L, Feron O, Trochu JN, Gauthier C, Balligand JL. Upregulation of beta(2)-adrenoceptors and altered contractile response to inotropic amines in human failing myocardium. *Circulation*. 2001;103:1649-1655
69. Hurley JH. Structure, mechanism, and regulation of mammalian adenylyl cyclase. *Journal of Biological Chemistry*. 1999;274:7599-7602
70. Dessauer CW. Adenylyl cyclase-a-kinase anchoring protein complexes: The next dimension in camp signaling. *Molecular Pharmacology*. 2009;76:935-941
71. Defer N, Best-Belpomme M, Hanoune J. Tissue specificity and physiological relevance of various isoforms of adenylyl cyclase. *American Journal of Physiology-Renal Physiology*. 2000;279:F400-F416
72. Zaccolo M, Movsesian MA. Camp and cgmp signaling cross-talk - role of phosphodiesterases and implications for cardiac pathophysiology. *Circulation Research*. 2007;100:1569-1578
73. Zaccolo M. Camp signal transduction in the heart: Understanding spatial control for the development of novel therapeutic strategies. *British Journal of Pharmacology*. 2009;158:50-60
74. Bean BP, Nowycky MC, Tsien RW. Beta-adrenergic modulation of calcium channels in frog ventricular heart-cells. *Nature*. 1984;307:371-375
75. Yoshida A, Takahashi M, Imagawa T, Shigekawa M, Takisawa H, Nakamura T. Phosphorylation of ryanodine receptors in rat myocytes during beta-adrenergic stimulation. *Journal of Biochemistry*. 1992;111:186-190
76. Marx SO, Marks AR. Regulation of the ryanodine receptor in heart failure. *Basic Research in Cardiology*. 2002;97:I.49-I.51
77. Zhang R, Zhao JJ, Mandveno A, Potter JD. Cardiac troponin-i phosphorylation increases the rate of cardiac-muscle relaxation. *Circulation Research*. 1995;76:1028-1035
78. Lindemann JP, Jones LR, Hathaway DR, Henry BG, Watanabe AM. Beta-adrenergic stimulation of phospholamban phosphorylation and ca-2+-atpase activity in guinea-pig ventricles. *Journal of Biological Chemistry*. 1983;258:464-471

79. Cooper DMF. Compartmentalization of adenylate cyclase and camp signalling. *Biochemical Society Transactions*. 2005;33:1319-1322
80. Zaccolo M, Pozzan T. Discrete microdomains with high concentration of camp in stimulated rat neonatal cardiac myocytes. *Science*. 2002;295:1711-1715
81. Scott JD, McConnachie G, Langeberg LK. Akap signaling complexes: Getting to the heart of the matter. *Trends in Molecular Medicine*. 2006;12:317-323
82. Jarnaess E, Tasken K. Spatiotemporal control of camp signalling processes by anchored signalling complexes. *Biochemical Society Transactions*. 2007;35:931-937
83. Sterin-Borda L, Bernabeo G, Ganzinelli S, Joensen L, Borda E. Role of nitric oxide/cyclic gmp and cyclic amp in beta(3) adrenoceptor-chronotropic response. *Journal of Molecular and Cellular Cardiology*. 2006;40:580-588
84. Castro LRV, Verde I, Cooper DMF, Fischmeister R. Cyclic guanosine monophosphate compartmentation in rat cardiac myocytes. *Circulation*. 2006;113:2221-2228
85. Takimoto E, Belardi D, Tocchetti CG, Vahebi S, Cormaci G, Ketner EA, Moens AL, Champion HC, Kass DA. Compartmentalization of cardiac beta-adrenergic inotropy modulation by phosphodiesterase type 5. *Circulation*. 2007;115:2159-2167
86. Yang L, Liu G, Zakharov SI, Bellinger AM, Mongillo M, Marx SO. Protein kinase g phosphorylates ca(v)1.2 alpha(1c) and beta(2) subunits. *Circulation Research*. 2007;101:465-474
87. Layland J, Kentish JC. Myofilament-based relaxant effect of isoprenaline revealed during work-loop contractions in rat cardiac trabeculae. *Journal of Physiology-London*. 2002;544:171-182
88. Raeymaekers L, Hofmann F, Casteels R. Cyclic gmp-dependent protein-kinase phosphorylates phospholamban in isolated sarcoplasmic-reticulum from cardiac and smooth-muscle. *Biochemical Journal*. 1988;252:269-273
89. Sperelakis N, Schneider JA. Metabolic control mechanism for calcium-ion influx that may protect ventricular myocardial-cell. *American Journal of Cardiology*. 1976;37:1079-1085
90. Reuter H, Scholz H. Regulation of calcium conductance of cardiac-muscle by adrenaline. *Journal of Physiology-London*. 1977;264:49-62
91. Hartzell HC, Mery PF, Fischmeister R, Szabo G. Sympathetic regulation of cardiac calcium current is due exclusively to camp-dependent phosphorylation. *Nature*. 1991;351:573-576
92. Kamp TJ, Hell JW. Regulation of cardiac l-type calcium channels by protein kinase a and protein kinase c. *Circulation Research*. 2000;87:1095-1102
93. Yue DT, Herzig S, Marban E. Beta-adrenergic stimulation of calcium channels occurs by potentiation of high-activity gating modes. *Proceedings of the National Academy of Sciences of the United States of America*. 1990;87:753-757
94. Benitah J-P, Alvarez JL, Gomez AM. L-type ca2+ current in ventricular cardiomyocytes. *Journal of Molecular and Cellular Cardiology*. 2010;48:26-36
95. Leroy J, Abi-Gerges A, Nikolaev VO, Richter W, Lechene P, Mazet J-L, Conti M, Fischmeister R, Vandecasteele G. Spatiotemporal dynamics of beta-adrenergic camp signals and l-type ca2+ channel regulation in adult rat ventricular myocytes - role of phosphodiesterases. *Circulation Research*. 2008;102:1091-1100
96. Gao TY, Yatani A, DellAcqua ML, Sako H, Green SA, Dascal N, Scott JD, Hosey MM. Camp-dependent regulation of cardiac l-type ca2+ channels requires membrane targeting of pka and phosphorylation of channel subunits. *Neuron*. 1997;19:185-196
97. Moens AL, Leyton-Mange JS, Niu X, Yang R, Cingolani O, Arkenbout EK, Champion HC, Bedja D, Gabrielson KL, Chen J, Xia Y, Hale AB, Channon KM, Halushka MK, Barker N, Wuyts FL, Kaminski PM, Wolin MS, Kass DA, Barouch LA. Adverse ventricular remodeling and exacerbated nos uncoupling from pressure-overload in mice lacking the beta 3-adrenoreceptor. *Journal of Molecular and Cellular Cardiology*. 2009;47:576-585
98. Mongillo M, Tocchetti CG, Terrin A, Lissandron V, Cheung YF, Dostmann WR, Pozzan T, Kass DA, Paolocci N, Houslay MD, Zaccolo M. Compartmentalized phosphodiesterase-2

activity blunts beta-adrenergic cardiac inotropy via an no/cgmp-dependent pathway. *Circulation Research*. 2006;98:226-234

99. Hartzell HC, Fischmeister R. Opposite effects of cyclic-gmp and cyclic-amp on ca-2+ current in single heart-cells. *Nature*. 1986;323:273-275
100. Levi RC, Alloatti G, Fischmeister R. Cyclic-gmp regulates the ca-channel current in guinea-pig ventricular myocytes. *Pflugers Archiv-European Journal of Physiology*. 1989;413:685-687
101. Mery PF, Lohmann SM, Walter U, Fischmeister R. Ca2+ current is regulated by cyclic gmp-dependent protein-kinase in mammalian cardiac myocytes. *Proceedings of the National Academy of Sciences of the United States of America*. 1991;88:1197-1201
102. Schroder F, Klein G, Fiedler B, Bastein M, Schnasse N, Hillmer A, Ames S, Gambaryan S, Drexler H, Walter U, Lohmann SM, Wollert KC. Single l-type ca2+ channel regulation by cgmp-dependent protein kinase type i in adult cardiomyocytes from pkg i transgenic mice. *Cardiovascular Research*. 2003;60:268-277
103. Mery PF, Pavoine C, Belhassen L, Pecker F, Fischmeister R. Nitric-oxide regulates cardiac ca2+ current - involvement of cgmp-inhibited and cgmp-stimulated phosphodiesterases through guanylyl cyclase activation. *Journal of Biological Chemistry*. 1993;268:26286-26295
104. Ginsburg KS, Bers DM. Modulation of excitation-contraction coupling by isoproterenol in cardiomyocytes with controlled sr ca2+ load and ca2+ current trigger. *Journal of Physiology-London*. 2004;556:463-480
105. Suko J, Maurerfogy I, Plank B, Bertel O, Wyskovsky W, Hohenegger M, Hellmann G. Phosphorylation of serine-2843 in ryanodine receptor-calcium release channel of skeletal-muscle by camp-dependent, cgmp-dependent and cam-dependent protein-kinase. *Biochimica Et Biophysica Acta*. 1993;1175:193-206
106. Hussain M, Orchard CH. Sarcoplasmic reticulum ca2+ content, l-type ca2+ current and the ca2+ transient in rat myocytes during beta-adrenergic stimulation. *Journal of Physiology-London*. 1997;505:385-402
107. Simmerman HKB, Collins JH, Theibert JL, Wegener AD, Jones LR. Sequence-analysis of phospholamban - identification of phosphorylation sites and 2 major structural domains. *Journal of Biological Chemistry*. 1986;261:3333-3341
108. Li L, Desantiago J, Chu GX, Kranias EG, Bers DM. Phosphorylation of phospholamban and troponin i in beta-adrenergic-induced acceleration of cardiac relaxation. *American Journal of Physiology-Heart and Circulatory Physiology*. 2000;278:H769-H779
109. Luo W, Grupp IL, Harrer JM, Slack JP, Grupp G, Doetschman T, Kranias EG. Targeted disruption of the phospholamban gene is associated with enhanced sarcoplasmic reticulum ca-2+ transport and myocardial contractile parameters. *Circulation*. 1994;90:I633
110. Zhang QH, Scholz PM, He YQ, Tse J, Weiss HR. Cyclic gmp signaling and regulation of serca activity during cardiac myocyte contraction. *Cell Calcium*. 2005;37:259-266
111. Jin CZ, Jang JH, Wang Y, Kim JG, Bae YM, Shi J, Che CR, Kim SJ, Zhang YH. Neuronal nitric oxide synthase is up-regulated by angiotensin ii and attenuates nadph oxidase activity and facilitates relaxation in murine left ventricular myocytes. *Journal of Molecular and Cellular Cardiology*. 2012;52:1274-1281
112. Daaka Y, Luttrell LM, Lefkowitz RJ. Switching of the coupling of the beta(2)-adrenergic receptor to different g proteins by protein kinase a. *Nature*. 1997;390:88-91
113. Chesley A, Lundberg MS, Asai T, Xiao RP, Ohtani S, Lakatta EG, Crow MT. The beta(2)-adrenergic receptor delivers an antiapoptotic signal to cardiac myocytes through g(i)-dependent coupling to phosphatidylinositol 3 '-kinase. *Circulation Research*. 2000;87:1172-1179

114. Lefkowitz RJ. G protein-coupled receptors iii. New roles for receptor kinases and beta-arrestins in receptor signaling and desensitization. *Journal of Biological Chemistry*. 1998;273:18677-18680
115. Lin FB, Wang HY, Malbon CC. Gravin-mediated formation of signaling complexes in beta(2)-adrenergic receptor desensitization and resensitization. *Journal of Biological Chemistry*. 2000;275:19025-19034
116. Lefkowitz RJ, Luttrell LM. The role of beta-arrestins in the termination and transduction of g-protein-coupled receptor signals. *Journal of Cell Science*. 2002;115:455-465
117. Bathgate-Siryk A, Dabul S, Pandya K, Walklett K, Rengo G, Cannavo A, De Lucia C, Liccardo D, Gao E, Leosco D, Koch WJ, Lymperopoulos A. Negative impact of beta-arrestin-1 on post-myocardial infarction heart failure via cardiac and adrenal-dependent neurohormonal mechanisms. *Hypertension*. 2014;63:404-+
118. Abramow-Newerly M, Roy AA, Nunn C, Chidiac P. Rgs proteins have a signalling complex: Interactions between rgs proteins and gpcrs, effectors, and auxiliary proteins. *Cellular Signalling*. 2006;18:579-591
119. Chidiac P, Roy AA. Activity, regulation, and intracellular localization of rgs proteins. *Receptors & Channels*. 2003;9:135-147
120. Nunn C, Zou M-X, Sobiesiak AJ, Roy AA, Kirshenbaum LA, Chidiac P. Rgs2 inhibits beta-adrenergic receptor-induced cardiomyocyte hypertrophy. *Cellular Signalling*. 2010;22:1231-1239
121. Takimoto E, Koitabashi N, Hsu S, Ketner EA, Zhang M, Nagayarna T, Bedja D, Gabrielson KL, Blanton R, Siderovski DP, Mendelsohn ME, Kass DA. Regulator of g protein signaling 2 mediates cardiac compensation to pressure overload and antihypertrophic effects of pde5 inhibition in mice. *Journal of Clinical Investigation*. 2009;119:408-420
122. Sinnarajah S, Dessauer CW, Srikumar D, Chen J, Yuen J, Yilma S, Dennis JC, Morrison EE, Vodyanoy V, Kehrl JH. Rgs2 regulates signal transduction in olfactory neurons by attenuating activation of adenylyl cyclase iii. *Nature*. 2001;409:1051-1055
123. Takimoto E, Champion HC, Li MX, Belardi D, Ren SX, Rodriguez ER, Bedja D, Gabrielson KL, Wang YB, Kass DA. Chronic inhibition of cyclic gmp phosphodiesterase 5a prevents and reverses cardiac hypertrophy. *Nature Medicine*. 2005;11:214-222
124. Hayes JS, Brunton LL. Functional compartments in cyclic-nucleotide action. *Journal of Cyclic Nucleotide Research*. 1982;8:1-16
125. Pidoux G, Tasken K. Specificity and spatial dynamics of protein kinase a signaling organized by a-kinase-anchoring proteins. *Journal of Molecular Endocrinology*. 2010;44:271-284
126. Stangherlin A, Zaccolo M. Local termination of 3 '-5 '-cyclic adenosine monophosphate signals: The role of a kinase anchoring protein-tethered phosphodiesterases. *Journal of Cardiovascular Pharmacology*. 2011;58:345-353
127. Davare MA, Avdonin V, Hall DD, Peden EM, Burette A, Weinberg RJ, Horne MC, Hoshi T, Hell JW. A beta(2) adrenergic receptor signaling complex assembled with the ca2+ channel ca(v)1.2. *Science*. 2001;293:98-101
128. Fink MA, Zakhary DR, Mackey JA, Desnoyer RW, Apperson-Hansen C, Damron DS, Bond M. Akap-mediated targeting of protein kinase a regulates contractility in cardiac myocytes. *Circulation Research*. 2001;88:291-297
129. Nikolaev VO, Bunemann M, Hein L, Hannawacker A, Lohse MJ. Novel single chain camp sensors for receptor-induced signal propagation. *Journal of Biological Chemistry*. 2004;279:37215-37218
130. Francis SH, Turko IV, Corbin JD. Cyclic nucleotide phosphodiesterases: Relating structure and function. *Progress in Nucleic Acid Research and Molecular Biology, Vol 65*. 2001;65:1-52
131. Soderling SH, Beavo JA. Regulation of camp and cgmp signaling: New phosphodiesterases and new functions. *Current Opinion in Cell Biology*. 2000;12:174-179

132. Francis SH, Blount MA, Corbin JD. Mammalian cyclic nucleotide phosphodiesterases: Molecular mechanisms and physiological functions. *Physiological Reviews*. 2011;91:651-690
133. Brunton LL, Hayes JS, Mayer SE. Functional compartmentation of cyclic-amp and protein-kinase in heart. *Advances in Cyclic Nucleotide Research*. 1981;14:391-397
134. Verde I, Vandecasteele G, Lezoualc'h F, Fischmeister R. Characterization of the cyclic nucleotide phosphodiesterase subtypes involved in the regulation of the l-type ca2+ current in rat ventricular myocytes. *British Journal of Pharmacology*. 1999;127:65-74
135. Richter W, Jin SLC, Conti M. Splice variants of the cyclic nucleotide phosphodiesterase pde4d are, differentially expressed and regulated in rat tissue. *Biochemical Journal*. 2005;388:803-811
136. Abi-Gerges A, Richter W, Lefebvre F, Mateo P, Varin A, Heymes C, Samuel JL, Lugnier C, Conti M, Fischmeister R, Vandecasteele G. Decreased expression and activity of camp phosphodiesterases in cardiac hypertrophy and its impact on beta-adrenergic camp signals. *Circulation Research*. 2009;105:784-U161
137. Molina CE, Leroy J, Richter W, Xie M, Scheitrum C, Lee I-O, Maack C, Rucker-Martin C, Donzeau-Gouge P, Verde I, Llach A, Hove-Madsen L, Conti M, Vandecasteele G, Fischmeister R. Cyclic adenosine monophosphate phosphodiesterase type 4 protects against atrial arrhythmias. *Journal of the American College of Cardiology*. 2012;59:2182-2190
138. Perera RK, Nikolaev VO. Compartmentation of camp signalling in cardiomyocytes in health and disease. *Acta Physiologica*. 2013;207:650-662
139. Mongillo M, McSorley T, Evellin S, Sood A, Lissandron V, Terrin A, Huston E, Hannawacker A, Lohse MJ, Pozzan T, Houslay MD, Zaccolo M. Fluorescence resonance energy transfer-based analysis of camp dynamics in live neonatal rat cardiac myocytes reveals distinct functions of compartmentalized phosphodiesterases. *Circulation Research*. 2004;95:67-75
140. Xiang Y, Naro F, Zoudilova M, Jin SLC, Conti M, Kobilka B. Phosphodiesterase 4d is required for beta(2) adrenoceptor subtype-specific signaling in cardiac myocytes. *Proceedings of the National Academy of Sciences of the United States of America*. 2005;102:909-914
141. De Arcangelis V, Soto D, Xiang Y. Phosphodiesterase 4 and phosphatase 2a differentially regulate camp/protein kinase a signaling for cardiac myocyte contraction under stimulation of beta(1) adrenergic receptor. *Molecular Pharmacology*. 2008;74:1453-1462
142. Leroy J, Richter W, Mika D, Castro LRV, Abi-Gerges A, Xie M, Scheitrum C, Lefebvre F, Schittl J, Mateo P, Westenbroek R, Catterall WA, Charpentier F, Conti M, Fischmeister R, Vandecasteele G. Phosphodiesterase 4b in the cardiac l-type ca2+ channel complex regulates ca2+ current and protects against ventricular arrhythmias in mice. *Journal of Clinical Investigation*. 2011;121:2651-2661
143. Richter W, Day P, Agrawal R, Bruss MD, Granier S, Wang YL, Rasmussen SGF, Homer K, Wang P, Lei T, Patterson AJ, Kobilka B, Conti M. Signaling from beta 1-and beta 2-adrenergic receptors is defined by differential interactions with pde4. *Faseb Journal*. 2008;22
144. Lehnart SE, Wehrens XHT, Reiken S, Warrier S, Belevych AE, Harvey RD, Richter W, Jin SLC, Conti M, Marks AR. Phosphodiesterase 4d deficiency in the ryanodine-receptor complex promotes heart failure and arrhythmias (vol 123, pg 25, 2005). *Cell*. 2005;123:535-536
145. Beca S, Helli PB, Simpson JA, Zhao D, Farman GP, Jones PP, Tian X, Wilson LS, Ahmad F, Chen SRW, Movsesian MA, Manganiello V, Maurice DH, Conti M, Backx PH. Phosphodiesterase 4d regulates baseline sarcoplasmic reticulum ca2+ release and cardiac contractility, independently of l-type ca2+ current. *Circulation Research*. 2011;109:1024-U1119
146. Kerfant B-G, Zhao D, Lorenzen-Schmidt I, Wilson LS, Cai S, Chen SRW, Maurice DH, Backx PH. Pi3k gamma is required for pde4, not pde3, activity in subcellular microdomains

containing the sarcoplasmic reticular calcium atpase in cardiomyocytes. *Circulation Research*. 2007;101:400-408

147. Baillie GS, Sood A, McPhee I, Gall I, Perry SJ, Lefkowitz RJ, Houslay MD. Beta-arrestin-mediated pde4 camp phosphodiesterase recruitment regulates beta-adrenoceptor switching from g(s) to g(i). *Proceedings of the National Academy of Sciences of the United States of America*. 2003;100:940-945
148. Scott JD, Dodge KL, Khouangsathiene S, Kapiloff MS, Mouton R, Hill EV, Houslay MD, Langeberg LK. Makap assembles a protein kinase a/pde4 phosphodiesterase camp signaling module. *Embo Journal*. 2001;20:1921-1930
149. Carlisle Michel JJ, Dodge KL, Wong W, Mayer NC, Langeberg LK, Scott JD. Pka-phosphorylation of pde4d3 facilitates recruitment of the makap signalling complex. *Biochemical Journal*. 2004;381:587-592
150. Wehrens XHT, Marks AR. Altered function and regulation of cardiac ryanodine receptors in cardiac disease. *Trends in Biochemical Sciences*. 2003;28:671-678
151. Houslay MD, Baillie GS, Maurice DH. Camp-specific phosphodiesterase-4 enzymes in the cardiovascular system - a molecular toolbox for generating compartmentalized camp signaling. *Circulation Research*. 2007;100:950-966
152. Vandeput F, Wolda SL, Krall J, Hambleton R, Uher L, McCaw KN, Radwanski PB, Florio V, Movsesian MA. Cyclic nucleotide phosphodiesterase pde1c1 in human cardiac myocytes. *Journal of Biological Chemistry*. 2007;282:32749-32757
153. Osadchii OE. Myocardial phosphodiesterases and regulation of cardiac contractility in health and cardiac disease. *Cardiovascular Drugs and Therapy*. 2007;21:171-194
154. Mehel H EJ, Vettel C, Wittköpper K, Seppelt D, Dewenter M, Lutz S, Sossalla S, Maier LS, Lechêne P, Leroy J, Lefebvre F, Varin A, Eschenhagen T, Nattel S, Dobrev D, Zimmermann WH, Nikolaev VO, Vandecasteele G, Fischmeister R, El-Armouche A. Phosphodiesterase-2 is upregulated in human failing hearts and blunts β-adrenergic responses in cardiomyocytes. *J Am Coll Cardiol*. 2013
155. Bode DC, Kanter JR, Brunton LL. Cellular-distribution of phosphodiesterase isoforms in rat cardiac tissue. *Circulation Research*. 1991;68:1070-1079
156. Han X, Kobzik L, Balligand JL, Kelly RA, Smith TW. Nitric oxide synthase (nos3)-mediated cholinergic modulation of ca2+ current in adult rabbit atrioventricular nodal. *Circulation Research*. 1996;78:998-1008
157. Mery PF, Pavoine C, Pecker F, Fischmeister R. Erythro-9-(2-hydroxy-3-nonyl)adenine inhibits cyclic gmp-stimulated phosphodiesterase in isolated cardiac myocytes. *Molecular Pharmacology*. 1995;48:121-130
158. Vandecasteele G, Verde I, Rucker-Martin C, Donzeau-Gouge P, Fischmeister R. Cyclic gmp regulation of the l-type ca2+ channel current in human atrial myocytes. *Journal of Physiology-London*. 2001;533:329-340
159. Senzaki H, Smith CJ, Juang GJ, Isoda T, Mayer SP, Ohler A, Paolocci N, Tomaselli GF, Hare JM, Kass DA. Cardiac phosphodiesterase 5 (cgmp-specific) modulates beta-adrenergic signaling in vivo and is down-regulated in heart failure. *Faseb Journal*. 2001;15:1718-1726
160. Turko IV, Francis SH, Corbin JD. Binding of cgmp to both allosteric sites of cgmp-binding cgmp-specific phosphodiesterase (pde5) is required for its phosphorylation. *Biochemical Journal*. 1998;329:505-510
161. Gopal VK, Francis SH, Corbin JD. Allosteric sites of phosphodiesterase-5 (pde5) - a potential role in negative feedback regulation of cgmp signaling in corpus cavernosum. *European Journal of Biochemistry*. 2001;268:3304-3312
162. Takimoto E, Champion HC, Belardi D, Moslehi J, Mongillo M, Mergia E, Montrose DC, Isoda T, Aufiero K, Zaccolo M, Dostmann WR, Smith CJ, Kass DA. Cgmp catabolism by phosphodiesterase 5a regulates cardiac adrenergic stimulation by nos3-dependent mechanism. *Circulation Research*. 2005;96:100-109

163. Zhang M, Koitabashi N, Nagayama T, Rambaran R, Feng N, Takimoto E, Koenke T, O'Rourke B, Champion HC, Crow MT, Kass DA. Expression, activity, and pro-hypertrophic effects of pde5a in cardiac myocytes. *Cellular Signalling*. 2008;20:2231-2236
164. Nagayama T, Zhang ML, Hsu S, Takimoto E, Kass DA. Sustained soluble guanylate cyclase stimulation offsets nitric-oxide synthase inhibition to restore acute cardiac modulation by sildenafil. *Journal of Pharmacology and Experimental Therapeutics*. 2008;326:380-387
165. Borlaug BA, Melenovsky V, Marhin T, Fitzgerald P, Kass DA. Sildenafil inhibits beta-adrenergic-stimulated cardiac contractility in humans. *Circulation*. 2005;112:2642-2649
166. Wang H, Kohr MJ, Traynham CJ, Ziolo MT. Phosphodiesterase 5 restricts nos3/soluble guanylate cyclase signaling to l-type ca2+ current in cardiac myocytes. *Journal of Molecular and Cellular Cardiology*. 2009;47:304-314
167. Roy, Adami JG. Remarks on failure of the heart from overstrain. *British medical journal*. 1888;2:1321-1326
168. Jefferies JL, Towbin JA. Dilated cardiomyopathy. *Lancet*. 2010;375:752-762
169. Levine TB, Francis GS, Goldsmith SR, Simon AB, Cohn JN. Activity of the sympathetic nervous-system and renin-angiotensin system assessed by plasma-hormone levels and their relation to hemodynamic abnormalities in congestive heart-failure. *American Journal of Cardiology*. 1982;49:1659-1666
170. Lefkowitz RJ, Rockman HA, Koch WJ. Catecholamines, cardiac beta-adrenergic receptors, and heart failure. *Circulation*. 2000;101:1634-1637
171. Braunwald E. Biomarkers in heart failure. *New England Journal of Medicine*. 2008;358:2148-2159
172. Hunt SA, American College of C, American Heart Association Task Force on Practice G. Acc/aha 2005 guideline update for the diagnosis and management of chronic heart failure in the adult: A report of the american college of cardiology/american heart association task force on practice guidelines (writing committee to update the 2001 guidelines for the evaluation and management of heart failure). *Journal of the American College of Cardiology*. 2005;46:e1-82
173. Ghio S, Freemantle N, Scelsi L, Serio A, Magrini G, Pasotti M, Shankar A, Cleland JGF, Tavazzi L. Long-term left ventricular reverse remodelling with cardiac resynchronization therapy: Results from the care-hf trial. *European Journal of Heart Failure*. 2009;11:480-488
174. Birks EJ, Tansley PD, Hardy J, George RS, Bowles CT, Burke M, Banner NR, Khaghani A, Yacoub MH. Left ventricular assist device and drug therapy for the reversal of heart failure. *New England Journal of Medicine*. 2006;355:1873-1884
175. Massie BM, Fisher SG, Radford MJ, Deedwania PC, Singh BN, Fletcher RD, Singh SN. Effect of amiodarone on clinical status and left ventricular function in patients with congestive heart failure (vol 93, pg 2128, 1996). *Circulation*. 1996;94:2668-2668
176. Pieske B, Maier LS, Bers DM, Hasenfuss G. Ca2+ handling and sarcoplasmic reticulum ca2+ content in isolated failing and nonfailing human myocardium. *Circulation Research*. 1999;85:38-46
177. Kurihara S, Sakai T. Effects of rapid cooling on mechanical and electrical responses in ventricular muscle of guinea-pig. *Journal of Physiology-London*. 1985;361:361-378
178. Maier LS, Bers DM, Pieske B. Differences in ca2+-handling and sarcoplasmic reticulum ca2+-content in isolated rat and rabbit myocardium. *Journal of Molecular and Cellular Cardiology*. 2000;32:2249-2258
179. Trafford AW, Briston SJ, Caldwell JL, Horn MA, Clarke JD, Richards MA, Greensmith DJ, Graham HK, Hall MCS, Eisner DA, Dibb KM. Impaired beta-adrenergic responsiveness accentuates dysfunctional excitation-contraction coupling in an ovine model of tachypacing-induced heart failure. *Journal of Physiology-London*. 2011;589:1367-1382

180. Beuckelmann DJ, Nabauer M, Erdmann E. Intracellular calcium handling in isolated ventricular myocytes from patients with terminal heart-failure. *Circulation*. 1992;85:1046-1055
181. Diaz ME, Graham HK, Trafford AW. Enhanced sarcolemmal ca2+ efflux reduces sarcoplasmic reticulum ca2+ content and systolic ca2+ in cardiac hypertrophy. *Cardiovascular Research*. 2004;62:538-547
182. Hobai IA, O'Rourke B. Decreased sarcoplasmic reticulum calcium content is responsible for defective excitation-contraction coupling in canine heart failure. *Circulation*. 2001;103:1577-1584
183. Mukherjee R, Spinale FG. L-type calcium channel abundance and function with cardiac hypertrophy and failure: A review. *Journal of Molecular and Cellular Cardiology*. 1998;30:1899-1916
184. Balijepalli RC, Lokuta AJ, Maertz NA, Buck JM, Haworth RA, Valdivia HH, Kamp TJ. Depletion of t-tubules and specific subcellular changes in sarcolemmal proteins in tachycardia-induced heart failure. *Cardiovascular Research*. 2003;59:67-77
185. He JQ, Balijepalli RC, Haworth RA, Kamp TJ. Crosstalk of beta-adrenergic receptor subtypes through g(i) blunts beta- adrenergic stimulation of l-type ca2+ channels in canine heart failure. *Circulation Research*. 2005;97:566-573
186. Louch WE, Bito V, Heinzel FR, Macianskiene R, Vanhaecke J, Flameng W, Mubagwa K, Sipido KR. Reduced synchrony of ca2+ release with loss of t-tubules - a comparison to ca2+ release in human failing cardiomyocytes. *Cardiovascular Research*. 2004;62:63-73
187. Caldwell JL, Eisner DA, Dibb KM, Trafford AW. Amphiphysin ii controls t-tubule formation in cardiac muscle. *Proceedings 37th IUPS*. 2013;PCB020 Poster Communications
188. Perreault CL, Bing OHL, Brooks WW, Ransil BJ, Morgan JP. Differential-effects of cardiac-hypertrophy and failure on right versus left-ventricular calcium activation. *Circulation Research*. 1990;67:707-712
189. Lindner M, Erdmann E, Beuckelmann DJ. Calcium content of the sarcoplasmic reticulum in isolated ventricular myocytes from patients with terminal heart failure. *Journal of Molecular and Cellular Cardiology*. 1998;30:743-749
190. Mercadier JJ, Lompre AM, Duc P, Boheler KR, Fraysse JB, Wisnewsky C, Allen PD, Komajda M, Schwartz K. Altered sarcoplasmic-reticulum ca-2+-atpase gene-expression in the human ventricle during end-stage heart-failure. *Journal of Clinical Investigation*. 1990;85:305-309
191. Meyer M, Lehnart S, Pieske B, Giljum M, Hasenfuss G. Sr-ca2+-atpase inhibition by cyclopiazonic acid - effects on the force-frequency relation in human ventricular myocardium. *Circulation*. 1995;92:1212-1212
192. Frank KF, Boelck B, Brixius K, Kranias EG, Schwinger RHG. Modulation of serca: Implications for the failing human heart. *Basic Research in Cardiology*. 2002;97:I.72-I.78
193. Mulieri LA, Leavitt BJ, Ittleman FP, Martin BJ, Haeberle JR, Alpert NR. Depressed myocardial force-frequency curve in mitral regurgitation heart-failure is partially reversed by forskolin. *Circulation*. 1992;86:861-861
194. Schwinger RHG, Munch G, Bolck B, Karczewski P, Krause EG, Erdmann E. Reduced ca2+-sensitivity of serca 2a in failing human myocardium due to reduced serin-16 phospholamban phosphorylation. *Journal of Molecular and Cellular Cardiology*. 1999;31:479-491
195. del Monte F, Harding SE, Schmidt U, Matsui T, Kang ZB, Dec W, Gwathmey JK, Rosenzweig A, Hajjar RJ. Restoration of contractile function in isolated cardiomyocytes from failing human hearts by gene transfer of serca2a. *Circulation*. 1999;100:2308-2311
196. Lyon AR, Nikolaev VO, Miragoli M, Sikkel MB, Paur H, Benard L, Hulot J-S, Kohlbrenner E, Hajjar RJ, Peters NS, Korchev YE, Macleod KT, Harding SE, Gorelik J. Plasticity of surface structures and beta(2)-adrenergic receptor localization in failing ventricular

cardiomyocytes during recovery from heart failure. *Circulation-Heart Failure*. 2012;5:357-365
197. Song LS, Sobie EA, McCulle S, Lederer WJ, Balke CW, Cheng HP. Orphaned ryanodine receptors in the failing heart. *Proceedings of the National Academy of Sciences of the United States of America*. 2006;103:4305-4310
198. Reiter E, Lefkowitz RJ. Grks and beta-arrestins: Roles in receptor silencing, trafficking and signaling. *Trends in Endocrinology and Metabolism*. 2006;17:159-165
199. Ferguson SSG. Evolving concepts in g protein-coupled receptor endocytosis: The role in receptor desensitization and signaling. *Pharmacological Reviews*. 2001;53:1-24
200. Lymperopoulos A, Rengo G, Funakoshi H, Eckhart AD, Koch WJ. Adrenal grk2 upregulation mediates sympathetic overdrive in heart failure. *Nature Medicine*. 2007;13:315-323
201. Bristow MR, Hershberger RE, Port JD, Minobe W, Rasmussen R. Beta-1-adrenergic and beta-2-adrenergic receptor-mediated adenylate-cyclase stimulation in nonfailing and failing human ventricular myocardium. *Molecular Pharmacology*. 1989;35:295-303
202. Feldman AM, Cates AE, Veazey WB, Hershberger RE, Bristow MR, Baughman KL, Baumgartner WA, Vandop C. Increase of the 40,000-mol wt pertussis toxin substrate (g-protein) in the failing human-heart. *Journal of Clinical Investigation*. 1988;82:189-197
203. Zhu PL, Karliner JS, Zhou HZ, Honbo N, Messing RO, Mochly-Rosen D, Gray MO. Does chronically upregulated delta pkc confer cardioprotection in the adult mouse? *Circulation*. 2001;104:209-209
204. Napp A, Brixius K, Pott C, Ziskoven C, Boelck B, Mehlhorn U, Schwinger RHG, Bloch W. Efftuects of the beta(3)-adrenergic agonist brl 37344 on endothelial nitric oxide synthase phosphorylation and force of contraction in human failing myocardium. *Journal of Cardiac Failure*. 2009;15:57-67
205. Reiken S, Gaburjakova M, Gaburjakova J, He KL, Prieto A, Becker E, Yi GH, Wang J, Burkhoff D, Marks AR. Beta-adrenergic receptor blockers restore cardiac calcium release channel (ryanodine receptor) structure and function in heart failure. *Circulation*. 2001;104:2843-2848
206. Reiken S, Wehrens XHT, Vest JA, Barbone A, Klotz S, Mancini D, Burkhoff D, Marks AR. Beta-blockers restore calcium release channel function and improve cardiac muscle performance in human heart failure. *Circulation*. 2003;107:2459-2466
207. Masunaga R, Nagasaka A, Sawai Y, Hayakawa N, Nakai A, Hotta K, Kato Y, Hishida H, Takahashi H, Naka M, Shimada Y, Tanaka T, Hidaka H, Itoh M. Changes in cyclic nucleotide phosphodiesterase activity and calmodulin concentration in heart muscle of cardiomyopathic hamsters. *Journal of Molecular and Cellular Cardiology*. 2004;37:767-774
208. Sato N, Asai K, Okumura S, Takagi G, Shannon RP, Fujita-Yamaguchi Y, Ishikawa Y, Vatner SF, Vatner DE. Mechanisms of desensitization to a pde inhibitor (milrinone) in conscious dogs with heart failure. *American Journal of Physiology-Heart and Circulatory Physiology*. 1999;276:H1699-H1705
209. Ding B, Abe JI, Wei H, Huang QH, Walsh RA, Molina CA, Zhao A, Sadoshima J, Blaxall BC, Berk BC, Yan C. Functional role of phosphodiesterase 3 in cardiomyocyte apoptosis - implication in heart failure. *Circulation*. 2005;111:2469-2476
210. Miller CL, Oikawa M, Cai Y, Wojtovich AP, Nagel DJ, Xu X, Xu H, Florio V, Rybalkin SD, Beavo JA, Chen Y-F, Li J-D, Blaxall BC, Abe J-i, Yan C. Role of ca(2+)/calmodulin-stimulated cyclic nucleotide phosphodiesterase 1 in mediating cardiomyocyte hypertrophy. *Circulation Research*. 2009;105:956-U959
211. Pokreisz P, Vandenwijngaert S, Bito V, Van den Bergh A, Lenaerts I, Busch C, Marsboom G, Gheysens O, Vermeersch P, Biesmans L, Liu XS, Gillijns H, Pellens M, Van Lommel A, Buys E, Schoonjans L, Vanhaecke J, Verbeken E, Sipido K, Herijgers P, Bloch KD, Janssens SP. Ventricular phosphodiesterase-5 expression is increased in patients with advanced heart failure and contributes to adverse ventricular remodeling after myocardial infarction in mice. *Circulation*. 2009;119:408-U493

212. Failli P, Fazzini A, Franconi F, Stendardi I, Giotti A. Taurine antagonizes the increase in intracellular calcium-concentration induced by alpha-adrenergic stimulation in freshly isolated guinea-pig cardiomyocytes. *Journal of Molecular and Cellular Cardiology*. 1992;24:1253-1265
213. Jong CJ, Azuma J, Schaffer S. Mechanism underlying the antioxidant activity of taurine: Prevention of mitochondrial oxidant production. *Amino Acids*. 2012;42:2223-2232
214. Satoh H, Delbridge LMD, Blatter LA, Bers DM. Surface:Volume relationship in cardiac myocytes studied with confocal microscopy and membrane capacitance measurements: Species-dependence and developmental effects. *Biophysical Journal*. 1996;70:1494-1504
215. Varro A, Negretti N, Hester SB, Eisner DA. An estimate of the calcium content of the sarcoplasmic-reticulum in rat ventricular myocytes. *Pflugers Archiv-European Journal of Physiology*. 1993;423:158-160
216. Dibb KM, Rueckschloss U, Eisner DA, Isenberg G, Trafford AW. Mechanisms underlying enhanced cardiac excitation contraction coupling observed in the senescent sheep myocardium. *Journal of Molecular and Cellular Cardiology*. 2004;37:1171-1181
217. Kass DA, Bronzwaer JGF, Paulus WJ. What mechanisms underlie diastolic dysfunction in heart failure? *Circulation Research*. 2004;94:1533-1542
218. Martinez SE, Wu AY, Glavas NA, Tang XB, Turley S, Hol WGJ, Beavo JA. The two gaf domains in phosphodiesterase 2a have distinct roles in dimerization and in cgmp binding. *Proceedings of the National Academy of Sciences of the United States of America*. 2002;99:13260-13265
219. Gauthier C, Seze-Goismier C, Rozec B. Beta 3-adrenoceptors in the cardiovascular system. *Clinical Hemorheology and Microcirculation*. 2007;37:193-204
220. Varghese P, Harrison RW, Lofthouse RA, Georgakopoulos D, Berkowitz DE, Hare JM. Beta(3)-adrenoceptor deficiency blocks nitric oxide-dependent inhibition of myocardial contractility. *Journal of Clinical Investigation*. 2000;106:697-703
221. Lee DI, Vahebi S, Tocchetti CG, Barouch LA, Solaro RJ, Takimoto E, Kass DA. Pde5a suppression of acute beta-adrenergic activation requires modulation of myocyte beta-3 signaling coupled to pkg-mediated troponin i phosphorylation. *Basic Research in Cardiology*. 2010;105:337-347
222. RivetBastide M, Vandecasteele G, Hatem S, Verde I, Benardeau A, Mercadier JJ, Fischmeister R. Cgmp-stimulated cyclic nucleotide phosphodiesterase regulates the basal calcium current in human atrial myocytes. *Journal of Clinical Investigation*. 1997;99:2710-2718
223. Bischoff E. Potency, selectivity, and consequences of nonselectivity of pde inhibition. *International Journal of Impotence Research*. 2004;16:S11-S14
224. Vandeput F, Krall J, Ockaili R, Salloum FN, Florio V, Corbin JD, Francis SH, Kukreja RC, Movsesian MA. Cgmp-hydrolytic activity and its inhibition by sildenafil in normal and failing human and mouse myocardium. *Journal of Pharmacology and Experimental Therapeutics*. 2009;330:884-891
225. Sumii K, Sperelakis N. Cgmp-dependent protein-kinase regulation of the l-type ca2+ current in rat ventricular myocytes. *Circulation Research*. 1995;77:803-812
226. Pelzmann B, Schaffer P, Bernhart E, Lang P, Machler H, Rigler B, Koidl B. L-type calcium current in human ventricular myocytes at a physiological temperature from children with tetralogy of fallot. *Cardiovascular Research*. 1998;38:424-432
227. Chiang CE, Luk HN, Wang TM, Ding PYA. Effects of sildenafil on cardiac repolarization. *Cardiovascular Research*. 2002;55:290-299
228. Dunkem TR, Hatzelmann A. The effect of sildenafil on human platelet secretory function is controlled by a complex interplay between phosphodiesterases 2, 3 and 5. *Cellular Signalling*. 2005;17:331-339

229. Trafford AW, Diaz ME, Negretti N, Eisner DA. Enhanced ca2+ current and decreased ca2+ efflux restore sarcoplasmic reticulum ca2+ content after depletion. *Circulation Research*. 1997;81:477-484
230. Trafford AW, Diaz ME, O'Neill SC, Eisner DA. Integrative analysis of calcium signalling in cardiac muscle. *Frontiers in Bioscience*. 2002;7:D843-D852
231. Castro LRV, Schittl J, Fischmeister R. Feedback control through cgmp-dependent protein kinase contributes to differential regulation and compartmentation of cgmp in rat cardiac myocytes. *Circulation Research*. 2010;107:1232-1240
232. Marston SB, de Tombe PP. Troponin phosphorylation and myofilament ca(2+) -sensitivity in heart failure: Increased or decreased? *Journal of Molecular and Cellular Cardiology*. 2008;45:603-607
233. Findlay I. Beta-adrenergic and muscarinic agonists modulate inactivation of l-type ca2+ channel currents in guinea-pig ventricular myocytes. *Journal of Physiology-London*. 2002;545:375-388
234. Katz AM. Role of phosphorylation of the sarcoplasmic reticulum in the cardiac response to catecholamines. *European heart journal*. 1980;Suppl A:29-33
235. Dibb KM, Eisner DA, Trafford AW. Regulation of systolic ca2+ (i) and cellular ca2+ flux balance in rat ventricular myocytes by sr ca2+, l-type ca2+ current and diastolic ca2+ (i). *Journal of Physiology-London*. 2007;585:579-592
236. Fischmeister R, Hartzell HC. Mechanism of action of acetylcholine on calcium current in single cells from frog ventricle. *Journal of Physiology-London*. 1986;376:183-202
237. Ziolo MT, Lewandowski SJ, Smith JM, Romano FD, Wahler GM. Inhibition of cyclic gmp hydrolysis with zaprinast reduces basal and cyclic amp-elevated l-type calcium current in guinea-pig ventricular myocytes. *British Journal of Pharmacology*. 2003;138:986-994
238. Montgomery DE, Rundell VLM, Goldspink PH, Urboniene D, Geenen DL, de Tombe PP, Buttrick PM. Protein kinase c epsilon induces systolic cardiac failure marked by exhausted inotropic reserve and intact frank-starling mechanism. *American Journal of Physiology-Heart and Circulatory Physiology*. 2005;289:H1881-H1888
239. Ginsburg R, Bristow MR, Billingham ME, Stinson EB, Schroeder JS, Harrison DC. Study of the normal and failing isolated human-heart - decreased response of failing heart to isoproterenol. *American Heart Journal*. 1983;106:535-540
240. Packer M, Carver JR, Rodeheffer RJ, Ivanhoe RJ, Dibianco R, Zeldis SM, Hendrix GH, Bommer WJ, Elkayam U, Kukin ML, Mallis GI, Sollano JA, Shannon J, Tandon PK, Demets DL. Effect of oral milrinone on mortality in severe chronic heart-failure. *New England Journal of Medicine*. 1991;325:1468-1475
241. Lechat P, Brunhuber KW, Hofmann R, Kuhn P, Nesser HJ, Slany J, al e. The cardiac insufficiency bisoprolol study ii (cibis-ii): A randomised trial.353:9-13
242. Chidsey CA, Braunwald E, Harrison DC. Augmentation of plasma nor-epinephrine response to exercise in patients with congestive heart failure. *New England Journal of Medicine*. 1962;267:650-&
243. Feldman MD, Copelas L, Gwathmey JK, Phillips P, Warren SE, Schoen FJ, Grossman W, Morgan JP. Deficient production of cyclic-amp - pharmacological evidence of an important cause of contractile dysfunction in patients with end-stage heart-failure. *Circulation*. 1987;75:331-339
244. Wang S, Cone J, Fong M, Yoshitake M, Kambayashi J, Liu YG. Interplay between inhibition of adenosine uptake and phosphodiesterase type 3 on cardiac function by cilostazol, an agent to treat intermittent claudication. *Journal of Cardiovascular Pharmacology*. 2001;38:775-783
245. Calverley PMA, Sanchez-Torill F, McIvor A, Teichmann P, Bredenbroeker D, Fabbri LM. Effect of 1-year treatment with roflumilast in severe chronic obstructive pulmonary disease. *American Journal of Respiratory and Critical Care Medicine*. 2007;176:154-161

246. Ghofrani HA, Grimminger F. Treatment of pulmonary arterial hypertension with phosphodiesterase-5 inhibitors. *Deutsche Medizinische Wochenschrift*. 2006;131:S311-S314
247. Corbin JD. Mechanisms of action of pde5 inhibition in erectile dysfunction. *International Journal of Impotence Research*. 2004;16:S4-S7
248. Lewis GD, Lachmann J, Camuso J, Lepore JJ, Shin J, Martinovic ME, Systrom DM, Bloch KD, Semigran MJ. Sildenafil improves exercise hemodynamics and oxygen uptake in patients with systolic heart failure. *Circulation*. 2007;115:59-66
249. Smith CJ, He J, Ricketts SG, Ding J-Z, Moggio RA, Hintze TH. Downregulation of right ventricular phosphodiesterase pde-3a mrna and protein before the development of canine heart failure. *Cell Biochemistry and Biophysics*. 1998;29:67-88
250. Yan C, Miller CL, Abe J. Regulation of phosphodiesterase 3 and inducible camp early repressor in the heart. *Circulation Research*. 2007;100:489-501
251. Masciarelli S, Horner K, Liu CY, Park SH, Hinckley M, Hockman S, Nedachi T, Jin C, Conti M, Manganiello V. Cyclic nucleotide phosphodiesterase 3a-deficient mice as a model of female infertility. *Journal of Clinical Investigation*. 2004;114:196-205
252. Baim DS, McDowell AV, Cherniles J, Monrad ES, Parker JA, Edelson J, Braunwald E, Grossman W. Evaluation of a new bipyridine inotropic agent - milrinone - in patients with severe congestive heart-failure. *New England Journal of Medicine*. 1983;309:748-756
253. Uretsky BF, Generalovich T, Reddy PS, Spangenberg RB, Follansbee WP. The acute hemodynamic-effects of a new agent, mdl-17,043, in the treatment of congestive heart-failure. *Circulation*. 1983;67:823-828
254. Jaski BE, Fifer MA, Wright RF, Braunwald E, Colucci WS. Positive inotropic and vasodilator actions of milrinone in patients with severe congestive heart-failure - dose-response relationships and comparison to nitroprusside. *Journal of Clinical Investigation*. 1985;75:643-649
255. Benotti JR, Grossman W, Braunwald E, Davolos DD, Alousi AA. Hemodynamic assessment of amrinone - new inotropic agent. *New England Journal of Medicine*. 1978;299:1373-1377
256. Osadchii OE, Woodiwiss AJ, Norton GR. Contractile responses to selective phosphodiesterase inhibitors following chronic beta-adrenoreceptor activation. *Pflugers Archiv-European Journal of Physiology*. 2006;452:155-163
257. Yano M, Kohno M, Ohkusa T, Mochizuki M, Yamada J, Hisaoka T, Ono K, Tanigawa T, Kobayashi S, Matsuzaki M. Effect of milrinone on left ventricular relaxation and ca2+ uptake function of cardiac sarcoplasmic reticulum. *American Journal of Physiology-Heart and Circulatory Physiology*. 2000;279:H1898-H1905
258. Amsallem E, Kasparian C, Haddour G, Boissel JP, Nony P. Phosphodiesterase iii inhibitors for heart failure. *Cochrane Database of Systematic Reviews*. 2005
259. Friis UG, Jensen BL, Sethi S, Andreasen D, Hansen PB, Skott O. Control of renin secretion from rat juxtaglomerular cells by camp-specific phosphodiesterases. *Circulation Research*. 2002;90:996-1003
260. Feneck RO. Effects of variable dose milrinone in patients with low cardiac-output after cardiac-surgery. *American Heart Journal*. 1991;121:1995-1999
261. Doolan LA, Jones EF, Kalman J, Burton BF, Tonkin AM. A placebo-controlled trial verifying the efficacy of milrinone in weaning high-risk patients from cardiopulmonary bypass. *Journal of Cardiothoracic and Vascular Anesthesia*. 1997;11:37-41
262. Huang Z, Mancini JA. Phosphodiesterase 4 inhibitors for the treatment of asthma and copd. *Current Medicinal Chemistry*. 2006;13:3253-3262
263. Goldstein I, Lue TF, Padma-Nathan H, Rosen RC, Steers WD, Wicker PA, Sildenafil Study G. Oral sildenafil in the treatment of erectile dysfunction. *New England Journal of Medicine*. 1998;338:1397-1404

264. Galie N, Ghofrani HA, Torbicki A, Barst RJ, Rubin LJ, Badesch D, Fleming T, Parpia T, Burgess G, Branzi A, Grimminger F, Kurzyna M, Simonneau G, Grp SS. Sildenafil citrate therapy for pulmonary arterial hypertension. *New England Journal of Medicine*. 2005;353:2148-2157
265. Guazzi M, Vicenzi M, Arena R, Guazzi MD. Pde5 inhibition with sildenafil improves left ventricular diastolic function, cardiac geometry, and clinical status in patients with stable systolic heart failure results of a 1-year, prospective, randomized, placebo-controlled study. *Circulation-Heart Failure*. 2011;4:8-17
266. Murry CE, Jennings RB, Reimer KA. Preconditioning with ischemia - a delay of lethal cell injury in ischemic myocardium. *Circulation*. 1986;74:1124-1136
267. Ockaili R, Salloum F, Hawkins J, Kukreja RC. Sildenafil (viagra) induces powerful cardioprotective effect via opening of mitochondrial k-atp channels in rabbits. *American Journal of Physiology-Heart and Circulatory Physiology*. 2002;283:H1263-H1269
268. Salloum F, Yin C, Xi L, Kukreja RC. Sildenafil induces delayed preconditioning through inducible nitric oxide synthase-dependent pathway in mouse heart. *Circulation Research*. 2003;92:595-597
269. Mokni W, Keravis T, Etienne-Selloum N, Walter A, Kane MO, Schini-Kerth VB, Lugnier C. Concerted regulation of cgmp and camp phosphodiesterases in early cardiac hypertrophy induced by angiotensin ii. *Plos One*. 2010;5:15
270. Miller CL, Yan C. Targeting cyclic nucleotide phosphodiesterase in the heart: Therapeutic implications. *Journal of Cardiovascular Translational Research*. 2010;3:507-515
271. Nagy O, Hajnal A, Parratt JR, Vegh A. Sildenaril (viagra) reduces arrhythmia severity during ischaemia 24h after oral administration in dogs. *British Journal of Pharmacology*. 2004;141:549-551
272. Lu Z, Xu X, Hu X, Lee S, Traverse JH, Zhu G, Fassett J, Tao Y, Zhang P, dos Remedios C, Pritzker M, Hall JL, Garry DJ, Chen Y. Oxidative stress regulates left ventricular pde5 expression in the failing heart. *Circulation*. 2010;121:1474-U1448
273. Sugiyama A, Satoh Y, Shiina H, Takahara A, Yoneyama M, Hashimoto K. Cardiac electrophysiologic and hemodynamic effects of sildenafil, a pde5 inhibitor, in anesthetized dogs. *Journal of Cardiovascular Pharmacology*. 2001;38:940-946
274. Nagayama T, Hsu S, Zhang ML, Koitabashi N, Bedja D, Gabrielson KL, Takimoto E, Kass DA. Sildenafil stops progressive chamber, cellular, and molecular remodeling and improves calcium handling and function in hearts with pre-existing advanced hypertrophy caused by pressure overload. *Journal of the American College of Cardiology*. 2009;53:207-215
275. Thompson WJ, Appleman MM. Multiple cyclic nucleotide phosphodiesterase activities from rat brain. *Biochemistry*. 1971;10:311-&
276. Horn MA, Graham HK, Richards MA, Clarke JD, Greensmith DJ, Briston SJ, Hall MCS, Dibb KM, Trafford AW. Age-related divergent remodeling of the cardiac extracellular matrix in heart failure: Collagen accumulation in the young and loss in the aged. *Journal of Molecular and Cellular Cardiology*. 2012;53:82-90
277. Dibb KM, Clarke JD, Horn MA, Richards MA, Graham HK, Eisner DA, Trafford AW. Characterization of an extensive transverse tubular network in sheep atrial myocytes and its depletion in heart failure. *Circulation-Heart Failure*. 2009;2:482-489
278. Goonasekera SA, Hammer K, Auger-Messier M, Bodi I, Chen X, Zhang H, Reiken S, Elrod JW, Correll RN, York AJ, Sargent MA, Hofmann F, Moosmang S, Marks AR, Houser SR, Bers DM, Molkentin JD. Decreased cardiac l-type ca2+ channel activity induces hypertrophy and heart failure in mice. *Journal of Clinical Investigation*. 2012;122:280-290
279. Chavey WE. The importance of beta blockers in the treatment of heart failure. *American Family Physician*. 2000;62:2453-2462
280. Liu YG, Shakur Y, Yoshitake M, Kambayashi J. Cilostazol (pletal (r)): A dual inhibitor of cyclic nucleotide phosphodiesterase type 3 and adenosine uptake. *Cardiovascular Drug Reviews*. 2001;19:369-386

281. Trafford AW, Diaz ME, Eisner DA. Coordinated control of cell ca2+ loading and triggered release from the sarcoplasmic reticulum underlies the rapid inotropic response to increased l-type ca2+ current. *Circulation Research*. 2001;88:195-201
282. Pogwizd SM, Schlotthauer K, Li L, Yuan WL, Bers DM. Arrhythmogenesis and contractile dysfunction in heart failure - roles of sodium-calcium exchange, inward rectifier potassium current, and residual beta-adrenergic responsiveness. *Circulation Research*. 2001;88:1159-1167
283. Ungerer M, Bohm M, Elce JS, Erdmann E, Lohse MJ. Altered expression of beta-adrenergic-receptor kinase and beta-1-adrenergic receptors in the failing human heart. *Circulation*. 1993;87:454-463
284. Netticadan T, Temsah RM, Kawabata K, Dhalla NS. Sarcoplasmic reticulum ca2+/calmodulin-dependent protein kinase is altered in heart failure. *Circulation Research*. 2000;86:596-605
285. Soeller C, Cannell MB. Examination of the transverse tubular system in living cardiac rat myocytes by 2-photon microscopy and digital image-processing techniques. *Circulation Research*. 1999;84:266-275
286. Maggi M, Filippi S, Ledda F, Magini A, Forti G. Erectile dysfunction: From biochemical pharmacology to advances in medical therapy. *European Journal of Endocrinology*. 2000;143:143-154
287. Eardley I, Cartledge J. Tadalafil (cialis (tm)) for men with erectile dysfunction. *International Journal of Clinical Practice*. 2002;56:300-304
288. Gerometta R, Alvarez LJ, Candia OA. Effects of sildenafil and tadalafil on intraocular pressure in sheep: Implications for aqueous humor dynamics. *Investigative Ophthalmology & Visual Science*. 2010;51:3139-3144
289. Bristow MR, Ginsburg R, Minobe W, Cubicciotti RS, Sageman WS, Lurie K, Billingham ME, Harrison DC, Stinson EB. Decreased catecholamine sensitivity and beta-adrenergic-receptor density in failing human hearts. *New England Journal of Medicine*. 1982;307:205-211
290. Houser SR, Margulies KB, Murphy AM, Spinale FG, Francis GS, Prabhu SD, Rockman HA, Kass DA, Molkentin JD, Sussman MA, Koch WJ, Amer Heart Assoc Council B, Council Clinical C, Council Functional G. Animal models of heart failure a scientific statement from the american heart association. *Circulation Research*. 2012;111:131-150
291. Whipple GH, Sheffield LT, Woodman EG, Theophilis C, Friedman S. Reversible congestive heart failure due to rapid stimulation of the normal heart. *Proc New Engl Cardiovasc Soc*. 1961-1962:39-40
292. Armstrong PW, Stopps TP, Ford SE, Debold AJ. Rapid ventricular pacing in the dog - pathophysiologic studies of heart-failure. *Circulation*. 1986;74:1075-1084
293. Paslawska U, Gajek J, Kiczak L, Noszczyk-Nowak A, Skrzypczak P, Bania J, Tomaszek A, Zacharski M, Sambor I, Dziegiel P, Zysko D, Banasiak W, Jankowska EA, Ponikowski P. Development of porcine model of chronic tachycardia-induced cardiomyopathy. *International Journal of Cardiology*. 2011;153:36-41
294. Byrne MJ, Raman JS, Alferness CA, Esler MD, Kaye DM, Power JM. An ovine model of tachycardia-induced degenerative dilated cardiomyopathy and heart failure with prolonged onset. *Journal of Cardiac Failure*. 2002;8:108-115
295. Wilson JR, Douglas P, Hickey WF, Lanoce V, Ferraro N, Muhammad A, Reichek N. Experimental congestive-heart-failure produced by rapid ventricular pacing in the dog - cardiac effects. *Circulation*. 1987;75:857-867
296. Hoskins DE, Ignasiak DP, Saganek LJ, Gallagher KP, Peterson JT. Myocardial infarct size is smaller in dogs with pacing-induced heart failure. *Cardiovascular Research*. 1996;32:238-247

297. Binkley PF, Murray KD, Watson KM, Myerowitz PD, Leier CV. Dobutamine increases cardiac-output of the total artificial-heart - implications for vascular contribution of inotropic agents to augmented ventricular-function. *Circulation*. 1991;84:1210-1215
298. Franz MR, Swerdlow CD, Liem LB, Schaefer J. Cycle length dependence of human action-potential duration invivo - effects of single extrastimuli, sudden sustained rate acceleration and deceleration, and different steady-state frequencies. *Journal of Clinical Investigation*. 1988;82:972-979
299. Luo S, Michler K, Johnston P, Macfarlane PW. A comparison of commonly used qt correction formulae: The effect of heart rate on the qtc of normal ecgs. *Journal of Electrocardiology*. 2004;37:81-90
300. Beuckelmann DJ, Nabauer M, Erdmann E. Alterations of k+ currents in isolated human ventricular myocytes from patients with terminal heart-failure. *Circulation Research*. 1993;73:379-385
301. Nattel S, Maguy A, Le Bouter S, Yeh Y-H. Arrhythmogenic ion-channel remodeling in the heart: Heart failure, myocardial infarction, and atrial fibrillation. *Physiological Reviews*. 2007;87:425-456
302. Song B, Wang BN, Chen DN, Luo ZG. Myocardial remodeling and bioelectric changes in tachycardia-induced heart failure in dogs. *Brazilian Journal of Medical and Biological Research*. 2013;46:797-802
303. Jackson G, Benjamin N, Jackson N, Allen MJ. Effect of sildenafil citrate on human hemodynamics. *American Journal of Cardiology*. 1999;83:13C-20C
304. Zhuang X-D, Long M, Li F, Hu X, Liao X-X, Du Z-M. Pde5 inhibitor sildenafil in the treatment of heart failure: A meta-analysis of randomized controlled trials. *International Journal of Cardiology*. 2014;172:581-587
305. Guazzi M, Tumminello G, Di Marco F, Fiorentini C, Guazzi MD. The effects of phosphodiesterase-5 inhibition with sildenafil on pulmonary hemodynamics and diffusion capacity, exercise ventilatory efficiency, and oxygen uptake kinetics in chronic heart failure. *Journal of the American College of Cardiology*. 2004;44:2339-2348
306. Guazzi M, Tumminello G, Di Marco F, Guazzi MD. Influences of sildenafil on lung function and hemodynamics in patients with chronic heart failure. *Clinical Pharmacology & Therapeutics*. 2004;76:371-378
307. Urbanowicz T, Straburzynska-Migaj E, Katynska I, Araszkiewicz A, Oko-Sarnowska Z, Grajek S, Jemielity M. Sustained improvement of clinical status and pulmonary hypertension in patients with severe heart failure treated with sildenafil. *Annals of transplantation : quarterly of the Polish Transplantation Society*. 2014;19:325-330
308. Kim K-H, Kim Y-J, Ohn J-H, Yang J, Lee S-E, Lee S-W, Kim H-K, Seo J-W, Sohn D-W. Long-term effects of sildenafil in a rat model of chronic mitral regurgitation benefits of ventricular remodeling and exercise capacity. *Circulation*. 2012;125:1390-U1157
309. Giannetta E, Isidori AM, Galea N, Carbone I, Mandosi E, Vizza CD, Naro F, Morano S, Fedele F, Lenzi A. Chronic inhibition of cgmp phosphodiesterase 5a improves diabetic cardiomyopathy a randomized, controlled clinical trial using magnetic resonance imaging with myocardial tagging. *Circulation*. 2012;125:2323-+
310. Borgdorff MA, Bartelds B, Dickinson MG, van Wiechen MPH, Steendijk P, de Vroomen M, Berger RMF. Sildenafil treatment in established right ventricular dysfunction improves diastolic function and attenuates interstitial fibrosis independent from afterload. *American journal of physiology. Heart and circulatory physiology*. 2014;307:H361-369
311. Eisner DA, Dibb KM, Trafford AW. The mechanism and significance of the slow changes of ventricular action potential duration following a change of heart rate. *Experimental Physiology*. 2009;94:520-528
312. Kass DA. Cardiac role of cyclic-gmp hydrolyzing phosphodiesterase type 5: From experimental models to clinical trials. *Current heart failure reports*. 2012;9:192-199

313. Frantz R, Durst L, Burger C, Oudiz R, RC Bourge, V Franco, AB Waxman, S McDevitt, Walker S. Conversion from sildenafil to tadalafil: Results from the sildenafil to tadalafil in pulmonary arterial hypertension (sitar) study. *Journal Of Cardiovascular Pharmacology And Therapeutics*. 2014;epub ahead of print
314. Tanaka R, Fulbright BM, Mukherjee R, Burchell SA, Crawford FA, Zile MR, Spinale FG. The cellular basis for the blunted response to beta-adrenergic stimulation in supraventricular tachycardia-induced cardiomyopathy. *Journal of Molecular and Cellular Cardiology*. 1993;25:1215-1233
315. Redfield MM, Chen HH, Borlaug BA, Semigran MJ, Lee KL, Lewis G, LeWinter MM, Rouleau JL, Bull DA, Mann DL, Deswal A, Stevenson LW, Givertz MM, Ofili EO, O'Connor CM, Felker GM, Goldsmith SR, Bart BA, McNulty SE, Ibarra JC, Lin G, Oh JK, Patel MR, Kim RJ, Tracy RP, Velazquez EJ, Anstrom KJ, Hernandez AF, Mascette AM, Braunwald E, Trial R. Effect of phosphodiesterase-5 inhibition on exercise capacity and clinical status in heart failure with preserved ejection fraction a randomized clinical trial. *Jama-Journal of the American Medical Association*. 2013;309:1268-1277
316. Akhter SA, Luttrell LM, Rockman HA, Iaccarino G, Lefkowitz RJ, Koch WJ. Targeting the receptor-g(q) interface to inhibit in vivo pressure overload myocardial hypertrophy. *Science*. 1998;280:574-577
317. Hao J, Michalek C, Zhang W, Zhu M, Xu X, Mende U. Regulation of cardiomyocyte signaling by rgs proteins: Differential selectivity towards g proteins and susceptibility to regulation. *Journal of Molecular and Cellular Cardiology*. 2006;41:51-61
318. Tokudome T, Kishimoto I, Horio T, Arai Y, Schwenke DO, Hino J, Okano I, Kawano Y, Kohno M, Miyazato M, Nakao K, Kangawa K. Regulator of g-protein signaling subtype 4 mediates antihypertrophic effect of locally secreted natriuretic peptides in the heart. *Circulation*. 2008;117:2329-2339
319. Tsutsui H, Kinugawa S, Matsushima S. Oxidative stress and heart failure. *American Journal of Physiology-Heart and Circulatory Physiology*. 2011;301:H2181-H2190
320. Irving EA, Bamford M. Role of mitogen- and stress-activated kinases in ischemic injury. *Journal of Cerebral Blood Flow and Metabolism*. 2002;22:631-647
321. Strohm C, Barancik M, Von Bruhl ML, Kilian SAR, Schaper W. Inhibition of the er-kinase cascade by pd98059 and uo126 counteracts ischemic preconditioning in pig myocardium. *Journal of Cardiovascular Pharmacology*. 2000;36:218-229
322. Fryer RM, Wang YG, Hsu AK, Nagase H, Gross GJ. Dependence of delta(1)-opioid receptor-induced cardioprotection on a tyrosine kinase-dependent but not a src-dependent pathway. *Journal of Pharmacology and Experimental Therapeutics*. 2001;299:477-482
323. Das A, Xi L, Kukreja RC. Protein kinase g-dependent cardioprotective mechanism of phosphodiesterase-5 inhibition involves phosphorylation of erk and gsk3 beta. *Journal of Biological Chemistry*. 2008;283:29572-29585
324. Zou YZ, Yao A, Zhu WD, Kudoh S, Hiroi Y, Shimoyama M, Uozumi H, Kohmoto O, Takahashi T, Shibasaki F, Nagai R, Yazaki Y, Komuro I. Isoproterenol activates extracellular signal-regulated protein kinases in cardiomyocytes through calcineurin. *Circulation*. 2001;104:102-108
325. Molkentin JD, Lu JR, Antos CL, Markham B, Richardson J, Robbins J, Grant SR, Olson EN. A calcineurin-dependent transcriptional pathway for cardiac hypertrophy. *Cell*. 1998;93:215-228
326. Fiedler B, Lohmann SM, Smolenski A, Linnemuller S, Pieske B, Schroder F, Molkentin JD, Drexler H, Wollert KC. Inhibition of calcineurin-nfat hypertrophy signaling by cgmp-dependent protein kinase type i in cardiac myocytes. *Proceedings of the National Academy of Sciences of the United States of America*. 2002;99:11363-11368
327. Brette F, Salle L, Orchard CH. Quantification of calcium entry at the t-tubules and surface membrane in rat ventricular myocytes. *Biophysical Journal*. 2006;90:381-389

328. Xie Y-P, Chen B, Sanders P, Guo A, Li Y, Zimmerman K, Wang L-C, Weiss RM, Grumbach IM, Anderson ME, Song L-S. Sildenafil prevents and reverses transverse-tubule remodeling and ca2+ handling dysfunction in right ventricle failure induced by pulmonary artery hypertension. *Hypertension*. 2012;59:355-+
329. Chen B, Li Y, Jiang S, Xie Y-P, Guo A, Kutschke W, Zimmerman K, Weiss RM, Miller FJ, Anderson ME, Song L-S. Beta-adrenergic receptor antagonists ameliorate myocyte t-tubule remodeling following myocardial infarction. *Faseb Journal*. 2012;26:2531-2537